

Na⁺,K⁺-ATPase in human skeletal muscle: the effects of glucose and sodium bicarbonate, and determination of cellular localisation via immunofluorescence

Submitted by

Collene H Steward, M App Sci

Institute of Sport, Exercise and Active Living

College of Exercise and Sports Science

Victoria University, Melbourne, Australia

A thesis submitted in fulfilment of the requirements for the degree

Doctor of Philosophy

Supervisor: Prof. Michael J. McKenna

September, 2014

ABSTRACT

The sodium-potassium adenosine triphosphatase enzyme (Na^+, K^+ -ATPase; NKA) is a heterodimeric protein comprising catalytic alpha (α -) and regulatory beta (β -) subunits. It drives active coupled transport of Na^+ and K^+ ions across the plasma membrane of most eukaryotic cells, including skeletal muscle cells, thereby also contributing to regulation of membrane potential. Tight control of Na^+/K^+ transport and of NKA is essential to maintaining ion homeostasis, excitability and thus muscle function. This thesis comprises two intervention studies investigating different supplementation protocols whose direct or indirect actions target the NKA in skeletal muscle, with the potential to modulate Na^+/K^+ homeostasis and enhance exercise performance. The first intervention used acute oral glucose supplementation to elevate endogenous insulin, thereby stimulating skeletal muscle NKA activity and modifying K^+ homeostasis, under conditions of rest and intense exercise. The second intervention involved chronic sodium bicarbonate ingestion during training, as induced metabolic alkalosis is expected to increase NKA activity in skeletal muscle and lower circulating K^+ . The third and final study had a methodological focus using immunofluorescence techniques. This study investigated cellular distribution patterns of the NKA isoforms in human skeletal muscle cells and their localisation, contrasting the plasma membrane and intracellular regions, as well as fibre-type differences.

Study 1.

The effects of acute oral glucose supplementation on carbohydrate metabolism are well established, however the effects on muscle NKA and K^+ homeostasis and are not well known. This study therefore investigated the effects of glucose supplementation on endogenous insulin and arterial plasma electrolyte and acid-base homeostasis, before, during and after high-intensity intermittent cycling exercise; in addition the effects on

skeletal muscle NKA isoform protein abundance were examined. Participants performed two trials in a randomised cross over design, ingesting either 75 g glucose (CHO) or a placebo (CON). Sixty min later they commenced exercise, which comprised three cycling exercise bouts (EB) for 45 s at 130% $\dot{V}O_{2peak}$, followed by a fourth bout at 130% $\dot{V}O_{2peak}$ continued until fatigue. Radial arterial (a) and antecubital venous (v) blood samples were taken simultaneously throughout the rest, exercise and recovery phases and analysed for plasma K^+ , Na^+ , H^+ , glucose and Lac^- concentrations ([ion]), and their arterio-venous [ion] differences calculated. A vastus lateralis muscle biopsy was taken prior to glucose/placebo ingestion, immediately before exercise and at fatigue, and analysed for muscle NKA α_{1-3} and β_{1-3} isoform protein abundance (western blotting).

The $[glucose]_a$ was greater during CHO than CON (main effect; $p < 0.001$). The $[glucose]_a$ during CHO was greater than CON from 10 min after ingestion through until EB3 ($p < 0.001$); a similar temporal pattern was observed for $[glucose]_v$ ($p < 0.001$). Arterial plasma [insulin] was increased at each time point measured ($p < 0.001$) and was greater during CHO than CON ($p < 0.001$). During CHO, both $[K^+]_a$ and $[K^+]_v$ were lower after glucose ingestion compared to CON, with the effect most prominent during exercise and early recovery ($p < 0.05$). The $[K^+]_{a-v}$ across the forearm increased during exercise and was more positive in CHO ($p < 0.05$), indicating a greater net uptake of K^+ into the relatively inactive forearm muscles during exercise. Arterial $[Na^+]_a$ was higher in CHO ($p < 0.05$) increasing throughout the exercise period, with the $[Na^+]_{a-v}$ more positive in CHO than CON ($p < 0.05$) during exercise and early recovery. There was no difference in time to fatigue during the final bout between trials. There were no significant main effects for time, treatment or time-by-treatment interactions for any of the skeletal muscle NKA α or β_1 or β_2 isoform abundances following glucose ingestion,

or with exercise. The muscle NKA β_3 protein abundance was increased following exercise during CON only ($p < 0.05$). Hence glucose ingestion attenuated the exercise-induced rise in plasma $[K^+]$ during exercise, likely consequent to increased [insulin]. These systemic K^+ -lowering effects probably indicate increased skeletal muscle NKA activity. This increased activity was not due to increased NKA isoform protein abundance and was not accompanied by improved exercise performance.

Study 2

Alkalosis, induced by sodium bicarbonate (NaHCO_3), affects systemic K^+ regulation, lowering circulating $[K^+]$ at rest and during exercise, and with an increased K^+ reuptake by skeletal muscle during recovery suggesting an increase in muscle NKA activity. Alkalosis also enhances short-term intense exercise performance and when induced during training has also been shown to enable athletes to train at higher intensities. Short-term high-intensity training has been shown to increase skeletal muscle NKA isoform protein expression. Therefore this study investigated the effects of acute NaHCO_3 supplementation on skeletal muscle NKA protein abundance after repeated sprint exercise (RSE), and whether NaHCO_3 -induced alkalosis during training would result in greater adaptations in muscle NKA protein expression post-training. Participants initially ingested a placebo ($0.3 \text{ g}\cdot\text{kg}^{-1}$ calcium carbonate, CaCO_3) and then completed a pre-training RSE session (Pre- CaCO_3). In a second pre-training trial, participants ingested NaHCO_3 prior to performing RSE (Pre- NaHCO_3). Participants then undertook four weeks of RSE training, with 3 sessions/wk and after ingesting $0.3 \text{ g}\cdot\text{kg}^{-1}$ NaHCO_3 prior to each session with water *ad libitum*. In the final trial post-training, participants ingested CaCO_3 and then completed a RSE session (Post- CaCO_3). A vastus lateralis muscle biopsy was taken after placebo/ NaHCO_3 ingestion prior to the warm-up, and then immediately following completion of the final sprint effort, for each

of the three trials (total 6 biopsies), and analysed for muscle NKA α_{1-3} and β_{1-3} isoform protein abundance (western blotting). The NKA α_{1-3} protein isoform abundances were unaltered by acute exercise or training (no significant time or treatment main effects, or time-by-treatment interactions). The muscle NKA β_1 protein abundance was greater ($p<0.01$) in Pre-NaHCO₃ than both Pre-CaCO₃ (20%) and Post-CaCO₃ (40%) trials. The Post-CaCO₃ β_1 was 27% less than Pre-CaCO₃ ($p<0.01$; treatment main effect). The β_3 protein abundance was increased in Post-CaCO₃ compared to Pre-CaCO₃ (35%; $p<0.05$). Thus acute RSE under placebo conditions did not alter muscle NKA isoform abundance, whereas acute RSE with prior NaHCO₃ supplementation increased the abundance of NKA β_1 protein. RSE training combined with chronic NaHCO₃ supplementation decreased NKA β_1 , but increased NKA β_3 protein abundance. These results suggest that acute exercise did not increase NKA abundance whilst chronic supplementation of NaHCO₃ during RSE training may reduce the NKA upregulation typically seen in response to training.

Study 3

In skeletal muscles taken from animal studies, the NKA isoforms have previously been shown to be located in both the plasma membrane and t-tubule membranes. However, the NKA distribution in human skeletal muscle cells is still largely unknown. This study investigated the distribution patterns of the six NKA isoforms (α_1 - α_3 and β_1 - β_3) expressed in human skeletal muscle, also exploring any fibre-type specific distribution. A vastus lateralis muscle biopsy was taken from seven healthy, recreationally-active young adults. Localisation in the plasma membrane (PM) and intracellular (IC) regions, defined as all areas/structures within the plasma membrane envelope and including the t-tubules, were investigated utilising immunofluorescence techniques. The fibre type distribution was approximately 55% type I and 45% type II fibres for each NKA

isoform analysed. The density of NKA α_1 abundance was 24% higher in type II compared to type I fibres ($p<0.01$). The NKA α_2 density was over 2-fold greater in the PM compared to IC ($p<0.05$), with no difference in density between fibre types. However, NKA α_3 was 63% greater in type I than type II fibres ($p<0.05$). The density of NKA β_1 was 58% greater in the PM compared to IC ($p<0.05$), and NKA β_2 was 25% greater in the PM compared to IC ($p<0.05$). There was no difference between fibres types for either NKA β_1 or β_2 . Co-localisation analysis of NKA β_2 with nuclei found a strong correlation (0.69), and showed that 64.8% of the NKA β_2 co-localised with nuclei. The density of NKA β_3 was 21% greater in the PM compared to IC ($p<0.01$). These results demonstrate a higher density of NKA α_2 and β_1 isoforms in the plasma membrane compared to the intracellular region, and a higher density of NKA α_1 in type II fibres and α_3 in type I fibres. Hence NKA expression and localisation differs markedly from previous reports in rat and mouse muscle.

Conclusions

This thesis demonstrated that oral supplementation of glucose prior to exercise modulated $[K^+]$ during exercise and recovery, lowering arterial $[K^+]$ and increasing the $[K^+]_{a-v}$ across the forearm, consistent with an increase in NKA activity, but without affecting NKA protein abundance. Whilst acute supplementation of $NaHCO_3$ increased NKA β_1 protein abundance, following 4 wks RSE training with chronic $NaHCO_3$ supplementation, only the NKA β_3 protein was increased, suggesting that prolonged $NaHCO_3$ supplementation during training does not enhance and may even impair training responses of augmented NKA expression. Immunofluorescence analyses revealed an isoform-specific distribution pattern for NKA isoforms in human vastus lateralis muscle, with a higher density of NKA α_1 in type II fibres and of α_3 in type I fibres, and with a higher density of NKA α_2 and β_1 isoforms in the plasma membrane

compared to the intracellular region. These results suggest that analysis of mixed muscle homogenates, as used in the first two studies, may also be less sensitive to measuring intervention-induced changes in NKA abundance and distribution.

DECLARATION

I, Collene Helen Steward, declare that the PhD thesis entitled *Na⁺,K⁺-ATPase in human skeletal muscle: the effects of glucose and sodium bicarbonate, and determination of cellular localisation via immunofluorescence* is no more than 100,000 words in length including quotes and exclusive of tables, figures, appendices, bibliography, references and footnotes. This thesis contains no material that has been submitted previously, in whole or in part, for the award of any other academic degree or diploma. Except where otherwise indicated, this thesis is my own work.

Signature

Date

ACKNOWLEDGEMENTS

There are many people I would like to thank for their support and involvement at various stages throughout the process of this thesis, whom without this would not have been possible.

To my supervisor Professor Mike McKenna, thank you for taking me on as a PhD student. It has been a bumpy road, but you have always supported me, been patient when needed, and given a push forward when needed. I don't think I could have got there with a different supervisor. Your knowledge, experience and demand for quality, made me strive to always aim for the best. Your encouragement to expand my research into the biochemistry area and develop my skills into new areas is something that I am very grateful for.

To the other research students and staff who I have had the pleasure of getting to know over the years, I appreciate all your assistance on trial days, teaching me analysis techniques, answering my statistics questions, and listening to me complain occasionally. While there are too many people to mention all of them, I would like to give special thanks to Ben Perry, Vicky Wyckelsma, Fabio Serpiello, Samantha Cassar and James Zois. As well as Chris Shaw and Nigel Stepto for their suggestions and feedback on my immunofluorescence work.

I would also like to thank Matthew Varley for collaboration with him on the muscle analysis for the sodium bicarbonate project. To my work colleagues Brad Gatt, Jessica Meilak and Samantha Cassar, thank you for your patience and understanding during this process. I am also especially grateful for the people who donated their time (blood and muscle) to be subjects in my projects, and the doctors who did the muscle biopsies (Andrew Garnham, Mitch Anderson and Jo Parkin) and the arterial lines (Mal Brown, Bob Smith and Irene Ng). Without people like you, none of this would be possible.

I would also like to thank my friends Rebecca, Judy, Suda and Houn for their patience and understanding when I said I couldn't come out because I had to work on my thesis. Finally, my biggest thank you must go to my family. It was nearly 20 yrs ago when I decided that I wanted to do a PhD in exercise physiology, and despite thinking that my dream was over after being told by my high school careers advisor that 'girls don't do sports science' you provided unwavering encouragement throughout every step of the way. I am eternally grateful for all your support; from letting me stay at home and not hurrying me up to move out, all the way through to the meals in my freezer these last couple of months. I appreciate every last bit of it. And now I look forward to being able to visit you more often and get in some more fishing together.

ABBREVIATIONS

		Units
[ion]	Ion concentration	
Δ [ion]	Change in ion concentration	mmol.L ⁻¹
[ion] _a	Arterial plasma ion concentration	mmol.L ⁻¹
[ion] _{a-v}	Arterio-venous plasma ion concentration difference	mmol.L ⁻¹
[ion] _o	Extracellular ion concentration	mmol.L ⁻¹
[ion] _i	Intracellular ion concentration	mmol.L ⁻¹
[ion] _v	Venous plasma ion concentration	mmol.L ⁻¹
[³ H]ouabain binding	Tritiated ouabain binding	
3- <i>O</i> -MFPase	3- <i>O</i> -methylfluorescein phosphatase	
ATP	Adenosine 5'triphosphate	
CaCO ₃	Calcium carbonate	
Cl ⁻	Chloride ion	mmol.L ⁻¹
H ⁺	Hydrogen ion	nmol.L ⁻¹
Hb	Haemoglobin	g.dl ⁻¹
HCO ₃ ⁻	Bicarbonate ion	mmol.L ⁻¹
Hct	Haematocrit	%
K ⁺	Potassium ion	mmol.L ⁻¹
Lac ⁻	Lactate ion	mmol.L ⁻¹
mRNA	Messenger ribonucleic acid	
Na ⁺	Sodium ion	mmol.L ⁻¹
NaHCO ₃	Sodium bicarbonate	
Na ⁺ ,K ⁺ -ATPase	Sodium-Potassium Adenosine Triphosphatase	

Na ⁺ ,K ⁺ -pump	Sodium-Potassium Adenosine Triphosphatase	
NKA	Sodium-Potassium Adenosine Triphosphatase	
RSE	Repeated sprint exercise	
VO ₂	Oxygen consumption	l.min ⁻¹
VO _{2peak}	Peak oxygen consumption (absolute)	l.min ⁻¹
VO _{2peak}	Peak oxygen consumption (relative)	ml.kg ⁻¹ .min ⁻¹

PUBLICATIONS AND PRESENTATIONS

This thesis is supported by the following presentation:

CONFERENCE PRESENTATION

C Steward, R Smith, N Stepto, F Serpiello, A Petersen, M Brown, R Aughey, J Zois, I Ng, M McKenna. *Effects of glucose ingestion on potassium homeostasis during rest and exercise*. 3rd Biennial MyoNaK Conference. Ionic regulation in heart and skeletal muscle: functional implications in health and in disease. Palm Cove, Queensland, Australia, 2009.

MANUSCRIPTS

C Steward, R Smith, N Stepto, M Brown, I Ng, M McKenna. *A single oral glucose load decreases arterial plasma K^+ during exercise and recovery*. In preparation for submission to Journal of Applied Physiology. (Study 1, Chapter 3)

C Steward and M McKenna. *Cellular localisation of NKA isoforms in human skeletal muscle determined by immunofluorescence microscopy*. In preparation for submission to Journal of Histochemistry and Cytochemistry. (Study 3, Chapter 5)

CONTENTS

ABSTRACT	ii
DECLARATION	viii
ACKNOWLEDGEMENTS	ix
ABBREVIATIONS	xi
PUBLICATIONS AND PRESENTATIONS.....	xiii
CONTENTS	xiv
LIST OF TABLES	xxi
LIST OF FIGURES	xxii
CHAPTER 1. INTRODUCTION	28
CHAPTER 2. Review of Literature	31
SECTION I: Muscle contraction, ionic regulation and fatigue	31
2.1 Skeletal muscle structure and function	31
2.2 Muscle ion regulation during membrane excitation	35
2.2.1 Membrane potential	35
2.2.2 K ⁺ Concentrations and fluxes with exercise	36
2.2.2.1 Insulin effects on plasma [K ⁺]	38
2.2.2.2 Sodium bicarbonate effects on plasma [K ⁺].....	40
2.2.3 Na ⁺ concentrations and fluxes with exercise.....	40
2.2.4 Lactate and hydrogen ions	41
2.2.5 Muscle water content and exercise	43
SECTION II: Na ⁺ ,K ⁺ -ATPase in skeletal muscle.....	44
2.3 NKA subunits and isoforms	44
2.4 Location	49

2.4.1	NKA isoform specific location.....	50
2.5	Quantification of NKA in skeletal muscle.....	53
2.5.1	Measurement of NKA content	53
2.5.2	Measurement of NKA <i>in-vitro</i> activity.....	54
2.6	Regulation of NKA.....	55
2.6.1	Acute regulation	55
2.6.1.1	Excitation.....	55
2.6.1.2	Insulin.....	56
2.6.1.3	Acute exercise.....	57
2.6.2	Chronic regulation	58
2.6.2.1	Insulin.....	58
2.6.2.2	Exercise training	58
	SECTION III: Aims and hypotheses	60
2.7	Aims.....	60
2.8	Hypotheses	60
CHAPTER 3. The effects of an oral glucose load on plasma K ⁺ and electrolyte		
homeostasis at rest, during high intensity intermittent exercise and recovery on skeletal		
muscle NKA isoform abundance.....		
3.1	Introduction.....	62
3.2	Methods	66
3.2.1	Participants.....	66
3.2.2	Experimental design	66
3.2.3	Incremental exercise testing.....	66
3.2.4	High-intensity intermittent cycling.....	67
3.2.5	Experimental trials.....	68

3.2.5.1	Participant preparation	68
3.2.5.2	Blood sampling and analyses	68
3.2.5.3	Muscle biopsies	69
3.2.6	Skeletal muscle NKA isoform protein abundance measures	70
3.2.6.1	Protein extraction	70
3.2.6.2	Immunoblotting	71
3.2.6.3	Antibodies.....	72
3.2.7	Statistical analyses	72
3.3	Results.....	74
3.3.1	Exercise performance	74
3.3.2	Plasma [glucose].....	74
3.3.3	Arterial plasma insulin concentration	75
3.3.4	Plasma [K ⁺]	77
3.3.5	ΔPlasma [K ⁺].....	79
3.3.6	Plasma [Na ⁺].....	81
3.3.7	Plasma [Lac ⁻].....	83
3.3.8	Plasma [H ⁺]	85
3.3.9	Haematology and fluid shifts	87
3.3.10	Skeletal muscle NKA alpha isoform protein abundances	91
3.3.11	Skeletal muscle NKA beta isoform protein abundances.....	93
3.4	Discussion	95
3.4.1	Glycaemic and metabolic responses.....	96
3.4.2	CHO effects on K ⁺ homeostasis	97
3.4.3	CHO Effects on Exercise Performance	99
3.4.4	Exercise and CHO Effects on NKA Protein Abundance.....	99

3.4.5	Limitations	101
3.4.6	Conclusions	101
CHAPTER 4. The effects of acute and chronic sodium bicarbonate supplementation		
and repeat sprint exercise on skeletal muscle NKA protein abundance		103
4.1	Introduction	103
4.2	Methods	107
4.2.1	Participants	107
4.2.2	Experimental design	107
4.2.3	Incremental exercise test	108
4.2.4	RSE Protocol	109
4.2.5	Supplementation	109
4.2.6	Experimental trials	110
4.2.7	Muscle biopsies	110
4.2.8	NKA isoform protein abundance	110
4.2.8.1	Protein extraction	110
4.2.8.2	Immunoblotting	111
4.2.8.3	Antibodies	112
4.2.9	Statistical analysis	112
4.3	Results	114
4.3.1	NKA alpha isoform protein abundances	114
4.3.2	NKA beta isoform protein abundances	117
4.4	Discussion	119
4.4.1	Acute exercise and NKA isoform abundance	119
4.4.2	Acute exercise and NaHCO ₃ supplementation	120
4.4.3	RSE training and NaHCO ₃ supplementation	121

4.4.4	Limitations	123
4.4.5	Conclusions	124
CHAPTER 5. Cellular localisation of NKA isoforms in human skeletal muscle		
	determined by immunofluorescence microscopy	125
5.1	Introduction	125
5.2	Methods	128
5.2.1	Participants	128
5.2.2	Muscle biopsies	128
5.2.3	Tissue sectioning	128
5.2.4	Immunofluorescence labelling	129
5.2.4.1	Antibodies	129
5.2.4.2	Fluorescence microscopy	131
5.2.5	Plasma membrane and intracellular NKA analysis	131
5.2.6	Colocalisation analysis	132
5.2.7	Line profile intensity analysis	133
5.2.8	Statistics	135
5.3	Results	136
5.3.1	NKA isoform antibody specificity	136
5.3.2	Comparison of plasma membrane markers	137
5.3.3	Fibre type distribution and area	138
5.3.4	NKA α_1	140
5.3.5	NKA α_2	142
5.3.6	NKA α_3	144
5.3.7	NKA β_1	146
5.3.8	NKA β_2	148

5.3.8.1	NKA β_2 nuclei colocalisation	150
5.3.9	NKA β_3	151
5.3.10	Further qualitative analysis of intracellular localisation	152
5.3.10.1	α isoforms	152
5.3.10.2	β isoforms	153
5.4	Discussion	155
5.4.1	Increased density in plasma membrane for NKA α_2 and β_1	155
5.4.2	Fibre-type specific expression of NKA α_1 and α_3	157
5.4.3	Intracellular localisation in t-tubules	159
5.4.4	Limitations	160
5.4.5	Conclusions	161
CHAPTER 6.	General Discussion and Conclusion	163
6.1	General Discussion.....	163
6.1.1	Introduction	163
6.1.2	Acute oral glucose load enhances K^+ regulation.....	163
6.1.3	Exercise, supplementation and NKA protein abundance	165
6.1.4	Cellular localisation.....	167
6.2	Conclusions.....	170
6.3	Recommendations for future studies	171
REFERENCES	173
Appendix 1.	Participant information, consent form, and risk factor questionnaires ...	193
Appendix 2.	Individual data from Study 1 (Chapter 3)	203
Appendix 3.	Individual data from Study 2 (Chapter 4)	233
Appendix 4.	Plasma K^+ data from Study 2 (Chapter 4).....	236
Appendix 5.	Western blot protein linearity	239

Appendix 6. Individual data from Study 3 (Chapter 5) 242

LIST OF TABLES

Table 3.1 Arterial plasma insulin concentration ($\text{pmol}\cdot\text{L}^{-1}$) measured at baseline, and subsequent 60 min rest and during high intensity intermittent exercise at 130% $\dot{V}\text{O}_2$ peak continued to fatigue, following either carbohydrate (CHO), or placebo (CON) ingestion.	75
Table 3.2 Arterial haemoglobin concentration ($[\text{Hb}]_a$; $\text{g}\cdot\text{dl}^{-1}$) and haematocrit (Hct_a ; %) measured at baseline, during 60 min rest and during high intensity intermittent exercise at 130% $\dot{V}\text{O}_2$ peak continued to fatigue and recovery, following either carbohydrate (CHO), or placebo (CON) ingestion.	88
Table 3.3 Venous haemoglobin concentration ($[\text{Hb}]_v$; $\text{g}\cdot\text{dl}^{-1}$) and haematocrit (Hct_v ; %) measured at baseline, during 60 min rest and during high intensity intermittent exercise at 130% $\dot{V}\text{O}_2$ peak continued to fatigue and recovery, following either carbohydrate (CHO), or placebo (CON) ingestion.	89
Table 3.4 Change in plasma volume relative to baseline in arterial (ΔPV_a) and venous blood (ΔPV_v), and the calculated arterio-venous plasma volume difference ($\Delta\text{PV}_{a-v\text{diff}}$), measured at baseline, during 60 min rest and high intensity intermittent exercise at 130% $\dot{V}\text{O}_2$ peak continued to fatigue and recovery, following either carbohydrate (CHO), or placebo (CON) ingestion.	90
Table 4.1 Participant Characteristics ($n = 7$)	107
Table 5.1 Colocalisation analysis of laminin and Cav-3.....	138
Table 5.2 Total number of type I and type II fibres analysed (participant mean \pm SD), proportion of fibres labelled positive for MHCI, and the (mean \pm SD) for each isoform is also shown for cross-sectional analyses of NKA α_{1-3} and β_{1-2}	139
Table 5.3 Colocalisation analysis of NKA β_2 and nuclei.....	150
Table 6.1 Summary of immunofluorescence localisation in human vastus lateralis muscle results from Study 3.....	168
Table 6.2 Summary of NKA immunofluorescence density in human vastus lateralis muscle results from Study 3.....	169

LIST OF FIGURES

- Figure 2.1 Electron micrograph of the extracellular matrix/muscle interface illustrating the basement membrane. (1b) in close association with the cell membrane/sarcolemma (2) and the cytoplasm where the cytoskeleton and contractile proteins (3) are located (Grounds *et al.*, 2005)..... 32
- Figure 2.2 Cross-section of a single muscle fibre showing the vastly complex t-tubule network in a frog Sartorius muscle fibre (Peachey & Eisenberg, 1978). 32
- Figure 2.3 Sequence of events in the excitation-contraction-relaxation cycle and of the major subcellular components in a skeletal muscle fibre. (1) Initiation and propagation of an action potential along the sarcolemma (SM) and the transverse tubular system (TS); (2) detection of the TS depolarization signal and signal transmission from the TS to the sarcoplasmic reticulum (SR) membrane; (3) Ca²⁺ release from the SR via SR Ca²⁺ release channel (CRC); (4) rise of myoplasmic [Ca²⁺]; (5) activation of the Ca²⁺ regulatory system and the contractile apparatus (MF, myosin filament; AF, actin filament); (6) Ca²⁺ reuptake by the SR Ca²⁺ pump (SCP) and Ca²⁺ binding to myoplasmic sites. TC, SR terminal cisternae; CS, calsequestrin; VS, voltage sensors in the transverse tubular membrane (Stephenson *et al.*, 1998). 34
- Figure 2.5 Time related decrease in plasma [K⁺] during hyperglycaemic clamp (+125 hyper) and euglycaemic insulin clamp studies of varying insulin concentrations (mU.kg⁻¹.min⁻¹) (DeFronzo *et al.*, 1980). 39
- Figure 2.6 Potential integrated physiological mechanisms by which ion–ion interactions, ion–metabolite interactions and catecholamines influence muscle force production during fatiguing exercise (Cairns & Lindinger, 2008). 42
- Figure 2.7 Membrane topology of the α- and β-isoforms of the NKA. Sequences of rat α₁- and β₁-isoforms are shown. Residues are coloured to indicate the amino acid homology among the different α-isoforms (α₁, α₂, α₃ and α₄) or β-isoforms (β₁, β₂ and β₃) (Blanco & Mercer, 1998)..... 45
- Figure 2.8 Architecture of the NKA αβγ complex and the K⁺/Rb⁺ sites. The cytoplasmic side is up. The α-, β- and γ-subunits are coloured blue, wheat and red, respectively. Helices are represented by cylinders and b-strands by arrows. The β-ectodomain is shown by surface representation of the experimental electron density. The transmembrane segments of the α-subunit are numbered (yellow) starting with the most N-terminal. The small C-terminal helix (S, for switch) is light red. Mg²⁺, MgF₄²⁻ and Rb⁺ ions are grey, orange and pink, respectively (Morth *et al.*, 2007). 46
- Figure 2.9 Subcellular localisation of NKA α₂ in rat EDL. Cross sections are labelled for NKA α₂ (A); DHPR (B). The composite image (C) show NKA α₂ in red, DHPR in green and structures containing both structures in yellow (Williams *et al.*, 2001)..... 52

Figure 3.1 Effects of an oral glucose load on plasma [glucose] measured at baseline (0), and subsequent 60 min rest, during high intensity intermittent cycling at 130% $\dot{V}O_2$ peak continued to fatigue, and in 30 min recovery, following either carbohydrate (CHO), or placebo (CON) ingestion. A) Arterial (a), B) venous (v), and C) calculated arterio-venous differences (a-v) in plasma [Gluc], under CON (●) and CHO (▽) conditions. ★ Different from baseline ($p < 0.05$, Time main effect). † CHO different from CON ($p < 0.05$, Treatment main effect). ‡ CHO greater than CON at that timepoint ($p < 0.05$). All data mean \pm SD, n = 8. Shaded bars represent exercise bout (EB), with EB1-EB3 of 45 s duration each and EB4 continued till fatigue (F). 76

Figure 3.2 Effects of an oral glucose load on plasma [K⁺] measured at baseline (0), and subsequent 60 min rest, during high intensity intermittent cycling at 130% $\dot{V}O_2$ peak continued to fatigue, and in 30 min recovery, following either carbohydrate (CHO), or placebo (CON) ingestion. A) Arterial (a), B) venous (v), and C) calculated arterio-venous differences (a-v) in plasma [K⁺], under CON (●) and CHO (▽) conditions. ★ Different from baseline ($p < 0.05$, Time main effect). † CHO different from CON ($p < 0.05$, Treatment main effect). ‡ CHO different from CON at that timepoint ($p < 0.05$). All data mean \pm SD, n = 8. Shaded bars represent exercise bout (EB), with EB1-EB3 of 45 s duration each and EB4 continued till fatigue (F). 78

Figure 3.3 Effects of an oral glucose load on plasma Δ [K⁺] measured at baseline (0), and subsequent 60 min rest, during high intensity intermittent cycling at 130% $\dot{V}O_2$ peak continued to fatigue, and in 30 min recovery, following either carbohydrate (CHO), or placebo (CON) ingestion. A) Arterial (a), B) venous (v), and C) calculated arterio-venous differences (a-v) in Δ [K⁺], under CON (●) and CHO (▽) conditions. ★ Different from baseline ($p < 0.05$, Time main effect). † CHO different from CON ($p < 0.05$, Treatment main effect). ‡ CHO different from CON at that timepoint ($p < 0.05$). All data mean \pm SD, n = 8. Shaded bars represent exercise bout (EB), with EB1-EB3 of 45 s duration each and EB4 continued till fatigue (F). 80

Figure 3.4 Effects of an oral glucose load on plasma [Na⁺] measured at baseline (0), and subsequent 60 min rest, during high intensity intermittent cycling at 130% $\dot{V}O_2$ peak continued to fatigue, and in 30 min recovery, following either carbohydrate (CHO), or placebo (CON) ingestion. A) Arterial (a), B) venous (v), and C) calculated arterio-venous differences (a-v) in plasma [Na⁺], under CON (●) and CHO (▽) conditions. ★ Different from baseline ($p < 0.05$, Time main effect). † CHO different from CON ($p < 0.05$, Treatment main effect). All data mean \pm SD, n = 8. Shaded bars represent exercise bout (EB), with EB1-EB3 of 45 s duration each and EB4 continued till fatigue (F). 82

Figure 3.5 Effects of an oral glucose load on plasma [Lac⁻] measured at baseline (0), and subsequent 60 min rest, during high intensity intermittent cycling at 130% $\dot{V}O_2$ peak continued to fatigue, and in 30 min recovery, following either carbohydrate (CHO), or placebo (CON) ingestion. A) Arterial (a), B) venous (v), and C) calculated arterio-venous differences (a-v) in plasma [Lac⁻], under CON (●) and CHO (▽) conditions. ★ Different from baseline ($p < 0.05$, Time main effect).

All data mean \pm SD, n = 8. Shaded bars represent exercise bout (EB), with EB1-EB3 of 45 s duration each and EB4 continued till fatigue (F).....	84
Figure 3.6 Effects of an oral glucose load on plasma $[H^+]$ measured at baseline (0), and subsequent 60 min rest, during high intensity intermittent cycling at 130% $\dot{V}O_{2peak}$ continued to fatigue, and in 30 min recovery, following either carbohydrate (CHO), or placebo (CON) ingestion. A) Arterial (a), B) venous (v), and C) calculated arterio-venous differences (a-v) in plasma $[H^+]$, under CON (\bullet) and CHO (∇) conditions. \star Greater than baseline ($p < 0.05$; Time main effect). All data mean \pm SD, n = 8. Shaded bars represent exercise bout (EB), with EB1-EB3 of 45 s duration each and EB4 continued till fatigue (F).	86
Figure 3.7 Representative immunoblots of NKA α_1 , α_2 , α_3 , β_1 , β_2 and β_3 isoforms in homogenates of the humans vastus lateralis muscle. Values at left indicate molecular weight of bands. Protein bands from left to right are Baseline, 60 min post ingestion and Fatigue, with lanes 1-3 CON, lanes 4-6 CHO.	91
Figure 3.8 Muscle NKA α isoform relative protein abundance at Baseline, 60 min rest following either carbohydrate (CHO) or placebo (CON) ingestion and at Fatigue. NKA α_1 (A); NKA α_2 (B); NKA α_3 (C). All results are normalised against total protein loaded and expressed relative to baseline from the CON trial. Data are mean \pm SD, n = 8.....	92
Figure 3.9 Muscle NKA β isoform relative protein abundance at Baseline, 60 min rest following either carbohydrate (CHO) or placebo (CON) ingestion and at Fatigue. NKA β_1 (A); NKA β_2 (B); NKA β_3 (C). All results are normalised against total protein loaded and expressed relative to baseline from the CON trial. Data are mean \pm SD, n = 8. \ast CON 60 min rest < CON Fatigue (interaction main effect, $p < 0.05$). \ddagger Tendency to higher CON than CHO.	94
Figure 4.1 Representative immunoblots of NKA α_1 , α_2 , α_3 , β_1 , β_2 and β_3 in muscle homogenates of human vastus lateralis muscle. Values at left indicate molecular weight of bands. Protein bands from left to right are, lanes 1 and 2 – PRE- $CaCO_3$; lanes 3 and 4 – PRE- $NaHCO_3$; lanes 5 and 6 – POST- $CaCO_3$ and are rest and exercise, respectively.....	114
Figure 4.2 NKA α protein abundance in the vastus lateralis muscle at rest and following acute RSE. The exercise test was conducted pre-training after placebo ingestion (PRE- $CaCO_3$); pre-training after $NaHCO_3$ ingestion (PRE- $NaHCO_3$); and post-training after placebo ingestion (POST- $CaCO_3$). NKA α_1 (A); NKA α_2 (B); NKA α_3 (C). All results are normalised to total protein and then expressed relative to PRE- $CaCO_3$ rest. All data are mean \pm SD, n = 7.	116
Figure 4.3 NKA β protein abundance in the vastus lateralis muscle at rest and following acute RSE. The exercise test was conducted pre-training after placebo ingestion (PRE- $CaCO_3$); pre-training after $NaHCO_3$ ingestion (PRE- $NaHCO_3$); and post-training after placebo ingestion (POST- $CaCO_3$). NKA β_1 (A); NKA β_2 (B); NKA β_3 (C). All results are normalised to total protein and then expressed relative to PRE- $CaCO_3$ rest. All data are mean \pm SD, n = 7. \dagger PRE- $NaHCO_3$ > PRE- $CaCO_3$; \ddagger POST- $CaCO_3$ < PRE- $CaCO_3$; \S PRE- $NaHCO_3$ > POST- $CaCO_3$ (treatment main	

effect, $p < 0.01$). *POST-CaCO₃ > PRE-NaHCO₃ (treatment main effect, $p < 0.05$).
 118

Figure 5.1 Example of analysis steps for intracellular and plasma membrane fluorescence analysis. A) Thresholded image from laminin stained section identifying individual muscle fibres; B) outline of intracellular areas analysed for fluorescence intensity; C) inverted threshold image identifying the plasma membrane; D) segmented plasma membrane outline; E) segments of plasma membrane from adjacent type I fibres for myosin type I plasma membrane analysis; F) segments of plasma membrane from adjacent type II fibres for myosin type II plasma membrane analysis. 134

Figure 5.2 Western blot results of antibody specificity testing for antibodies specific to NKA $\alpha_1 - \alpha_3$ and $\beta_1 - \beta_3$ 136

Figure 5.3 Line profile analysis of laminin and cav-3 colocalisation in human vastus lateralis muscle fibre membranes. Location of the line drawn across four cell walls for analysis of laminin (A); cav-3 (B); composite image (C) showing laminin in red, cav-3 in green and areas of colocalisation in yellow; fluorescence profile for the line (D) with peaks for laminin (red) and cav-3 (green) occurring at the same location. 137

Figure 5.4 Cellular localisation of NKA α_1 abundance in human skeletal muscle fibres. Serial sections of the vastus lateralis muscle were double labelled with laminin (A, D), and antibody to NKA α_1 (B) or MHC I (E). The composite image (C) show the NKA subunit in green, laminin in red, and nucleus in blue; composite image (F) shows MHCI in green, laminin in red, and nucleus in blue; areas of colocalisation of primary antibodies are yellow. 140

Figure 5.5 Calculated density for NKA α_1 abundance in human vastus lateralis muscle. * type I < type II; main effect, $p < 0.01$. All data mean \pm SD; type I fibres (n = 307; N = 6); type II fibres (n = 256; N = 6); (n = number of fibres; N = number of subjects). 141

Figure 5.6 Cellular localisation of NKA α_2 abundance in human skeletal muscle fibres. Serial sections of the vastus lateralis muscle were double labelled with cav-3 (A) or laminin (D), and antibody to NKA α_2 (B) or MHC I (E). The composite image (C) show the NKA subunit in green, cav-3 in red, and nucleus in blue; composite image (F) shows MHCI in green, Cav-3 in red, and nucleus in blue; areas of colocalisation of primary antibodies are yellow. 142

Figure 5.7 Calculated density for NKA α_2 abundance in human vastus lateralis muscle. * PM > IC; location main effect; $p < 0.01$. All data mean \pm SD; type I fibres (n = 339; N = 6); type II fibres (n = 232; N = 6); (n = number of fibres; N = number of subjects). 143

Figure 5.8 Cellular localisation of NKA α_3 abundance in human skeletal muscle fibres. Serial sections of the vastus lateralis muscle were double labelled with laminin (A, D), and antibody to NKA α_3 (B) or MHC I (E). The composite image (C) show the NKA subunit in green, laminin in red, and nucleus in blue; composite image (F)

shows MHCI in green, laminin in red, and nucleus in blue; areas of colocalisation of primary antibodies are yellow.	144
Figure 5.9 Calculated density for NKA α_3 abundance in human vastus lateralis muscle. * type I > type II; fibre type main effect; $p < 0.05$. All data mean \pm SD; type I fibres (n = 348; N = 6); type II fibres (n = 268; N = 6); (n = number of fibres; N = number of subjects).	145
Figure 5.10 Cellular localisation of NKA β_1 abundance in human skeletal muscle fibres. Serial sections of the vastus lateralis muscle were double labelled with laminin (A, D), and antibody to NKA β_1 (B) or MHC I (E). The composite image (C) show the NKA subunit in green, laminin in red, and nucleus in blue; composite image (F) shows MHCI in green, laminin in red, and nucleus in blue; areas of colocalisation of primary antibodies are yellow.	146
Figure 5.11 Calculated density for NKA β_1 abundance in human vastus lateralis muscle. * PM > IC; location main effect; $p < 0.05$. All data mean \pm SD; type I fibres (n = 387; N = 6); type II fibres (n = 286; N = 6); (n = number of fibres; N = number of subjects).	147
Figure 5.12 Cellular localisation of NKA β_2 abundance in human skeletal muscle fibres. Serial sections of the vastus lateralis muscle were double labelled with laminin (A, D), and antibody to NKA β_2 (B) or MHC I (E). The composite image (C) show the NKA subunit in green, laminin in red, and nucleus in blue; composite image (F) shows MHCI in green, laminin in red, and nucleus in blue; areas of colocalisation of primary antibodies are yellow.	148
Figure 5.13 Calculated density for NKA β_2 abundance in human vastus lateralis muscle. * PM > IC; location main effect; $p < 0.05$. All data mean \pm SD; type I fibres (n = 128; N = 3); type II fibres (n = 70; N = 3); (n = number of fibres; N = number of subjects).	149
Figure 5.14 Cellular colocalisation of NKA β_2 and nuclei in human vastus lateralis muscle fibres. Cross-section labelled with antibody specific to NKA β_2 (A); nuclei labelled with bis-benzimide (B); merged image with NKA β_2 shown in green and nuclei blue (C); analysis results showing areas of colocalisation in orange/red (D).	150
Figure 5.15 Cellular localisation of NKA β_3 abundance in human skeletal muscle fibres. Serial sections of the vastus lateralis muscle were double labelled with laminin (A), and antibody to NKA β_3 (B). The composite image (C) show the NKA subunit in green, laminin in red, and nucleus in blue; areas of colocalisation of primary antibodies are yellow.	151
Figure 5.16 Calculated density for NKA β_3 abundance in human vastus lateralis muscle. * PM > IC; $p < 0.01$. All data mean \pm SD; (n = 810 ; N = 6); (n = number of fibres; N = number of subjects).	152
Figure 5.17 Higher magnification images of intracellular localisation of DHPR and NKA α isoforms. A) DHPR shown in green, laminin in red; B) NKA α_1 shown in	

green, laminin in red, areas of colocalisation in yellow; C) NKA α_2 shown in red (due to different antibody host species); D) NKA α_3 shown in green, laminin in red, areas of colocalisation in yellow. Nuclei where visible are blue. 153

Figure 5.18 High magnification images of intracellular localisation of NKA β_1 and β_2 .

A) NKA β_1 shown in green, laminin in red, areas of colocalisation in yellow; B)

NKA β_2 shown in green, laminin in red, areas of colocalisation in yellow. Nuclei where visible are blue. 154

_Toc424151550

CHAPTER 1. INTRODUCTION

High-intensity exercise demands marked elevations of glycolytic metabolism and ATP utilisation, and leads to pronounced metabolic and ionic disturbances in contracting skeletal muscle. These ionic disturbances include a loss of potassium (K^+) and a concurrent gain of sodium (Na^+) ions and have been linked with a pronounced decline in power output due to fatigue (Lindinger *et al.*, 1992; McKenna *et al.*, 1993; McKenna *et al.*, 1997; Harmer *et al.*, 2000; Clausen, 2013). During high intensity exercise, increased cellular K^+ efflux increases muscle interstitial $[K^+]$, which has been linked with muscular fatigue (de Paoli *et al.*, 2007). The plasma K^+ concentration ($[K^+]$) during and following exercise is dependent on the balance between K^+ release by contracting cells, and rates of K^+ uptake by contracting and non-contracting, (inactive) skeletal muscle and other tissues (Lindinger & Sjøgaard, 1991). Plasma $[K^+]$ increases from approximately 4 up to 7-8 $mmol.L^{-1}$ during intense exercise (Kowalchuk *et al.*, 1988a; McKenna *et al.*, 1997), and upon cessation of exercise, the combination of rapid cellular K^+ reuptake and an initial high post-exercise blood flow result in a rapid decrease of plasma $[K^+]$ to or below resting concentration (Lindinger & Sjøgaard, 1991; Lindinger *et al.*, 1992; Nordsborg *et al.*, 2008).

Whilst the kidneys are responsible for long-term K^+ regulation, extra-renal tissues such as skeletal muscle contain the largest pool of exchangeable K^+ and directly influence systemic K^+ regulation. The sodium-potassium adenosine triphosphatase (Na^+,K^+ -ATPase, Na^+,K^+ -pump, NKA) is primarily responsible for maintaining the large $[Na^+]$ and $[K^+]$ gradients across the plasma membrane of excitable cells (Therien & Blostein, 2000). There are seven isoforms of the NKA, of which six are expressed in human skeletal muscle (Murphy *et al.*, 2004). Supplements with ergogenic properties have long been used to enhance exercise performance and many of these have either a

primary or secondary effect on the NKA in skeletal muscle. The first two studies of this thesis examined two of these ergogenic aids, glucose and sodium bicarbonate. Physiological increases in plasma insulin induce a significant decrease in plasma $[K^+]$ (DeFronzo *et al.*, 1980). Glucose ingestion increases endogenous insulin concentration, and a 75g glucose load was sufficient to induce hypokalaemia (Natali *et al.*, 1993). However the effects on plasma $[K^+]$ during exercise and or muscle NKA abundance in human skeletal muscle are unknown. This thesis examined glucose effects on K^+ homeostasis in arterial and venous plasma and on NKA isoform protein abundance in skeletal muscle. Supplementation with $NaHCO_3$ has been shown to induce metabolic alkalosis, decrease arterial and venous $[K^+]$, enhance short-term intense exercise performance, as well as increase K^+ reuptake during recovery, suggesting an increase in muscle NKA activity (Sostaric *et al.*, 2006). However, the effects of $NaHCO_3$ supplementation on skeletal muscle NKA following acute exercise are unknown. Exercise training has previously been shown to up-regulate NKA α_2 protein expression in muscle (Bangsbo *et al.*, 2009; Thomassen *et al.*, 2010) but the effects of chronic sodium bicarbonate supplementation during training on skeletal muscle NKA protein expression are also unknown and are explored here.

Studies in animal muscles have reported NKA isoforms to be located in both the sarcolemmal and t-tubular systems of skeletal muscle cells (Fambrough & Bayne, 1983; Juel *et al.*, 2001; Williams *et al.*, 2001; Summa *et al.*, 2004; Kristensen *et al.*, 2008). However their cellular location in human muscle is largely unknown. Analysis of the NKA isoform abundance in red gastrocnemius muscle in rats demonstrated highest NKA α_1 and β_1 in type I fibres, similar α_2 in the different fibre types and strongest β_2 labelling in type IIB fibres (Zhang *et al.*, 2006). The localisation of NKA isoforms in human skeletal muscle is addressed with the third study of this thesis which adapted the

technique of immunofluorescence microscopy to conduct a semi-quantitative analysis of the NKA isoforms in type I and type II fibres in human skeletal muscle, comparing sarcolemmal and intracellular localisations and fibre-type differences.

CHAPTER 2. Review of Literature

SECTION I: Muscle contraction, ionic regulation and fatigue

This literature review is divided into three sections. Section I briefly describes the events involved in muscular contraction, sodium and potassium transport within the muscle cell, and muscular fatigue. Section II discusses the Na^+, K^+ -ATPase ion transport protein in skeletal muscle, whilst Section III details the specific aims and hypotheses of studies within the thesis.

2.1 Skeletal muscle structure and function

Skeletal muscle fibres are grouped into bundles of 10-20 fibres called fascicles. Each fibre within the fascicle is surrounded by a delicate membrane of connective tissue called the endomysium, while the fascicle itself is surrounded by a thicker layer of connective tissue called the perimysium. Thin-section microscopic studies of the surface of a muscle fibre demonstrate that it is composed of three major components: the endomysial fibrous network, the basal lamina and the plasmalemma (sarcolemma) (Fig. 2.1) (Mauro & Adams, 1961).

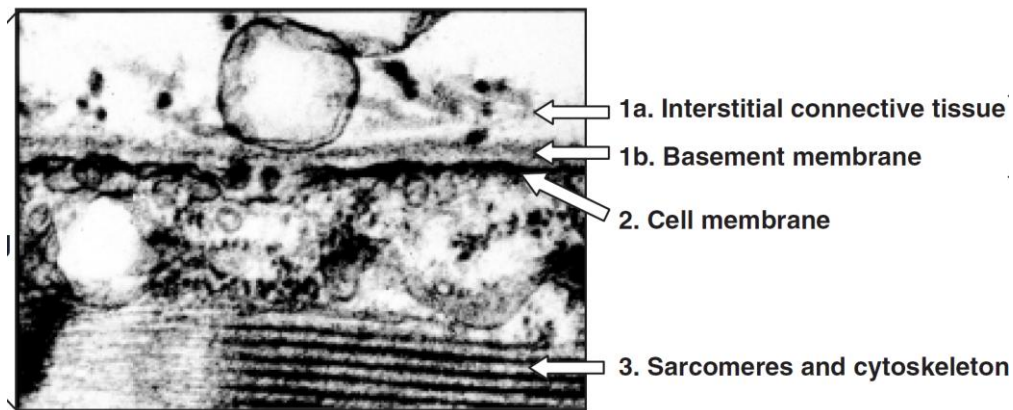


Figure 2.1 Electron micrograph of the extracellular matrix/muscle interface illustrating the basement membrane. (1b) in close association with the cell membrane/sarcolemma (2) and the cytoplasm where the cytoskeleton and contractile proteins (3) are located (Grounds *et al.*, 2005).

Enclosed within the sarcolemma is the sarcoplasm (cytoplasm), which surrounds the sarcoplasmic reticulum (SR) and contractile proteins. The transverse tubules (t-tubules) extend inward from the sarcolemma and pass completely through the muscle fibre in an extremely complex branched network (Fig. 2.2).

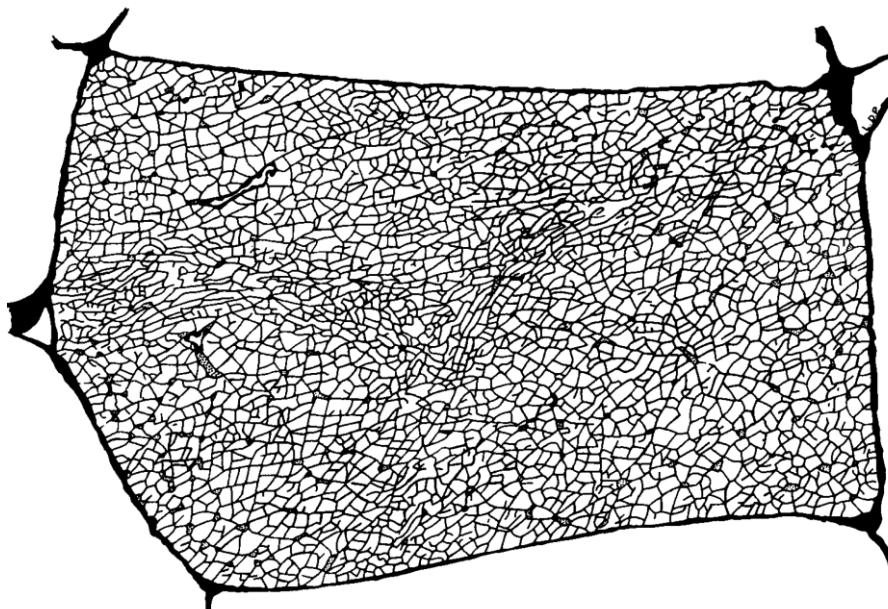


Figure 2.2 Cross-section of a single muscle fibre showing the vastly complex t-tubule network in a frog Sartorius muscle fibre (Peachey & Eisenberg, 1978).

Muscle fibre types can be classified according to differences in their structural and functional properties. Actin and myosin are the major contractile proteins in muscle fibres, with myosin made up of two heavy chains (MHC) and four light chains, are the major determinants of the force velocity properties of the muscle fibre (Liu *et al.*, 2002). A common method of fibre type classification is based on specific profiles of the myosin proteins, particularly the MHC composition (Pette & Staron, 2000). Analyses using various methodological approaches including myofibrillar ATP histochemistry, immunohistochemistry with antibodies specific to MHC isoforms, and electrophoretic analysis in microdissected single fibres, have revealed the existence of muscle fibres that contain either a single MHC isoform (“pure fibre type”) or two or more MHC isoforms (“hybrid fibre types”), with the pure fibre types categorized as slow type I, and three fast types, type IIA, type IID (considered equivalent to type IIX), and type IIB (Pette & Staron, 2000).

The contractile apparatus comprises a parallel arrangement of overlapping myosin and actin filaments. Elevation of the myoplasmic $[Ca^{2+}]$ allows strong and rapid cyclic interactions to occur between the myosin cross-bridges and actin, resulting in force development. Muscle relaxation is enabled through Ca^{2+} being re-sequestered into the SR Ca^{2+} ATPase, which acts as a Ca^{2+} -pump, restoring the myoplasmic $[Ca^{2+}]$ to resting levels (Stephenson *et al.*, 1998). Excitation-contraction coupling is thought to follow the same sequence of events in all mammalian skeletal muscle (Fig 2.3) (Stephenson *et al.*, 1998).

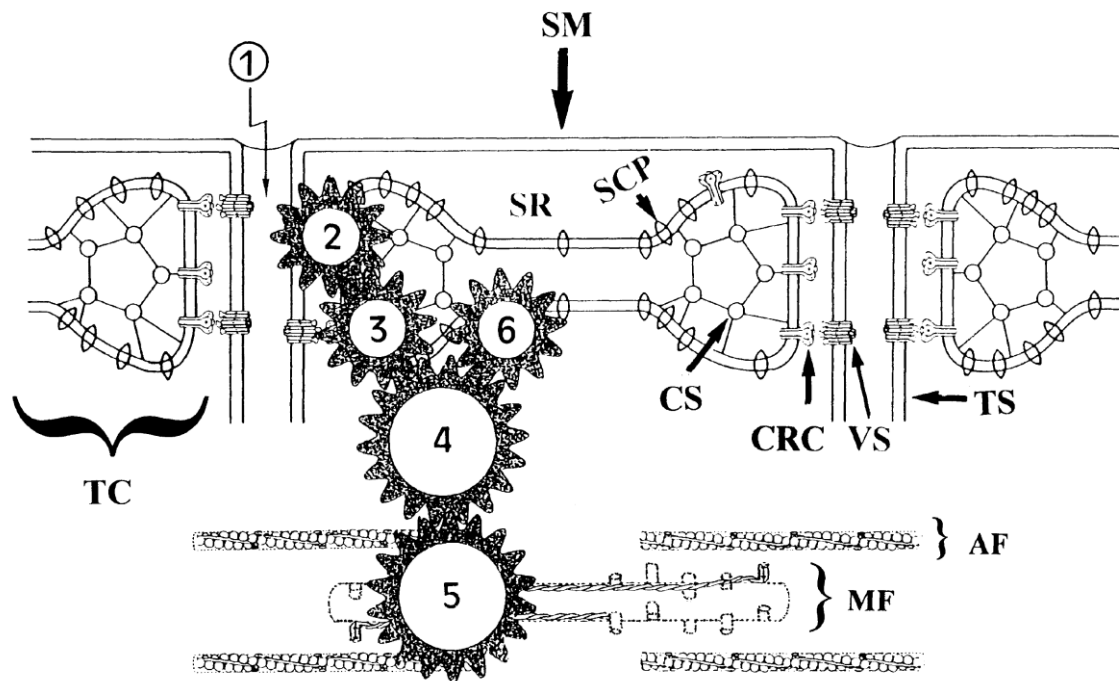


Figure 2.3 Sequence of events in the excitation-contraction-relaxation cycle and of the major subcellular components in a skeletal muscle fibre. (1) Initiation and propagation of an action potential along the sarcolemma (SM) and the transverse tubular system (TS); (2) detection of the TS depolarization signal and signal transmission from the TS to the sarcoplasmic reticulum (SR) membrane; (3) Ca^{2+} release from the SR via SR Ca^{2+} release channel (CRC); (4) rise of myoplasmic $[\text{Ca}^{2+}]$; (5) activation of the Ca^{2+} regulatory system and the contractile apparatus (MF, myosin filament; AF, actin filament); (6) Ca^{2+} reuptake by the SR Ca^{2+} pump (SCP) and Ca^{2+} binding to myoplasmic sites. TC, SR terminal cisternae; CS, calsequestrin; VS, voltage sensors in the transverse tubular membrane (Stephenson et al., 1998).

The release of acetylcholine from the terminal of the motor nerve causes depolarisation at the motor end plate at the neuromuscular junction, which causes generation and propagation of the action potentials along the sarcolemma and into the t-tubule system, decreasing the membrane potential (E_m) from its resting value of approximately -90 mV to close to +20 mV (Cunningham *et al.*, 1971; Sjøgaard *et al.*, 1985; Fitts & Balog, 1996). As the action potential spreads throughout the t-tubules, the depolarisation wave is sensed by the dihydropyridine receptors (DHPR), which are regularly arranged in groups of four, called tetrads and are located in the junctional region of the t-tubule system with the SR terminal cisternae, with alternating tetrads opposing the SR

(Stephenson *et al.*, 1998; Di Biase & Franzini-Armstrong, 2005). The action potential results in a mechanical interaction between the DHPR and the SR Ca^{2+} release channel, known as the ryanodine receptor (RyR) and Ca^{2+} release is induced. This results in an increased myoplasmic $[\text{Ca}^{2+}]$, as fully discussed by Stephenson *et al.* (1998).

2.2 Muscle ion regulation during membrane excitation

Intense exercise results in a marked elevation of glycolytic metabolism and ATP utilisation leading to considerable metabolic and ionic disturbances in contracting skeletal muscle. This is characterised by a rapid onset and pronounced degree of fatigue, which is evidenced by a decline in power output (Lindinger *et al.*, 1992; McKenna *et al.*, 1993; McKenna *et al.*, 1997; Harmer *et al.*, 2000). Movements of inorganic and organic ions (Na^+ , K^+ , Cl^- , Lac^-) across the plasma membrane, in combination with fluid shifts, contribute to changes in extracellular and intracellular ion concentrations (Lindinger *et al.*, 1992). There is a loss of K^+ from exercising muscle, and a concurrent gain of Na^+ , Cl^- , Ca^{2+} and water, whilst H^+ becomes elevated in both the muscle and interstitial fluid and in plasma (Cairns & Lindinger, 2008). The magnitude of these ionic shifts are dependent upon the intensity of exercise and the size of the muscle groups involved (Cairns & Lindinger, 2008).

2.2.1 Membrane potential

The transmembranous electrochemical charge known as resting membrane potential (resting E_m) is influenced by Cl^- , Na^+ and K^+ ions, with the major influence coming from K^+ due to its high conductance (Hodgkin & Huxley, 1952; Cunningham *et al.*, 1971). In the anterior tibialis muscle in resting humans, E_m is approximately -90 mV (Cunningham *et al.*, 1971; Sjøgaard *et al.*, 1985; Fitts & Balog, 1996). The action potential generation

comprises an initial E_m increase to approximately -50 mV, facilitating the opening of Na^+ channels, resulting in further depolarisation of the membrane, and with E_m peaking at approximately +20 to +35 mV during the action potential overshoot (Balog *et al.*, 1994). The return to resting E_m occurs through the rapid inactivation of the Na^+ channels, and the opening of the voltage-sensitive K^+ channels (Sejersted & Sjøgaard, 2000) leading to an increase in K^+ permeability and resultant K^+ efflux (Balog *et al.*, 1994). Therefore, the successful propagation of an action potential depends upon the maintenance of steep chemical gradients for both Na^+ and K^+ as well as active Na^+/K^+ transport (Sjøgaard *et al.*, 1985; Fitts & Balog, 1996).

2.2.2 K^+ Concentrations and fluxes with exercise

At rest, intracellular $[\text{K}^+]$ ($[\text{K}^+]_i$) in skeletal muscle is $\sim 168 \text{ mmol.L}^{-1}$, while extracellular $[\text{K}^+]$ ($[\text{K}^+]_o$) is $\sim 4.5 \text{ mmol.L}^{-1}$ (Sjøgaard *et al.*, 1985). This $[\text{K}^+]_o$ is closely related to plasma $[\text{K}^+]$ which is kept within the narrow limits of $3.5 - 5.5 \text{ mmol.L}^{-1}$ (Sejersted & Sjøgaard, 2000; Kristensen & Juel, 2010). Although the kidneys are responsible for long-term K^+ regulation, it is extra-renal tissues such as skeletal muscle which contains the largest pool of exchangeable K^+ , and probably plays the most important role in the acute control of plasma $[\text{K}^+]$ (Lindinger & Sjøgaard, 1991; Sejersted & Sjøgaard, 2000). Each action potential results in a small efflux of K^+ from the cell via voltage-dependent K^+ channels (Sejersted & Sjøgaard, 2000); during high-intensity dynamic exercise this can result in a doubling or more of the $[\text{K}^+]_o$ as measured via microdialysis probes inserted into the vastus lateralis (Juel *et al.*, 2000b). Hence studies have demonstrated increases in plasma $[\text{K}^+]$ from approximately 4 mmol.L^{-1} at rest up to $7-8 \text{ mmol.L}^{-1}$ during intense exercise (Kowalchuk *et al.*, 1988a; Vollestad & Sejersted, 1988; Lindinger *et al.*, 1992; McKenna *et al.*, 1997). Mathematical modelling of electrical stimulation of

surface fibres of the EDL muscle of rats demonstrated that $[K^+]$ in the innermost t-tubules reached approximately 8 mmol.L^{-1} when stimulated at 6 Hz and 13 mmol.L^{-1} when stimulated at 30 Hz (Fig 2.4) (Fraser *et al.*, 2011).

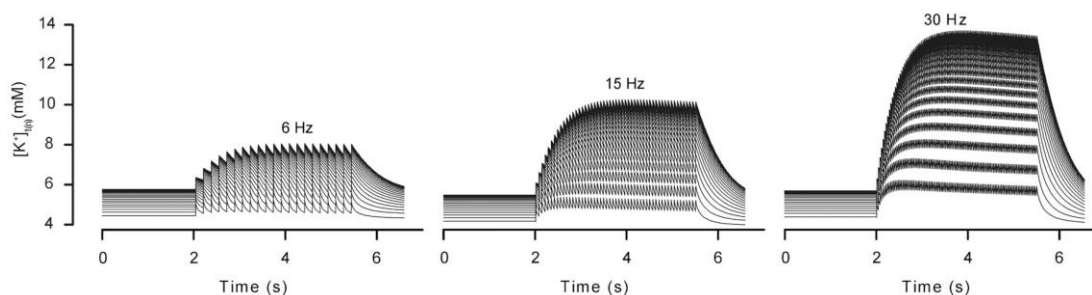


Figure 2.4 Trains of action potentials show K^+ build-up in the t-system that was greatest in the innermost t-system shell (uppermost traces), and least in the outermost shell (lowest traces) (Fraser *et al.*, 2011).

In-vitro studies have demonstrated that increasing the $[K^+]_o$ to $10\text{-}12 \text{ mmol.L}^{-1}$ leads to a $10\text{-}20 \text{ mV}$ depolarization of the muscle fibre, resulting in a corresponding reduction of force development (Cairns *et al.*, 1997; Nielsen *et al.*, 2001). Studies in isolated rat soleus muscle demonstrated that a $[K^+]$ of 10 mmol.L^{-1} reduced twitch and tetanic force by 40%, whilst $[K^+]$ of 12.5 mmol.L^{-1} resulted in a 95% reduction of tetanic force (Clausen *et al.*, 1993). In isolated mouse soleus muscle, an increase in $[K^+]_o$ to 10 mmol.L^{-1} resulted in a 40% reduction in tetanic (Juel, 1988). In frog sartorius muscle, an increase in $[K^+]_o$ from 3 to 7 mmol.L^{-1} resulted in a 41% decrease in tetanic force production (Bouclin *et al.*, 1995). These findings have supported the hypothesis that elevated extracellular K^+ , and imbalances in its regulation, may play an important role in muscular fatigue (Fig 2.6).

However, while elevated $[K^+]_o$ in skeletal muscle has been linked with the development of fatigue, experiments on isolated muscles have shown that when force is depressed due to high $[K^+]_o$, acidification by lactic acid produced a pronounced recovery of force, and

therefore may actually protect against fatigue (Nielsen *et al.*, 2001; de Paoli *et al.*, 2007). Chloride (Cl^-) exerts a protective effect against the depolarising effect of K^+ accumulation via the relatively high Cl^- permeability of the t-tubule membrane, meaning that the membrane potential is strongly biased towards the Cl^- equilibrium potential, thereby maintaining excitability and force responses (Cairns *et al.*, 2004; Dutka *et al.*, 2008). However, this relationship between acidosis, K^+ homeostasis and muscle function in humans is still not completely understood.

The main mechanisms regulating $[\text{K}^+]$ during and following exercise are K^+ release by contracting cells, distribution in the muscle interstitium and other extracellular spaces, rates of reuptake by contracting muscle and uptake by non-contracting tissues, including inactive skeletal muscle and clearance by increases in muscle blood flow (Lindinger & Sjøgaard, 1991). Several studies have demonstrated that inactive muscles play an active role in the regulation of $[\text{K}^+]$, $[\text{Na}^+]$ and lactate both during and following intense leg exercise (Kowalchuk *et al.*, 1988a; Lindinger *et al.*, 1990a). Upon cessation of exercise, the combination of rapid muscular reuptake of K^+ and an initial high post-exercise blood flow as a result of high cardiac output (through increased heart rate), results in a rapid decrease of plasma $[\text{K}^+]$ to or below resting levels (Lindinger & Sjøgaard, 1991; Lindinger *et al.*, 1992).

2.2.2.1 Insulin effects on plasma $[\text{K}^+]$

The polypeptide hormone insulin modulates plasma $[\text{K}^+]$ through its effect on the NKA, which is discussed further in Section II. The rise in plasma [insulin] following a standard glucose load produces hypokalaemia (Natali *et al.*, 1993). It was also demonstrated long ago that physiological concentrations of insulin stimulated K^+ uptake by skeletal muscle in the human forearm (Zierler & Rabinowitz, 1964). Several studies have used insulin

infusion to induce hyperinsulinaemia, and demonstrated a dose-related decrease in plasma $[K^+]$, which was progressive over time (Fig. 2.5) (DeFronzo *et al.*, 1980). Local hyperinsulinaemia in the perfused forearm resulted in a net uptake of K^+ which was suppressed by the cardiac glycoside ouabain, independent of glucose uptake (Ferrannini *et al.*, 1988).

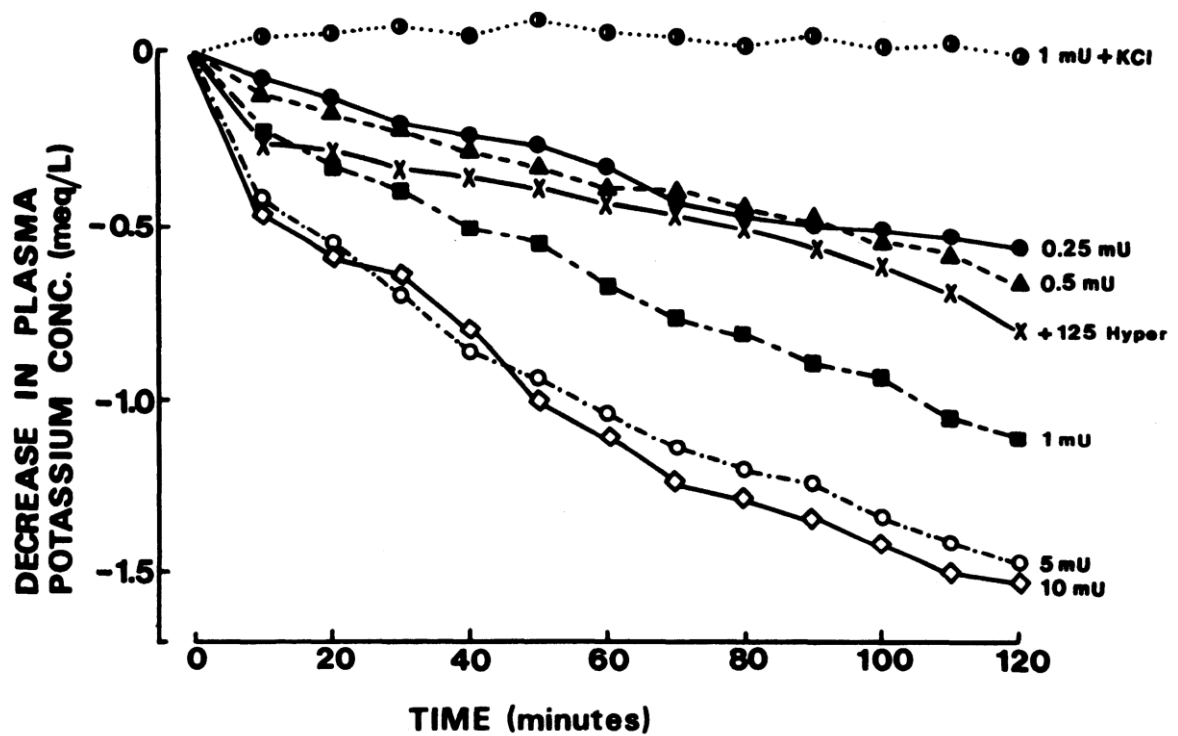


Figure 2.5 Time related decrease in plasma $[K^+]$ during hyperglycaemic clamp (+125 hyper) and euglycaemic insulin clamp studies of varying insulin concentrations ($mU.kg^{-1}.min^{-1}$) (DeFronzo *et al.*, 1980).

In order to understand the causes of K^+ imbalance during exercise, it is necessary to investigate which K^+ -transporting proteins are present in skeletal muscle (Kristensen & Juel, 2010) and the mechanisms involved in K^+ regulation. Chapter 3 investigates the effects of glucose-induced increases in endogenous insulin on K^+ homeostasis and NKA protein expression.

2.2.2.2 Sodium bicarbonate effects on plasma [K⁺]

Ingestion of sodium bicarbonate (NaHCO₃) also affects K⁺ homeostasis, probably via an induced metabolic alkalosis (Stephens *et al.*, 2002). NaHCO₃ ingestion (0.3 g.kg⁻¹) resulted in a lowering of arterial and venous [K⁺] during finger flexion exercise and a greater reuptake of K⁺ into muscle at fatigue and during recovery (Sostaric *et al.*, 2006). However, ingestion of 3.5 mmol.kg⁻¹ (0.21 g.kg⁻¹) did not alter plasma [K⁺] in the 3.5 hrs rest following ingestion (Lindinger *et al.*, 2000). Ingestion of NaHCO₃ has also been shown to improve repeat sprint performance (Bishop *et al.*, 2004); however, the mechanisms involved are still unclear.

2.2.3 Na⁺ concentrations and fluxes with exercise

In human skeletal muscle at rest, [Na⁺]_i is approximately 6 mmol.L⁻¹, while [Na⁺]_o was calculated at ~135 mmol.L⁻¹ after measurement of total body water, extracellular and intracellular fluid volume (Sjøgaard *et al.*, 1985). The initial phase of an action potential is due to the opening of voltage-gated Na⁺ channels, allowing an influx of Na⁺ and depolarisation of the plasma membrane (Stephenson *et al.*, 1998), hence excitation is associated with an initial cellular Na⁺ influx (Fig 2.6).

Electrical stimulation of frog semitendinosus at 150 Hz, with one stimulus per second for 5 min increased muscle [Na⁺]_i from 16 to 49 mmol.L⁻¹ (Balog & Fitts, 1996). In isolated mouse soleus and EDL muscle, reducing the [Na⁺]_o by half, which reduces the [Na⁺]_o/[Na⁺]_i ratio by half and is equivalent to a doubling the [Na⁺]_i, there was a fall in peak tetanic force by 10-15% (Cairns *et al.*, 2003). However, this needs to be considered in the context of the potential benefit of raised [Na⁺]_i also stimulating the NKA (Clausen, 2003). While a rather large reduction in the Na⁺ gradient causes a reduction in force production, in muscles also exposed to elevated [K⁺]_o, only a small reduction in the Na⁺

gradient can reduce muscle excitability substantially (Bouclin *et al.*, 1995; Overgaard *et al.*, 1997). Therefore it is likely that the synergistic combination of effects of both Na⁺ influx and K⁺ efflux have an important adverse effects on muscle contractility (Overgaard *et al.*, 1997; Overgaard *et al.*, 1999). This makes the activity of the NKA vital in maintenance of cellular excitability for optimal functioning.

2.2.4 Lactate and hydrogen ions

Lactic acid accumulation and the resultant decrease in pH have long been considered major factors in fatigue (Cairns & Lindinger, 2008). This has primarily been based on the large body of research demonstrating a correlation between reduced pH_i and lactate accumulation and fatigue development (Nielsen & de Paoli, 2007). *In-vitro* experiments in skinned rat muscle fibres have demonstrated acidosis depression of Ca²⁺ sensitivity and peak force (Nelson & Fitts, 2014). However, reduced excitability in high K⁺-depressed muscle demonstrated a pronounced recovery of force and muscle excitability following the addition of 20 mmol.L⁻¹ lactate (Nielsen *et al.*, 2001). This restorative effect of acidosis has been reproduced several times (Pedersen *et al.*, 2004; Kristensen *et al.*, 2005; Pedersen *et al.*, 2005) and demonstrates that although acidosis does not abolish the depressive effects of K⁺, it does shift the peak tetanic force-membrane potential relationship in resting muscle rightwards towards a more depolarised E_m, so that muscles can withstand a 2-3 mmol.L⁻¹ higher [K⁺]_o (Cairns & Lindinger, 2008). Therefore it is suggested that acidification counteracts the depressing effects of elevated [K⁺]_o, and rather than causing fatigue, may actually protect against it (Nielsen *et al.*, 2001). The mechanism for the effect of acidification on the excitability of muscle cells is related to an improved balance between excitatory Na⁺ currents and the inhibitory K⁺ and Cl⁻ currents in K⁺ depressed muscles (Nielsen & de Paoli, 2007). The effect has been

attributed to a decrease in Cl^- channel conductance, rather than to an increase in NKA activity (de Paoli *et al.*, 2007).

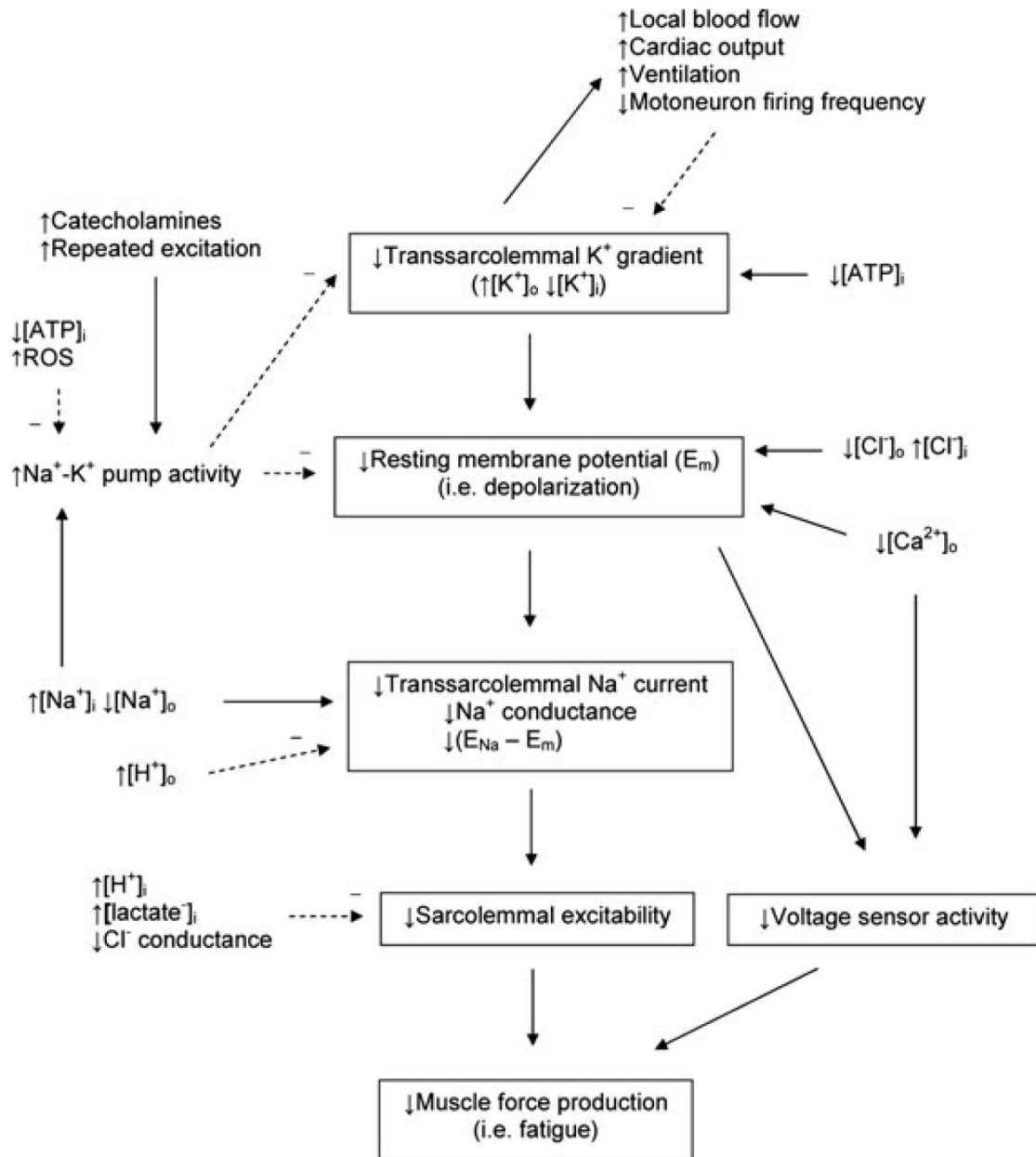


Figure 2.6 Potential integrated physiological mechanisms by which ion-ion interactions, ion-metabolite interactions and catecholamines influence muscle force production during fatiguing exercise such as a decline of $[\text{ATP}]_i$, muscle glycogen depletion or glucose depletion and/or elevation of ROS may all contribute to fatigue by exacerbating the effects of a diminished K^+ gradient (Cairns & Lindinger, 2008). Continuous lines with arrow indicate support for the subsequent process. Dashed lines with arrow indicate resistance to the following process.

2.2.5 Muscle water content and exercise

The human body is composed of approximately 50-60% water, which corresponds to 70% of lean body mass being water (Sejersted & Sjøgaard, 2000). During exercise there is a shift of water from blood into contracting muscles. This occurs as a result of complex mechanisms which include, but are not limited to, increased capillary hydrostatic pressure and increased capillary openings, causing a net flux of fluid from the plasma into the interstitial space, where exchanges between the intra- and extravascular compartments take place and increase interstitial oncotic pressure (Harrison, 1985; Sejersted & Sjøgaard, 2000). This increased osmolality is driven by an accumulation of lactate and K^+ ions in the interstitial space (Juel *et al.*, 2004). This initial uptake of fluid by the muscle cells leads to a rapid decline of plasma volume (McKenna *et al.*, 1997) resulting in increased haematocrit (Hct) and an increased net haemoconcentration effect on all extracellular and plasma ions and a corresponding decrease in the concentration of all intracellular ions (Sjøgaard, 1983; Sjøgaard *et al.*, 1985; Lindinger & Heigenhauser, 1988). This increase in total muscle water content can occur within seconds of muscle stimulation (Sjøgaard *et al.*, 1985; Lindinger & Heigenhauser, 1988), without any change in total body water content (Harrison, 1985). These changes are intensity- and duration-specific, with increases in muscle water content of ~21% seen during high-intensity cycling at 100% VO_{2peak} , compared to changes of only ~10% during exercise at 50-70% VO_{2peak} (Sjøgaard *et al.*, 1985). Experiments in isolated mouse EDL and soleus muscle demonstrated impaired cell volume regulatory responses during exposure to increased extracellular osmolarity when incubated with ouabain, this indicated that the activity of the NKA is necessary to maintain inward movement of Na^+ as is Cl^- to maintain activity of the $Na^+-K^+-Cl^-$ cotransporter (Lindinger *et al.*, 2011).

SECTION II: Na⁺,K⁺-ATPase in skeletal muscle

The sodium-potassium adenosine triphosphatase (Na⁺,K⁺-ATPase), also known as the Na⁺,K⁺-pump (NKA), is a protein responsible for the active, coupled transport of Na⁺ and K⁺ ions across the plasma membrane of most eukaryotic cells. In 1997 the Nobel Prize for Chemistry was awarded to Danish researcher Jens Skou, who first identified this enzyme in 1957 (Skou, 1998). While the existence of a “sodium pump” had already been hypothesized, Skou was the first to suggest an association between the transport of Na⁺ and K⁺ across the plasma membrane and an ATPase activity activated by Na⁺ and K⁺ (Skou, 1998).

The NKA belongs to a widely distributed class of P-type ATPases which are responsible for the active transport of various cations across cellular membranes (Blanco & Mercer, 1998). P-type ATPases can be found in both eukaryotic and prokaryotic cells and derive energy from the hydrolysis of the terminal phosphate bond of ATP to drive the transport of cations against the electrochemical gradient (Blanco & Mercer, 1998; Kaplan, 2002). For each ATP molecule hydrolysed, three Na⁺ ions are transported into the cell and two K⁺ ions are transported out of the cell.

2.3 NKA subunits and isoforms

The basic function of the NKA is to maintain high Na⁺ and K⁺ gradients across the plasma membrane of animal cells (Therien & Blostein, 2000). The NKA is especially important in regulating the cytoplasmic [Na⁺], playing important roles in regulating cell volume, maintaining the resting membrane potential in excitable cells, and is also responsible for driving a number of secondary transport processes such as Na⁺-dependent glucose and amino acid transport (Therien & Blostein, 2000).

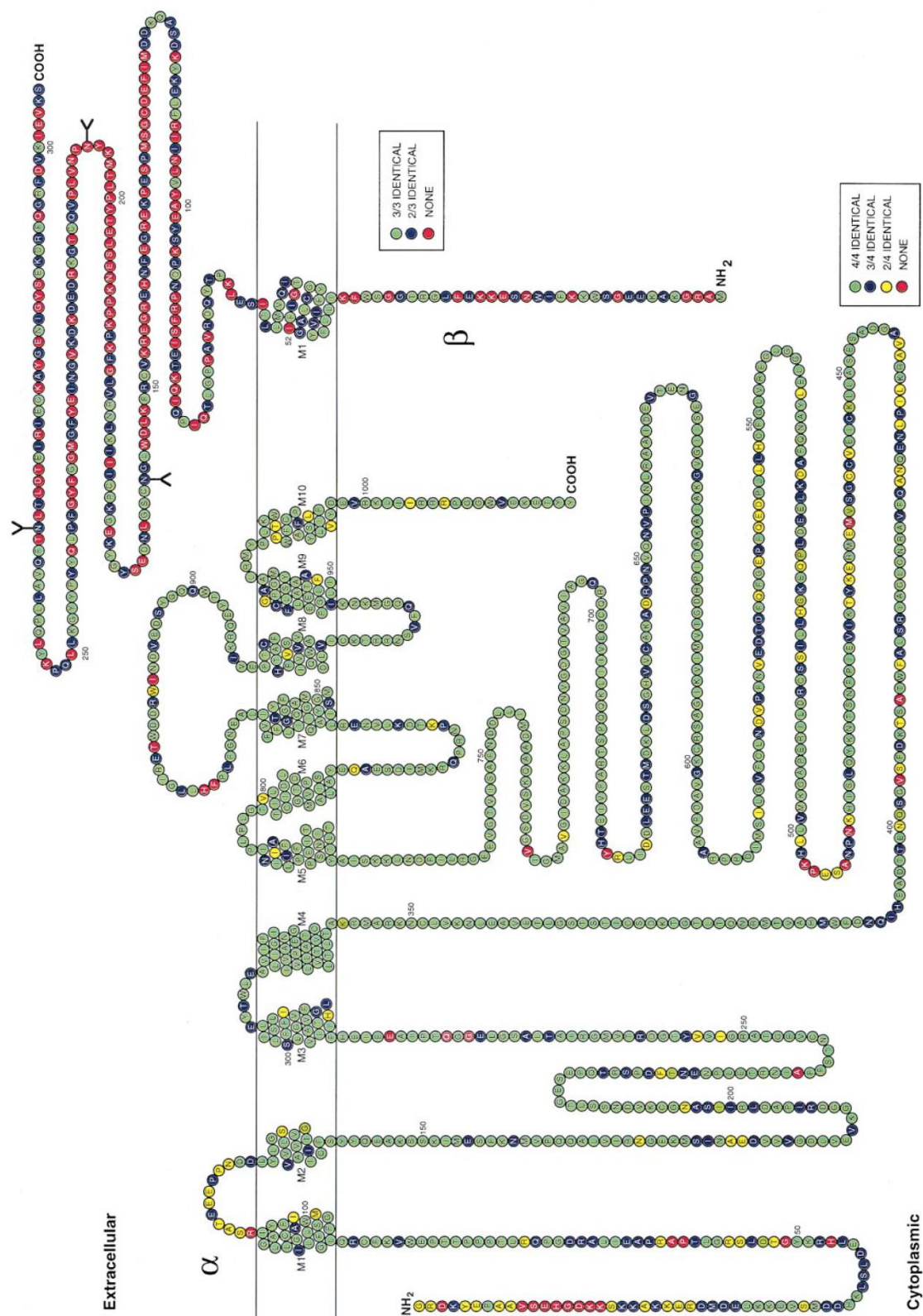


Figure 2.7 Membrane topology of the α - and β -isoforms of the NKA. Sequences of rat α_1 - and β_1 -isoforms are shown. Residues are coloured to indicate the amino acid homology among the different α -isoforms (α_1 , α_2 , α_3 and α_4) or β -isoforms (β_1 , β_2 and β_3) (Blanco & Mercer, 1998).

The NKA is a heterodimeric protein consisting of an alpha (α -) and a beta (β -) subunit, as well as a third, tissue-specific regulatory gamma (γ) subunit (Kaplan, 2002). The catalytic α -subunit is a multi-spanning membrane protein with 5 exposed extracellular loops and 10 transmembrane segments, composed of approximately 1000 amino acids with a molecular mass of approximately 112 kDa (Fig 2.7 and Fig 2.8) (Hu & Kaplan, 2000; Kaplan, 2002). The α -subunit contains the binding sites for Na^+ , K^+ , ATP as well as the specific inhibitor ouabain and transports Na^+ and K^+ across the membrane (Clausen, 2003).

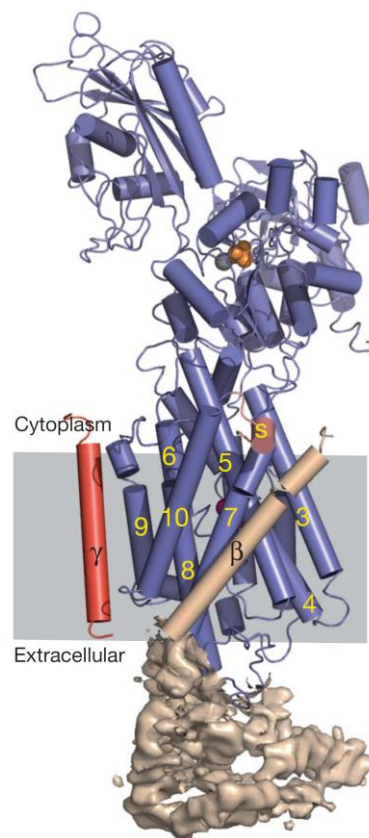


Figure 2.8 Architecture of the NKA $\alpha\beta\gamma$ complex and the K^+/Rb^+ sites. The cytoplasmic side is up. The α -, β - and γ -subunits are coloured blue, wheat and red, respectively. Helices are represented by cylinders and b-strands by arrows. The β -ectodomain is shown by surface representation of the experimental electron density. The transmembrane segments of the α -subunit are numbered (yellow) starting with the most N-terminal. The small C-terminal helix (S, for switch) is light red. Mg^{2+} , MgF_4^{2-} and Rb^+ ions are grey, orange and pink, respectively (Morth *et al.*, 2007).

The β -subunit is a glycoprotein polypeptide consisting of approximately 370 amino acids and it crosses the membrane only once, with its N-terminus in the cytoplasm. There are 3 disulfide bonds and several N-glycosylation sites in the extracellular domain. Depending on the degree of glycosylation in different tissues, it has a molecular weight of between 40 and 60 kDa (Beggah *et al.*, 1997; Blanco & Mercer, 1998; Kaplan, 2002). A third γ protein, called phospholemman (PLM) in skeletal and cardiac muscle, is a small, hydrophobic polypeptide of between 8-14 kDa that consists of between 61-95 amino acids and preferentially associates with $\alpha_1\beta$ -complexes (Mercer *et al.*, 1993; Blanco & Mercer, 1998; Geering *et al.*, 2003; Geering, 2006). The PLM protein belongs to the family of FXYD proteins, which contains seven members, including FXYD1 (PLM). Although not all functions of FXYD proteins are known, it is believed that all FXYD proteins are tissue-specific auxiliary subunits of the NKA, with PLM being specific to skeletal muscle (Geering, 2006).

The NKA is expressed in various isoforms which can be detected using specific antibodies. Four isoforms of the α -subunit have been identified (α_1 - α_4), with α_1 , α_2 and α_3 found in human skeletal muscle (Murphy *et al.*, 2004) and α_4 in rat testes (Blanco & Mercer, 1998). The molecular diversity of the NKA is also evident in the β -subunit with three different isoforms identified (β_1 , β_2 , and β_3) all of which are found in skeletal muscle (Clausen, 2003; Murphy *et al.*, 2004; Green *et al.*, 2007b).

The α isoforms exhibit a tissue-specific pattern of expression, with α_2 being the predominant isoform in skeletal muscle (Hundal *et al.*, 1992; Lavoie *et al.*, 1997). A comparison of the NKA affinities for Na^+ and K^+ found no significant difference in isoform affinities for K^+ ; whereas, α_3 exhibited a lower affinity for intracellular Na^+ compared to α_1 and α_2 (Jewell & Lingrel, 1991). In cells containing mainly α_3 , the $[\text{Na}^+]_i$

appears to be higher (Jewell & Lingrel, 1991; Munzer *et al.*, 1994), while apparent affinity for ATP is slightly higher for α_3 compared to α_1 and α_2 (Jewell & Lingrel, 1991). The functional significance of variations in the proportions of isoforms in various tissues has not yet been clearly identified, but a possible isoform-specific role in muscle contractility has been suggested. The NKA α_1 isoform has been found in nearly all tissues (Sweadner, 1989; Blanco & Mercer, 1998) and this widespread distribution has led to the suggestion that it serves a “housekeeping” role maintaining basal ion gradients (Blanco & Mercer, 1998; Shelly *et al.*, 2004). Studies in gene-targeted mice showed that reductions of the α_2 isoform resulted in increased isometric force, whereas reduced α_1 resulted in reduced force in mouse muscle *in situ* (He *et al.*, 2001). Whereas gene-targeted mice which expressed an ouabain-insensitive α_2 isoform exhibited an enhanced ability to perform physical exercise, as well as an increased ability to transport $^{86}\text{Rb}^+$ during treadmill running compared to wild type mice (Radzyukevich *et al.*, 2009). Studies in NKA α_2 knockout mice, showed a reduced ability to produce force, and an increased susceptibility to fatigue, despite a 2.5-fold increase in the α_1 isoform (Radzyukevich *et al.*, 2013). The NKA α_2 has also been shown to be associated with the regulation of Ca^{2+} homeostasis in cardiomyocytes where specific inhibition of the α_2 isoform caused slowing of Ca^{2+} extrusion by the $\text{Na}^+/\text{Ca}^{2+}$ -exchanger (Swift *et al.*, 2010). These results suggest that the NKA α_2 isoform is crucial for optimal cellular functioning, and therefore also exercise performance.

While all the β subunits are glycosylated, the number of glycosylations varies with each isoform (Chow & Forte, 1995; Blanco & Mercer, 1998). The β subunit is necessary for the transfer of the entire enzyme from its location of synthesis in the endoplasmic reticulum to its site of insertion in the plasma membrane (Renaud *et al.*, 1991), as well as

stabilisation and maturation of the NKA (Chow & Forte, 1995). Studies on xenopus oocytes have demonstrated that the prevention of the formation of only one of the disulfide bonds of the β subunits was sufficient to abolish its ability to correctly assemble with an α subunit, which consequently led to an impedance of the maturation and expression of functional pumps (Beggah *et al.*, 1997). Studies in MDCK cells reported that normal glycosylation of the β_1 isoform was essential for the stable association of the NKA for the adherens junctions, and played an important roles in cell-cell adhesion (Vagin *et al.*, 2006). The β subunit is also essential for the normal functioning of the NKA as it appears to be involved in the regulation of Na^+ and K^+ affinity of the enzyme and regulating the enzymatic activity levels (Blanco & Mercer, 1998).

Phospholemman is mainly expressed in the heart, liver and in skeletal muscle where it is believed to play roles in both muscle contractility and cell volume regulation (Geering, 2006). PLM interacts specifically with the $\alpha_1\beta$ -isozymes where it decreases the apparent Na^+ affinity, and to a lesser extent the K^+ affinity of the NKA. PLM was originally discovered as a major substrate for protein kinase A and C accompanying α - and β -adrenergic stimulation of the heart (Presti *et al.*, 1985a; Presti *et al.*, 1985b) and isolated membranes from ischemic rat hearts have been found to be strongly stimulated in association of PKA and PKC and phosphorylation of PLM (Fuller *et al.*, 2004). It has also been demonstrated that the phosphorylation of PLM is required for the translocation of PLM from the endoplasmic reticulum to the plasma membrane in mammalian cells (Lansbery *et al.*, 2006).

2.4 Location

In skeletal muscle cells the NKA has been found to be located in both the sarcolemma and t-tubule systems, as determined via numerous studies using varied techniques such as

sarcolemmal giant vesicles (Juel *et al.*, 2001), isolated membrane preparations, differential centrifugation of whole muscle homogenates and immunofluorescence labelling of cultured chicken myotubes (Fambrough & Bayne, 1983), rat EDL and mouse tibialis anterior (Williams *et al.*, 2001). T-tubules isolated from rabbit skeletal muscle have been found to accumulate Na⁺ via an ATP-dependent, K⁺-sensitive and digitoxin-suppressible process, thus implicating NKA (Lau *et al.*, 1979). Early analysis utilising the [³H]ouabain binding technique in glycerol-treated muscle found 80% of the skeletal muscle NKA to be located in the sarcolemma and the remaining 20% located in the t-tubules (Venosa & Horowicz, 1981). However, the use of glycerol pre-treatment is unlikely to cause complete disruption of the t-tubular connections to the sarcolemma, resulting in a large underestimate of the density of pumps in the t-tubules (Clausen, 2003). Analysis of frog sartorius muscle [³H]ouabain found the binding capacity of NKA in the t-tubules to be 215pmol.mg protein⁻¹ compared to 163pmol.mg protein⁻¹ in the sarcolemma (Jaimovich *et al.*, 1986). Additionally, through the use of a monoclonal antibody and immunofluorescent staining, NKA have also been detected in the t-tubules of chicken skeletal muscle (Fambrough & Bayne, 1983).

2.4.1 NKA isoform specific location

Numerous studies analysing the location of the NKA in skeletal muscle have focused on the isolation and purification of the enzyme through the process of subcellular fractionation (Hundal *et al.*, 1994; Dombrowski *et al.*, 1996; Rasmussen *et al.*, 2008). Studies have utilised this method to demonstrate that exercise results in large increases in the relative amount of α_2 in the outer-membrane-enriched fraction (Kristensen *et al.*, 2008). In rat kidney proximal convoluted tubules, NKA activation via the protein kinase A pathway resulted in a 40% increase in cell-surface NKA protein expression, which

occurred in conjunction with a 30% decrease in subcellular fraction NKA protein expression (Carranza *et al.*, 1998). In cultured rat skeletal muscle cells, cyclic stretch also increased α_1 and α_2 isoform protein expression in plasma membrane fractions with a concurrent decrease in endosomal fractions (Yuan *et al.*, 2006). This has resulted in the suggestion of translocation of the NKA protein between the plasma membrane and intracellular stores in response to various stimuli including exercise (Juel *et al.*, 2000a) and insulin (Hundal *et al.*, 1992; Lavoie *et al.*, 1996). Translocation of NKA isoforms to the plasma membrane has also been found in rat hindlimb muscle with 30-60% increases in plasma membrane abundance of α_1 and α_2 isoforms following 1 hr of treadmill running (Tsakiridis *et al.*, 1996) and 5 min of electrical stimulation of isolated soleus (Juel *et al.*, 2001). However, due to the loss of protein when separating the plasma membrane from other cell structures, the recovery of the NKA is usually quite low, with recovery values ranging from 0.2-8.9% (Clausen, 1986). This makes it very difficult to ascertain whether the sample measured is an accurate representation of the total population of the NKA (Clausen, 1986).

Other researchers have utilised the technique of immunofluorescence microscopy on skeletal muscle cross-sections, and have demonstrated in rat EDL muscle that the α_2 isoform revealed a distinctive reticular pattern in the sarcoplasm, that co-labelled with the DHPR, consistent with the presence of the NKA α_2 isoform in t-tubules (Fig. 2.9). However, immunolabelling of the α_1 isoform did not show significant intracellular labelling and gave no overlap with DHPR (Williams *et al.*, 2001). The immunofluorescence labelled longitudinal sections of rat EDL demonstrated that the distribution of the NKA α and α_2 isoforms was nearly identical to β -spectrin, indicating localisation in costameres (Williams *et al.*, 2001).

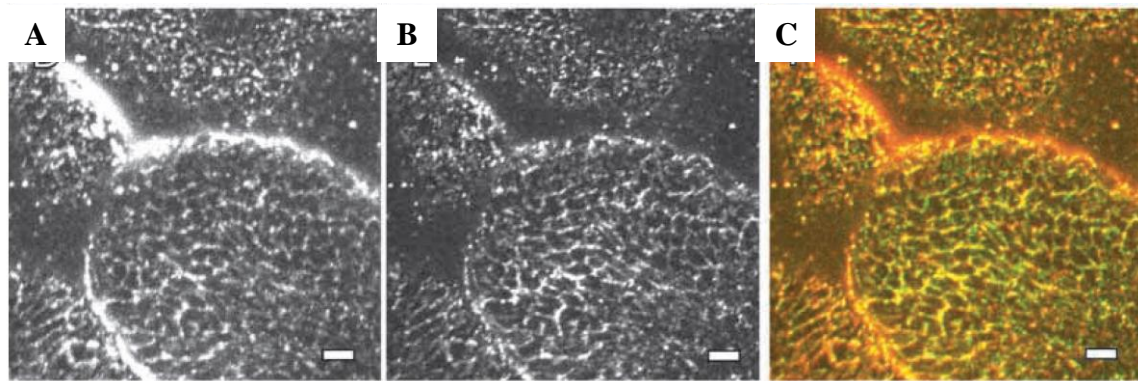


Figure 2.9 Subcellular localisation of NKA α_2 in rat EDL. Cross sections are labelled for NKA α_2 (A); DHPR (B). The composite image (C) show NKA α_2 in red, DHPR in green and structures containing both structures in yellow (Williams *et al.*, 2001).

Immunolabelling of the NKA isoforms in red and white gastrocnemius muscle of the rat showed fibre-type specific distribution patterns, with fluorescence from α_1 and α_2 isoforms evenly distributed among the fibres of white gastrocnemius and red gastrocnemius, with the exception of higher α_1 levels in slow-twitch oxidative type I fibres of red gastrocnemius (Zhang *et al.*, 2006). In contrast, labelling for the β_1 and β_2 isoforms in mostly oxidative and mostly glycolytic fibres, respectively, was almost mutually exclusive (Zhang *et al.*, 2006). Studies in the guinea pig heart have demonstrated that the α_1 isoform is distributed uniformly in the sarcolemma and t-tubules, whereas in the rat heart, the α_1 isoform labelled the t-tubules more intensively, while the α_2 and β_1 isoforms were evenly distributed throughout the t-tubules and sarcolemma (McDonough *et al.*, 1996). In contrast to this, other research in guinea pig ventricular myocytes has found that α_2 was mainly located in the t-tubules and α_1 was predominantly expressed on the sarcolemma (Silverman *et al.*, 2005). In one study that examined NKA location in human skeletal muscle, using the open biopsy technique, it was observed in soleus cross-sections that the α_2 isoform was predominantly located in

the sarcolemma but also diffusely dispersed throughout the intracellular region, while α_1 was detected largely in the plasma membrane (Hundal *et al.*, 1994). However all these studies have been of a qualitative nature, and did not report differences between regions examined. This is examined in chapter 5, where the density of NKA isoform fluorescence is calculated for both type I and type II fibres, within the plasma membrane and intracellular region and abundance compared.

2.5 Quantification of NKA in skeletal muscle

2.5.1 Measurement of NKA content

Studies using purified NKA demonstrate that cardiac glycosides bind to the α -subunit with a 1:1 stoichiometry and this has become the basis for the widespread use of [3 H]ouabain for the quantification of NKA content in tissues, cells and isolated membrane preparations (Clausen, 2003). The initial rate of [3 H]ouabain binding can be measured by exposing muscle to [3 H]ouabain, with vanadate (VO_4) used to facilitate this process by binding to the phosphorylation site of the NKA on the intracellular surface of the plasma membrane. The high-affinity binding of VO_4 maintains the NKA in a configuration capable of binding [3 H]ouabain to the extracellular surface of the molecule (Clausen, 2003). Therefore the VO_4 -facilitated assay for [3 H]ouabain binding has been widely used for measurement of NKA content (in pmol.g.ww^{-1}) on human muscle biopsy specimens from the vastus lateralis muscle (Norgaard *et al.*, 1984; McKenna *et al.*, 1993; Green *et al.*, 2004; Aughey *et al.*, 2005; Petersen *et al.*, 2005; Murphy *et al.*, 2007) with values typically ranging from 300-400 pmol.g.ww^{-1} in human skeletal muscle.

2.5.2 Measurement of NKA *in-vitro* activity

Crude homogenates of skeletal muscle contain large concentrations of various ATPases, of which only a small fraction is specifically activated by Na⁺, K⁺, and Mg²⁺, or suppressed by cardiac glycosides (Clausen, 2003). NKA activity has been measured in crude homogenates by a highly sensitive fluorometric assay using 3-*O*-methylfluorescein (3-*O*-MFPase) as a substrate, and on the basis of the K⁺-stimulated, maximal 3-*O*-MFPase activity the NKA activity has been quantified (Fraser & McKenna, 1998). In biopsies of human vastus lateralis muscle a significant correlation was found between [³H]ouabain binding site content and 3-*O*-MFPase activity (Fraser *et al.*, 2002).

In skeletal muscle the 3-*O*-MFPase activity of muscle homogenates has only reached its optimum levels when deoxycholate was added. This has been attributed to the opening of inside-out vesicles of the sarcolemma, formed during the homogenisation process. Later studies have demonstrated that repeated freeze-thaw cycles produces a similar effect, possibly by opening t-tubules or vesicles (Fowles *et al.*, 2002). It is possible that both these phenomena reflect the opening of t-tubules and that most of the NKA in skeletal muscle therefore resides in the lumens of these structures (Clausen, 2003).

However, this method uses 3-*O*-MFP as an artificial substrate and does not involve the hydrolysis of ATP. It also cannot analyse the Na⁺-dependent activation, and the K⁺ sensitivity obtained may not reflect the sensitivity of the intact ATPase; therefore these ion-induced activity values may not reflect the NKA activity in the intact organism (Juel, 2009). A recent study comparing methods of measuring NKA activity found that the 3-*O*-MFPase activity assay was unable to detect changes in NKA activity and is therefore unsuitable for detecting changes in NKA activity with exercise (Juel *et al.*, 2013).

2.6 Regulation of NKA

Skeletal muscle excitability and contractility rely on the membrane potential and chemical gradients for Na^+ and K^+ . At rest passive Na^+/K^+ fluxes are low, but during muscle contraction both the influx of Na^+ and efflux of K^+ are dramatically increased; if unopposed these would lead to a rapid decrease of the Na^+ and K^+ chemical gradients and depolarisation, leading to a loss of excitability and contractility (Nielsen & Harrison, 1998). Therefore, in order to maintain optimal muscle function, tight control of the Na^+/K^+ exchange is essential, and the NKA is the common target for a wide variety of control mechanisms which determine the Na^+/K^+ distribution and the membrane potential in skeletal muscle (Clausen, 1986). These mechanisms can be broadly categorised as either acute (eg. excitation, insulin and contraction) or chronic (eg. insulin and exercise training) regulators of the NKA

2.6.1 Acute regulation

Many stimuli acutely regulate the NKA, including catecholamines and other hormones and energy depletion/repletion, but the largest single acute stimulus to the activity of the NKA appears to be related to excitation (Clausen, 2003).

2.6.1.1 Excitation

Action potentials comprise a cellular influx of Na^+ and efflux of K^+ , leading to a rapid increase in the concentrations of Na^+ and K^+ in the intracellular and extracellular regions, respectively, as shown in isolated frog muscles (Balog & Fitts, 1996), as well as in human skeletal muscle (Sjøgaard *et al.*, 1985; Juel *et al.*, 2000b). Studies in isolated rat soleus stimulated for 10 s at 60 Hz showed muscle $[\text{Na}^+]_i$ increased by 58%, and in the following rest period, re-extrusion of Na^+ to resting levels was completed in 2 min (Everts & Clausen, 1994), and 5 min of intermittent tetanic contractions in the rat

hindlimb demonstrated a decreased $[K^+]_i$ which was associated with an increased $[Na^+]_i$, $[Cl^-]_i$ and $[La^-]_i$ as well as an increased plasma $[K^+]$ (Lindinger & Heigenhauser, 1988). Electrical stimulation of isolated rat soleus at 120 Hz for 10 s showed no significant changes in the max $[^3H]$ ouabain binding for either EDL or soleus (McKenna *et al.*, 2003) but an almost two-fold increase in ouabain-suppressible $^{86}Rb^+$ uptake (Everts & Clausen, 1994).

2.6.1.2 Insulin

In addition to its vital role in regulating carbohydrate homeostasis (Yki-Jarvinen *et al.*, 1987), insulin plays an important role in Na^+ and K^+ homeostasis (Ewart & Klip, 1995). Insulin increases the NKA activity, as demonstrated via an increase in ouabain-sensitive $^{86}Rb^+$ uptake in cultured adipocytes (Sargeant *et al.*, 1995), rat collecting duct (Feraille *et al.*, 1995) and in isolated rat soleus muscles (McKenna *et al.*, 2003). An early study found that insulin increased both Na^+ efflux and K^+ influx in rat soleus, which were blocked by ouabain (Clausen & Kohn, 1977); these same results have also been demonstrated with insulin-like growth factor I (Dorup & Clausen, 1995). This insulin-NKA activation link is further supported by the results of a euglycaemic-hyperinsulinaemic clamp which showed a ouabain-suppressible increase in $[^{13}C]$ lactate from tibialis anterior dialysate, suggesting an increase in glycolysis as a result of increased NKA activity (Novel-Chate *et al.*, 2001).

Numerous studies have investigated the effects of insulin on NKA, with many finding that insulin increased NKA subunits in the sarcolemma in cultured human skeletal muscle cells (Al-Khalili *et al.*, 2003b), HEK-293 cells (Sweeney *et al.*, 2001), frog skeletal muscle (Omatsu-Kanbe & Kitasato, 1990), rat skeletal muscle (Lavoie *et al.*, 1996) and mouse skeletal muscle (Ramlal *et al.*, 1996). This increase in NKA subunits

in the sarcolemma has been suggested to be the result of translocation of NKA subunits from intracellular locations, which is supported by results from rat skeletal muscle where insulin treatment increased the α_2 abundance in the plasma membrane, with a parallel decrease in its abundance in the internal membrane pool as measured via western blotting (Hundal *et al.*, 1992).

2.6.1.3 Acute exercise

Analysis of NKA isoform abundance following an acute bout of high intensity one-legged knee extensor exercise (Juel *et al.*, 2000a; Murphy *et al.*, 2004), or high-intensity interval cycling (Aughey *et al.*, 2007) found that NKA α_{1-3} and β_{1-3} protein abundance were unchanged. However, NKA α_2 protein abundance was increased less than one hour after the first 6 min high intensity bout of a 16 h intermittent protocol (Green *et al.*, 2007b). Exercise-induced increases in the NKA mRNA have been demonstrated immediately following knee extensor exercise for the α_1 , α_2 , α_3 , β_1 , and β_3 isoforms (Murphy *et al.*, 2004; Nordsborg *et al.*, 2005). Acute prolonged submaximal cycling showed increases in muscle NKA content measured via [3 H]ouabain binding after only 30 min cycling (Green *et al.*, 2007a). These results suggest that NKA changes following acute exercise may be dependent on the mode and intensity of the exercise performed, and further investigation is needed. Supplementation of HCO_3^- prior to repeat sprint treadmill exercise has tended to increase mean power, peak power and total work (Gaitanos *et al.*, 1991), and improved exercise performance following HCO_3^- ingestion has also been associated with a lowering of plasma $[\text{K}^+]$ (Raymer *et al.*, 2004; Sostaric *et al.*, 2006). However the acute effect of HCO_3^- supplementation on the NKA are largely unknown. The effects of acute exercise on NKA isoform abundance is investigated in both chapters 3 and 4.

2.6.2 Chronic regulation

Repeated stimuli over time can result in long-term adaptations of the NKA. These include, but are not limited to, different forms of exercise training and various hormones.

2.6.2.1 Insulin

Changes in response to the sustained presence of insulin include changes in NKA protein levels and gene transcription as well as the half-life of the corresponding mRNA (Ewart & Klip, 1995). Studies in untreated diabetic rats have demonstrated that insulin deficiency resulted in a decrease of [³H]ouabain binding in the soleus muscle of ~18%, and when treated with insulin, levels increased to ~23% above control levels (Schmidt *et al.*, 1994). Studies in humans have found a significant linear correlation between plasma insulin concentration and skeletal muscle pump content in both control subjects and patients with non-insulin dependent diabetes mellitus (Schmidt *et al.*, 1994). Analysis of hyperglycaemic in ventricular myocytes isolated from diabetic rabbits reported that diabetes-induced inhibition of sarcolemmal NKA electrogenic current was reversed following restoration of euglycaemia (Hansen *et al.*, 2007).

2.6.2.2 Exercise training

The NKA is a skeletal muscle protein highly adaptable to chronic changes in contractile activity levels. A 16% increase in muscle NKA content measured via [³H]ouabain binding was observed in humans following 7 wks sprint cycle training (McKenna *et al.*, 1993). These increases in pump content could provide beneficial effects in protecting contractility during repeated activity given the role of the NKA in membrane excitability (Clausen, 1996). NKA adaptations can occur quite quickly in response to training. After only 3 days of training, an increase in vanadate facilitated [³H]ouabain-binding NKA content and α_2 isoform protein abundance were found, while β_1 protein abundance

increased after 6 days of prolonged cycling training in untrained humans (Green *et al.*, 2004). Up-regulation of isoform protein abundance in skeletal muscle is also seen in trained athletes after only 2 weeks high intensity sprint training, with α_2 isoform expression increasing by 15% at the end of the intervention (Thomassen *et al.*, 2010). Long term training also induces increases in [³H]ouabain binding, being 16% higher following 5 months training of moderate or high intensity exercise in cross-country skiers (Evertsen *et al.*, 1997). Training status is also important, with endurance trained males having higher NKA content and activity levels compared to recreationally active males, but no difference was found between male and female athletes for NKA content or activity (Murphy *et al.*, 2007). While acute ingestion of HCO₃ has been demonstrated to improve acute exercise performance (Bishop *et al.*, 2004; Raymer *et al.*, 2004; Sostaric *et al.*, 2006), the effects of chronic ingestion are largely unknown. However, given the acute performance benefits of HCO₃, chronic supplementation during repeat sprint training could potentially lead to greater post-training improvements in performance (Varley, 2013). The effect of repeat sprint training will be examined on NKA isoform protein abundance in chapter 4.

SECTION III: Aims and hypotheses

2.7 Aims

Study 1 (Chapter 3) examined the effects of exogenous glucose and the induced increases in insulin, as well as intense exercise on arterial and venous plasma K^+ homeostasis and on skeletal muscle NKA protein isoform abundance.

Study 2 (Chapter 4) investigated the effects of acute pre-exercise $NaHCO_3$ supplementation, and chronic $NaHCO_3$ supplementation during 4 wks of repeat sprint training (RSE), on skeletal muscle NKA isoform abundance.

Study 3 (Chapter 5) investigated the distribution patterns of the six NKA isoforms (α_1 - α_3 and β_1 - β_3) expressed in human skeletal muscle, exploring any fibre-type specific distribution and examining localisation within the plasma membrane and intracellular regions.

2.8 Hypotheses

Study 1 (Chapter 3) hypotheses tested were that an oral glucose load would:

1. Lower arterial and venous plasma $[K^+]$ at rest and during subsequent high-intensity exercise;
2. increase the arterio-venous K^+ difference across inactive skeletal muscle;
3. that improved K^+ homeostasis would enhance high-intensity intermittent exercise performance;
4. Not modify skeletal muscle NKA α_{1-3} and β_{1-3} isoform protein abundances following acute exercise.

Study 2 (Chapter 4) hypotheses tested were that:

1. Skeletal muscle NKA α_{1-3} and β_{1-3} isoform protein abundances would remain unchanged following acute exercise and after acute NaHCO_3 supplementation.
2. Skeletal muscle NKA α_2 and β_1 isoform protein abundance would increase following 4 wks RSE training with chronic NaHCO_3 supplementation.

Study 3 (Chapter 5) hypotheses tested were that in human skeletal muscle:

1. Skeletal muscle NKA α_1 isoform density would be greater in the plasma membrane than the intracellular region, whereas NKA α_2 isoform density would be greater in the intracellular region.
2. Skeletal muscle NKA α_1 and β_1 isoforms would have a higher density in type I than type II fibres.

CHAPTER 3. The effects of an oral glucose load on plasma K^+ and electrolyte homeostasis at rest, during high intensity intermittent exercise and recovery on skeletal muscle NKA isoform abundance

3.1 Introduction

During muscle contraction, increased rates of myocytic Na^+ influx and K^+ efflux lead to increased interstitial $[K^+]$, decreased intracellular $[K^+]$ and membrane potential, with these changes linked with muscular fatigue (de Paoli *et al.*, 2007; Cairns & Lindinger, 2008). Skeletal muscle also exerts major impacts on plasma $[K^+]$, with even modest increases in the exercise-induced release of K^+ from contracting skeletal muscles markedly elevating plasma $[K^+]$ (Lindinger & Sjøgaard, 1991; Sejersted & Sjøgaard, 2000; Clausen, 2010). The main mechanisms regulating $[K^+]$ during and following exercise are K^+ release by contracting cells, and rates of reuptake by contracting muscle and uptake by non-contracting tissues, including inactive skeletal muscle (Lindinger & Sjøgaard, 1991). Several studies have shown that inactive muscles play an important role in the regulation of $[K^+]$, $[Na^+]$ and lactate both during and following intense leg exercise (Kowalchuk *et al.*, 1988a; Lindinger *et al.*, 1990a). Upon cessation of exercise, the rapid reuptake of K^+ by previously active muscle induces a rapid decrease of plasma $[K^+]$ to reach or even fall below resting levels within the first 5 min of recovery (Lindinger & Sjøgaard, 1991; Lindinger *et al.*, 1992).

Elevated extracellular $[K^+]$ strongly depresses muscle force (Cairns *et al.*, 1997; de Paoli *et al.*, 2007). In isolated rat soleus muscles, $10 \text{ mmol.L}^{-1} [K^+]$ induced a 40% reduction in tetanic force, whilst $12.5 \text{ mmol.L}^{-1} [K^+]$ inhibited 95% of the tetanic force (Clausen *et al.*, 1993). However, experiments on isolated muscles have also shown that when force

is depressed due to high extracellular $[K^+]$, acidification by lactic acid produced a pronounced recovery of force, and therefore acidosis may protect against fatigue (Nielsen *et al.*, 2001; de Paoli *et al.*, 2007). This effect is mediated via reduced Cl^- conductance, with the membrane potential strongly biased towards the Cl^- equilibrium potential, aiding in maintaining excitability and force responses (Cairns *et al.*, 2004; Dutka *et al.*, 2008). Nonetheless, K^+ regulation is critical to muscle excitation, force production and fatigue, and it is important to understanding the mechanisms involved in K^+ regulation.

In skeletal muscle the NKA contributes to the maintenance of intracellular $[Na^+]$ and $[K^+]$ via re-uptake of K^+ , Na^+ extrusion and electrogenic effects, which makes it vitally important to cellular excitability and muscle contraction (Everts & Clausen, 1994; Blanco & Mercer, 1998; Chibalin *et al.*, 2001; Kaplan, 2002). Skeletal muscle comprises the largest pool of NKA in the body (Clausen, 1996) and expresses three α - (α_1 - α_3) and three β - (β_1 - β_3) isoforms at the protein level (Murphy *et al.*, 2004; Nordsborg *et al.*, 2005). The acute effects of exercise on NKA isoform abundance have been scarcely studied. The NKA α_{1-3} and β_{1-3} protein abundances were unchanged after an acute bout of high intensity, one-legged knee extensor exercise (Juel *et al.*, 2000a; Murphy *et al.*, 2004), or high-intensity interval cycling (Aughey *et al.*, 2007). In contrast, NKA α_2 protein abundance was increased less than one hour after the first 6 min high intensity bout of a 16 h intermittent protocol (Green *et al.*, 2007b). Possible exercise effects on muscle NKA isoforms were investigated here.

Insulin is an important regulator of skeletal muscle NKA and K^+ . An early reported effect of insulin was a reduction in plasma $[K^+]$ (Andres *et al.*, 1962; Zierler & Rabinowitz, 1964), primarily via uptake of K^+ into skeletal muscle (Ewart & Klip, 1995). Several studies have used insulin infusion to induce hyperinsulinaemia, and

demonstrated an accompanying decrease in plasma $[K^+]$ (DeFronzo *et al.*, 1980; Alvestrand *et al.*, 1984; DeFronzo, 1988; Ferrannini *et al.*, 1988). However, little research has investigated the more physiological glucose-induced hyperinsulinaemia and its effects on plasma $[K^+]$. Whilst a 75g glucose load was sufficient to induce hypokalaemia in one study (Natali *et al.*, 1993), another study reported a decrease in serum K^+ in haemodialysis patients, but not in the healthy control group (Muto *et al.*, 2005).

Insulin has also been found to lower extracellular K^+ in isolated muscle preparations (Erlj & Grinstein, 1976; Clausen & Kohn, 1977). This was mainly attributed to a rapid stimulation of NKA (Moore, 1973; Gavryck *et al.*, 1975) and occurred independent of increased muscle glucose transport (Clausen, 1986). The effects of insulin on NKA can be seen in humans *in vivo*, where physiological concentrations of insulin stimulated K^+ uptake into the forearm at rest (Zierler & Rabinowitz, 1964). Insulin also stimulated ouabain suppressible muscle lactate release, indicating this was due to NKA activation (Novel-Chate *et al.*, 2001). However, it is unknown if insulin induces changes in NKA isoform protein abundance in skeletal muscle, and whether these may be isoform-specific.

The aim of this study was to investigate whether glucose-induced increases in plasma insulin concentration can lower plasma $[K^+]$ during rest, high-intensity intermittent exercise and recovery. It was hypothesised firstly that an oral glucose load would lower plasma $[K^+]$ at rest and during subsequent high-intensity exercise, increase the K^+ arterio-venous difference across non-contracting skeletal muscle and that improved K^+ homeostasis may increase high-intensity intermittent exercise performance, and finally,

that NKA α_{1-3} and β_{1-3} isoform protein abundances would remain unchanged following acute exercise and after glucose ingestion.

3.2 Methods

3.2.1 Participants

Eight recreationally active individuals (6 males and 2 females; age 24.8 ± 4.9 yrs; height 175.0 ± 9.8 cm; body mass 74.1 ± 11.0 kg; mean \pm SD) gave their written informed consent to participate in the study, which was approved by the Victoria University Human Research Ethics Committee.

3.2.2 Experimental design

Participants attended the laboratory on six occasions. The first visit involved initial screening and included an incremental exercise test on a cycle ergometer to determine peak oxygen consumption ($\dot{V}O_{2\text{peak}}$). During the second visit, participants were familiarised with the high-intensity intermittent cycling protocol. This protocol was then repeated during all subsequent trials, comprising visits 3 and 4 to establish exercise performance variability for each participant, as well as the final two visits, which comprised the experimental and placebo trials. During the experimental trial the participants ingested a carbohydrate solution (CHO) consisting of 75 g glucose, and in the placebo trial, an artificially sweetened placebo solution (CON) (NutraSweet, Mt Prospect, USA) in 300 ml of water; both solutions were flavoured with an unsweetened, caffeine-free powder (Kool-Aid, Kraft Foods, Glenview, USA). The CHO and CON trials were conducted in a double-blind, randomised, crossover design with a minimum period of 4 weeks between trials.

3.2.3 Incremental exercise testing

The peak oxygen uptake ($\dot{V}O_{2\text{peak}}$) was measured during an incremental test to volitional exhaustion conducted on an electronically braked cycle ergometer (Lode, Groningen, The Netherlands). The ergometer position was modified to have the participant in a

partially-recumbent position seated on a custom-made chair, and was consistent for all subsequent experimental trials. Participants completed four, 4 min submaximal work periods at 60, 90, 120 and 150 W, performed continuously and at a cadence of 70 rpm, followed by a 5 min rest period. Exercise then recommenced at 175 W and was increased by 25 W every minute until volitional exhaustion, defined as an inability to maintain a pedalling cadence above 60 rpm. Participants breathed through a Hans Rudolph two-way non-rebreathing valve, with expired air passing through low resistance tubing into a 4 L mixing chamber. Expired air flow was analysed using a flow transducer (KL Engineering K520, California, USA); fractions of expired O₂ and carbon dioxide (CO₂) were measured continuously by rapidly responding analysers (Ametek S-3A/II and Ametek CD-3A, Ametek, Berwyn, PA, USA). The $\dot{V}O_2$ was calculated continuously and displayed every 15 s on a personal computer (Turbofit, VacuMed, Ventura, CA, USA). The ventilometer and gas analysers were calibrated prior to each test with a standard 3 L syringe and precision reference gases. The $\dot{V}O_{2peak}$ was calculated as the mean of the two highest consecutive 15 s values. A regression equation of $\dot{V}O_2$ versus power output was derived from the four submaximal workloads and the $\dot{V}O_{2peak}$ and used to determine a power output corresponding to 130% $\dot{V}O_{2peak}$ for each individual (Medved *et al.*, 2003).

3.2.4 High-intensity intermittent cycling

The high-intensity intermittent cycling protocol comprised four exercise bouts (EB), each performed at a power output corresponding to 130% $\dot{V}O_{2peak}$ power output with cadence to be kept above 70rpm; the first three EBs (EB1-3) were each for 45 s duration whilst the final EB (EB4) was continued until volitional exhaustion, defined as the inability to maintain a pedalling cadence above 50 rpm. All bouts were separated by a 135 s rest

period, giving a 1:3 work-to-rest ratio. During the two variability sessions, the time to fatigue on the final bout was measured to determine their individual performance variability.

3.2.5 Experimental trials

3.2.5.1 Participant preparation

All participants arrived in the lab at 8 am after an overnight fast and were allowed water *ad libitum*. Heart rate and rhythm were monitored via telemetry using a 12-lead electrocardiogram (Mortara, Boston, MA, USA). A 20G arterial catheter (Mayo Healthcare, Mulgrave, VIC, Australia) was inserted retrograde into the radial artery under local anaesthesia (1% Xylocaine, McFarlane Medical and Scientific, Surrey Hills, VIC, Australia), and a 20G catheter was inserted anterograde into the antecubital vein of the contralateral arm. Both catheters were connected to a saline filled arterial infusion kit (ITL Healthcare, Chelsea Heights, VIC, Australia) and kept patent by a slow pressurised infusion of 0.9% sodium chloride.

3.2.5.2 Blood sampling and analyses

Following cannulation participants rested for 30 min and the first blood sample was then taken (baseline). The participant then ingested either the CHO or CON solution and for the following 60 min remained passive in a supine position, with arterial and venous blood samples taken simultaneously at 10, 20, 40 and 60 min following ingestion. Subjects were then moved to an adjacent cycle ergometer where arterial (a) and venous (v) samples were drawn simultaneously, immediately prior to and during the final seconds of EB1-4, and at 1, 2, 5, 10, 20 and 30 min during recovery.

At each time point two samples were taken from each site. The first sample (~0.6 ml) was drawn into a blood gas syringe (Rapidlyte lithium heparin) for immediate analysis of

plasma electrolytes (Na^+ and K^+) and pH, on an automated blood gas analyser (Ciba Corning 865, Seimens, Bayswater, VIC, Australia). The second sample (~3 ml) was drawn into a plain, latex-free syringe and expelled into a tube containing lithium heparin (125 IU). Immediately, 400 μl of whole blood was transferred into a 1.5 ml microfuge tube for analysis of haemoglobin concentration ([Hb]) and haematocrit (Hct) using an automated analyser (Sysmex Automated Cell Counter, Roche Diagnostics, Dee Why, NSW, Australia). The remaining blood was centrifuged at 4500 rpm for 2 min and the separated plasma was removed and stored at $-20\text{ }^\circ\text{C}$ for later analyses of plasma glucose and Lac^- concentrations (YSI 2300 STAT plus Glucose Lactate Analyser, John Morris Scientific, Chatswood, NSW, Australia). Plasma insulin concentration was measured only on arterial blood samples taken at baseline, 20, 40, 60 min and at fatigue, using an enzyme-linked immunosorbent assay (ELISA, DAKO, North Sydney, NSW, Australia).

Calculations

Plasma hydrogen concentration (nmol.L^{-1}) was calculated from measured pH. Changes in arterial and venous plasma volume (PV_a and PV_v) and blood volume (BV_a and BV_v) from baseline, and changes in venous compared with arterial plasma (PV_{a-v}) and blood volume (BV_{a-v}) across the forearm were calculated before, during and after exercise, from changes in [Hb] and Hct, as previously described (Harrison, 1985; McKenna *et al.*, 1997).

3.2.5.3 Muscle biopsies

Needle muscle biopsies were taken from the middle third of the vastus lateralis muscle. A local anaesthetic (1% Xylocaine, McFarlane Medical and Scientific, Surrey Hills, Australia) was injected into the skin and subcutaneous tissue. A small incision was then made into the skin and fascia, and a small muscle sample was excised using a Stille

biopsy needle. The muscle sample was rapidly blotted on filter paper to remove blood and then snap frozen in liquid N₂ and stored at -80 °C for later analysis.

A muscle biopsy was taken at baseline and at 60 min after ingestion of either the CHO or CON solution. Subjects then moved to an adjacent cycle ergometer for the high-intensity intermittent exercise protocol. The final biopsy was taken immediately after the point of fatigue. A total of six biopsies were taken from each individual (three each trial).

3.2.6 Skeletal muscle NKA isoform protein abundance measures

3.2.6.1 Protein extraction

Frozen muscle samples of approximately 25 mg were homogenised in an ice-cold buffer (25 mM Tris-HCL, pH 6.8, 1% sodium dodecyl sulphate (SDS), 5 mM EGTA, 50 mM NaF, 1 mM sodium vanadate, 17.4 µg/µl phenylmethylsulphonyl fluoride (PMSF), 20 µl protease inhibitor cocktail (Sigma, Sydney, NSW, Australia) for 2 x 10 s using a tissue homogeniser (TH220, Omni International, Kennesaw, GA, USA). Samples were then heated on a thermoshaker for 20 min at 56 °C with a shaking speed of 750 rpm. Total protein concentration of each sample was determined using a BCA Assay Kit (BioRad, Sydney, NSW, Australia), with bovine serum albumin (BSA) as the standard (Murphy *et al.*, 2006; Aughey *et al.*, 2007).

Muscle homogenates were then deglycosylated to enhance identification of the β-isoforms. This involved adding 0.5% (v/v) Nonidet P40 and 3 units N-Glycosidase F (Roche Diagnostics, Dee Why, NSW, Australia) per 0.5 mg protein and incubating for 1 hr at 37 °C.

Previous studies utilising repeated steps of centrifugation of muscle and membrane separation have resulted in very low recovery of NKA, yielding a final sample that may be unrepresentative of the whole muscle NKA population (Hansen & Clausen, 1988).

Therefore, muscle sample analyses did not include any membrane isolation steps, to maximize recovery of NKA protein (Murphy *et al.*, 2004). Aliquots of each homogenate were diluted to a concentration of $3.5 \mu\text{g}\cdot\mu\text{l}^{-1}$, mixed with Laemmli sample buffer and stored at -80°C until analysed.

3.2.6.2 Immunoblotting

SDS-PAGE 10% gels were loaded with 10 (α_2, β_1) or 20 ($\alpha_1, \alpha_3, \beta_2, \beta_3$) μg protein and run for 10 min at 100 V then 2 hr at 75 V. The linearity of the blot signal for protein loaded was confirmed for each isoform. Following electrophoresis, proteins were wet transferred (90 min, 100 V) to $0.45 \mu\text{m}$ nitrocellulose membranes. Membranes were blocked in TBST (10 mM Tris, 100 mM NaCl, 0.02% Tween-20) containing 7.5% non-fat milk, for 1 hr at room temperature. Following washing, membranes were incubated overnight at 4°C with primary antibodies diluted in TBST buffer containing 0.1% NaN_3 and 0.1% BSA.

Membranes were washed in TBST and incubated with the appropriate anti-rabbit (NEFA812001EA) or anti-mouse (NEFA822001EA, PerkinElmer, Melbourne, VIC, Australia) horseradish peroxidase-conjugated secondary antibody for 1 hr at room temperature. Secondary antibodies were diluted 1:20,000 in TBST buffer containing 5% non-fat milk. After washing the membranes in TBST, proteins were detected using chemiluminescence reagents (Imobillon™ HRP Substrate, Millipore, Macquarie Park, NSW, Australia) and quantified via densitometric scanning (VersaDoc™ Imaging System, Bio-Rad) and dedicated software (Quantity One v4.6.6, BioRad, Sydney, NSW, Australia). All proteins were normalised against total protein loading detected via coomassie staining, then all protein was expressed relative to the baseline biopsy from the CON trial.

3.2.6.3 Antibodies

Primary antibodies specific to each NKA isoform were: α_1 (1:50): monoclonal $\alpha 6F$ (developed by D. Fambrough and obtained from the Developmental Studies Hybridoma Bank developed under the auspices of the NICHD and maintained by the University of Iowa, Department of Biological Sciences, Iowa City, IA, USA); α_2 (1:200): polyclonal anti-HERED (kindly donated by T. Pressley, Texas Tech University, USA); α_3 (1:500): monoclonal MA3-915 (Thermo Scientific Scoresby, VIC, Australia); β_1 (1:500): monoclonal MA3-930 (Thermo Scientific, Scoresby, VIC, Australia); β_2 (1:500): monoclonal 610915 (BD Biosciences, Franklin Lakes NJ, USA); and β_3 (1:500): monoclonal 610993 (BD Biosciences, Franklin Lakes NJ, USA).

3.2.7 Statistical analyses

All results are expressed as mean \pm SD. All data were tested for normality using the Shapiro-Wilk W test. When normality criteria were not met ($p < 0.05$), data were log transformed to reduce bias of the error. Balanced data sets (no missing variables) were analysed using a two-way repeated measure ANOVA. Data sets which contained missing values were analysed using a linear mixed model, with time and treatment (CHO or CON) as fixed effects, and restricted maximum likelihood as the estimation method for missing values. For each variable, two covariance methods were tested (first-order autoregressive and compound symmetry), the appropriate structure was chosen according to which covariance type had the lowest Aikake Information Criterion (AIC). Least Significant Difference post-hoc tests were used for all analyses. Time-by-treatment interactions were not significant unless stated. Significance was accepted at $p < 0.05$. Effect size was calculated with 90% confidence intervals (ES \pm 90% CI) used to compare magnitudes of effect between and within trials. Magnitudes of change using Cohen's

effect size were classified as; trivial <0.2 ; small, 0.2-0.6; moderate, 0.6-1.2; large, 1.2-2.0; and very large, 2.0-4.0 (Batterham & Hopkins, 2006; Hopkins, 2006). Effects with less certainty (magnitude of $< 75\%$) were classified as no meaningful difference (Batterham & Hopkins, 2006; Hopkins, 2006). Statistical analyses were performed using PASW Statistics 20 (SPSS Inc, Quarry Bay, Hong Kong) and effect size calculated via a custom spreadsheet (Hopkins, 2006).

3.3 Results

3.3.1 Exercise performance

The subjects had a $\dot{V}O_{2\text{peak}}$ of $3.33 \pm 0.52 \text{ L}\cdot\text{min}^{-1}$ ($45.5 \pm 8.6 \text{ ml}\cdot\text{kg}^{-1}\cdot\text{min}^{-1}$) and a peak power output of $293 \pm 47 \text{ W}$. The calculated work rate corresponding to 130% $\dot{V}O_{2\text{peak}}$ was $360 \pm 75 \text{ W}$. Time to fatigue during the final Exercise Bout to fatigue (EB4) did not differ in the two variability trials (69.4 ± 17.9 and $68.9 \pm 24.4 \text{ s}$ respectively; Mean \pm SD, CV 8.6%) or in the experimental trials (CON 64.7 ± 19.7 vs CHO $56.3 \pm 22.8 \text{ s}$).

3.3.2 Plasma [glucose]

Arterial [glucose]. The $[\text{glucose}]_a$ rose above baseline at 10 min rest and remained elevated 20 min post-fatigue (time main effect; $p < 0.001$), with the $[\text{glucose}]_a$ during CHO greater than CON (treatment main effect; $p < 0.001$; Fig 3.1). The time-by-treatment interaction was significant ($p < 0.001$) and post-hoc tests revealed that $[\text{glucose}]_a$ during CHO was greater than CON from 10 min after ingestion through until end of EB3 (Fig. 3.1).

Venous [glucose]. A similar temporal pattern was observed for $[\text{glucose}]_v$ (time main effect; $p < 0.001$), with $[\text{glucose}]_v$ also greater during CHO than CON (treatment main effect; $p < 0.01$; Fig 3.1). The time-by-treatment interaction was significant ($p < 0.001$), with $[\text{glucose}]_v$ greater in CHO than CON for the period from 20 min after ingestion through until EB3 and becoming less than CON at 30 min recovery (Fig. 3.1).

Arterio-venous [glucose] difference. The $[\text{glucose}]_{a-v}$ was elevated above baseline indicating a large net glucose uptake into the forearm at each of EB1-EB4 and at 1 min recovery (time main effect; $p < 0.001$; Fig 3.1). The $[\text{glucose}]_{a-v}$ was more positive during CHO than CON (treatment main effect; $p < 0.001$). The time-by-treatment interaction was significant ($p < 0.01$; Fig. 3.1) with $[\text{glucose}]_{a-v}$ more positive in CHO

than CON from 10 min post-ingestion through to pre EB3, indicating a large net glucose uptake into the forearm.

3.3.3 Arterial plasma insulin concentration

Arterial plasma insulin concentration ($[\text{insulin}]_a$) was increased at all time points ($p < 0.001$, time main effect) and was greater during CHO compared to CON (trial main effect, $p < 0.01$; Table 3.1). There was a significant time-by-treatment interaction ($p < 0.01$), and post-hoc analysis indicated that during the CHO trial, $[\text{insulin}]_a$ was elevated above baseline more than four-fold at 20 and 40 min and remained elevated at 60 min and fatigue, and was also greater than CON at the same time points (Table 3.1).

Table 3.1 Arterial plasma insulin concentration ($\text{pmol}\cdot\text{L}^{-1}$) measured at baseline, and subsequent 60 min rest and during high intensity intermittent exercise at 130% $\dot{V}\text{O}_2$ peak continued to fatigue, following either carbohydrate (CHO), or placebo (CON) ingestion.

	Baseline	Rest			Fatigue
		20 min	40 min	60 min	
CON	60.0 ± 29.6	62.9 ± 21.0	65.1 ± 52.6	42.6 ± 15.5	60.0 ± 17.5
CHO	43.8 ± 10.2	209.0 ± 84.4*†	261.0 ± 85.6*†	212.7 ± 84.4*†	129.4 ± 33.5*†

†CHO greater than CON at that time point ($p < 0.001$); *CHO greater than baseline ($p < 0.001$). Mean ± SD, n = 8.

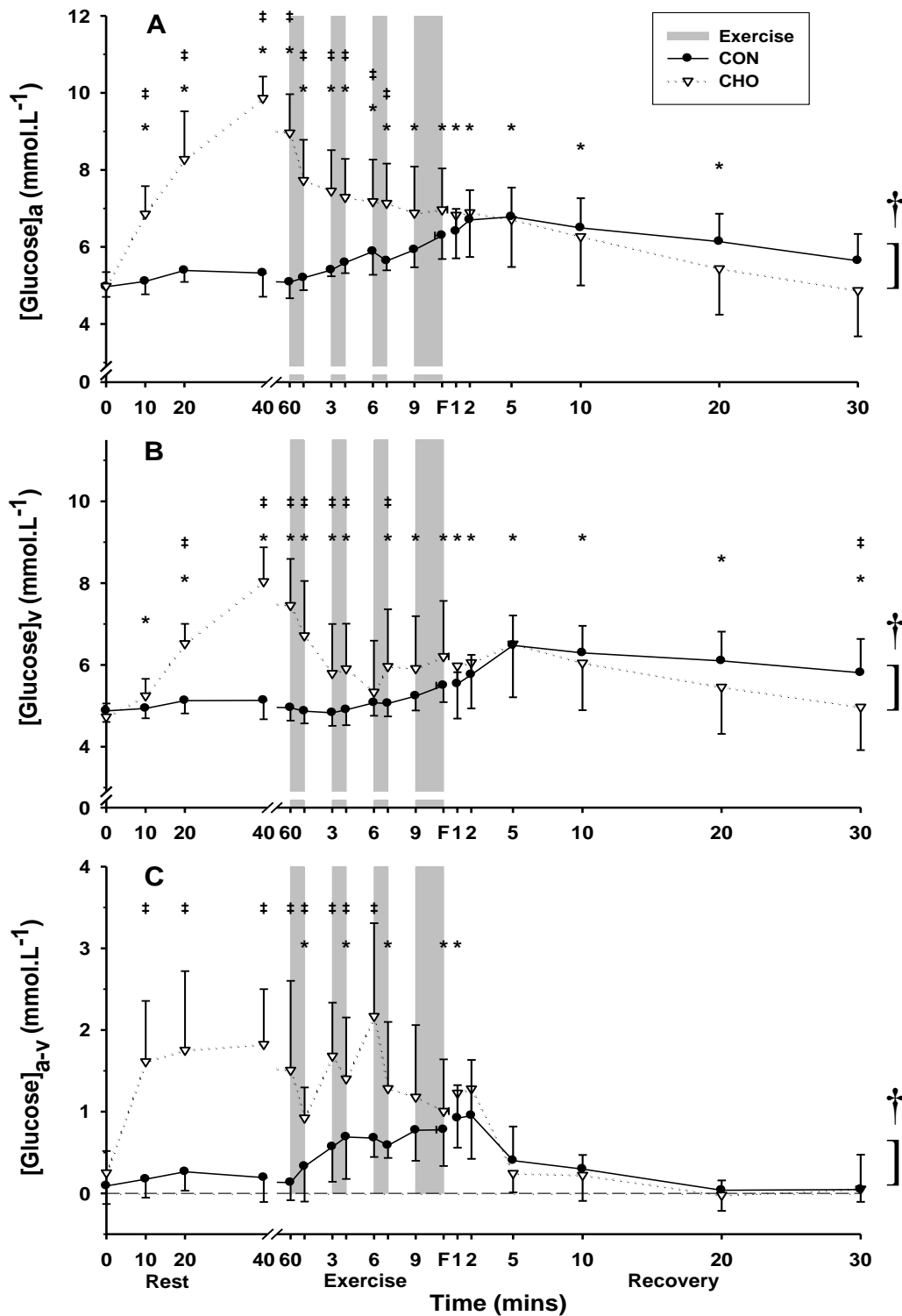


Figure 3.1 Effects of an oral glucose load on plasma [glucose] measured at baseline (0), and subsequent 60 min rest, during high intensity intermittent cycling at 130% $\dot{V}O_{2peak}$ continued to fatigue, and in 30 min recovery, following either carbohydrate (CHO), or placebo (CON) ingestion. A) Arterial (a), B) venous (v), and C) calculated arterio-venous differences (a-v) in plasma [Gluc], under CON (●) and CHO (▽) conditions. * Different from baseline ($p < 0.05$, Time main effect). † CHO different from CON ($p < 0.05$, Treatment main effect). ‡ CHO greater than CON at that timepoint ($p < 0.05$). All data mean \pm SD, $n = 8$. Shaded bars represent exercise bout (EB), with EB1-EB3 of 45 s duration each and EB4 continued till fatigue (F).

3.3.4 Plasma $[K^+]$

Arterial $[K^+]$. Plasma $[K^+]_a$ was elevated above baseline at the end of each EB, including at fatigue, remained elevated at 1 min post-exercise and then fell below baseline at 5 min post-fatigue (time main effect; $p < 0.01$, Fig. 3.2). The $[K^+]_a$ was lower in CHO than in CON (treatment main effect; $p < 0.05$).

Venous $[K^+]$. In contrast the $[K^+]_v$ did not differ from baseline during exercise, but fell below baseline at 5 and 10 min post-fatigue (time main effect; $p < 0.001$). The $[K^+]_v$ was lower in CHO than in CON (treatment main effect; $p < 0.01$). The time-by-treatment interaction was significant with post-hoc analyses revealing a lower $[K^+]_v$ during CHO than CON at the end of EB1 through to 2 min post-fatigue ($p < 0.05$, Fig. 3.2).

Arterio-venous $[K^+]$ difference. The $[K^+]_{a-v}$ was greater (more positive) than baseline at the end of exercise for each of EB1-EB4 and at 1 min post-fatigue, representing a greater net K^+ uptake into the (inactive) forearm muscle (time main effect; $p < 0.001$; Fig. 3.2). The $[K^+]_{a-v}$ was greater in CHO than CON (treatment main effect; $p < 0.001$). The time-by-treatment interaction was significant, with $[K^+]_{a-v}$ more positive for CHO during each of EB1, EB2 and EB3 than CON ($p < 0.01$), representing a greater net K^+ uptake into the forearm during exercise in CHO (Fig. 3.2).

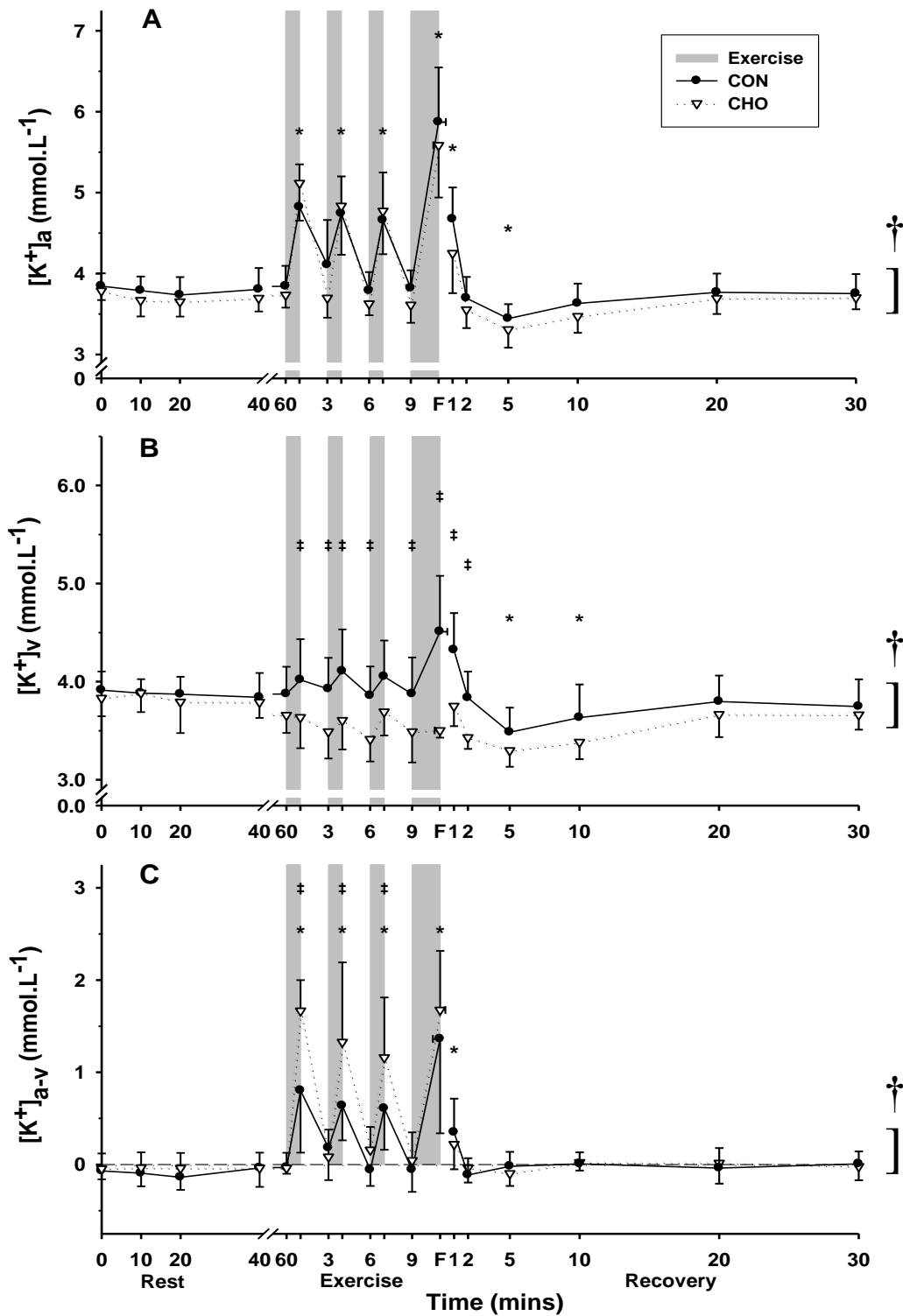


Figure 3.2 Effects of an oral glucose load on plasma $[K^+]$ measured at baseline (0), and subsequent 60 min rest, during high intensity intermittent cycling at $130\% \dot{V}O_{2peak}$ continued to fatigue, and in 30 min recovery, following either carbohydrate (CHO), or placebo (CON) ingestion. A) Arterial (a), B) venous (v), and C) calculated arterio-venous differences (a-v) in plasma $[K^+]$, under CON (\bullet) and CHO (∇) conditions. *Different from baseline ($p < 0.05$, Time main effect). † CHO different from CON ($p < 0.05$, Treatment main effect). ‡ CHO different from CON at that timepoint ($p < 0.05$). All data mean \pm SD, $n = 8$. Shaded bars represent exercise bout (EB), with EB1-EB3 of 45 s duration each and EB4 continued till fatigue (F).

3.3.5 Δ Plasma $[K^+]$

The changes in plasma $[K^+]$ from baseline ($\Delta[K^+]$) for each trial were also calculated, with similar time effects as seen for plasma $[K^+]$ (Fig. 3.3).

Arterial $\Delta[K^+]$. The $\Delta[K^+]_a$ was elevated above baseline at the end of each EB, remained elevated at 1 min post-exercise and became negative (i.e. fell below baseline) at 5 and 10 min post-fatigue (time main effect; $p < 0.001$; Fig. 3.3). However, no difference in $\Delta[K^+]_a$ was found between CON and CHO, and no interaction effect was present.

Venous $\Delta[K^+]$. The $\Delta[K^+]_v$ was below baseline at pre-EB3 and at 2, 5, and 10 min post-fatigue (time main effect; $p < 0.001$) and was more negative (larger decline) in CHO than CON (treatment main effect; $p < 0.001$). A significant interaction was detected ($p < 0.01$) and post-hoc analysis revealed $\Delta[K^+]_v$ was more negative for CHO than CON from post-EB1 to pre-EB3 and at fatigue, 1 and 2 min post-fatigue ($p < 0.05$; Fig. 3.3).

Arterio-venous $\Delta[K^+]$ difference. The $\Delta[K^+]_{a-v}$ was more positive at the end of each EB and at 1 min post-fatigue (time main effect; $p < 0.001$) and was more positive in CHO than in CON (treatment main effect; $p < 0.01$). The time-by-treatment interaction ($p < 0.01$) showed a more positive $\Delta[K^+]_{a-v}$ during EB1, EB2 and EB3 for CHO than CON, representing a greater net K^+ uptake into the forearm during exercise (Fig. 3.3).

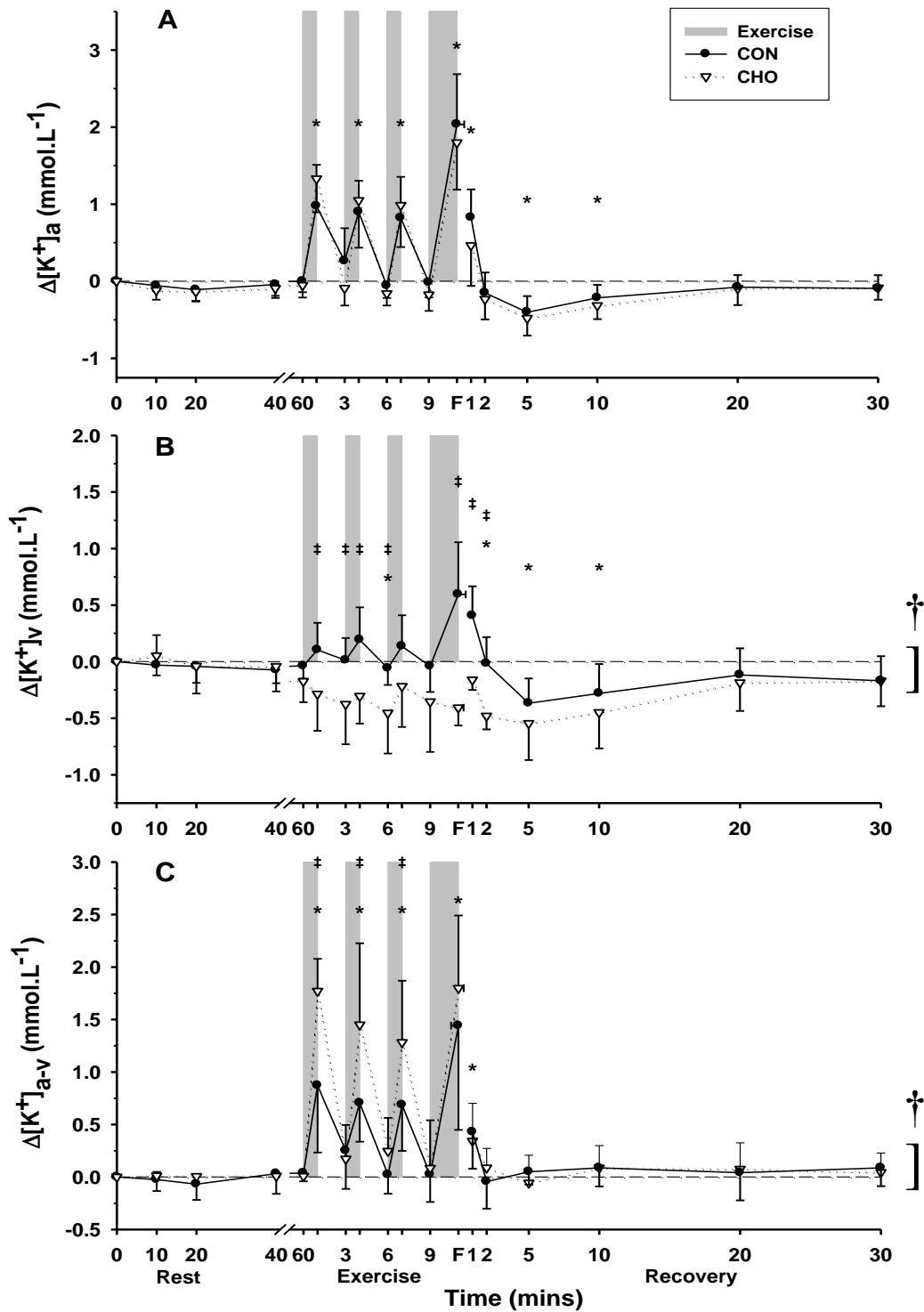


Figure 3.3 Effects of an oral glucose load on plasma $\Delta[K^+]$ measured at baseline (0), and subsequent 60 min rest, during high intensity intermittent cycling at 130% $\dot{V}O_{2peak}$ continued to fatigue, and in 30 min recovery, following either carbohydrate (CHO), or placebo (CON) ingestion. A) Arterial (a), B) venous (v), and C) calculated arterio-venous differences (a-v) in $\Delta[K^+]$, under CON (●) and CHO (▽) conditions. *Different from baseline ($p < 0.05$, Time main effect). † CHO different from CON ($p < 0.05$, Treatment main effect). ‡ CHO different from CON at that timepoint ($p < 0.05$). All data mean \pm SD, $n = 8$. Shaded bars represent exercise bout (EB), with EB1-EB3 of 45 s duration each and EB4 continued till fatigue (F).

3.3.6 Plasma $[\text{Na}^+]$

Arterial $[\text{Na}^+]$. Plasma $[\text{Na}^+]_a$ was elevated above baseline throughout the exercise period and up to 10 min recovery (time main effect; $p < 0.001$; Fig. 3.4). The $[\text{Na}^+]_a$ was consistently greater during CHO than in CON (treatment main effect; $p < 0.05$).

Venous $[\text{Na}^+]$. Venous $[\text{Na}^+]$ was elevated above baseline from EB3 through until 5 min post-fatigue (time main effect; $p < 0.001$; Fig. 3.4), with no difference in $[\text{Na}^+]_v$ between CHO and CON.

Arterio-venous $[\text{Na}^+]$ difference. The $[\text{Na}^+]_{a-v}$ was more positive during EB1-EB4 and at 1 min recovery (time main effect; $p < 0.001$), reflecting a net Na^+ uptake from plasma across the forearm. The $[\text{Na}^+]_{a-v}$ was more positive in CHO representing a greater net Na^+ uptake into the forearm compared to CON (treatment main effect; $p = 0.001$; Fig. 3.4).

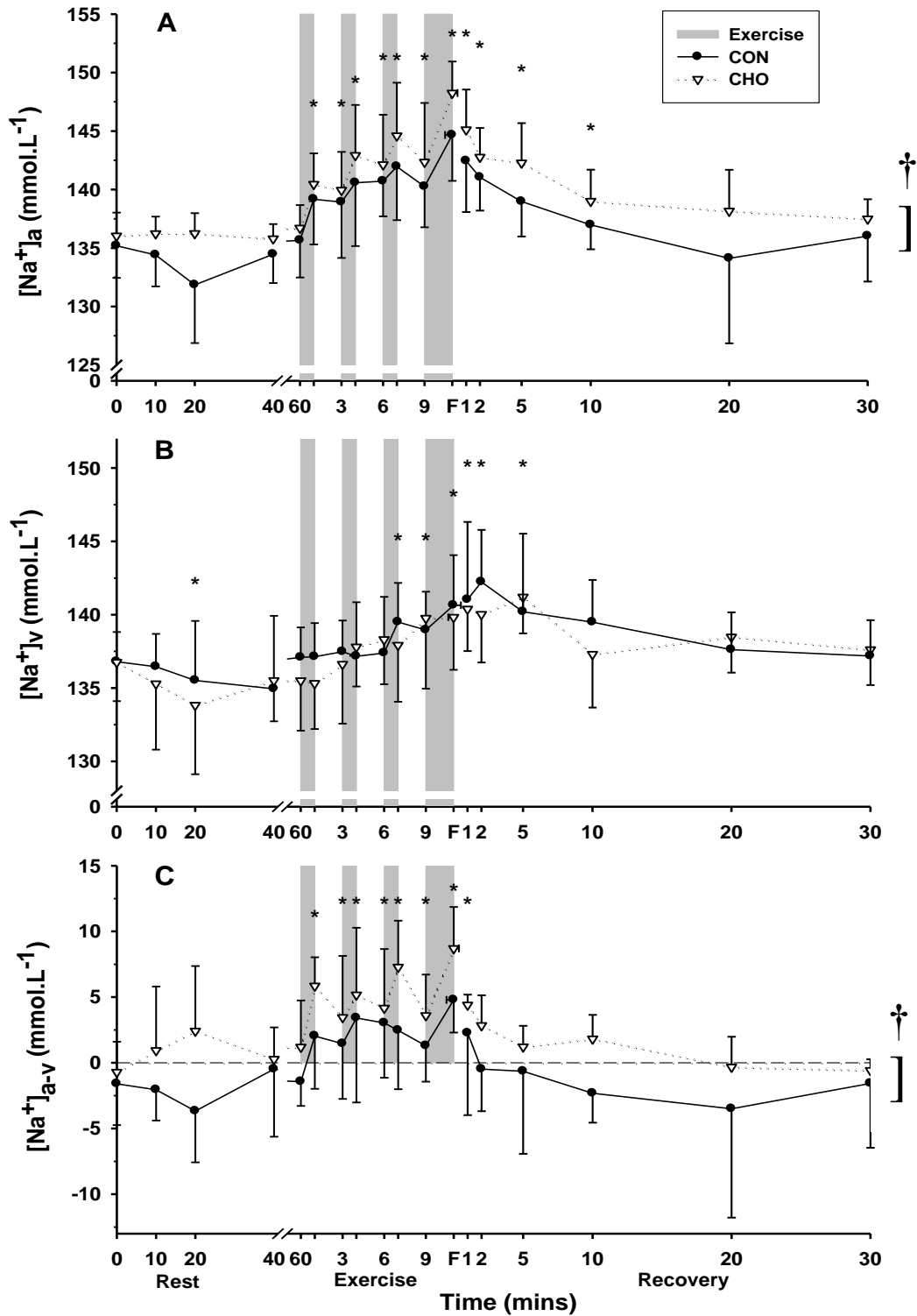


Figure 3.4 Effects of an oral glucose load on plasma $[Na^+]$ measured at baseline (0), and subsequent 60 min rest, during high intensity intermittent cycling at 130% $\dot{V}O_{2peak}$ continued to fatigue, and in 30 min recovery, following either carbohydrate (CHO), or placebo (CON) ingestion. A) Arterial (a), B) venous (v), and C) calculated arterio-venous differences (a-v) in plasma $[Na^+]$, under CON (●) and CHO (▽) conditions. * Different from baseline ($p < 0.05$, Time main effect). † CHO different from CON ($p < 0.05$, Treatment main effect). All data mean \pm SD, $n = 8$. Shaded bars represent exercise bout (EB), with EB1-EB3 of 45 s duration each and EB4 continued till fatigue (F).

3.3.7 Plasma [Lac⁻]

Arterial [Lac⁻]. The [Lac⁻]_a was elevated above baseline at EB1 and until at 1 min post-fatigue where it reached ~20 mmol.L⁻¹, and remained elevated at 30 min post-fatigue (time main effect; $p < 0.001$; Fig. 3.5). There was no difference in [Lac⁻]_a between CHO and CON.

Venous [Lac⁻]. Venous [Lac⁻] was elevated above baseline from pre-EB2 to 5 min post-fatigue where it reached ~16 mmol.L⁻¹, and remained elevated throughout recovery (time main effect; $p < 0.001$; Fig. 3.5). There was no difference in [Lac⁻]_v between CHO and CON.

Arterio-venous [Lac⁻] difference. The [Lac⁻]_{a-v} remained positive throughout the exercise period and until 10 min post-fatigue, representing a large net uptake of lactate into the forearm before returning to baseline (time main effect; $p < 0.001$) (Fig. 3.5). There was no difference in the [Lac⁻]_{a-v} between CHO and CON.

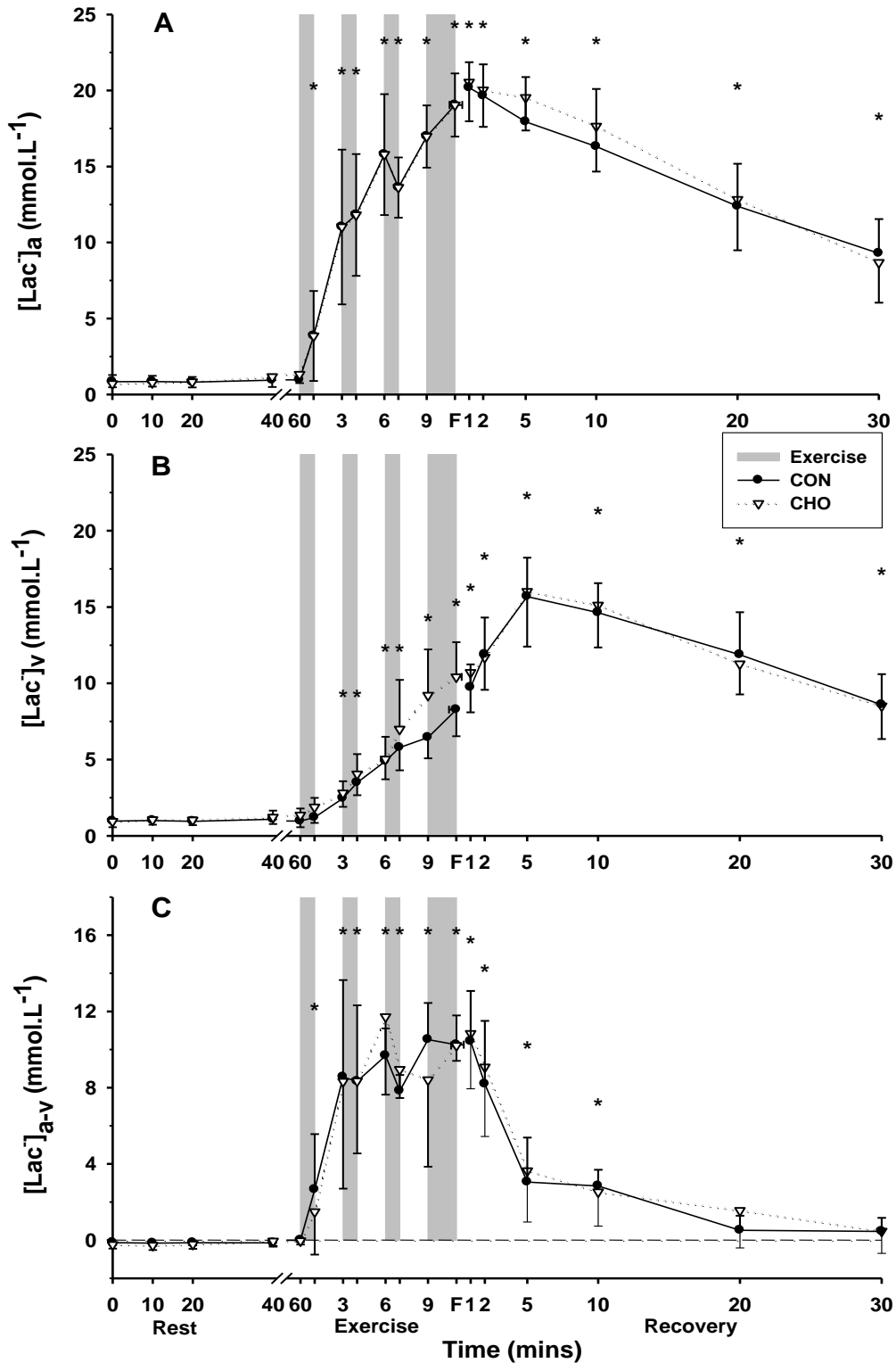


Figure 3.5 Effects of an oral glucose load on plasma [Lac⁻] measured at baseline (0), and subsequent 60 min rest, during high intensity intermittent cycling at 130% $\dot{V}O_{2peak}$ continued to fatigue, and in 30 min recovery, following either carbohydrate (CHO), or placebo (CON) ingestion. A) Arterial (a), B) venous (v), and C) calculated arterio-venous differences (a-v) in plasma [Lac⁻], under CON (●) and CHO (▽) conditions. * Different from baseline ($p < 0.05$, Time main effect). All data mean \pm SD, $n = 8$. Shaded bars represent exercise bout (EB), with EB1-EB3 of 45 s duration each and EB4 continued till fatigue (F).

3.3.8 Plasma $[H^+]$

Arterial $[H^+]$. The $[H^+]_a$ was elevated from pre-EB2 until 30 min post-fatigue, reaching $\sim 67 \text{ nmol.L}^{-1}$ ($\sim \text{pH} = 7.18$) at 5 min post-fatigue (time main effect; $p < 0.001$; Fig. 3.6).

There was no difference in $[H^+]_a$ between CHO and CON.

Venous $[H^+]$. The $[H^+]_v$ was slightly elevated at 10 min rest and then increased during EB2, EB3 and EB4, reaching $\sim 65 \text{ nmol.L}^{-1}$ ($\sim \text{pH} = 7.19$) at 5 min post-fatigue and remained elevated throughout the recovery period (time main effect; $p < 0.001$; Fig. 3.6).

There was no difference between CHO and CON.

Arterio-venous $[H^+]$ difference. The $[H^+]_{a-v}$ was slightly greater (more positive) than baseline at pre-EB2, pre-EB3 and pre-EB4, and at fatigue until 10 min post-fatigue (time main effect; $p < 0.001$; Fig. 3.6).

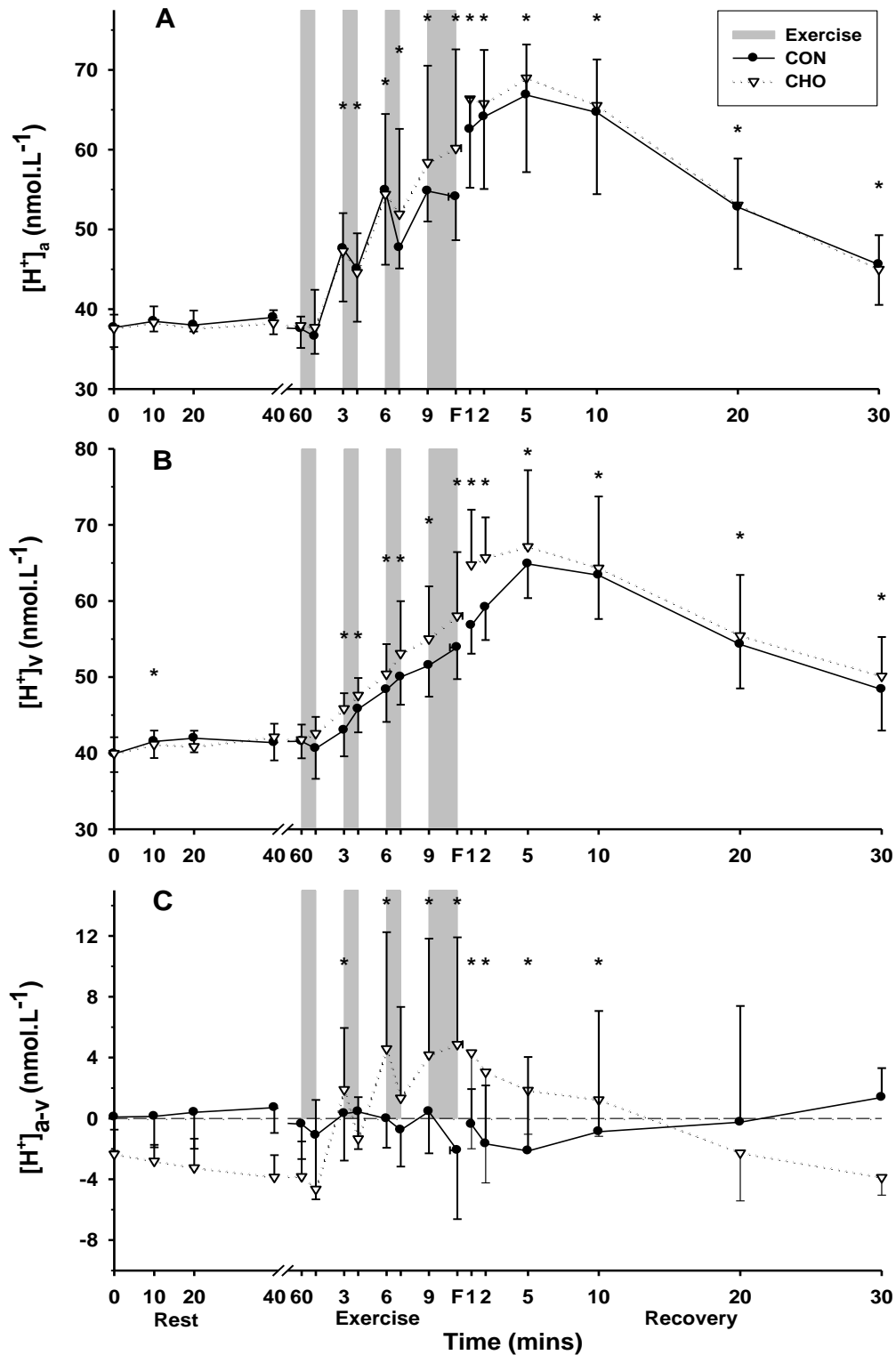


Figure 3.6 Effects of an oral glucose load on plasma $[H^+]$ measured at baseline (0), and subsequent 60 min rest, during high intensity intermittent cycling at $130\% \dot{V}O_{2\text{peak}}$ continued to fatigue, and in 30 min recovery, following either carbohydrate (CHO), or placebo (CON) ingestion. A) Arterial (a), B) venous (v), and C) calculated arterio-venous differences (a-v) in plasma $[H^+]$, under CON (\bullet) and CHO (∇) conditions. *Greater than baseline ($p < 0.05$; Time main effect). All data mean \pm SD, $n = 8$. Shaded bars represent exercise bout (EB), with EB1-EB3 of 45 s duration each and EB4 continued till fatigue (F).

3.3.9 Haematology and fluid shifts

Arterial and Venous Hb and Hct. Arterial (Table 3.2) and venous (Table 3.3) [Hb] and Hct remained unchanged from baseline to 60 min, with the exception of Hct_a which was slightly reduced only at 20 min; all variables then increased from EB1 to fatigue and remained elevated above baseline until 20 min recovery, returning to resting levels at 30 min post fatigue (time main effect, $p < 0.001$). There were no differences in Hb or Hct between CHO and CON.

Arterial plasma volume changes. The arterial plasma volume (PV_a) was unchanged during the pre-exercise rest period with the exception of a slight increase at 20 min. The PV_a decreased during exercise and by around 20% at fatigue, was gradually restored during the recovery period, but remained ~3% less than baseline at 30 min post-fatigue ($p < 0.05$; time main effect; Table 3.4). There was no difference between CHO and CON.

Venous plasma volume changes. The venous plasma volume (PV_v) was unchanged from baseline during the pre-exercise rest, declined during exercise by 13% at fatigue ($p < 0.001$), and continued to decline during recovery, by around 16-17% at 2 and 5 min post-fatigue for CON and CHO, respectively ($p < 0.05$; time main effect; Table 3.4). There was no difference between CHO and CON.

Arterio-venous plasma volume difference. As the blood transversed the forearm there was a positive change in plasma volume (ΔPV_{a-v}) indicating a gain in plasma volume across the forearm, of between 4-10% during CON and 3 - 10% during CHO ($p < 0.05$; time main effect; Table 3.4).

There were no treatment or interaction effects found for BV_a, BV_v or BV_{a-v}; the time main effects ($p < 0.05$) indicated similar trends as reported for PV (see Appendix 2).

Table 3.2 Arterial haemoglobin concentration ([Hb]_a; g.dl⁻¹) and haematocrit (Hct_a; %) measured at baseline, during 60 min rest and during high intensity intermittent exercise at 130% $\dot{V}O_{2peak}$ continued to fatigue and recovery, following either carbohydrate (CHO), or placebo (CON) ingestion.

	Rest (min)						
	Baseline	10	20	40	60		
CON							
[Hb] _a	14.3 ± 0.8	14.3 ± 0.9	14.2 ± 0.9	14.2 ± 0.7	14.5 ± 0.8		
Hct _a	39.6 ± 2.2	39.5 ± 2.4	39.0 ± 2.2 [†]	39.3 ± 2.3	40.1 ± 2.5		
CHO							
[Hb] _a	14.4 ± 0.7	14.5 ± 0.7	14.3 ± 0.6	14.3 ± 0.7	14.4 ± 0.5		
Hct _a	39.8 ± 1.7	39.6 ± 1.5	38.8 ± 1.5 [†]	39.0 ± 1.6	39.4 ± 1.2		
	Exercise Bouts						
	EB1	PreEB2	EB2	PreEB3	EB3	PreEB4	Fatigue
CON							
[Hb] _a	15.1 ± 0.7 [*]	15.4 ± 0.7 [*]	15.7 ± 0.7 [*]	15.7 ± 0.8 [*]	15.8 ± 1.0 [*]	16.0 ± 0.8 [*]	16.4 ± 0.9 [*]
Hct _a	41.5 ± 2.1 [†]	43.4 ± 2.4 [†]	43.2 ± 1.7 [†]	43.2 ± 2.6 [†]	44.0 ± 3.2 [†]	44.2 ± 2.6 [†]	45.5 ± 3.0 [†]
CHO							
[Hb] _a	15.2 ± 0.5 [*]	15.3 ± 0.6 [*]	15.7 ± 0.6 [*]	15.6 ± 0.8 [*]	16.0 ± 0.5 [*]	15.9 ± 0.7 [*]	16.2 ± 0.8 [*]
Hct _a	41.5 ± 1.4 [†]	42.3 ± 1.6 [†]	43.5 ± 1.7 [†]	43.3 ± 1.6 [†]	43.7 ± 1.6 [†]	44.2 ± 1.6 [†]	44.7 ± 2.2 [†]
	Recovery Time (min)						
	1	2	5	10	20	30	
CON							
[Hb] _a	16.1 ± 1.0 [*]	15.9 ± 1.0 [*]	15.8 ± 1.0 [*]	15.4 ± 1.0 [*]	14.8 ± 1.0 [*]	14.7 ± 1.0	
Hct _a	45.8 ± 3.8 [†]	44.4 ± 3.4 [†]	44.4 ± 3.4 [†]	42.9 ± 3.1 [†]	41.4 ± 3.5 [†]	40.7 ± 2.8	
CHO							
[Hb] _a	16.1 ± 0.8 [*]	16.0 ± 0.8 [*]	15.7 ± 0.7 [*]	15.3 ± 0.8 [*]	14.9 ± 0.8 [*]	14.7 ± 0.8	
Hct _a	44.8 ± 2.2 [†]	44.2 ± 1.9 [†]	44.0 ± 1.8 [†]	43.1 ± 2.1 [†]	41.2 ± 2.0 [†]	40.5 ± 2.2	

* [Hb]_a greater than baseline (time main effect; $p < 0.05$); † Hct_a greater than baseline (time main effect; $p < 0.05$). All data mean ± SD, n = 8.

Table 3.3 Venous haemoglobin concentration ($[\text{Hb}]_v$; $\text{g}\cdot\text{dL}^{-1}$) and haematocrit (Hct_v ; %) measured at baseline, during 60 min rest and during high intensity intermittent exercise at 130% $\dot{V}\text{O}_{2\text{peak}}$ continued to fatigue and recovery, following either carbohydrate (CHO), or placebo (CON) ingestion.

	Rest (min)						
	Baseline	10	20	40	60		
CON							
$[\text{Hb}]_v$	14.3 ± 0.8	14.3 ± 0.8	14.3 ± 0.9	14.2 ± 0.7	14.4 ± 0.9		
Hct_v	39.2 ± 2.7	39.5 ± 2.0	39.2 ± 2.4	39.2 ± 1.9	39.2 ± 2.3		
CHO							
$[\text{Hb}]_v$	14.3 ± 0.7	14.3 ± 0.7	14.3 ± 0.7	14.2 ± 0.7	14.4 ± 0.6		
Hct_v	39.3 ± 1.2	39.5 ± 1.5	39.2 ± 1.4	38.8 ± 1.7	39.0 ± 1.9		
	Exercise Bouts						
	EB1	PreEB2	EB2	PreEB3	EB3	PreEB4	Fatigue
CON							
$[\text{Hb}]_v$	$14.6 \pm 0.8^*$	$14.9 \pm 0.9^*$	$15.1 \pm 0.7^*$	$15.1 \pm 0.9^*$	$15.2 \pm 1.2^*$	$15.6 \pm 0.8^*$	$15.5 \pm 1.1^*$
Hct_v	$40.3 \pm 2.3^\dagger$	$41.0 \pm 2.5^\dagger$	$41.4 \pm 2.6^\dagger$	$42.1 \pm 2.7^\dagger$	$42.0 \pm 2.8^\dagger$	$42.9 \pm 2.4^\dagger$	$43.2 \pm 2.9^\dagger$
CHO							
$[\text{Hb}]_v$	$14.8 \pm 0.6^*$	$14.7 \pm 0.5^*$	$14.8 \pm 0.5^*$	$15.0 \pm 0.6^*$	$15.0 \pm 0.3^*$	$15.6 \pm 0.7^*$	$15.7 \pm 0.9^*$
Hct_v	$41.3 \pm 1.8^\dagger$	$40.3 \pm 2.2^\dagger$	$40.7 \pm 1.8^\dagger$	$41.8 \pm 1.0^\dagger$	$42.1 \pm 2.3^\dagger$	$42.2 \pm 1.9^\dagger$	$43.0 \pm 1.9^\dagger$
	Recovery Time (min)						
	1	2	5	10	20	30	
CON							
$[\text{Hb}]_v$	$15.7 \pm 1.3^*$	$15.7 \pm 1.3^*$	$15.6 \pm 0.9^*$	$15.4 \pm 1.0^*$	$14.9 \pm 1.1^*$	14.6 ± 1.1	
Hct_v	$43.9 \pm 3.3^\dagger$	$44.0 \pm 3.0^\dagger$	$43.5 \pm 2.8^\dagger$	$43.2 \pm 2.9^\dagger$	$41.3 \pm 3.0^\dagger$	40.3 ± 3.1	
CHO							
$[\text{Hb}]_v$	$15.2 \pm 0.4^*$	$15.6 \pm 0.9^*$	$15.6 \pm 0.9^*$	$15.3 \pm 0.9^*$	$14.9 \pm 0.8^*$	14.4 ± 0.8	
Hct_v	$42.2 \pm 1.7^\dagger$	$43.6 \pm 3.5^\dagger$	$43.7 \pm 2.6^\dagger$	$42.6 \pm 2.6^\dagger$	$40.9 \pm 1.0^\dagger$	40.0 ± 1.9	

* $[\text{Hb}]_v$ greater than baseline (time main effect; $p < 0.05$); $^\dagger\text{Hct}_v$ greater than baseline (time main effect; $p < 0.05$). All data mean \pm SD, $n = 8$.

Table 3.4 Change in plasma volume relative to baseline in arterial (ΔPV_a) and venous blood (ΔPV_v), and the calculated arterio-venous plasma volume difference ($\Delta PV_{a-v \text{ diff}}$), measured at baseline, during 60 min rest and high intensity intermittent exercise at 130% $\dot{V}O_2$ peak continued to fatigue and recovery, following either carbohydrate (CHO), or placebo (CON) ingestion.

	Rest (min)						
	Baseline	10	20	40	60		
CON							
ΔPV_a	-	0.0 ± 2.0	$1.8 \pm 2.0^*$	1.1 ± 2.5	-2.0 ± 2.4		
ΔPV_v	-	-0.7 ± 4.3	1.0 ± 5.2	1.0 ± 5.3	-0.5 ± 5.3		
$\Delta PV_{a-v \text{ diff}}$	0.8 ± 3.2	-0.1 ± 2.0	-0.7 ± 2.0	0.5 ± 1.7	2.1 ± 2.3		
CHO							
ΔPV_a	-	-0.3 ± 2.6	$2.3 \pm 3.7^*$	1.7 ± 3.6	0.07 ± 4.6		
ΔPV_v	-	-0.0 ± 2.6	0.8 ± 1.9	2.2 ± 3.7	-0.5 ± 3.9		
$\Delta PV_{a-v \text{ diff}}$	1.6 ± 0.1	0.9 ± 1.6	-0.5 ± 1.2	1.0 ± 1.9	1.1 ± 2.7		
	Exercise Bouts						
	EB1	PreEB2	EB2	PreEB3	EB3	PreEB4	Fatigue
CON							
ΔPV_a	$-8.5 \pm 3.6^*$	$-13.3 \pm 4.2^*$	$-14.5 \pm 3.0^*$	$-14.3 \pm 4.2^*$	$-15.4 \pm 7.1^*$	$-16.7 \pm 4.3^*$	$-20.9 \pm 3.0^*$
ΔPV_v	-3.8 ± 6.2	$-6.9 \pm 4.9^\dagger$	$-8.6 \pm 5.6^\dagger$	$-10.1 \pm 5.8^\dagger$	$-9.4 \pm 6.5^\dagger$	$-13.2 \pm 5.1^\dagger$	$-13.0 \pm 5.3^\dagger$
$\Delta PV_{a-v \text{ diff}}$	5.8 ± 5.0	$8.1 \pm 4.4^\ddagger$	$7.6 \pm 5.1^\ddagger$	5.6 ± 5.6	$7.9 \pm 2.8^\ddagger$	4.8 ± 2.7	$10.8 \pm 7.6^\ddagger$
CHO							
ΔPV_a	$-8.2 \pm 5.2^*$	$-9.8 \pm 3.5^*$	$-13.5 \pm 3.3^*$	$-12.2 \pm 4.9^*$	$-15.8 \pm 2.7^*$	$-15.5 \pm 3.3^*$	$-18.2 \pm 4.1^*$
ΔPV_v	$-6.0 \pm 4.6^\dagger$	$-5.0 \pm 5.2^\dagger$	$-6.5 \pm 7.9^\dagger$	$-10.0 \pm 2.3^\dagger$	$-11.8 \pm 5.0^\dagger$	$-12.3 \pm 1.7^\dagger$	$-13.8 \pm 5.0^\dagger$
$\Delta PV_{a-v \text{ diff}}$	3.7 ± 3.1	$7.3 \pm 3.8^\ddagger$	$10.3 \pm 8.2^\ddagger$	5.0 ± 2.2	$6.6 \pm 3.7^\ddagger$	3.6 ± 2.7	$6.8 \pm 4.0^\ddagger$
	Recovery Time (min)						
	1	2	5	10	20	30	
CON							
ΔPV_a	$-20.0 \pm 4.9^*$	$-17.5 \pm 3.5^*$	$-16.8 \pm 3.9^*$	$-12.4 \pm 4.2^*$	$-6.3 \pm 5.4^*$	$-3.3 \pm 4.7^*$	
ΔPV_v	$-15.3 \pm 6.0^\dagger$	$-15.5 \pm 4.9^\dagger$	$-16.3 \pm 5.8^\dagger$	$-12.7 \pm 5.5^\dagger$	$-6.9 \pm 7.3^\dagger$	$-3.2 \pm 6.8^\dagger$	
$\Delta PV_{a-v \text{ diff}}$	$7.0 \pm 8.7^\ddagger$	3.8 ± 5.8	2.0 ± 2.1	0.9 ± 3.7	0.3 ± 3.0	-0.3 ± 1.3	
CHO							
ΔPV_a	$-17.8 \pm 3.4^*$	$-16.5 \pm 2.9^*$	$-14.7 \pm 3.9^*$	$-11.0 \pm 3.5^*$	$-5.6 \pm 3.3^*$	$-3.2 \pm 2.9^*$	
ΔPV_v	$-14.2 \pm 5.0^\dagger$	$-17.1 \pm 6.1^\dagger$	$-14.7 \pm 4.9^\dagger$	$-11.1 \pm 4.9^\dagger$	$-5.9 \pm 3.2^\dagger$	$-2.5 \pm 4.0^\dagger$	
$\Delta PV_{a-v \text{ diff}}$	$5.1 \pm 2.2^\ddagger$	0.2 ± 3.9	0.9 ± 3.46	0.88 ± 2.4	0.57 ± 1.1	1.6 ± 1.5	

* ΔPV_a greater than baseline (time main effect; $p < 0.05$); $^\dagger \Delta PV_v$ greater than baseline (time main effect; $p < 0.05$); $^\ddagger \Delta PV_{a-v \text{ diff}}$ greater than baseline (time main effect; $p < 0.05$). All data mean \pm SD, n = 8.

3.3.10 Skeletal muscle NKA alpha isoform protein abundances

Representative blots for all six NKA isoforms analysed are displayed in Fig. 3.7.

There were no significant main effects for time or treatment or significant time-by-treatment interaction for any of the NKA α isoforms (Fig. 3.8). The main effect for time for NKA α_3 tended to significance, ($p = 0.07$; Fig. 3.8), and a small effect size ($ES = 0.38 \pm 0.18$) for decreased α_3 protein abundance at fatigue compared to 60 min but only within CON.

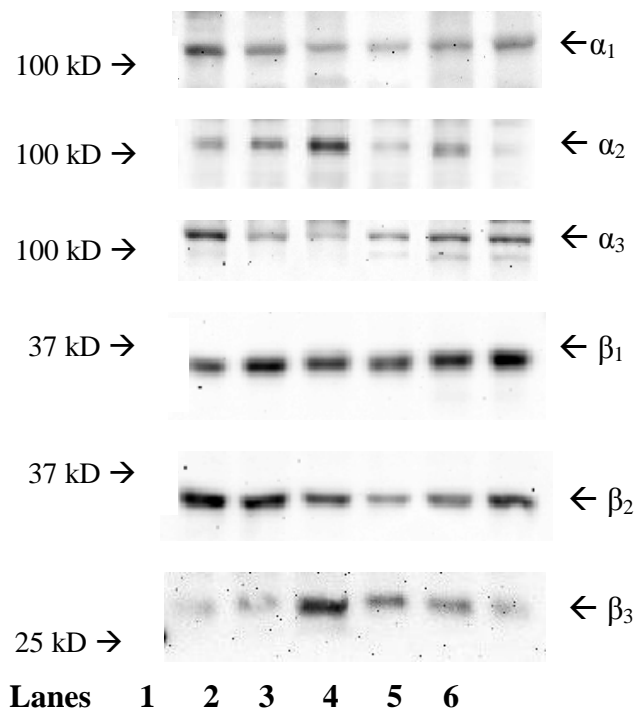


Figure 3.7 Representative immunoblots of NKA α_1 , α_2 , α_3 , β_1 , β_2 and β_3 isoforms in homogenates of the human vastus lateralis muscle. Values at left indicate molecular weight of bands. Protein bands from left to right are Baseline, 60 min post ingestion and Fatigue, with lanes 1-3 CON, lanes 4-6 CHO.

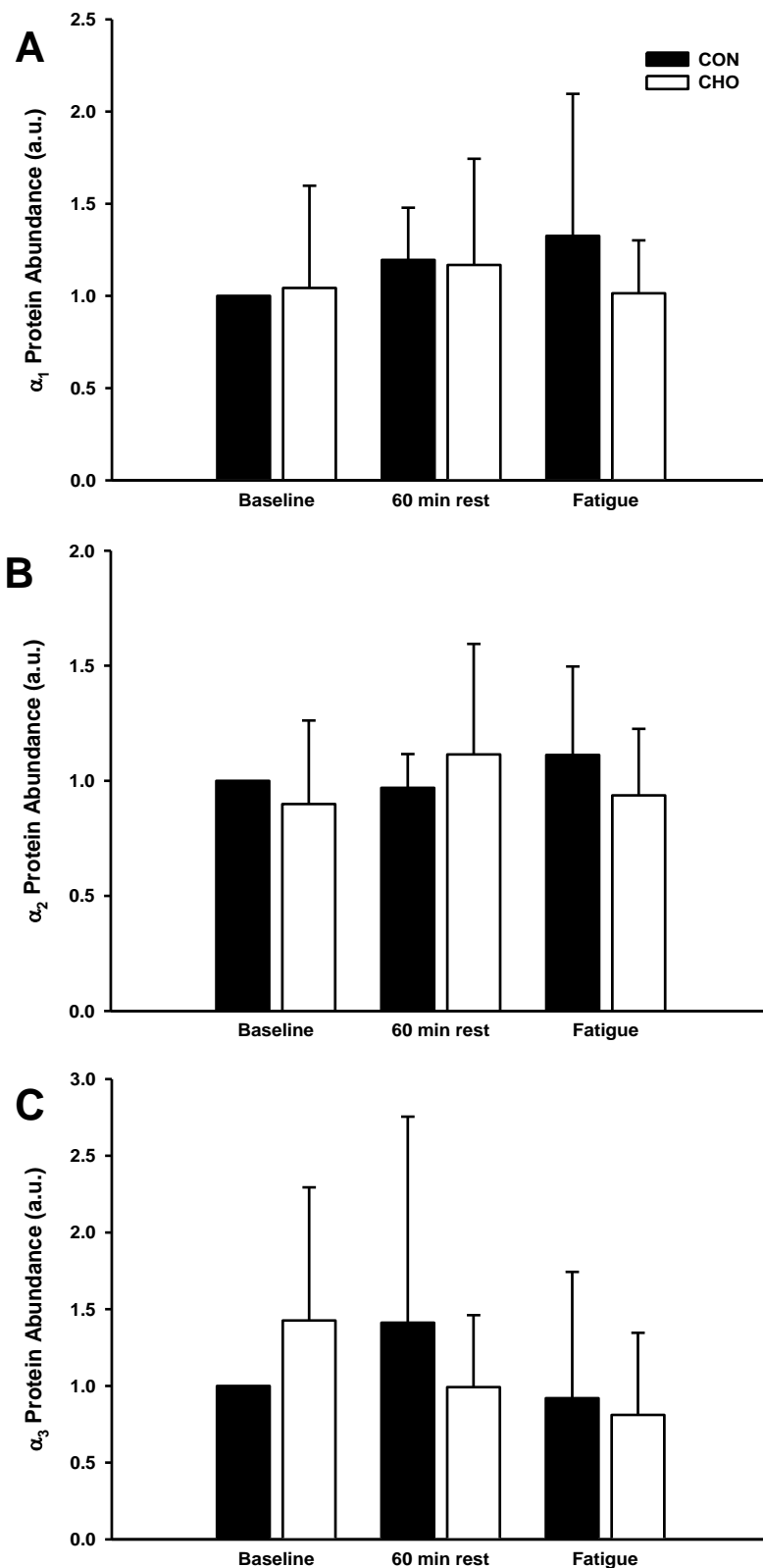


Figure 3.8 Muscle NKA α isoform relative protein abundance at Baseline, 60 min rest following either carbohydrate (CHO) or placebo (CON) ingestion and at Fatigue. NKA α_1 (A); NKA α_2 (B); NKA α_3 (C). All results are normalised against total protein loaded and expressed relative to baseline from the CON trial. Data are mean \pm SD, n = 8.

3.3.11 Skeletal muscle NKA beta isoform protein abundances

There were no significant main effects for the NKA β_1 or β_2 isoforms. There was a small effect size ($ES = 0.36 \pm 0.26$) for increased β_1 protein abundance at fatigue compared to 60 min but only within CON; and a small effect size ($ES = 0.27 \pm 0.32$; Fig. 3.9) for an increased β_2 protein abundance at fatigue in CHO compared to CON.

There was no significant main effect for time or treatment for NKA β_3 (Fig. 3.9), but a significant time-by-treatment interaction was found ($p < 0.01$). Post-hoc analyses revealed a greater NKA β_3 at fatigue than 60 min rest within CON ($p = 0.004$; $ES = 1.29 \pm 0.42$), and a tendency to greater β_3 in CHO than CON at 60 min rest ($p = 0.06$, $ES = 1.00 \pm 0.86$). A moderate effect size was found for decreased β_3 protein at fatigue in CHO compared to CON ($ES = 0.61 \pm 0.82$).

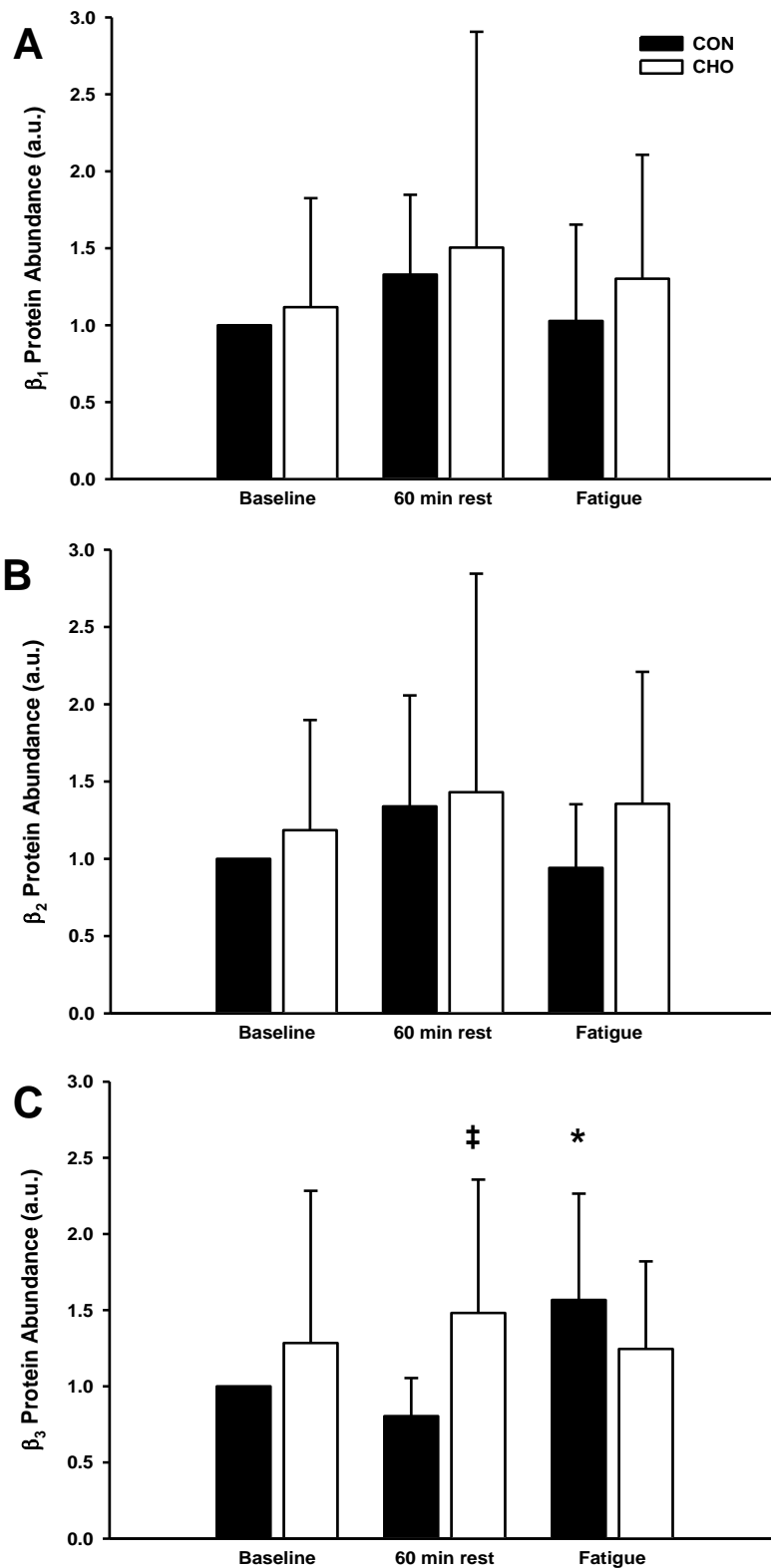


Figure 3.9 Muscle NKA β isoform relative protein abundance at Baseline, 60 min rest following either carbohydrate (CHO) or placebo (CON) ingestion and at Fatigue. NKA β_1 (A); NKA β_2 (B); NKA β_3 (C). All results are normalised against total protein loaded and expressed relative to baseline from the CON trial. Data are mean \pm SD, $n = 8$. *CON 60 min rest < CON Fatigue (interaction main effect, $p < 0.05$). ‡ Tendency to higher CON than CHO.

3.4 Discussion

This study investigated the effects of an oral glucose load, which induced an endogenous insulin increase to high physiological levels, on plasma K^+ and electrolyte homeostasis and on skeletal muscle NKA isoform abundance prior to, during and after high-intensity interval exercise that included a final bout continued until fatigue. Glucose ingestion significantly affected plasma $[K^+]$, lowering both arterial and venous $[K^+]$ and with a more positive K^+_{a-v} across the forearm following CHO ingestion, suggesting an increased K^+ uptake into the forearm muscle during and following high intensity intermittent exercise. However, no significant changes were detected in vastus lateralis muscle NKA protein abundance following CHO ingestion, and no change in exercise performance was recorded.

Intense exercise is associated with a net movement of fluid into the active muscles and a corresponding decrease in plasma volume by up to 20% (Lundvall *et al.*, 1972) as was seen in the present study with a large decrease in arterial plasma, of up to 20% at fatigue. These plasma volume shifts are most likely due to a net osmotic flux of water from plasma as well as from the extravascular space of inactive tissues to protect the vascular volume (Lundvall *et al.*, 1972; Lindinger *et al.*, 1994) as indicated by a net gain in plasma water as blood traversed the forearm, suggesting that a greater net K^+ uptake wasn't simply due to a haemoconcentration effect, as this would have lowered the arterio-venous $[K^+]$ difference. While there was an increase in the measured $[Hb]$ and Hct, and a decrease in plasma volume with exercise, there was no difference between conditions, indicating that glucose ingestion and the subsequent increase in endogenous insulin had no effect on blood flow, this is despite increases in forearm blood flow seen previously during hyperinsulinaemic clamps (Fugmann *et al.*, 1998). However, during

leg exercise an increase in blood flow to inactive arm muscles by 2-3-fold has been previously reported (Bevegard & Shepherd, 1966; Tanaka *et al.*, 2006), and this increased perfusion of inactive tissue is suggested to aid the correction of arterial ionic disturbances as a result of intense exercise in humans (Lindinger *et al.*, 1990a).

3.4.1 Glycaemic and metabolic responses

Glucose ingestion increased $[\text{insulin}]_a$ to 5-fold greater than at baseline, and induced large rises in $[\text{glucose}]_a$ at rest to $\sim 10 \text{ mmol.L}^{-1}$; this increase persisted throughout the exercise period, demonstrating the efficacy of the glucose ingestion protocol. In contrast during CON, a slow increase in plasma $[\text{glucose}]$ occurred as exercise progressed and in early recovery, consistent with liver glycogenolysis and hepatic glucose release (Wahren *et al.*, 1971). Similar temporal responses were seen for $[\text{glucose}]_v$ as in arterial blood, whilst the wide positive $[\text{glucose}]_{a-v}$ indicated a large net glucose uptake into the forearm, which is consistent with peripheral glucose disposal (McConnell *et al.*, 1994).

The exercise protocol induced considerable metabolic disturbances. The intense nature of the exercise was indicated by the large increase in $[\text{Lac}]_a$ which exceeded 20 mmol.L^{-1} . Whilst the $[\text{Lac}]_{a-v}$ indicated a net uptake of lactate by the forearm, presumably by the forearm skeletal muscles, there was no difference with glucose ingestion compared to placebo. There was also a large increase in $[\text{H}^+]_a$ and $[\text{H}^+]_v$ representing increased plasma acidity, but with no difference between CON and CHO trials.

The NKA cycle relies on glycolytic ATP production/supply (Dutka & Lamb, 2007), and previous research has linked increased NKA activity with increased lactate production in skeletal muscle (James *et al.*, 1996). Insulin increases NKA activity in skeletal muscle (Clausen & Kohn, 1977). Hence it was anticipated that increased endogenous insulin with oral glucose ingestion would increase skeletal muscle NKA activity, muscle lactate

production and therefore increase plasma [lactate]. However, there was no measured effect of glucose ingestion on plasma [lactate] in the current study. However, lactate is both produced and utilised by skeletal muscle fibres (Stainsby *et al.*, 1991) and it is therefore possible that any insulin-induced increase in lactate production as a result of increased NKA activity could be masked by a simultaneous increase in lactate utilisation (Novel-Chate *et al.*, 2001) as well as the large metabolic changes in the contracting muscle (Green, 1997). It is likely that the intense nature of the exercise swamped any smaller glycolytic effects of the NKA due to insulin stimulation.

3.4.2 CHO effects on K⁺ homeostasis

The large increases in plasma glucose and hence insulin, were however sufficient to lower [K⁺] in arterial and venous plasma, and to increase the [K⁺]_{a-v} difference across the forearm (treatment main effects). A most notable effect was plasma [K⁺]_v decreasing during exercise in CHO, compared to increases during CON, with a resultant 1.0 mmol.L⁻¹ lower plasma [K⁺] at the point of fatigue following glucose ingestion. These findings extend previous reports that insulin infusion can elicit a decrease in plasma [K⁺] (Andres *et al.*, 1962; DeFronzo *et al.*, 1980) by demonstrating that an oral glucose load elevating insulin to physiological concentrations also markedly affects K⁺ homeostasis. Previous research (Muto *et al.*, 2005) failed to detect a decrease in [K⁺]_v in response to an oral glucose load in control subjects. This is consistent with the current study, where, despite significant main effects for decreased arterial and venous [K⁺], post-hoc analysis failed to find differences between the trials at rest. However, analysis of the exercise and recovery data revealed a clear glucose lowering effect on K⁺. With [K⁺]_v significantly lower during the exercise phase following glucose ingestion, with the exception of EB3. This was also in conjunction with [Na⁺]_a being consistently elevated during exercise for

CHO. This lowering of plasma $[K^+]_v$ could be due to an insulin-induced increase in NKA activity of the forearm muscles, as previously demonstrated in the plasma membranes of rat skeletal muscles (Hundal *et al.*, 1992; Marette *et al.*, 1993).

Plasma $[K^+]$ is tightly regulated between extrarenal disposal and renal excretion. During the first hour of an insulin clamp, around 30% of K^+ uptake was attributable to peripheral tissues including skeletal muscles, with the splanchnic bed responsible for the remaining 70% of the K^+ uptake (Andres *et al.*, 1962). The wide $[K^+]_{a-v}$ seen across the forearm in the current study, strongly suggests that skeletal muscle uptake was primarily responsible for the lowering of plasma $[K^+]$ seen. It has also been suggested that a high plasma [glucose] increases the supply of energy to fuel glycolytic ATP for the NKA (Okamoto *et al.*, 2001; Dufer *et al.*, 2009) thus providing the energetic basis for an increase in NKA activity. This association is consistent with greater $[K^+]_{a-v}$ and $\Delta[K^+]_{a-v}$ in CHO compared to CON for the first 3 exercise bouts.

Previous studies have demonstrated that nonworking tissues take up large amounts of lactate, as well as K^+ and Na^+ , and play an active role in ion regulation during intense exercise (Poortmans *et al.*, 1978; Kowalchuk *et al.*, 1988a; Lindinger *et al.*, 1990a). The more positive arterio-venous $[K^+]$ difference seen following glucose ingestion likely represents a greater net uptake of K^+ into the relatively inactive forearm, at a rate almost double compared to the CON.

There was also an increase in arterial and venous plasma $[Na^+]$, however plasma $[Na^+]$ does not increase in proportion to plasma volume decrease (Lindinger *et al.*, 1994), and also increases proportionately less than plasma $[K^+]$ (Harrison, 1985). The 4-6% increase in plasma $[Na^+]$ in the present study was much less than could be accounted for by the up to 20% decrease seen in plasma volume, thereby indicating the net loss of Na^+

from the plasma compartment. Previous research has suggested that Na^+ may be taken up by contracting muscle (Kowalchuk *et al.*, 1988b) and inactive tissues (Kowalchuk *et al.*, 1988a; Lindinger *et al.*, 1990a) during exercise. This is consistent with the positive $[\text{Na}^+]_{\text{a-v}}$ seen in this study.

3.4.3 CHO Effects on Exercise Performance

There was no improvement in exercise performance, measured via time to fatigue in the fourth bout of high-intensity intermittent cycling exercise when performed 60 min following CHO ingestion. Hence any insulin-stimulated skeletal muscle NKA activity and cellular K^+ uptake, resulting in less membrane depolarisation was insufficient to enhance muscle function. Previous research has demonstrated that oral glucose ingestion can enhance glucose utilisation, improve exercise performance and attenuate fatigue, in humans (Coyle *et al.*, 1983; Coyle *et al.*, 1986; Green *et al.*, 2007a), and animal models (Karelis *et al.*, 2002). However, these studies all examined prolonged submaximal exercise, where increased plasma [glucose] is more closely aligned with the attenuation of muscle fatigue compared to increased plasma [insulin] (Karelis *et al.*, 2003). This contrasts the high-intensity intermittent exercise protocol utilised here, where factors such as glucose supply and glucose delivery to the contracting muscles are less likely to relate to fatigue than impairments to excitability or the sequelae from severe metabolic disturbances.

3.4.4 Exercise and CHO Effects on NKA Protein Abundance

There was no effect of intense intermittent cycling exercise on NKA isoform protein abundance for any of the α_{1-3} or β_{1-2} isoforms, indicating that there was no increase in protein synthesis, or unmasking of isoforms from latent storage pools occurring, or an

inability to detect these changes within a short time frame. This finding supports previous research that found no change in NKA isoform protein abundance following acute high intensity exercise (Juel *et al.*, 2000a; Murphy *et al.*, 2004). However, there was a significant increase in NKA β_3 for CON following high-intensity intermittent exercise, which contrasts to the single bout of exercise utilised previously (Murphy *et al.*, 2004; Aughey *et al.*, 2007). There were no effects of CHO on skeletal muscle NKA protein abundance. It has also been suggested that insulin is responsible for translocation of the NKA protein between the plasma membrane and intracellular stores (Hundal *et al.*, 1992; Lavoie *et al.*, 1996). However, studies analysing the location of the NKA in skeletal muscle have focused on the isolation and purification of the enzyme through the process of subcellular fractionation (Hundal *et al.*, 1994; Dombrowski *et al.*, 1996; Rasmussen *et al.*, 2008), and due to the loss of protein when separating the plasma membrane from other cell structures, the recovery of the NKA protein is usually quite low, with values ranging from 0.2-8.9% (Clausen, 1986). This makes it very difficult to ascertain whether the sample measured is an accurate representation of the total population of the NKA (Clausen, 1986).

Insulin has been shown to increase NKA activity in studies examining ouabain-suppressible $^{86}\text{Rb}^+$ uptake in rat adipocytes and kidney (Resh *et al.*, 1980; Feraille *et al.*, 1995). In humans, NKA activity has been measured in crude muscle homogenates by a highly sensitive fluorometric assay using 3-*O*-methylfluorescein (3-*O*-MFPase), and on the basis of the 3-*O*-MFPase activity the NKA activity can be quantified (Fraser *et al.*, 2002). However, this method uses 3-*O*-MFP as an artificial substrate and does not involve the hydrolysis of ATP. It also cannot analyse the Na^+ -dependent activation, and the K^+ sensitivity obtained may not reflect the sensitivity of the intact ATPase, therefore

these ion-induced activity values may not reflect the activity in the intact organism (Juel, 2009). A recent study comparing methods of measuring NKA activity found that the 3-O-MFPase activity assay was unable to detect changes in NKA activity and was unsuitable for detecting changes in NKA activity with exercise (Juel *et al.*, 2013). Further research is required to determine the best method of measuring changes in NKA activity in human skeletal muscle.

3.4.5 Limitations

Care should be taken when interpreting the protein expression results due to the variability evident in the results, partly due to variability in the individual responses to the protocol utilised. Also the small number of subjects and the lack of additional post-exercise biopsy sampling times prevented the detection of any delayed responses in isoform protein abundance. Total NKA protein content was also not measured in the current study. Whilst the VO_4 -facilitated assay for [^3H]ouabain binding has been widely used for measurement of NKA content on human muscle biopsy specimens from the vastus lateralis muscle (Clausen, 1996), this technique does not distinguish between the different NKA α isoforms and was not used here.

The inclusion of measures of forearm blood flow would have enabled the calculation of ion uptake by the forearm muscles, as well as the measurement of intracellular and interstitial $[\text{K}^+]$ could have provided more detailed information on the K^+ kinetics.

3.4.6 Conclusions

This study combined the well established protocol of a glucose tolerance test with performing high intensity intermittent exercise. This provided a novel approach to examine the effects of a physiological (endogenous) increase in plasma insulin concentration on the regulation of K^+ and other electrolytes, skeletal muscle NKA

isoform protein abundance and exercise performance. The results provide support for the first hypothesis, demonstrating that there was a significant effect of glucose ingestion on plasma K^+ regulation, however this was only seen during exercise (and recovery) and not at rest. Most interestingly, plasma $[K^+]_v$ decreased during the CHO exercise trial, compared to an increase during the CON trial exercise, such that plasma $[K^+]$ was 1.0 mmol.L^{-1} less at the point of fatigue following CHO ingestion compared to CON, however these effects on K^+ homeostasis were insufficient to improve exercise performance. Given that there was no effect on NKA isoform protein abundance the second hypothesis was accepted, with the exception of β_3 which showed an increase, it is likely that this $[K^+]_v$ lowering was due to increased activity of the NKA. Whilst this was not measured, *in vivo* NKA activity was reflected in the calculated $\Delta[K^+]$ which showed a treatment main effect for decreased $\Delta[K^+]_v$ and increased $\Delta[K^+]_{a-v}$ following glucose ingestion. These results showed that physiological concentrations of insulin induced through an oral glucose load can have a significant K^+ lowering effect during high-intensity intermittent exercise, probably via K^+ uptake by skeletal muscles. Further investigation is required to determine the signalling mechanisms involved in this process.

CHAPTER 4. The effects of acute and chronic sodium bicarbonate supplementation and repeat sprint exercise on skeletal muscle NKA protein abundance

4.1 Introduction

High intensity exercise causes a loss of K^+ from the contracting muscles (Bangsbo *et al.*, 1996), and a large rise in muscle interstitial $[K^+]$ (Juel *et al.*, 2000b; Nordsborg *et al.*, 2003; Mohr *et al.*, 2004). Increases in $[K^+]$ in the t-tubules and interstitium and declines in $[K^+]_i$ have been proposed to depolarise of the muscle membrane, leading to excitation failure and reduced exercise performance (Sejersted & Sjøgaard, 2000; Clausen, 2003). Intense muscle contractions also lead to marked reductions in intracellular pH, due primarily to increased glycolysis (Spriet *et al.*, 1989; Broch-Lips *et al.*, 2007). This acidosis has also been suggested to be a major cause of fatigue in isolated muscle preparations by reducing the sensitivity of the contractile apparatus to calcium (Fitts, 1994; Nelson & Fitts, 2014). However, experiments on isolated muscles have shown that when force is depressed due to high $[K^+]_o$, acidification by lactic acid produced a pronounced recovery of force, and therefore may actually protect against K^+ -induced fatigue (Nielsen *et al.*, 2001; de Paoli *et al.*, 2007). The interactions between acidosis, K^+ homeostasis, and muscle function remain incompletely understood, especially *in-vivo* in humans.

Although the role of acidosis per se in muscle fatigue remains controversial, it is clear that sodium bicarbonate ($NaHCO_3$) ingestion can enhance high intensity exercise performance, including a one minute bout of high-intensity cycle exercise (McNaughton, 1992; McNaughton *et al.*, 1999) and repeated 6 s sprints with 30 s recovery between sprints (Bishop *et al.*, 2004). Whilst the underlying mechanisms of this are still unclear,

many early studies suggested that the performance-enhancing effects of NaHCO₃ were largely associated with metabolic alkalosis, attenuating the rate of free H⁺ accumulation in the sarcoplasm, in turn delaying the onset of fatigue (Fitts, 2008). However, NaHCO₃ had no effect on pre- or post-exercise muscle pH or resting *in-vitro* muscle buffer capacity, yet improved repeat sprint performance was observed (Bishop *et al.*, 2004). Furthermore, ingestion of NaHCO₃ decreased both muscle and blood [H⁺] at rest and during prolonged submaximal exercise, but without affecting performance (Stephens *et al.*, 2002). This suggests that alternative or at least additional factors might be involved in the ergogenic effects of NaHCO₃.

Studies on perfused rat hindlimb demonstrated that respiratory alkalosis significantly lowered resting [K⁺]_i, and attenuated the decline in [K⁺]_i following electrical stimulation compared to controls (Lindinger *et al.*, 1990b). In humans, ingestion of NaHCO₃ lowered circulating [K⁺] at rest and during finger flexion exercise and increased K⁺ reuptake into muscle at fatigue and during recovery; this was associated with a greater time to fatigue during exercise (Sostaric *et al.*, 2006). Thus, NaHCO₃ ingestion can enhance intense exercise performance, which may be in part be due to enhanced K⁺ regulation. The effect of chronic NaHCO₃ supplementation is of interest for K⁺ regulation during training. Supplementation of NaHCO₃ for 5 days increased time to exhaustion during constant load cycling exercise, relative to placebo (Mueller *et al.*, 2013). Hence it is possible that chronic NaHCO₃ ingestion, repeated prior to training sessions improves both K⁺ homeostasis and training adaptations. The major factor influencing K⁺ homeostasis in muscle during exercise is the NKA in skeletal muscle, which contributes to the maintenance of cellular excitability increasing uptake of K⁺ by

contracting and inactive muscle (Clausen, 2003) thereby attenuating the increase in $[K^+]_o$ and plasma $[K^+]$.

Few studies have investigated the acute effects of exercise on NKA isoform protein abundance. Common findings were that NKA α_{1-3} and β_{1-3} protein abundance were unchanged in muscle following an acute bout of high intensity one-legged knee extensor exercise (Juel *et al.*, 2000a; Murphy *et al.*, 2004), or high-intensity interval cycling (Aughey *et al.*, 2007). However, an exception to this was a 26% increase in NKA α_2 protein abundance less than one hour after the first 6 min high intensity bout of a 16 hr intermittent protocol (Green *et al.*, 2007b). Increases in NKA α_2 protein expression have occurred after 3 days of prolonged submaximal cycle training (9%) in previously untrained adults (Green *et al.*, 2004), after 2 wks intensified training (15%) in trained athletes (Thomassen *et al.*, 2010), and after 9 wks of training (68%) in endurance trained runners (Bangsbo *et al.*, 2009). In contrast, NKA α_{1-3} and β_{1-3} isoform protein abundance measured in whole muscle homogenate was unchanged following 3 wks high-intensity interval training in trained cyclists (Aughey *et al.*, 2007). Intense exercise training is likely to increase the NKA protein abundance and also enhances exercise performance. Repeated high-intensity sprints of short duration are a common component of many team sports, making the ability to recover quickly an important attribute of the team sport athlete.

Therefore the effect of chronic pre-training $NaHCO_3$ supplementation on skeletal muscle NKA isoform protein abundance will be examined in this study. The effects of repeated $NaHCO_3$ ingestion combined with intense training on muscle NKA are unknown and were investigated here. This was part of a larger collaborative study which included analysis of the effects of $NaHCO_3$ supplementation on venous plasma $[K^+]$ and repeated

sprint exercise (RSE) performance (Varley, 2013). The RSE and $[K^+]$ data do not however, form part of this thesis and will not be presented here. Due to the limitations regarding the measurement of NKA activity (see section 2.5.2) in skeletal muscle following exercise this was not measured. Therefore the aim of this study was to investigate the effects of acute and chronic (pre-exercise) $NaHCO_3$ supplementation, as well as acute and chronic exercise, on NKA isoform protein abundance in skeletal muscle. It was hypothesised that NKA α_{1-3} and β_{1-3} isoform protein abundance would each remain unchanged following acute exercise and $NaHCO_3$ supplementation, whereas NKA α_2 and β_1 isoform protein abundance would be increased after 4 wks RSE training with chronic $NaHCO_3$ supplementation.

4.2 Methods

4.2.1 Participants

Seven healthy, recreationally active young adults (5 males and 2 females, Table 4.1) who were involved in various club level sports (soccer, netball, Australian football) gave their written informed consent to participate in the study, which was approved by the Victoria University Human Research Ethics Committee.

Table 4.1 Participant Characteristics (n = 7)

Variable	Mean	SD
Age (yrs)	21.6	1.6
Height (cm)	174.4	9.6
Body mass (kg)	70.0	8.1
$\dot{V}O_{2\text{peak}}$ (ml.kg ⁻¹ .min ⁻¹)	51.6	5.1

4.2.2 Experimental design

Participants initially underwent an incremental exercise test on a motorised treadmill and on two subsequent visits, performed a familiarisation session of repeat sprint exercise (RSE). Participants then completed an initial pre-training RSE session during which participants ingested a placebo, calcium carbonate (CaCO₃), prior to RSE (PRE-CaCO₃). Participants completed a second pre-training trial where participants ingested sodium bicarbonate (NaHCO₃) prior to RSE to determine the acute effects of supplementation on RSE (PRE-NaHCO₃). Following these two pre-training trials, participants then undertook four weeks of RSE training, comprising 3 sessions per week, each separated by at least 48 h for a total of 12 sessions, with participants ingesting NaHCO₃ prior to

each session. Forty-eight hours after the final training session all participants then repeated the pre-training RSE placebo trial during which CaCO_3 was ingested prior to exercise (POST- CaCO_3). Participants were instructed to refrain from consuming alcohol, caffeine and performing vigorous exercise for 48 h prior to all testing sessions. All participants were asked to fast for 12 h prior to all experimental trials. Pre- and post-exercise biopsies were taken during the PRE- CaCO_3 , PRE- NaHCO_3 and POST- CaCO_3 trials.

4.2.3 Incremental exercise test

The incremental exercise test was performed on a motorised treadmill (Quinton Q65, Seattle, WA, USA) with speed commencing at $8 \text{ km}\cdot\text{hr}^{-1}$ and subsequently increased by $1 \text{ km}\cdot\text{hr}^{-1}$ every minute, with no change in gradient, until volitional exhaustion. Participants breathed through a Hans Rudolph two-way non-rebreathing valve, with expired air passing through low resistance tubing into a 4 L mixing chamber. Expired air flow was analysed using a flow transducer (KL Engineering K520, California, USA); fractions of expired O_2 and CO_2 were measured continuously by rapidly responding analysers (Ametek S-3A/II and Ametek CD-3A, Berwyn, PA, USA). The $\dot{V}\text{O}_2$ was calculated continuously and displayed every 15 s on a personal computer (Turbofit, VacuMed, Ventura, CA, USA). The ventilometer and gas analysers were calibrated prior to each test with a standard 3 L syringe and precision reference gases. The $\dot{V}\text{O}_{2\text{peak}}$ was calculated as the mean of the two highest consecutive 15 s values in two consecutive 15 s periods. The speed at $\dot{V}\text{O}_{2\text{peak}}$ was the speed at the final 1 min stage was completed in full.

4.2.4 RSE Protocol

At least 3 days after completing the incremental exercise test, participants performed the first RSE familiarisation trial. This comprised a 4 min standardised warm up on a motorised treadmill at a running speed of 60% of the speed at $\dot{V}O_{2\text{peak}}$, followed by three warm-up runs on a non-motorised treadmill (Woodway Force, Waukesha, WI, USA), each comprising two 4 s runs at 13 km.hr⁻¹, with an intervening 20 s passive recovery, followed by 1 min of rest with a final 4 s run at 15 km.hr⁻¹. Following 1 min of passive rest, RSE commenced and comprised three sets of five, 4 s maximal sprints with 20 s of passive recovery between sprints and 4.5 min of passive rest between sets (Serpello *et al.*, 2011). Participants were instructed to run maximally during each sprint and were verbally encouraged throughout. This protocol was repeated for the second familiarisation session one week later and for all experimental trials. During the subsequent training and testing sessions the three warm-up runs were performed at 70%, 70% and 90%, respectively, of the peak speed attained during the first familiarisation trial.

4.2.5 Supplementation

Prior to each training session, participants ingested 0.3 g.kg⁻¹ NaHCO₃ encased in gelatin capsules (Sodibic, Aspen Pharmacare, St Leonards, NSW, Australia). All NaHCO₃ capsules were ingested with water *ad libitum* over a 1 h period, in 3 even doses, at 90, 60 and 30 min prior to exercise. This dosage and ingestion protocol was chosen because 0.3 g.kg⁻¹ of NaHCO₃ ingested 90 min prior to exercise lowered venous plasma [K⁺] during forearm exercise (Raymer *et al.*, 2004; Sostaric *et al.*, 2006) and pilot testing determined that this protocol did not result in any gastrointestinal disturbances. The same dose and

ingestion regime was used for the experimental trials, with either CaCO_3 or NaHCO_3 contained within the capsules.

4.2.6 Experimental trials

During the PRE- CaCO_3 , PRE- NaHCO_3 and POST- CaCO_3 experimental trials, participants arrived at the laboratory 2 hrs prior to commencement of the RSE. Participants remained in a supine position from 10 min prior to ingestion until the warm-up on the motorised treadmill and again throughout the entire recovery period. A resting biopsy was taken immediately prior to the warm-up (after CaCO_3 or NaHCO_3 ingestion) and immediately following completion of the final sprint effort.

4.2.7 Muscle biopsies

Needle muscle biopsies were taken from the middle third of the vastus lateralis muscle via incisions made after local anaesthetic (1% Xylocaine, McFarlane Medical and Scientific, Surrey Hills, VIC, Australia) was injected into the skin and subcutaneous tissue. A small incision was then made into the skin and fascia, and a small muscle sample was excised using a Stille biopsy needle. The muscle sample was blotted on filter paper to remove blood and snap frozen in liquid N_2 and stored at -80°C for later analyses.

4.2.8 NKA isoform protein abundance

4.2.8.1 Protein extraction

Frozen muscle samples of approximately 25 mg were homogenised in ice cold buffer (25 mM Tris-HCL, pH 6.8, 1% sodium dodecyl sulphate (SDS), 5 mM EGTA, 50 mM NaF, 1 mM sodium vanadates, 17.4 $\mu\text{g}/\mu\text{l}$ phenylmethylsulphonyl fluoride (PMSF), and Protease Inhibitor Cocktail (Sigma Aldrich, Sydney, NSW, Australia) for 2 x 10 s using a tissue homogeniser (TH220, Omni International, Kennesaw, GA, USA). Samples were then heated on a thermoshaker for 20 min at 56°C with a shaking speed of 750 rpm.

Total protein concentration of each sample was determined using a BCA Assay Kit (Pierce, Rockford, IL, USA), with bovine serum albumin (BSA) as the standard (Murphy *et al.*, 2006; Aughey *et al.*, 2007).

Muscle homogenates were then deglycosylated to enhance identification of the β -isoforms. This involved adding 0.5% (v/v) Nonidet P40 and 3 units N-Glycosidase F (Roche Diagnostics, Dee Why, NSW, Australia) per 0.5 mg protein and incubating for 1 hr at 37°C. Aliquots of each homogenate were mixed with Laemmli sample buffer and stored at -80°C until analysed.

4.2.8.2 Immunoblotting

SDS-PAGE 10% gels were loaded with 10 μ g (α_2 , β_1) or 20 μ g (α_1 , α_3 , β_2 , β_3) protein and run for 10 min at 100 V then 2 hr at 75 V. The linearity of the blot signal against protein loaded was confirmed for each antibody (see Appendix 5). Following electrophoresis, proteins were wet transferred (90 min, 100 V) to 0.45 μ m nitrocellulose membranes. Membranes were blocked in TBST (10 mM Tris, 100 mM NaCl, 0.02% Tween-20) containing 7.5% non-fat milk, for 1 hr at room temperature. Following washing, membranes were incubated with primary antibodies diluted in TBST buffer containing 0.1% NaN₃ and 0.1% BSA overnight at 4°C.

Membranes were washed in TBST and incubated with the appropriate anti-rabbit (NEFA812001EA) or anti-mouse (NEFA822001EA, PerkinElmer, Melbourne, VIC, Australia) horseradish peroxidase-conjugated secondary antibody for 1 hr at room temperature. Secondary antibodies were diluted 1:20,000 in TBST buffer containing 5% non-fat milk. After washing the membranes in TBST, proteins were detected using chemiluminescence reagents (Imobilon™ HRP Substrate, Millipore, Macquarie Park, NSW, Australia) and quantified via densitometric scanning (VersaDoc™ Imaging

System, Bio-Rad, Sydney, NSW, Australia) and dedicated software (Quantity One v4.6.6, BioRad, Sydney, NSW, Australia). All proteins were normalised against total protein loading detected via coomassie staining (Welinder & Ekblad, 2011).

4.2.8.3 Antibodies

Primary antibodies specific to each NKA isoform were: α_1 (1:50): monoclonal $\alpha 6F$ (developed by D. Fambrough and obtained from the Developmental Studies Hybridoma Bank developed under the auspices of the NICHD and maintained by the University of Iowa, Department of Biological Sciences, Iowa City, IA, USA); α_2 (1:200): polyclonal anti-HERED (kindly donated by T. Pressley, Texas Tech University, USA); α_3 (1:500): monoclonal MA3-915 (Thermo Scientific, Scoresby, VIC, Australia); β_1 (1:500): monoclonal MA3-930 (Thermo Scientific, Scoresby, VIC, Australia); β_2 (1:500): monoclonal 610915 (BD Biosciences, Franklin Lakes NJ, USA) and β_3 (1:500): monoclonal 610993 (BD Biosciences, Franklin Lakes NJ, USA).

4.2.9 Statistical analysis

All results are expressed as mean \pm SD. All results were normalised relative to the rest biopsy from the PRE-CaCO₃ trial for each individual. Data were analysed using a two-way repeated measures ANOVA, with post-hoc analyses using the least significant difference. Significance was accepted at $p < 0.05$. Main effects and time-by-treatment interactions were not significant unless stated. Effect size (ES) was also calculated with 90% confidence intervals (ES \pm 90% CI) used to compare magnitudes of effect between and within trials. Magnitudes of change using Cohen's effect size were classified as; trivial < 0.2 ; small, 0.2-0.6; moderate, 0.6-1.2; large, 1.2-2.0; and very large, 2.0-4.0 (Batterham & Hopkins, 2006; Hopkins, 2006). Effects with less certainty (magnitude of $< 75\%$) were classified as no meaningful difference (Batterham & Hopkins, 2006;

Hopkins, 2006). Statistical analyses were performed using PASW Statistics 20 (SPSS Inc, Quarry Bay, Hong Kong) and effect size calculated via a custom spreadsheet (Hopkins, 2006).

4.3 Results

4.3.1 NKA alpha isoform protein abundances

Representative blots for all NKA isoforms analysed are displayed in Fig. 4.1.

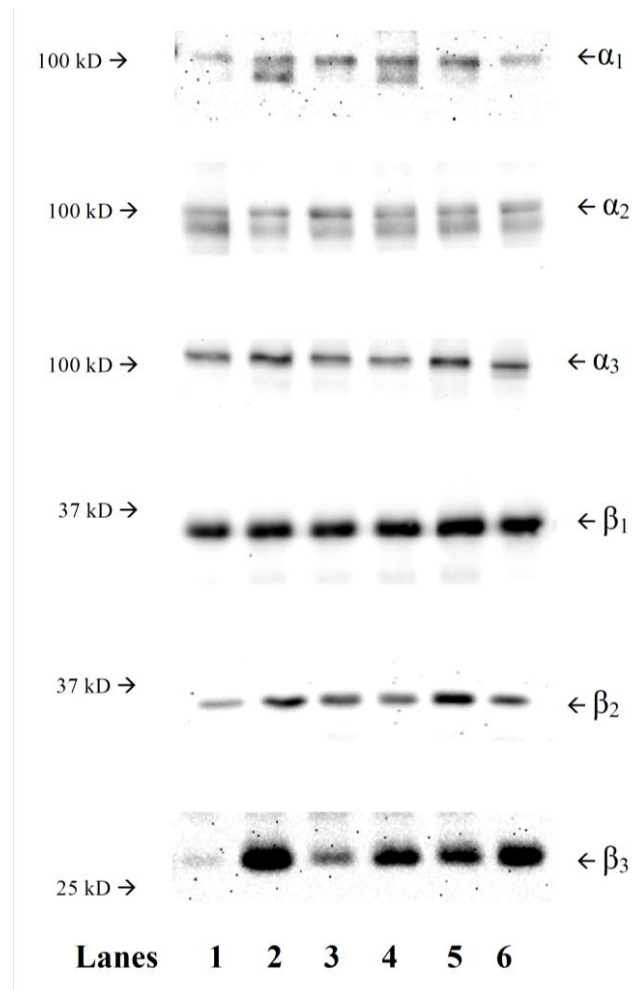


Figure 4.1 Representative immunoblots of NKA α_1 , α_2 , α_3 , β_1 , β_2 and β_3 in muscle homogenates of human vastus lateralis muscle. Values at left indicate molecular weight of bands. Protein bands from left to right are, lanes 1 and 2 – PRE- CaCO_3 ; lanes 3 and 4 – PRE- NaHCO_3 ; lanes 5 and 6 – POST- CaCO_3 and are rest and exercise, respectively.

There were no significant time or treatment main effects, or significant time-by-treatment interaction for any of the α isoforms (Fig. 4.2). The NKA α_2 protein abundance post-exercise had a moderate effect size ($ES = 0.62 \pm 0.73$; 21% increase) within the PRE-CaCO₃ trial, while the POST-CaCO₃ trial a small effect size ($ES = 0.57 \pm 0.72$; 14% decrease). There was also a small effect size for reduced NKA α_2 protein abundance post-exercise in POST-CaCO₃ compared to post-exercise for both PRE-NaHCO₃ (-7%; $ES = 0.57 \pm 0.72$) and PRE-CaCO₃ (-11%; $ES = 0.57 \pm 0.70$). There was a small effect size for a 7.5-fold increase in NKA α_3 protein abundance post-exercise ($ES = 0.45 \pm 0.43$), but only within the PRE-CaCO₃ trial, however variability in the results for NKA α_3 affected the ability to measure a significant difference.

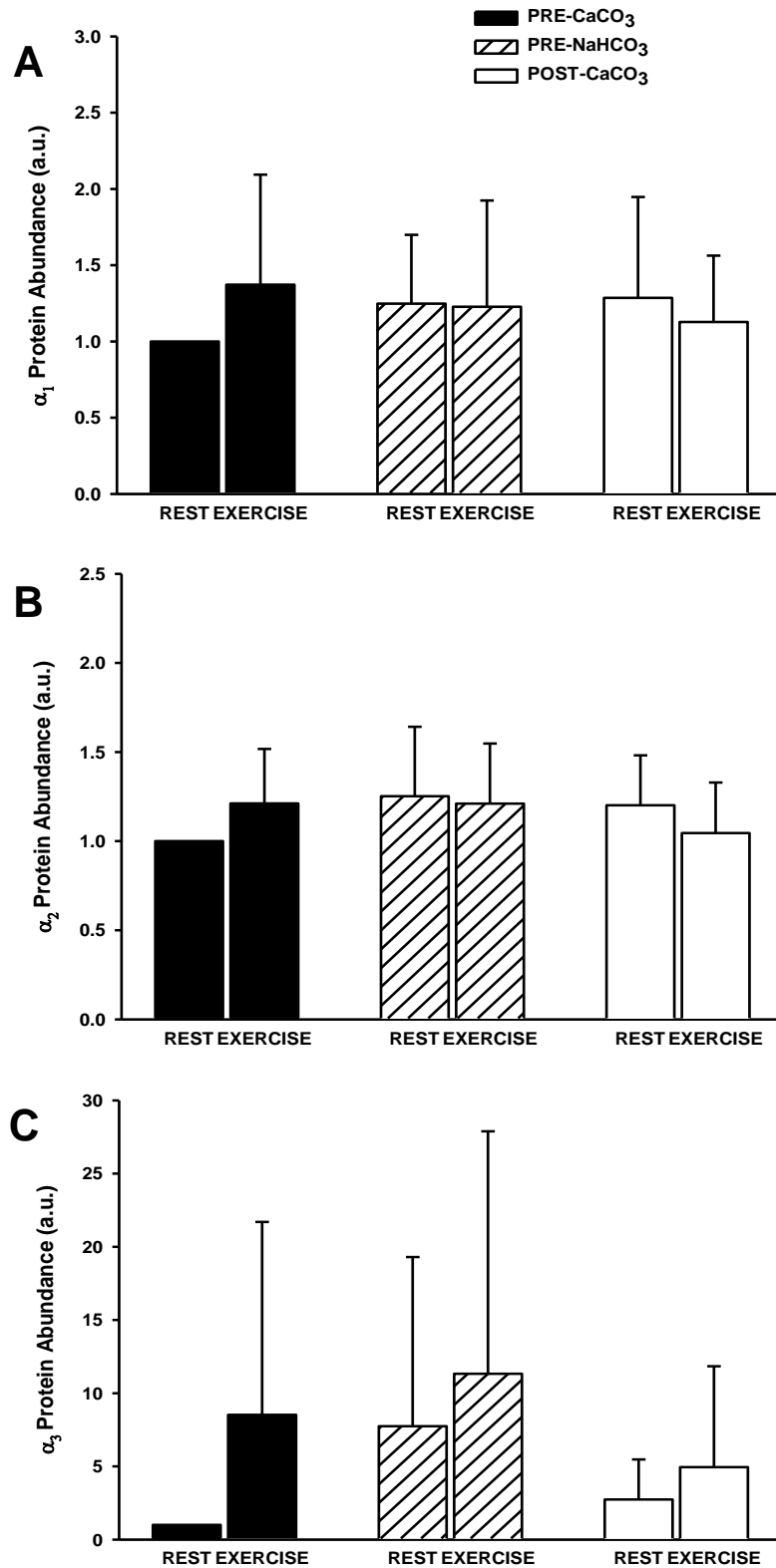


Figure 4.2 NKA α protein abundance in the vastus lateralis muscle at rest and following acute RSE. The exercise test was conducted pre-training after placebo ingestion (PRE-CaCO₃); pre-training after NaHCO₃ ingestion (PRE-NaHCO₃); and post-training after placebo ingestion (POST-CaCO₃). NKA α_1 (A); NKA α_2 (B); NKA α_3 (C). All results are normalised to total protein and then expressed relative to PRE-CaCO₃ rest. All data are mean \pm SD, n = 7.

4.3.2 NKA beta isoform protein abundances

The results of muscle NKA β isoform analyses are shown in Fig 4.3. For β_1 protein abundance there was no significant time (exercise) main effect ($p = 0.096$), but a treatment main effect was found ($p < 0.01$). Post-hoc analysis revealed that β_1 protein abundance was greater in PRE-NaHCO₃ than PRE-CaCO₃ ($p < 0.05$), which was in turn greater than POST-CaCO₃ ($p < 0.01$). There were very large and moderate ES for decreased β_1 protein abundance post exercise, within the PRE-NaHCO₃ (24%; ES = 2.42 \pm 2.20) and POST-CaCO₃ (16%; ES = 1.17 \pm 0.29) trials, respectively. There was no significant time-by-treatment interaction.

For β_2 protein abundance, there were no significant main effects for time, treatment or significant time-by-treatment interaction. A small-moderate ES was recorded for β_2 protein abundance post-exercise within POST-CaCO₃ (-61%; ES = 0.56 \pm 0.37). There were also a small ES for decreased β_2 protein abundance post-exercise in the POST-CaCO₃ trial compared to PRE-CaCO₃ (-32%; ES = 0.34 \pm 0.26) and PRE-NaHCO₃ (-41%; ES = 0.56 \pm 0.37).

For NKA β_3 protein abundance there was no significant time main effect ($p = 0.150$). There was a significant treatment main effect ($p < 0.05$) for β_3 protein abundance, with post-hoc analysis finding POST-CaCO₃ greater than PRE-NaHCO₃ ($p < 0.05$), however there was no significant interaction ($p = 0.224$). There was a moderate ES for increased post-exercise β_3 protein abundance by 5.3-fold in PRE-CaCO₃ (ES = 0.97 \pm 1.03), and for PRE-CaCO₃ post-exercise to be 1.7-fold greater than PRE-NaHCO₃ (ES = 0.62 \pm 0.0.72) post-exercise.

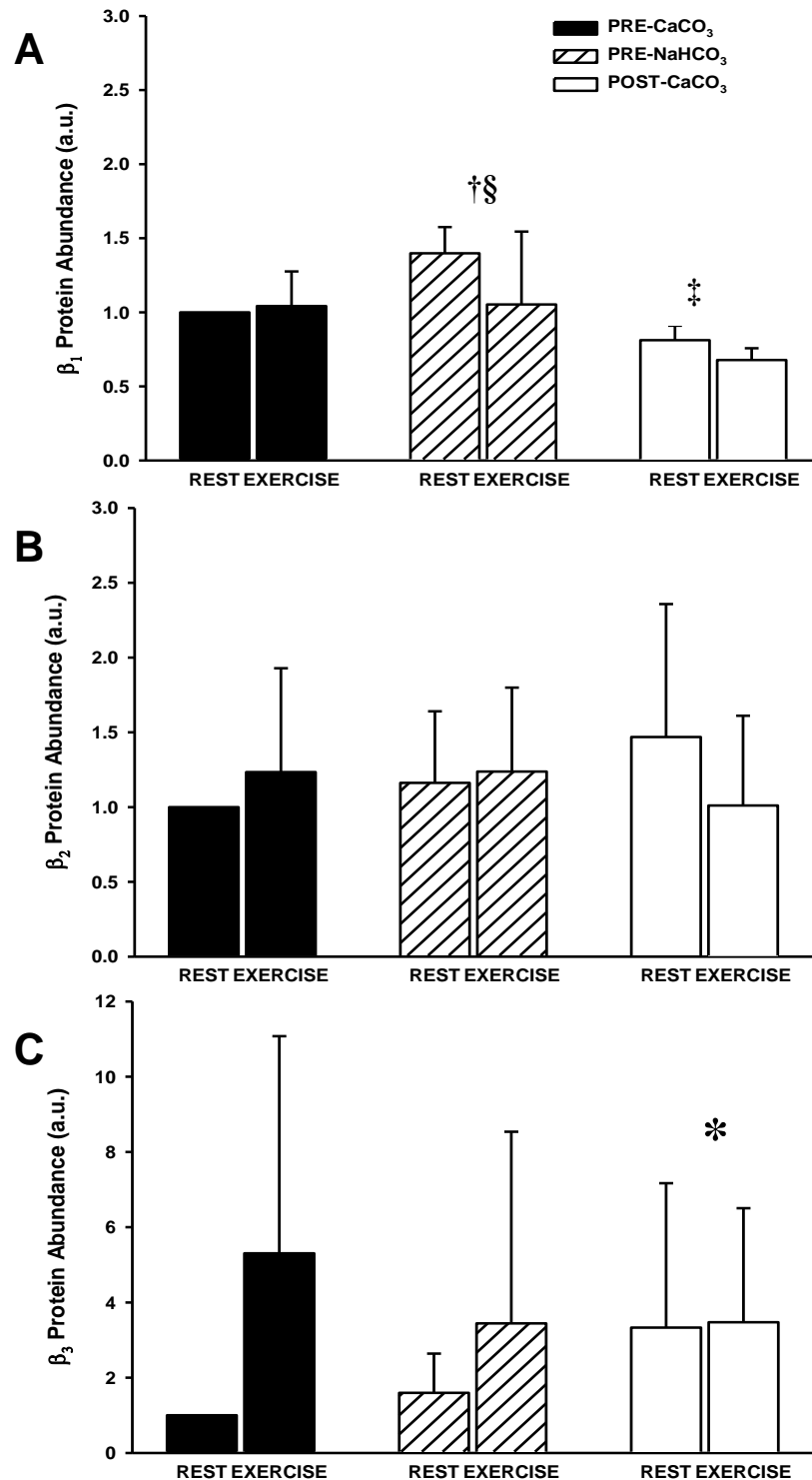


Figure 4.3 NKA β protein abundance in the vastus lateralis muscle at rest and following acute RSE. The exercise test was conducted pre-training after placebo ingestion (PRE-CaCO₃); pre-training after NaHCO₃ ingestion (PRE-NaHCO₃); and post-training after placebo ingestion (POST-CaCO₃). NKA β_1 (A); NKA β_2 (B); NKA β_3 (C). All results are normalised to total protein and then expressed relative to PRE-CaCO₃ rest. All data are mean \pm SD, $n = 7$. †PRE-NaHCO₃ > PRE-CaCO₃; ‡POST-CaCO₃ < PRE-CaCO₃; §PRE-NaHCO₃ > POST-CaCO₃ (treatment main effect, $p < 0.01$). *POST-CaCO₃ > PRE-NaHCO₃ (treatment main effect, $p < 0.05$).

4.4 Discussion

This study investigated the effects of acute NaHCO₃ supplementation on skeletal muscle NKA protein abundance before and after RSE, and whether chronic NaHCO₃ supplementation during training would result in greater adaptations in NKA protein expression post-training. It was firstly shown that there were no significant changes in NKA α or β isoform protein abundance with acute exercise in the placebo trials. A key finding was an increase in skeletal muscle NKA β_1 protein abundance following acute NaHCO₃ supplementation, without significant effects on the α , β_2 or β_3 isoforms. The second finding was that an increase in NKA β_3 protein abundance was found following RSE training with chronic NaHCO₃ supplementation, but that there were no significant changes in any α or other β isoform protein expression.

4.4.1 Acute exercise and NKA isoform abundance

There were no significant effects of an acute bout of RSE on the protein abundance of any of the NKA isoforms. These results may be due to the exercise protocol employed providing an insufficient stimulus to elicit a change in protein expression. Although the RSE protocol involved maximal intensity exercise, which was exhaustive, each sprint was of a very short duration (4 s) and the total exercise time for each trial was therefore only 60 s. This is the first report of effects of such high intensity intermittent exercise on muscle NKA isoforms. The lack of changes in NKA protein abundance with acute exercise are consistent with previous similar findings following acute intense interval cycling (Aughey *et al.*, 2007) or fatiguing knee extensor exercise (Murphy *et al.*, 2004), but contrasts other research findings after acute exercise (Overgaard *et al.*, 2002; Green *et al.*, 2007b). However, these latter two studies employed very prolonged exercise duration. Thus a significant up-regulation in NKA α_2 protein expression was

demonstrated following 16 hr heavy intermittent exercise in which a 6 min bout was performed at approximately 91% $\text{VO}_{2\text{peak}}$ every hour (Green *et al.*, 2007b), and increased NKA content measured via [^3H]ouabain binding was observed following a 100 km run (Overgaard *et al.*, 2002). There were small-moderate effect sizes observed for increased α_2 , α_3 and β_3 NKA protein abundance post-exercise in the PRE- CaCO_3 trial. So while changes in NKA protein abundance with acute exercise appears unlikely, this suggests further investigation of acute, but more prolonged exercise may be warranted.

4.4.2 Acute exercise and NaHCO_3 supplementation

Acute ingestion of NaHCO_3 resulted in an increased β_1 protein expression (treatment main effect), but was without significant effect on the protein abundance of any other NKA α or β isoforms. It has been shown previously that NaHCO_3 ingestion prior to sprint cycling exercise increased total work output (Bishop *et al.*, 2004). Whilst acute ingestion of NaHCO_3 may have been the stimulus for the increased β_1 protein expression in PRE- NaHCO_3 compared to PRE- CaCO_3 , this is unlikely given the small volume of exercise, and since mean power did not differ significantly between the three trials (Varley, 2013).

The primary role of the NKA in skeletal muscle is the regulation of trans-sarcolemmal $[\text{Na}^+]$ and $[\text{K}^+]$ gradients which are critical for the maintenance of membrane excitability and contraction (Clausen, 2003). The β_1 isoform regulates the Na^+ and K^+ affinity of the NKA and also NKA activity levels (Blanco & Mercer, 1998). Hence an increase in β_1 protein abundance with NaHCO_3 could improve K^+ regulation. Although plasma $[\text{K}^+]$ results are not reported here (see Appendix 4), there was no significant effect of acute NaHCO_3 supplementation on plasma $[\text{K}^+]$. However, a trend was noted for a lower rise in

venous plasma $[K^+]$ above baseline during PRE-NaHCO₃ compared to PRE-CaCO₃ (Varley, 2013).

It is unlikely that this increased β_1 protein expression is a result of unmasking or translocation between different cellular locations because crude homogenates of whole muscle were analysed, as opposed to techniques involving repeated centrifugation and membrane separation. This technique was chosen since membrane fractionation results in a very low recovery of NKA enzymes which may be unrepresentative of the total population (Clausen, 2013). However, it does have the weakness of not being able to determine the specific location of where changes occur. It should also be noted that the vastus lateralis is of mixed fibre composition and it is therefore unclear whether the changes observed were specific to one or both fibre types (Green *et al.*, 2007b). The mechanism via which NaHCO₃ acts upon NKA β_1 isoform expression are unknown.

4.4.3 RSE training and NaHCO₃ supplementation

Chronic NaHCO₃ supplementation taken during 4 wks of RSE training induced the opposite effect to acute NaHCO₃ with a decrease in β_1 and also an increase in β_3 protein abundance (treatment main effects). A consistent finding was the non-significant effect of chronic NaHCO₃ and training on the protein abundance of any NKA α isoform.

The lack of increase in NKA α_1 - α_3 and β_2 protein abundance following 4 wks RSE training was unexpected. Exercise training in humans results in an up-regulation of NKA content, as seen after 7 wks of high-intensity sprint interval training (McKenna *et al.*, 1993; Harmer *et al.*, 2000), and also endurance training (Green *et al.*, 2004). Provided that the stimulus is sufficient, up-regulation of the NKA can be seen within the first week of training (Green *et al.*, 1993). High intensity training increased α_2 protein abundance in both endurance-trained runners (Bangsbo *et al.*, 2009) and highly trained soccer players

(Thomassen *et al.*, 2010), while sprint training in runners increased the α_1 protein abundance (Iaia *et al.*, 2008). The lack of increased α abundance here may be due to the RSE training having an insufficient total load to stimulate increases in NKA isoform protein, via insufficient sprint duration, total exercise duration, or total work. Interestingly, only the β_3 isoform was found to have an elevated protein abundance following training here.

The effects of NaHCO_3 -induced hypokalaemia should be contrasted with previously demonstrated training induced changes in NKA protein abundance. Whilst acute NaHCO_3 ingestion and associated metabolic alkalosis reduces arterial $[\text{K}^+]$ at rest (Sostaric *et al.*, 2006), chronic alkalosis can lead to hypokalaemia through increased renal excretion of K^+ (Clausen, 2010). Studies utilising animal models have found that 2 wks of dietary-induced hypokalaemia resulted in a large decrease in NKA α_2 abundance (Azuma *et al.*, 1991; Hsu & Guidotti, 1991). Ten days K^+ deprivation resulted in large decreases in α_2 and β_2 abundances in rat red and white gastrocnemius and EDL, while β_1 was reduced in red gastrocnemius (Thompson & McDonough, 1996), a muscle of similar fibre composition to the human vastus lateralis sampled in this study (Hundal *et al.*, 1993). Whilst not inducing hypokalaemia at rest, the NaHCO_3 supplementation protocol utilised in the current study resulted in a post-exercise lowering of antecubital venous plasma $[\text{K}^+]$ to $\sim 0.6 \text{ mmol.L}^{-1}$ below rest, compared to $\sim 0.3 \text{ mmol.L}^{-1}$ below rest for PRE- CaCO_3 (Varley, 2013). If this small difference in post-exercise $[\text{K}^+]$ was repeated during training it is possible that this may have induced signalling changes in muscle and contributed to the decrease seen in NKA β_1 protein abundance following RSE training with NaHCO_3 supplementation. Given that NKA β_1 is implicated in regulating NKA

activity levels (Geering, 2001), the reduced β_1 protein abundance seen post-training may then adversely affect K^+ regulation.

Performance measurements taken during the POST- CaCO_3 trial demonstrated that following 4 weeks training with HCO_3^- supplementation there was no improvement of mean power output during RSE testing (Varley, 2013). This finding contrasts previous research in this laboratory demonstrating improved RSE performance following similar training conducted without NaHCO_3 supplementation (Serpiello *et al.*, 2011). Therefore, whilst acute NaHCO_3 supplementation may improve acute exercise performance, it is possible that chronic supplementation may prevent or reduce training adaptations in NKA in skeletal muscle and therefore limit any performance gains. Further research is recommended to examine the effects of NaHCO_3 supplementation during training that comprises exercise of moderate-to-high intensities but of longer durations that are known to enhance NKA content.

4.4.4 Limitations

There were a number of limitations of this study, including the low number of subjects, the typical variability evident in the NKA isoform western blot results, and the lack of additional post-exercise biopsy sampling times to detect any delayed responses in NKA adaptations. Hence, care should be taken when interpreting these protein expression results. On the other hand, the repeated trials give strength to the study design, as the participants acted as their own controls. To reduce the inherent variability in western blotting the protein loading and antibody concentrations were optimised prior to analysis. Nevertheless, variability of results is typical of western blotting and an increased number of participants would have been beneficial. However, the training commitment and NaHCO_3 supplementation were very demanding and combined with the invasive

measures made recruitment more difficult than anticipated. It is also possible that the order of the pre-training trials had a time/learning effect on the results, and while the inclusion of familiarisations sessions was intended to minimise this, the randomisation of these trials should also been considered for future studies.

Measurement of muscle [³H]ouabain binding site content would also have been beneficial to demonstrate whether training increased total NKA content. Whilst the aim of this study was to investigate individual isoform responses, which was done via western blotting, the lack of changes seen in the individual α isoforms does however suggest that total NKA content would also be unlikely to have increased with RSE.

4.4.5 Conclusions

Acute RSE did not significantly increase the protein abundance of any NKA isoform post-exercise, which is consistent with previous research with short-term continuous exercise. Acute NaHCO₃ supplementation resulted in an increased skeletal muscle NKA β_1 isoform protein, which contrasts chronic NaHCO₃ supplementation during RSE training, which significantly decreased muscle β_1 , as well as increased β_3 protein abundance. It appears likely that the RSE protocol utilised was insufficient to induce training-related increases in skeletal muscle NKA isoform proteins and any upregulatory effect may in fact have been blocked by chronic NaHCO₃ supplementation.

CHAPTER 5. Cellular localisation of NKA isoforms in human skeletal muscle determined by immunofluorescence microscopy

5.1 Introduction

The NKA is responsible for the active transport of Na^+ and K^+ ions across cellular membranes (Blanco & Mercer, 1998). It is a heterodimeric protein consisting of an alpha (α -) and beta (β -) subunit as well as a third, γ subunit (PLM) (Kaplan, 2002) that co-immunoprecipitates with $\alpha\beta$ -complexes (Geering, 2006; Bossuyt *et al.*, 2009). The basic function of the NKA is to maintain high $[\text{Na}^+]$ and $[\text{K}^+]$ gradients across the plasma membrane of mammalian cells, maintaining the resting membrane potential (Nielsen & de Paoli, 2007; Clausen, 2008).

The NKA is expressed as different isoforms each encoded by a separate gene. Four isoforms of the α -subunit ($\alpha_1 - \alpha_4$) and three different beta isoforms ($\beta_1 - \beta_3$) have been identified (Blanco & Mercer, 1998; Clausen, 2003) with six of these ($\alpha_1 - \alpha_3$ and $\beta_1 - \beta_3$) expressed at the protein level in human skeletal muscle (Murphy *et al.*, 2004) (Chapters 3 and 4). Isoforms of the NKA have been detected in both the sarcolemmal and t-tubular systems of skeletal muscle cells using a variety of techniques. In developing hindlimb muscle from mice, the appearance of the α_2 isoform corresponded with t-tubule maturation marked by maximal DHPR protein expression, as measured via western blotting (Cougnon *et al.*, 2002). In mouse cardiac myocytes, where α_1 is the predominant α isoform, the NKA density was 60% higher in the t-tubules compared to sarcolemmal membranes, using formamide-induced detubulation of isolated ventricular myocytes (Berry *et al.*, 2007). An early study reported that 80% of the skeletal muscle NKA were

located in the sarcolemma and the remaining 20% located in the t-tubules, determined utilising [³H]ouabain binding after glycerol pre-treatment to disrupt the t-tubular network in frog sartorius muscle (Venosa & Horowicz, 1981). However, glycerol pre-treatment is unlikely to cause complete disruption of the t-tubular connections to the sarcolemma, resulting in a large underestimate of the density of NKA in the t-tubules (Clausen, 2003). Nonetheless, this indicates some localisation of NKA within the t-tubules.

In rat cardiomyocytes, using immunofluorescence analysis, t-tubules were found to label α_1 -specific antibodies more intensely than the sarcolemma (McDonough *et al.*, 1996). Analysis of rat EDL muscle utilising α_1 and α_2 specific antibodies, indicated that both the NKA α_1 and α_2 isoforms were present in the sarcolemma, but that only the α_2 was present in the t-tubules (Williams *et al.*, 2001). However, other researchers have been unable to conclusively detect intracellular NKA localisation in either the white or red gastrocnemius muscle of rats using immunofluorescence (Zhang *et al.*, 2006). Fluorescence analysis of NKA α_1 and α_2 in mouse EDL muscle found α_2 to be mainly expressed in the t-tubules, while the α_1 isoform was mainly located in the sarcolemma, with some longitudinal sections also demonstrating α_1 in the t-tubules (Radzyukevich *et al.*, 2013). The only study to have investigated NKA localisation with immunofluorescence in human skeletal muscle found in soleus muscle that α_1 fluorescence was largely contained to the plasma membrane (Hundal *et al.*, 1994). Further, α_2 was observed in the plasma membranes of the muscle fibres as well as being observed to be diffusely distributed throughout the muscle fibre (Hundal *et al.*, 1994) but a comparison of expression in different fibre types was not examined.

Muscle fibres can be classified according to differences in their structural and functional properties, with a common method of classification being according to the composition

of myosin heavy chain within the muscle fibre. Expression patterns of NKA isoforms have been reported to be muscle fibre type-specific. Immunofluorescence studies in the red gastrocnemius muscle of rats demonstrated that NKA α_1 and β_1 were highest in type I fibres, α_2 fluorescence was similar among the different fibre types, whereas β_2 labelling was strongest in type IIB fibres (Zhang *et al.*, 2006). Fibre type analysis of NKA expression in human vastus lateralis via western blot of single fibre segments found no difference between type I and type II fibres for NKA α_1 and β_1 , but that α_2 protein expression was higher in type II fibres (Thomassen *et al.*, 2013).

The aim of this study was to determine the distribution patterns of the six NKA isoforms that have been reported in human skeletal muscle ($\alpha_1 - \alpha_3$ and $\beta_1 - \beta_3$), investigate possible differences in NKA expression in type I and type II fibres, as well as explore plasma membrane and intracellular localisation utilising quantitative immunofluorescence techniques. It is hypothesized firstly that the NKA α_1 isoform density would be greater in the plasma membrane, whereas α_2 isoform density would be greater in the intracellular region, and secondly that NKA α_1 and β_1 isoforms will have a higher density in type I than type II fibres.

5.2 Methods

5.2.1 Participants

Six healthy, recreationally active young adults (4 males, 2 females; age 22.3 ± 1.7 yrs; height 165.0 ± 6.0 cm; body mass 63.6 ± 7.1 kg; mean \pm SD) gave their written informed consent to participate in the study, which was approved by the Victoria University Human Research Ethics Committee.

5.2.2 Muscle biopsies

A percutaneous muscle biopsy with a Stille biopsy needle, was taken from the middle third of the vastus lateralis muscle under resting conditions. After local anaesthetic (1% Xylocaine, McFarlane Medical and Scientific, Surrey Hills, VIC, Australia) was injected into the skin and subcutaneous tissue, a small incision was then made into the skin and fascia, and a small muscle sample was excised using a sterilised biopsy needle with suction. A small portion of each biopsy was mounted in Tissue-Tek O.C.T. compound (ProSciTech, Thuringowa, QLD, Australia) and frozen in isopentane (Merck, Bayswater, VIC, Australia) pre-cooled in liquid nitrogen (N_2). The remaining muscle sample was blotted on filter paper to remove excess blood and snap frozen in liquid N_2 and stored at -80°C for later analyses as part of a larger study (data not included in this thesis).

5.2.3 Tissue sectioning

Tissue samples were removed from -80°C storage and left at -20°C for 1 hr. Serial tissue sections of ~ 5 μm were cut at -20°C (HM 550 cryostat, Thermo Fisher, Scoresby, VIC, Australia) and thaw-mounted onto glass microscope slides (Starfrost, ProSciTech, Thuringowa, QLD, Australia). Slides were stored at -80°C until analysed.

5.2.4 Immunofluorescence labelling

Tissue sections were removed from -80°C storage and left to air dry for 30 min at room temperature, which reduces artefacts and morphological changes often seen as a result of immunological staining procedures (Boenisch, 2001), before being fixed for 10 min in 4% (wt/vol) Paraformaldehyde (Sigma-Aldrich, Sydney, NSW, Australia) in order to preserve the cell structure. However fixation often results in the loss of immunoreactivity (Boenisch, 2001), therefore sections were then permeabilised for 5 min with 5% (vol/vol) Triton X-100 (Sigma-Aldrich, Sydney, NSW, Australia) to unmask antigens and restore immunoreactivity (Boenisch, 2001). Finally, sections were blocked in 3% (wt/vol) Bovine Serum Albumin (BSA, Sigma-Aldrich, Sydney, NSW, Australia) for 1 hr at room temperature in a humid chamber. Sections were rinsed four times with phosphate buffered saline (PBS) in between each stage. Primary antibodies, diluted in 3% BSA in PBS, were applied and left to incubate in a humid chamber overnight at 4°C. The sections were washed four times in PBS. Secondary antibodies, diluted in 3% BSA in PBS, were applied and incubated for 2 hr in a humid chamber at room temperature in the dark. Sections were washed four times, and then incubated with the nuclear stain bis-benzimide (Hoechst 33258, Sigma-Aldrich, Sydney, NSW, Australia), then mounted in PBS, coverslips applied and sealed (Trenerry *et al.*, 2007).

5.2.4.1 Antibodies

Serial sections were incubated with primary antibodies specific to each NKA isoform. These were for α_1 : monoclonal $\alpha 6F$ (developed by D. Fambrough and obtained from the Developmental Studies Hybridoma Bank developed under the auspices of the NICHD and maintained by the University of Iowa, Department of Biological Sciences, Iowa City, IA, USA); α_2 : polyclonal anti-HERED (kindly donated by T. Pressley, Texas Tech

University, USA); α_3 : monoclonal MA3-915 (Thermo Scientific, Scoresby, VIC, Australia); β_1 : monoclonal MA3-930 (Thermo Scientific, Scoresby, VIC, Australia); β_2 : monoclonal 610915 (BD Biosciences, Franklin Lakes NJ, USA); β_3 : monoclonal 610993 (BD Biosciences, Franklin Lakes, NJ, USA).

Additional primary antibodies used to identify cellular structures were the polyclonal plasma membrane marker anti-laminin L9393 (Sigma-Aldrich, Sydney, NSW, Australia); monoclonal anti-DHPR α_1 MA3-920 (Thermo Scientific, Scoresby, VIC, Australia) used to identify the t-tubules; the monoclonal anti-Caveolin 3 (Cav-3) 610420 (BD Biosciences, Franklin Lakes, NJ, USA) was used to identify the plasma membrane when laminin could not be used due to cross reactivity of the antibody host species.

Fibre-typing of the cross-sections was performed using the monoclonal anti-myosin type I antibody A4.480 (developed by H. Blau and obtained from the Developmental Studies Hybridoma Bank developed under the auspices of the NICHD and maintained by the University of Iowa, Department of Biological Sciences, Iowa City, IA, USA). All unstained fibres were classified as myosin type II. Since a major aim of this study was to examine differences in NKA expression in type I and type II fibres, the type II fibres were not further subcategorized (Rudnick *et al.*, 2004).

Secondary antibody-coupled fluorophores used were Alex Fluor[®] 488 donkey anti-mouse A21202 and Alexa Fluor[®] 594 donkey anti-rabbit A21207 (Invitrogen, Carlsbad, CA, USA).

Western blot analysis was performed on all NKA isoform antibodies to verify (i) protein specificity at the correct molecular weight, and (ii) lack of reactivity to other proteins (Murphy & Lamb, 2013). For negative controls and the assessment of background

fluorescence, the primary antibody was omitted, and in all cases the fluorescence signal was absent.

5.2.4.2 Fluorescence microscopy

Immunolabelled sections were visualised with an Olympus BX51 fluorescent microscope and digital images were captured using a DP72 colour CCD camera and Cell*F software (Olympus Corporation, Tokyo, Japan) using either a 10x (numerical aperture 0.30) air immersion, or a 100x (numerical aperture 1.40) oil immersion objective. Filters specific to the wavelength of the secondary antibodies were used to visualise the Hoechst 33258, and Alex Fluor 488 and 594 fluorophores, respectively.

5.2.5 Plasma membrane and intracellular NKA analysis

Captured images were separated into individual colour channels and analysed using ImageJ Software (NIH, Bethesda, MD, USA). Using the membrane labelled image, a participant-specific intensity threshold (Fig 5.1A) was selected and used to identify and outline individual muscle fibres (Fig 5.1B). The thresholded image was inverted (Fig 5.1C) and the plasma membrane (PM) segmented (Fig 5.1D), using the watershed tool (ImageJ Software; NIH, Bethesda, MD). Segments of the PM situated between adjacent fibres expressing the same myosin heavy chain type were analysed to determine a mean fluorescence density, calculated as the sum of the fluorescence of all the pixels divided by the number of pixels for the PM of that fibre type. This was repeated for type I adjacent membrane segments of cells and type II membrane segments (Fig 5.1 E, F) for each NKA isoform.

The fibre outline was then overlaid onto the raw NKA isoform labelled image, for quantification of intracellular (IC) fluorescence. For the purpose of this investigation, the IC region was classified as including all locations within the plasma membrane envelope.

This therefore included the t-tubules and other areas within the t-tubular boundaries, such as the sarcoplasm and cytoskeleton. The interface between the PM and the t-tubules is included in the PM analysis, however a lack of sensitivity prevented further differentiation of cellular structures.

The fluorescence density was calculated as the sum of the fluorescence for all fibres divided by the number of fibres for each of type I and type II fibres, for each NKA isoform (Equation 1). By measuring density which is expressed in arbitrary units of fluorescence per pixel, it allows for direct comparison of NKA expression in regions of different size, such as PM compared to IC.

$$\text{Eq}^n 1 \quad \text{Density } (f.\text{pixel}^{-1}) = \frac{\text{sum fluorescence } (f)}{\text{number of pixels } (p)}$$

Fibres were classified as type I or type II using MHCI labelled serial sections. Only well cross-sectioned fibres with clear borders were measured, all fibres on the edge of the field of view were also excluded.

5.2.6 Colocalisation analysis

As the β_2 isoform was found not to be diffusely distributed, colocalisation analysis of NKA β_2 with the cell nucleus was performed using the ImageJ co-localisation threshold tool (NIH, Bethesda, MD, USA). Colocalisation was analysed using the Pearson's Correlation Coefficient, and Manders' Coefficient (Bolte & Cordelieres, 2006), where M1 equals the proportion of NKA β_2 which colocalises with nucleus; and M2 equals the proportion of nucleus that colocalises with NKA β_2 .

5.2.7 Line profile intensity analysis

A line profile intensity analysis was done to compare PM localisation of laminin and cav-3 antibodies. This was done with the ImageJ plot profile tool (NIH, Bethesda, MD). This created a plot of fluorescence intensity along a line drawn through a selected region of interest.

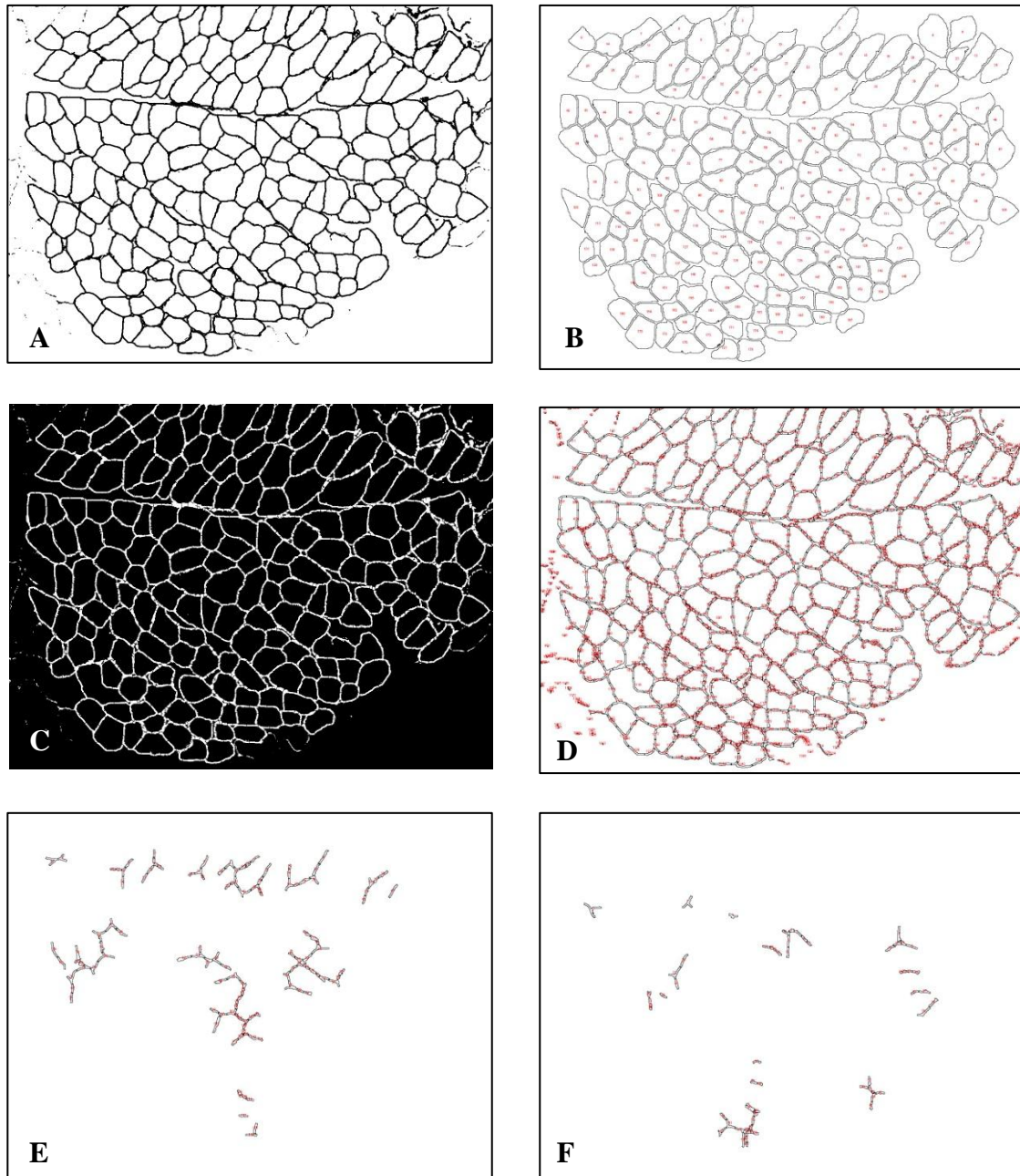


Figure 5.1 Example of analysis steps for intracellular and plasma membrane fluorescence analysis. A) Thresholded image from laminin stained section identifying individual muscle fibres; B) outline of intracellular areas analysed for fluorescence intensity; C) inverted threshold image identifying the plasma membrane; D) segmented plasma membrane outline; E) segments of plasma membrane from adjacent type I fibres for myosin type I plasma membrane analysis; F) segments of plasma membrane from adjacent type II fibres for myosin type II plasma membrane analysis.

5.2.8 Statistics

All results are expressed as mean \pm SD. Data were analysed using a two-way repeated measures ANOVA, for the main effects of fibre type (type I vs type II) and expression location (IC vs PM), and for fibre type-by-location interactions, with post-hoc analyses using the least significant difference test. Significance was accepted at $p < 0.05$. Main effects and interactions were not significant unless stated. Effect size was also calculated with 90% confidence intervals (ES \pm 90% CI) used to compare magnitudes of effect. Magnitudes of change using Cohen's effect size were classified as; trivial < 0.2 ; small, 0.2-0.6; moderate, 0.6-1.2; large, 1.2-2.0; and very large, 2.0-4.0 (Batterham & Hopkins, 2006; Hopkins, 2006). Effects with less certainty (magnitude of $< 75\%$) were classified as no meaningful difference (Batterham & Hopkins, 2006; Hopkins, 2006). Statistical analyses were performed using PASW Statistics 20 (SPSS Inc, Quarry Bay, Hong Kong) and effect size calculated via a custom spreadsheet (Hopkins, 2006).

5.3 Results

5.3.1 NKA isoform antibody specificity

Antibody specificity was tested for all NKA isoforms analysed via western blotting (Fig 5.2). Results demonstrated some non-specific binding for NKA α_1 at approximately 150 kD, and for NKA α_2 at approximately 15 kD which could potentially be the accessory protein PLM (FXYP1). It should also be noted that while western blotting can provide some validation of the antibody specificity, this is imperfect because during this analysis the proteins are in a denatured state compared to being in its natural folded form for immunofluorescence analysis (Murphy & Lamb, 2013). In the case of the β subunits, the crude homogenates were also deglycosylated for blotting.

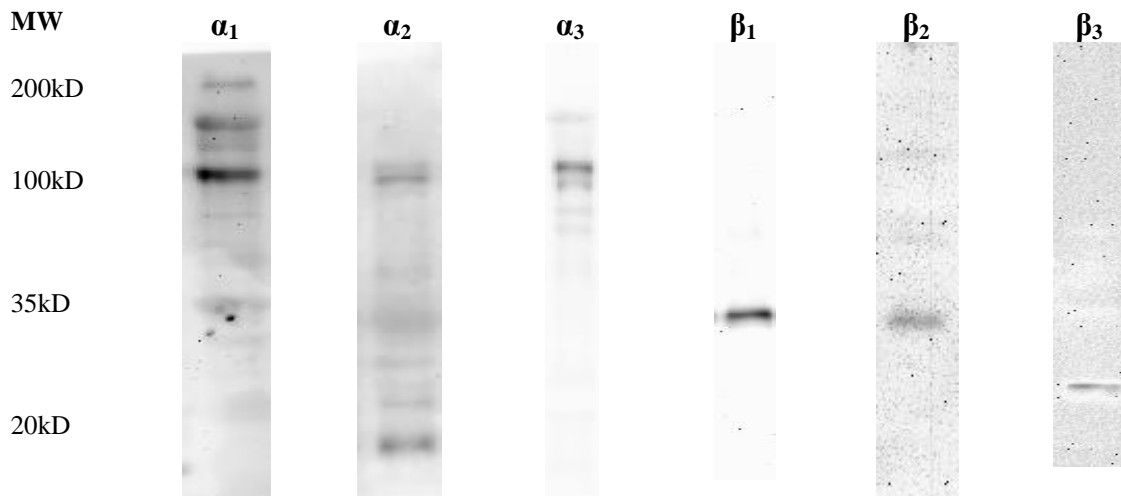


Figure 5.2 Western blot results of antibody specificity testing for antibodies specific to NKA $\alpha_1 - \alpha_3$ and $\beta_1 - \beta_3$.

5.3.2 Comparison of plasma membrane markers

Line profile analysis of the laminin and cav-3 antibodies indicated that both laminin and cav-3 fluorescence peaks were detected at the same location, demonstrating that they colocalise in the PM, and hence that they can be used interchangeably when required due to cross-reactivity of antibody host species (Fig 5.3). This was supported by correlation analysis, where the Pearson's correlation coefficient was $r=0.891$ (Table 5.1).

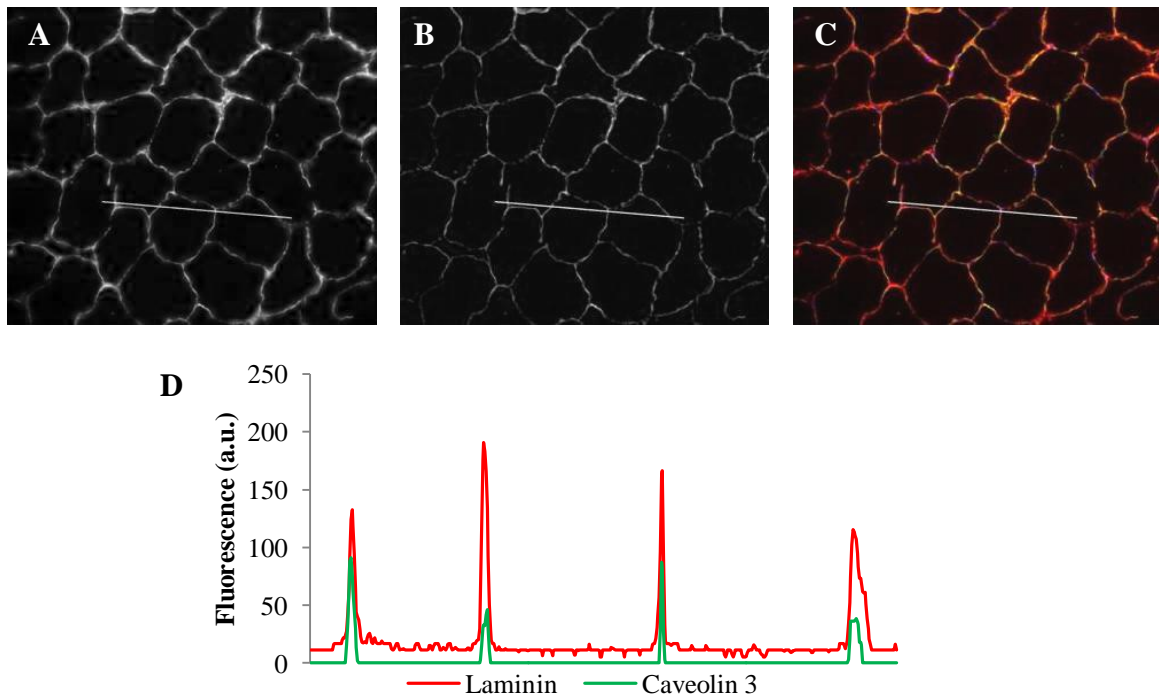


Figure 5.3 Line profile analysis of laminin and cav-3 colocalisation in human vastus lateralis muscle fibre membranes. Location of the line drawn across four cell walls for analysis of laminin (A); cav-3 (B); composite image (C) showing laminin in red, cav-3 in green and areas of colocalisation in yellow; fluorescence profile for the line (D) with peaks for laminin (red) and cav-3 (green) occurring at the same location.

Table 5.1 Colocalisation analysis of laminin and Cav-3.

Pearson's Correlation Coefficient	0.89
Manders' Coefficient M1	0.99
Manders' Coefficient M2	0.99

M1 is equal to the proportion of laminin which colocalises with cav-3; and M2 is equal to the proportion of cav-3 that colocalises with laminin.

5.3.3 Fibre type distribution and area

From each individual sample, fibres labelled positive for MHCI were classified as type I and all unlabelled fibres classified as type II. The fibre type distribution was approximately 55% type I and 45% type II fibres for each of the isoform analyses; findings were consistent across analyses and also with the expected mixed fibre composition of the vastus lateralis muscle (Table 5.2).

for NKA β_3 analysis, technical difficulties prevented fibre matching of serial cross-sections and fibre type classification, therefore only PM vs IC analysis were performed and not fibre type comparison (see section 5.3.10).

Table 5.2 Total number of type I and type II fibres analysed (participant mean \pm SD), proportion of fibres labelled positive for MHCI, and the (mean \pm SD) for each isoform is also shown for cross-sectional analyses of NKA α_{1-3} and β_{1-2} .

	Type I Fibres	Type II Fibres	% Type I	Range (min-max)
α_1	307 (51 \pm 27)	256 (43 \pm 9)	52%	30-67%
α_2	339 (57 \pm 32)	232 (38 \pm 13)	55%	28-70%
α_3	348 (58 \pm 37)	268 (45 \pm 15)	53%	28-68%
β_1	387 (65 \pm 29)	286 (48 \pm 13)	55%	28-66%
β_2	128 (45 \pm 52)	70 (24 \pm 22)	58%	30-74%

Number of subjects from which muscle was obtained was 6 for each isoform and each fibre type except β_2 where number of subjects was 3.

5.3.4 NKA α_1

Laminin labelling produced clearly defined fibre membranes (Fig 5.4A, D). Cross-sections labelled for NKA α_1 (Fig 5.3B) showed that the isoform is located in all fibres, but also that some fibres displayed a brighter fluorescence than others. Comparison with the MHCI stained serial section (Fig 5.4E) indicates that these more brightly labelled fibres for α_1 were type II fibres. Examination of the composite image (Fig. 5.4C) reveals some areas of colocalisation (yellow) between NKA α_1 and laminin, indicating that some NKA α_1 are located in the PM. Diffuse fluorescence of NKA α_1 throughout the fibres was also observed indicating that it is also located intracellularly. Quantification of these results is shown in Fig 5.5.

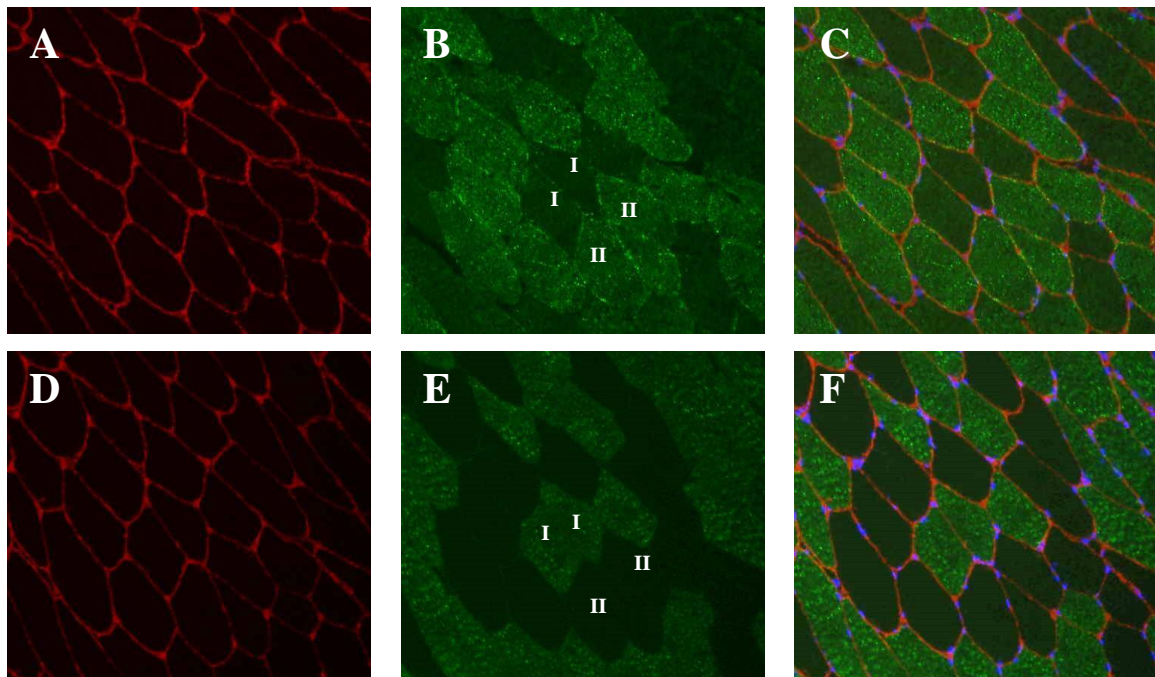


Figure 5.4 Cellular localisation of NKA α_1 abundance in human skeletal muscle fibres. Serial sections of the vastus lateralis muscle were double labelled with laminin (A, D), and antibody to NKA α_1 (B) or MHC I (E). The composite image (C) show the NKA subunit in green, laminin in red, and nucleus in blue; composite image (F) shows MHC I in green, laminin in red, and nucleus in blue; areas of colocalisation of primary antibodies are yellow.

To allow for direct comparison of areas of different size, fluorescence density was used to give a calculated relative value of isoform abundance. This was calculated as the sum of the fluorescence divided by the number of pixels for all regions of interest. The density of NKA α_1 was 24% higher in type II compared to type I fibres ($p < 0.01$; fibre type main effect; ES = 0.84 ± 0.46). However, the density of NKA α_1 did not differ between IC and PM (Fig. 5.5).

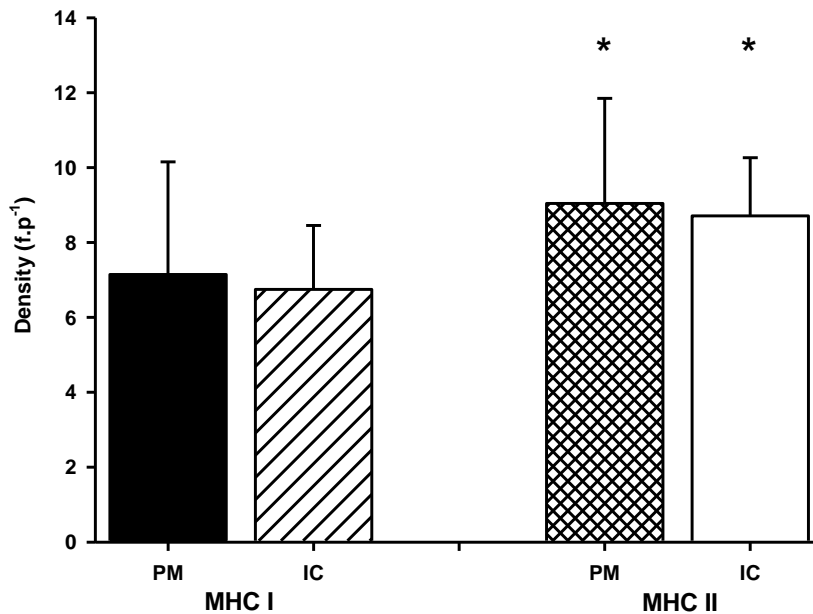


Figure 5.5 Calculated density for NKA α_1 abundance in human vastus lateralis muscle. * type I < type II; main effect, $p < 0.01$. All data mean \pm SD; type I fibres (n = 307; N = 6); type II fibres (n = 256; N = 6); (n = number of fibres; N = number of subjects).

5.3.5 NKA α_2

Due to cross-reactivity of the primary antibody host species, cav-3 was used to label the PM for NKA α_2 labelled sections (Fig 5.6A,C) and this clearly defined the muscle cells. Cross-sections labelled for NKA α_2 (Fig. 5.6B) demonstrated that the α_2 was located in all fibres, and exhibited a strong fluorescence in the PM. Examination of the composite image (Fig. 5.5C) revealed an apparent strong colocalisation (yellow) between NKA α_2 and cav-3, which indicated that NKA α_2 was present in the PM. There was also lighter fluorescence throughout the fibres indicating that α_2 is also located intracellularly. However, this appears uniform across the image suggesting there was no difference in α_2 abundance between fibre types. Quantification of these results is shown in Fig 5.7.

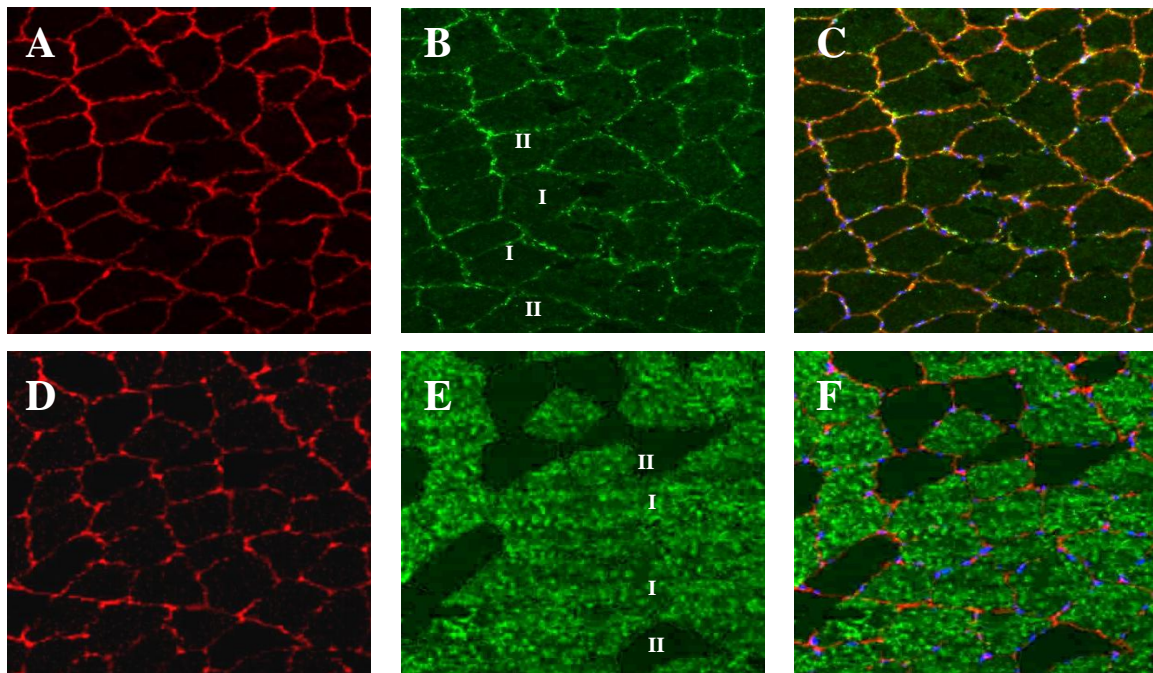


Figure 5.6 Cellular localisation of NKA α_2 abundance in human skeletal muscle fibres. Serial sections of the vastus lateralis muscle were double labelled with cav-3 (A) or laminin (D), and antibody to NKA α_2 (B) or MHC I (E). The composite image (C) show the NKA subunit in green, cav-3 in red, and nucleus in blue; composite image (F) shows MHCI in green, Cav-3 in red, and nucleus in blue; areas of colocalisation of primary antibodies are yellow.

Analysis of the calculated density found that NKA α_2 was 65% greater in the PM compared to IC ($p < 0.01$; location main effect; ES = 3.49 ± 2.48). There was no difference in NKA α_2 between fibre types (Fig. 5.7).

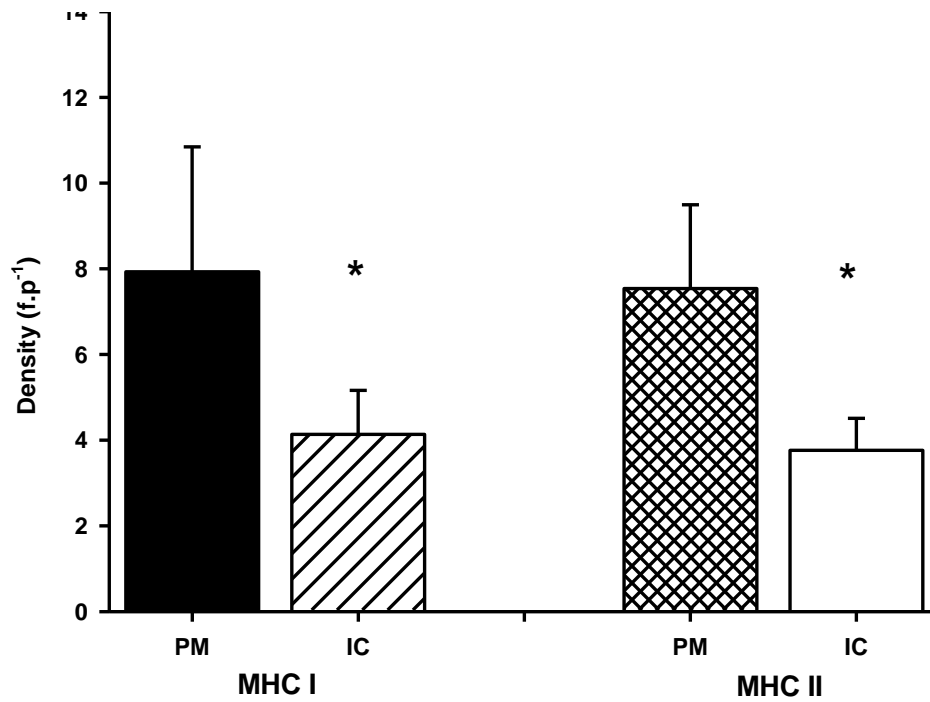


Figure 5.7 Calculated density for NKA α_2 abundance in human vastus lateralis muscle. * PM > IC; location main effect; $p < 0.01$. All data mean \pm SD; type I fibres ($n = 339$; $N = 6$); type II fibres ($n = 232$; $N = 6$); ($n =$ number of fibres; $N =$ number of subjects).

5.3.6 NKA α_3

Sections labelled for NKA α_3 indicated some fibres exhibited a strong fluorescence, while others appeared to have very little fluorescence. Comparison with MHCI stained serial sections (Fig. 5.8E) indicate these more brightly fluorescing fibres were type I fibres. Examination of the composite image (Fig. 5.8C) indicates some areas of colocalisation of NKA α_3 and laminin (yellow) suggesting that the NKA α_3 is located in the PM, also with diffuse labelling through the IC region (Fig. 5.8C). Quantification of these results is shown in Fig. 5.9.

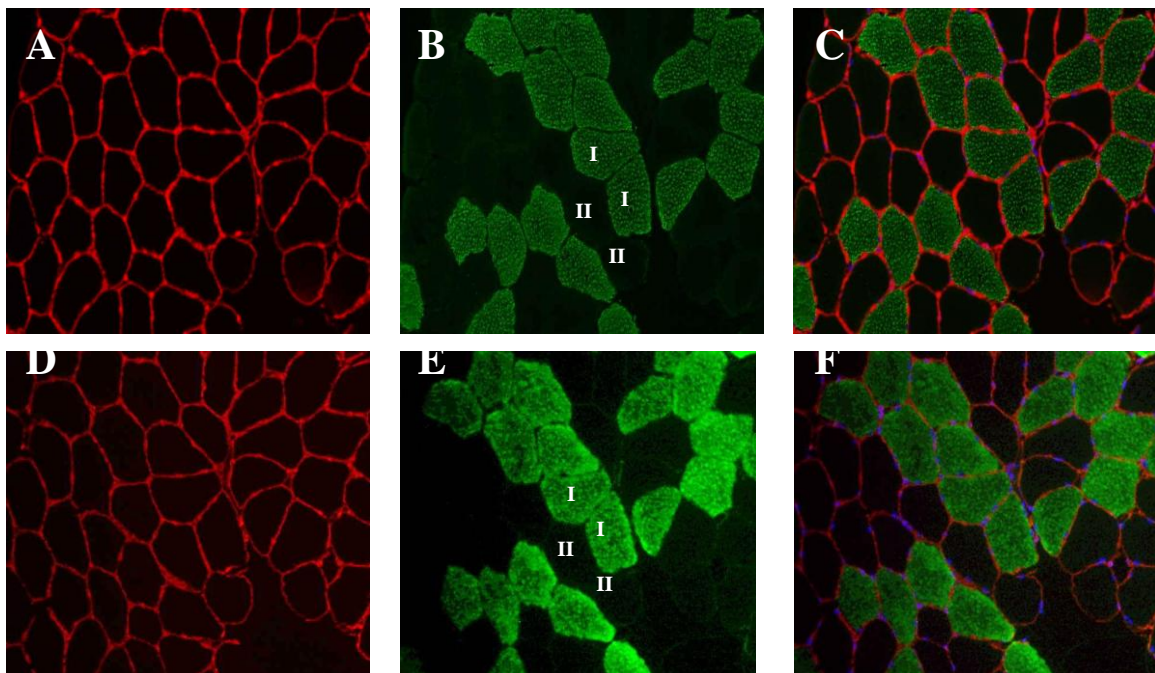


Figure 5.8 Cellular localisation of NKA α_3 abundance in human skeletal muscle fibres. Serial sections of the vastus lateralis muscle were double labelled with laminin (A, D), and antibody to NKA α_3 (B) or MHC I (E). The composite image (C) show the NKA subunit in green, laminin in red, and nucleus in blue; composite image (F) shows MHCI in green, laminin in red, and nucleus in blue; areas of colocalisation of primary antibodies are yellow.

The density of NKA α_3 in type I fibres was 90% greater than in type II fibres ($p < 0.05$; fibre type main effect; $ES = 1.49 \pm 0.88$); however, the NKA α_3 density for IC was not different to PM.

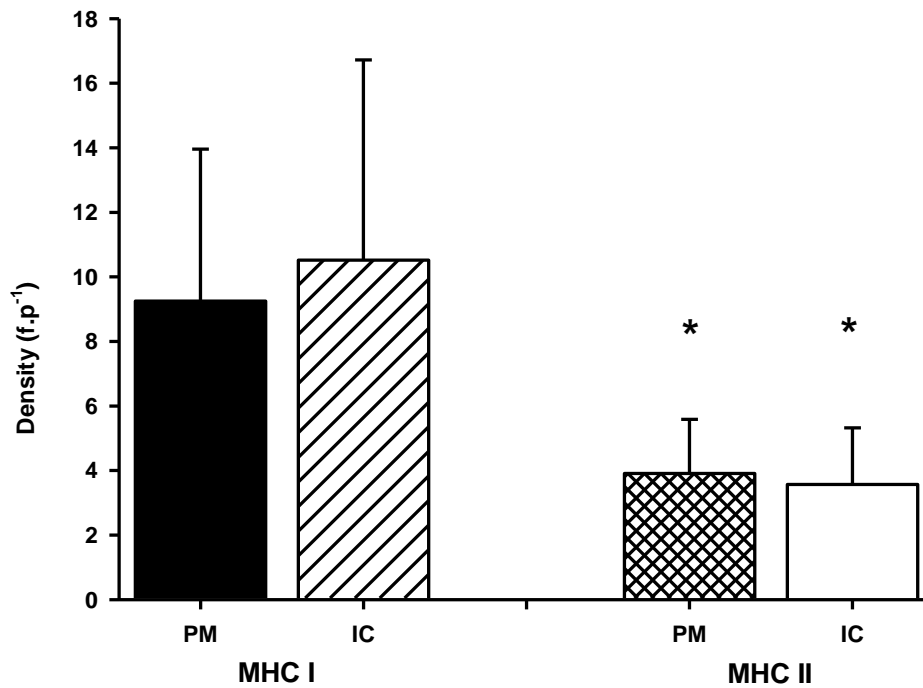


Figure 5.9 Calculated density for NKA α_3 abundance in human vastus lateralis muscle. * type I > type II; fibre type main effect; $p < 0.05$. All data mean \pm SD; type I fibres ($n = 348$; $N = 6$); type II fibres ($n = 268$; $N = 6$); ($n =$ number of fibres; $N =$ number of subjects).

5.3.7 NKA β_1

Cross-sections labelled for NKA β_1 showed strong fluorescence corresponding with the laminin labelled image (Fig. 5.10A and B). Examination of the composite image (Fig. 5.10C) revealed a strong colocalisation (yellow) between NKA β_1 and laminin, indicating that the NKA β_1 isoform is present in the PM. There was also diffuse fluorescence throughout the fibres indicating that β_1 is also located intracellularly. This labelling appeared to be uniform across the image suggesting there was no difference between fibre types. Quantification of these results is shown in Fig 5.11.

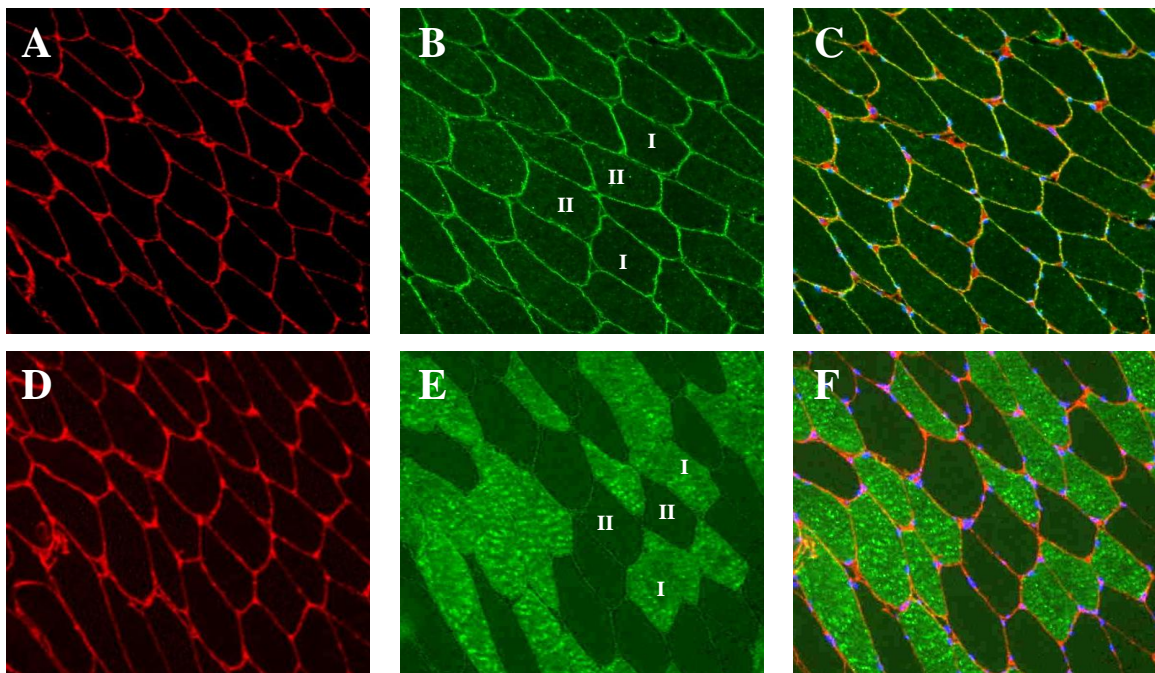


Figure 5.10 Cellular localisation of NKA β_1 abundance in human skeletal muscle fibres. Serial sections of the vastus lateralis muscle were double labelled with laminin (A, D), and antibody to NKA β_1 (B) or MHC I (E). The composite image (C) show the NKA subunit in green, laminin in red, and nucleus in blue; composite image (F) shows MHCI in green, laminin in red, and nucleus in blue; areas of colocalisation of primary antibodies are yellow.

The calculated density of NKA β_1 was 47% greater in the PM compared to IC ($p < 0.05$; location main effect; $ES=0.73\pm 0.26$). There was no difference in NKA β_1 density between type I and type II fibres (Fig. 5.11).

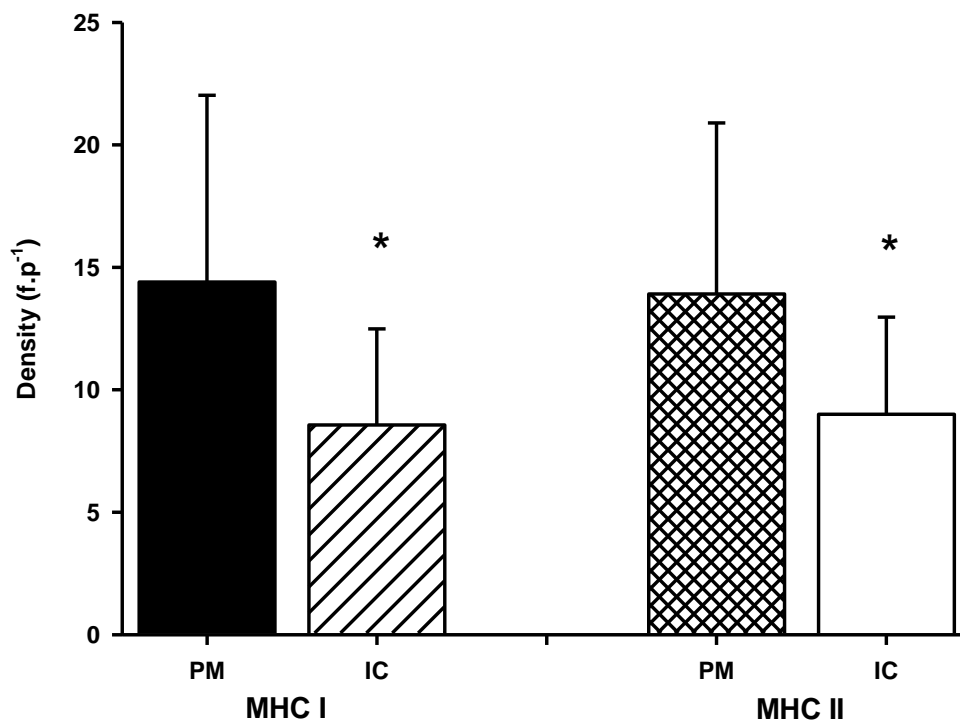


Figure 5.11 Calculated density for NKA β_1 abundance in human vastus lateralis muscle. * PM > IC; location main effect; $p < 0.05$. All data mean \pm SD; type I fibres ($n = 387$; $N = 6$); type II fibres ($n = 286$; $N = 6$); ($n =$ number of fibres; $N =$ number of subjects).

5.3.8 NKA β_2

Cross-sections labelled for NKA β_2 showed a strong fluorescence that corresponded with the laminin labelled image (Fig. 5.12A and B). In addition to this there were also small foci of bright staining interspersed along the plasma membrane. Examination of the composite image revealed a strong colocalisation (yellow) between NKA β_2 and laminin, indicating NKA β_2 is present in the plasma membrane. The bright spots of β_2 located on the plasma membrane appear to co-locate with the nuclei (Fig. 5.12C). There appeared to be very little staining throughout the fibres indicating lower abundance intracellularly. Quantification of these results is shown in Fig 5.13.

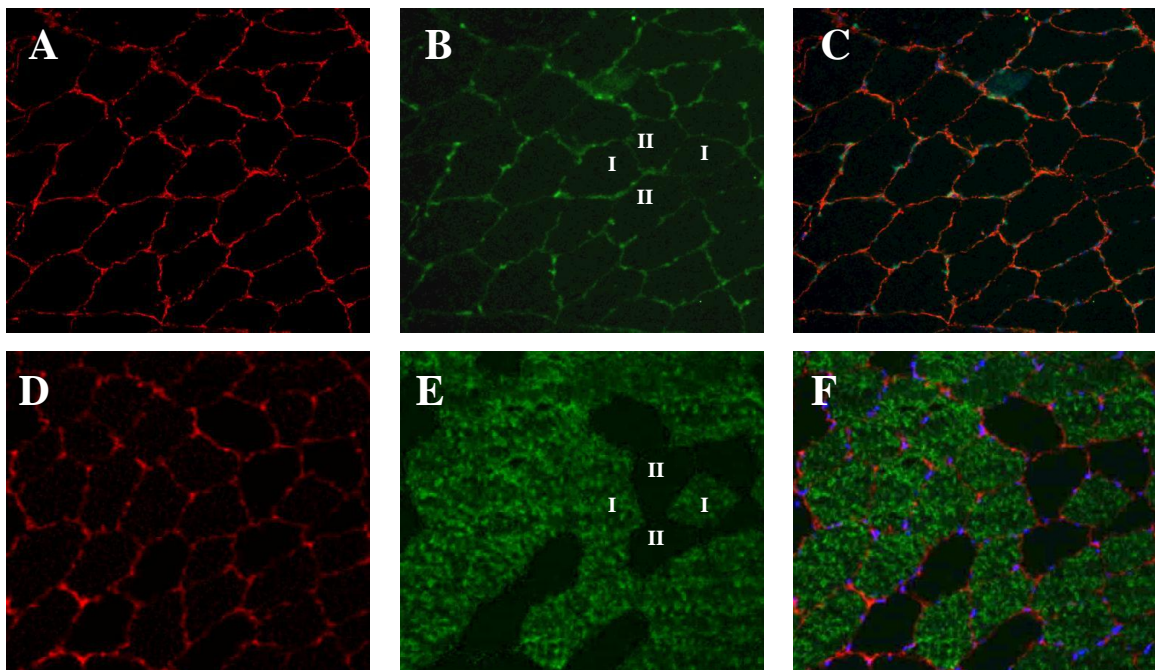


Figure 5.12 Cellular localisation of NKA β_2 abundance in human skeletal muscle fibres. Serial sections of the vastus lateralis muscle were double labelled with laminin (A, D), and antibody to NKA β_2 (B) or MHC I (E). The composite image (C) show the NKA subunit in green, laminin in red, and nucleus in blue; composite image (F) shows MHCI in green, laminin in red, and nucleus in blue; areas of colocalisation of primary antibodies are yellow.

The calculated density of NKA β_2 was 44% greater in the PM compared to IC ($p < 0.05$; location main effect; $ES = 0.81 \pm 0.34$). There was no difference in NKA β_2 density between type I and type II fibres.

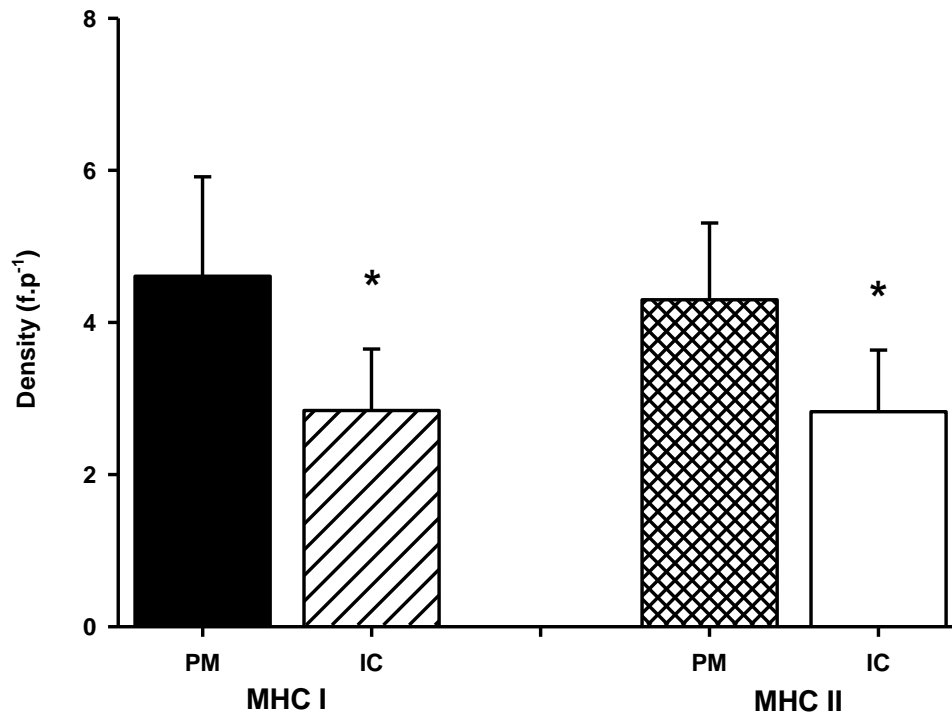


Figure 5.13 Calculated density for NKA β_2 abundance in human vastus lateralis muscle. * PM > IC; location main effect; $p < 0.05$. All data mean \pm SD; type I fibres ($n = 128$; $N = 3$); type II fibres ($n = 70$; $N = 3$); (n = number of fibres; N = number of subjects).

5.3.8.1 NKA β_2 nuclei colocalisation

The appearance of bright foci of NKA β_2 along the plasma membrane warranted further investigation. Analysis examining the co-localisation of NKA β_2 with nuclei revealed a strong correlation (0.69), and calculation of Manders' coefficient (Table 5.3) revealed that 64.8% of the NKA β_2 co-localised with nuclei, while 100% of nuclei colocalised with NKA β_2 .

Table 5.3 Colocalisation analysis of NKA β_2 and nuclei.

Pearson's Correlation Coefficient	0.69 ± 0.15
Manders' Coefficient M1	0.64 ± 0.24
Manders' Coefficient M2	0.99 ± 0.00

Mean \pm SD; N = 6. M1 is equal to the proportion of β_2 which colocalised with nuclei; and M2 is equal to the proportion of nuclei that colocalised with β_2 .

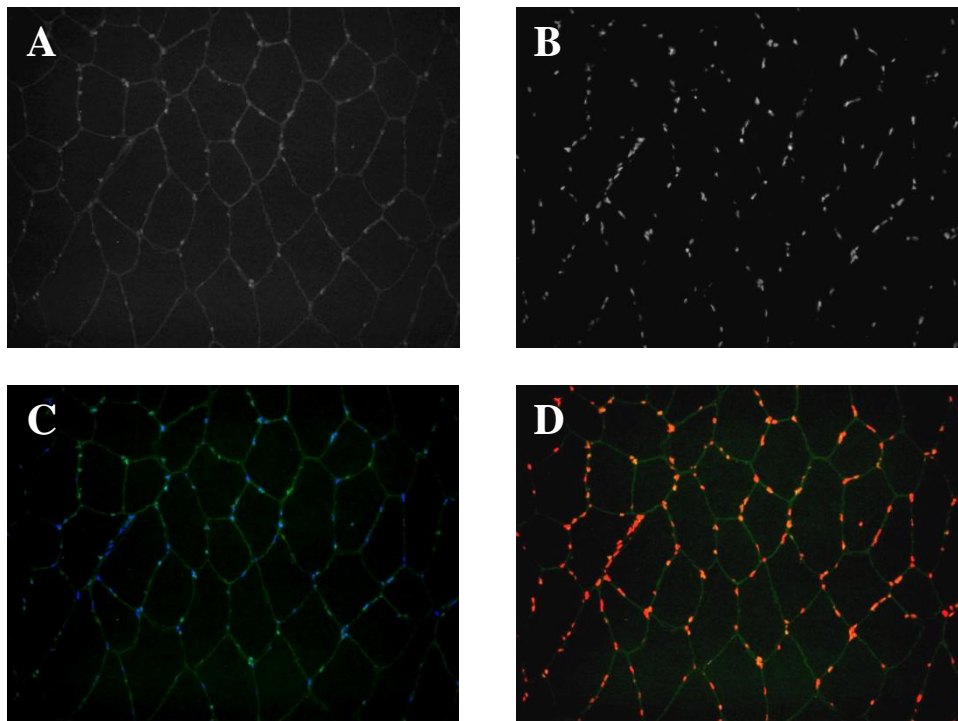


Figure 5.14 Cellular colocalisation of NKA β_2 and nuclei in human vastus lateralis muscle fibres. Cross-section labelled with antibody specific to NKA β_2 (A); nuclei labelled with bis-benzimide (B); merged image with NKA β_2 shown in green and nuclei blue (C); analysis results showing areas of colocalisation in orange/red (D).

5.3.9 NKA β_3

Due to small tissue samples resulting in limited usable cross-sections, difficulties with matching serial sections for NKA β_3 analysis were encountered and prevented matching of fibre type analysis for NKA β_3 , therefore only the PM vs IC analysis was performed. Cross-sections labelled for NKA β_3 showed random patches of fluorescence which appeared to have no pattern or regularity about them. Quantification of these results is shown in Fig 5.16.

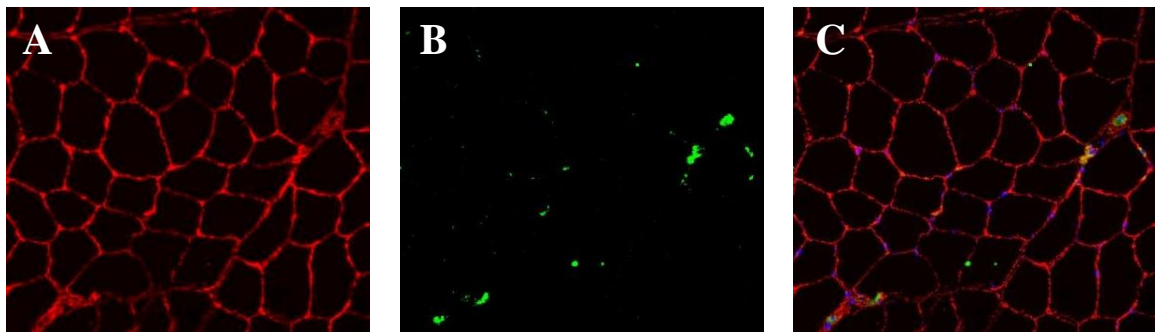


Figure 5.15 Cellular localisation of NKA β_3 abundance in human skeletal muscle fibres. Serial sections of the vastus lateralis muscle were double labelled with laminin (A), and antibody to NKA β_3 (B). The composite image (C) show the NKA subunit in green, laminin in red, and nucleus in blue; areas of colocalisation of primary antibodies are yellow.

The calculated density of NKA β_3 was 21% greater in the PM compared to IC ($p < 0.01$; ES = 4.04 ± 1.26).

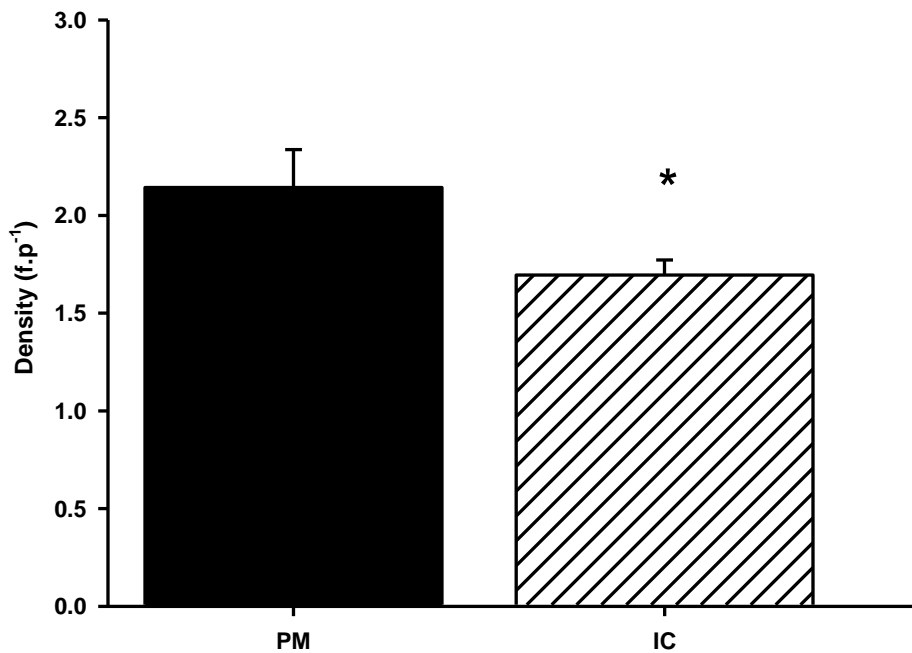


Figure 5.16 Calculated density for NKA β_3 abundance in human vastus lateralis muscle. * PM > IC; $p < 0.01$. All data mean \pm SD; (n = 810 ; N = 6); (n = number of fibres; N = number of subjects).

5.3.10 Further qualitative analysis of intracellular localisation

5.3.10.1 α isoforms

Sections were labelled with antibodies specific to DHPR in order to identify the t-tubules within the muscle fibres. DHPR labelled images (Fig 5.17A) revealed the very complex pattern of the t-tubules branching throughout the intracellular region. High magnification images (x100) of NKA α_1 , α_2 and α_3 (Fig 5.17B-D) also revealed a detailed pattern of a branched network throughout the intracellular region, similar to that seen with DHPR. This strongly suggests that the intracellular localisation of the NKA α isoforms is probably located mostly within the t-tubules.

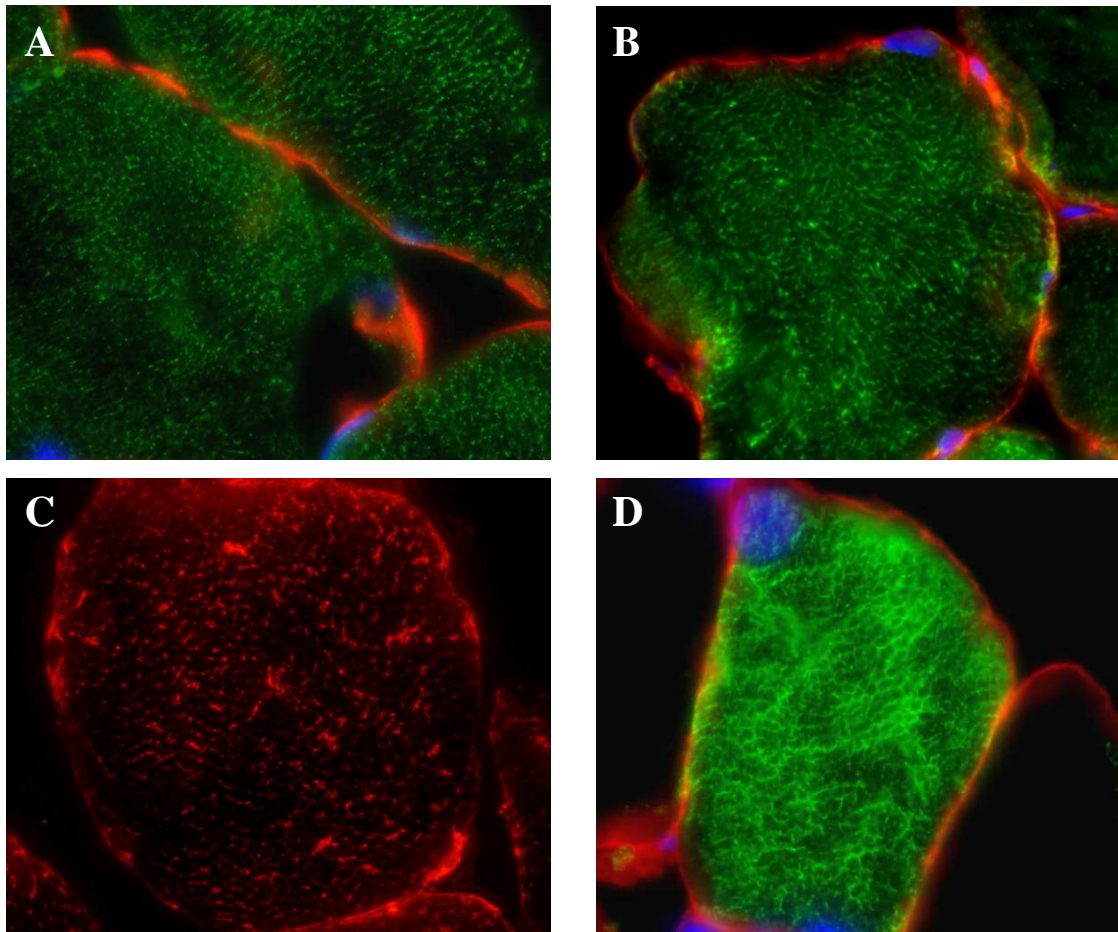


Figure 5.17 Higher magnification images of intracellular localisation of DHPR and NKA α isoforms. A) DHPR shown in green, laminin in red; B) NKA α_1 shown in green, laminin in red, areas of colocalisation in yellow; C) NKA α_2 shown in red (due to different antibody host species); D) NKA α_3 shown in green, laminin in red, areas of colocalisation in yellow. Nuclei where visible are blue.

5.3.10.2 β isoforms

Inspection of high magnification images of NKA β_1 (Fig 5.18A) revealed strong fluorescence in the PM as well as an intricate intracellular network suggesting that β_1 intracellularly is likely also located in the t-tubules. However, images of NKA β_2 (Fig 5.18B) gave no indication of localisation within the t-tubules, but strong foci of fluorescence located on the plasma membrane colocalising with the nuclei.

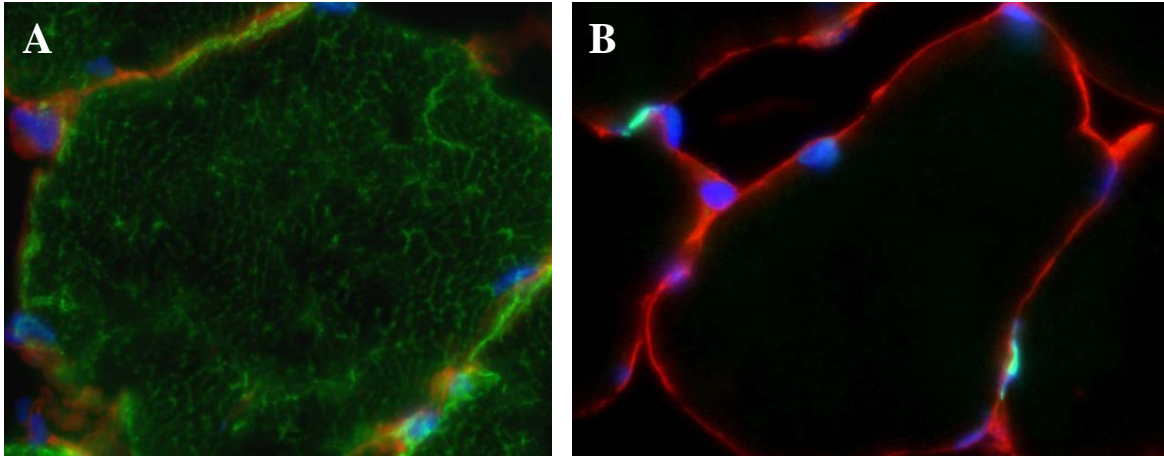


Figure 5.18 High magnification images of intracellular localisation of NKA β_1 and β_2 . A) NKA β_1 shown in green, laminin in red, areas of colocalisation in yellow; B) NKA β_2 shown in green, laminin in red, areas of colocalisation in yellow. Nuclei where visible are blue.

5.4 Discussion

This study analysed a very large number of individual muscle fibres to investigate the cellular localisation and fibre type expression of the six NKA isoforms previously reported in skeletal muscle, utilising immunofluorescence microscopy of human vastus lateralis muscle cross-sections. The NKA α_1 and α_3 were expressed in a fibre-type dependent pattern, with NKA α_1 expression higher in type II fibres and conversely with NKA α_3 having a higher expression in type I fibres. Each of the NKA α_2 , β_1 and β_2 isoforms were expressed with a higher density in the PM than in the IC region, but did not differ between Type I and II fibres. The IC measures are also likely to reflect t-tubular distribution. Finally, the NKA β_2 isoform appeared to colocalise with the muscle fibre nuclei, whereas the β_3 was less consistent in its localisation.

5.4.1 Increased density in plasma membrane for NKA α_2 and β_1

Fluorescence density analyses demonstrated that the NKA α_2 , β_1 and β_2 isoforms expressions were 65%, 47% and 44% higher in the PM, compared to the IC region. This opposes the hypothesis that NKA α_2 expression would be greater in the t-tubules, based on results from mouse EDL muscles in which α_2 was mainly expressed in the t-tubules (Radzyukevich *et al.*, 2013). These findings are consistent with the α_2 shown to be expressed in the PM of rat EDL (Williams *et al.*, 2001) and gastrocnemius muscles (Zhang *et al.*, 2006), as well as human soleus muscle (Hundal *et al.*, 1994). However, these previous studies have largely been of a qualitative nature, so the relative distribution between regions has not been quantitated as performed here.

The existence of multiple isoforms of the NKA suggests specialised functional roles. Studies examining the NKA α_2 isoform in cultured astrocytes from mice have found that it is involved in Ca^{2+} signalling via the $\text{Na}^+/\text{Ca}^{2+}$ exchanger (Golovina *et al.*, 2003) and

also in regulating contractility in mouse vascular smooth muscle (Shelly *et al.*, 2004). Studies in gene targeted mice have demonstrated that lacking one copy of the α_2 gene increased EDL force (He *et al.*, 2001), whereas force was reduced in both EDL and soleus muscles of α_2 knockout mice (Radzyukevich *et al.*, 2013) resulting in decreased exercise capacity.

The localisation of the NKA α_2 isoform in the plasma membrane in this study demonstrated a 65% co-location of α_2 with cav-3 in human muscle. This is consistent with analysis of rat mixed muscle where it was shown that 16% of NKA α_2 co-immunoprecipitated with cav-3, which they suggested was to facilitate translocation of NKA α_2 from intracellular locations to the plasma membrane (Kristensen *et al.*, 2008). The difference in percentages between these results could be due to the use of sarcolemmal giant vesicles in the latter study, where the recovery of NKA is usually quite low in fractionation techniques (Clausen, 1986) as well as potential differences in NKA expression between the species studied.

The strong PM labelling of the NKA β_1 isoform is consistent with results from rat cardiac myocytes where it was shown that more than 80% of the β_1 subunits were located in cav3-containing membranes (Liu & Askari, 2006). In the current study, the measured density of β_1 was 5-fold greater than β_2 , based simply on fluorescence measures, suggesting that NKA β_1 is the predominant β isoform in human skeletal muscle; this would be consistent with results from rat muscle where NKA β_1 isoform was 4-fold greater than β_2 (Lavoie *et al.*, 1997). However, due to different binding efficiencies for β_1 and β_s antibodies, differences in the fluorescence intensity cannot be argued as strong evidence for quantification of relative abundances of each isoform, but may be suggestive of a different expression pattern.

Surprisingly, it was found that the NKA β_2 isoform was localised to concentrated areas of fluorescence which had a strong correlation with the cell nuclei. This was similar to a report in the white and red gastrocnemius muscle of rats (Zhang *et al.*, 2006) and was suggested to represent satellite cells on the surface of the fibre. However, that is quite unlikely here as satellite cells constitute approximately only 4% of muscle nuclei in adult human muscle (Hawke & Garry, 2001) whereas this study found that 99% of nuclei co-located with β_2 . While the functional significance of this co-location is not known, it has been suggested that the β_2 isoform is important for modulating NKA activity via regulating K^+ affinity (Chow & Forte, 1995). Further importance of the β_2 was shown in a study using mice carrying a targeted deletion of the β_2 gene, which exhibited motor incoordination and subsequent paralysis (Magyar *et al.*, 1994). Therefore, it is likely that the β_2 isoform plays an important specific regulatory role and is possibly required for proper nuclear functioning.

There was very little fluorescence detected for NKA β_3 , which may be due to the suspected low abundance of this isoform in human skeletal muscle (McKenna *et al.*, 2012). However, the fluorescence detected appeared to positively label areas outside of the cell but still surrounded by the PM, which might be blood vessels within the muscle. As the laminin antibody used as a PM marker also labels the basement membranes in blood vessels (Colognato & Yurchenco, 2000), this may explain the higher density measures in the PM seen in the β_3 analysis as well as the diffuse intracellular fluorescence that was detected.

5.4.2 Fibre-type specific expression of NKA α_1 and α_3

The NKA α_1 was expressed 24% higher in type II fibres, while NKA α_3 had a 90% higher expression in type I fibres. This finding contradicts the hypotheses that NKA α_1

and β_1 isoform would have a higher density in type I than type II fibres, based on studies in the red gastrocnemius muscle of rats (Zhang *et al.*, 2006).

The functional significance of fibre type specific expression of the NKA α_1 and α_3 may relate to NKA activity. The rate of active Na^+/K^+ transport is largely determined by the Na^+ affinity (Clausen, 1986), with an increased Na^+ affinity allowing for an increased Na^+ efflux and subsequent maintenance of a steeper Na^+ gradient across the sarcolemma (Clausen, 2003).

In isolated HeLa cells transfected with NKA α isoforms, the NKA α_3 had a 4-fold lower affinity for intracellular Na^+ and a 3-fold higher affinity for extracellular K^+ compared with the α_1 and α_2 isoforms (Munzer *et al.*, 1994). This lower Na^+ -affinity could result in a lower NKA activity in type I fibres where more α_3 isoforms are located. It also suggests that NKA α_3 may only be activated when $[\text{Na}^+]_i$ reaches its highest concentration following repeated action potentials (Segall *et al.*, 2001). Studies in isolated rat muscles have demonstrated that the excitation-induced rates of Na^+ influx and K^+ efflux are appreciably lower in predominantly type I fibres (Everts & Clausen, 1992). This suggests that the NKA activity is not required to be as high in type I fibres compared to type II fibres and thereby explains the higher α_3 expression.

Conversely, NKA α_1 has a higher affinity for intracellular Na^+ , and is expressed with greater density in type II fibres. It has been suggested that the NKA α_1 performs a “housekeeping” role with regards to Na^+/K^+ exchange, responding to typical physiological demands (Jewell & Lingrel, 1991) and a high Na^+ affinity could enable it to respond efficiently to increases in $[\text{Na}^+]_i$. Recently it was also suggested that over half the NKA located in the plasma membrane was involved in non-pumping functions such as signal transduction (Xie & Askari, 2002; Liang *et al.*, 2007). Graded knock-down of

α_1 resulted in a loss of the “non-pumping” pool in order to preserve the pumping pool, but resulted in a loss of receptor function as evidenced by the failure of ouabain administration to induce activation of signalling pathways (Liang *et al.*, 2007).

Interestingly, there was no difference between fibre types for NKA α_2 isoform density. This is in contrast to studies in rat muscle where α_2 density was greater in red compared to white gastrocnemius (Fowles *et al.*, 2004), and in single fibre analysis of human vastus lateralis muscle where α_2 protein expression was higher in type II compared to type I fibres (Thomassen *et al.*, 2013), but is consistent with previous results in single fibres from our laboratory (Wyckelsma, 2014).

5.4.3 Intracellular localisation in t-tubules

All three α isoforms, as well as β_1 each demonstrated strong IC fluorescence, which from the higher magnification images, appears highly likely to be due to localisation within the t-tubular system. The t-tubules are an extensive network of invaginations on the surface membrane with a very high surface-to-volume ratio, constituting ~80% of the total fibre surface area but only ~1% of the total fibre volume (Dutka & Lamb, 2007). Early analysis of t-tubules isolated from rabbit skeletal muscle found they were able to accumulate Na^+ via an ATP-dependent, K^+ -sensitive and digitoxin-suppressible process, thus suggesting NKA presence (Lau *et al.*, 1979). Analysis of mechanically skinned EDL muscle fibres from the rat demonstrated that NKA subunits located within the t-tubules played an important role in restoring and maintaining excitability (Nielsen *et al.*, 2004b). Immunofluorescence labelling of NKA α_2 in rat EDL muscle demonstrated that the α_2 isoform displayed a distinctive reticular pattern in the intracellular region, that co-labelled with the DHPR (Williams *et al.*, 2001), consistent with the presence of the α_2 isoform in t-tubules, similar to what was found in the current study in human skeletal

muscle. As a result of K^+ efflux into the t-tubule with each action potential, the $[K^+]$ in the t-tubules may increase substantially above resting levels (Fraser *et al.*, 2011), which could depolarise the membrane and interfere with action potential generation and Ca^{2+} release (Sejersted & Sjøgaard, 2000; Clausen, 2003; Dutka & Lamb, 2007). Therefore, a high abundance of α_2 in both the PM and t-tubules in human muscle indicates that localisation of the NKA in the t-tubules is particularly important for maintaining Na^+/K^+ gradients and membrane potential necessary for continued excitability of the interior of the cell.

5.4.4 Limitations

The immunostaining methods used in this study are well established and widely used and published by experts in this field (Trenerry *et al.*, 2007; Murphy *et al.*, 2009; Radzyukevich *et al.*, 2013). There were a number of limitations to this study, including the apparent cross-reactivity of antibodies to the α -isoforms to other proteins as seen in the western blot results. However, the proteins are in a denatured state for western blotting compared to in their natural folded form for immunofluorescence analysis (Murphy & Lamb, 2013). This has the potential to alter the antibody binding properties and therefore limit the relevance of western blot results. The western blot results did show that the strongest band was located at the expected molecular weight for each NKA isoform, suggesting that the majority of the antibody is binding to the NKA, and any non-specific fluorescence likely to be small.

The use of a detergent is a common step in immunostaining procedures performed in order to unmask antigens and to restore immunoreactivity which can be reduced during the fixation process. While detergents are harsh chemicals that generally disrupt proteins when used at high concentrations for long periods of time (Boenisch, 2001), the

concentration and time used in this study (5% for 5 min) should not result in any significant protein disruption or damage. Therefore, the fluorescence results presented should provide an indication of NKA distribution in human skeletal muscle. Interestingly it was noted that the western blot for α_2 displayed some non-specific binding at approximately 10-15kD, which could possibly be PLM, and future studies should include localisation analysis of PLM.

It should also be noted that the possibility of any hybrid fibres with a mixed myosin type weren't identified and separated for individual analysis. However, previous analysis has shown that the vastus lateralis muscle in humans has very few hybrid fibres (~8%) (Staron *et al.*, 2000), so this is unlikely to have had a major influence on these results.

Possible labelling of blood vessels with β_3 suggests that future analysis be repeated with a different protein used to label the PM which is not expressed in blood vessels and also using a specific marker for smooth muscle tissue.

This technique also has limitations due to the inability to separate the intracellular region into the t-tubules and sarcoplasm. The results suggest that the intracellular localisation is largely based in the t-tubules, however because this result also includes the sarcoplasm, the NKA density in the t-tubules is likely to be greater than that calculated here. It is also not sensitive enough around the PM/IC interface and more detailed analysis using confocal microscopy is recommended, along with examination of NKA isoform location in relation to other membrane transport proteins.

5.4.5 Conclusions

This study took a novel approach in quantifying the cellular location of the six NKA isoforms expressed in human skeletal muscle. By utilising antibodies to label cellular proteins known to be expressed in the plasma membrane, individual fibres were able to

be separated into PM and IC regions and the fluorescence quantified for analysis and comparison. This methodology demonstrated firstly that each of the NKA α_2 , β_1 and β_2 isoforms were expressed with greater density in the PM than IC, and secondly, analysis of isoform expression in fibre types revealed NKA α_1 and α_3 were expressed with greater density in type II and type I fibres, respectively. These results reveal new information regarding isoform-specific expression of the NKA isoforms in human skeletal muscle, and provide a basis for future research into previously suggested isoform specific functions. These results also demonstrate that the NKA isoform distribution is distinctly different in human skeletal muscle compared to previous reports in mice and rats, hence the relevance and transferability of results from one species to human should be carefully considered.

CHAPTER 6. General Discussion and Conclusion

6.1 General Discussion

6.1.1 Introduction

This thesis investigated the effects of glucose ingestion on K^+ regulation at rest, during exercise and recovery, and each of exercise, glucose and $NaHCO_3$ intervention effects on skeletal muscle NKA isoform protein abundance. It also investigated the cellular localisation of the six NKA isoforms ($\alpha_1 - \alpha_3$ and $\beta_1 - \beta_3$) in human vastus lateralis muscle. The major findings have been discussed in detail in their respective chapters. Thus, this chapter summarises the main findings, integrates where possible, and makes concluding comments regarding these findings. Additionally, this chapter identifies areas of importance for future research regarding K^+ and skeletal muscle NKA regulation that arise from this thesis.

6.1.2 Acute oral glucose load enhances K^+ regulation

Glucose induced increases in endogenous insulin and this was probably primarily responsible for the modulation of plasma K^+ during rest, exercise and recovery; with a single oral glucose load lowering arterial and venous plasma $[K^+]$ and increasing the $[K^+]_{a-v}$ across the forearm. The latter suggests that these $[K^+]$ changes were consequent to an increased K^+ uptake into the (relatively) inactive forearm musculature during high intensity intermittent exercise. This is consistent with previous findings that physiological concentrations of insulin can decrease plasma $[K^+]$ (Andres *et al.*, 1962; DeFronzo *et al.*, 1980). Study 1 extends this by demonstrating that this K^+ -lowering effect is also possible via a single oral glucose load. It is likely that the lowering of plasma $[K^+]$ reflects an insulin-induced increase in NKA activity in skeletal muscle (Rosic *et al.*, 1985; Weil *et al.*, 1991) which has been demonstrated to occur in the

plasma membranes of rat skeletal muscles (Hundal *et al.*, 1992; Marette *et al.*, 1993). However, some of the K^+ -lowering effect is also likely to be due to increased K^+ uptake via the splanchnic bed (Andres *et al.*, 1962), but this was not quantified here. The results from Study 1 demonstrated the importance of examining the interaction of multiple systems in human physiology. In the case of Study 1, glucose ingestion likely induced the well described sequence of increased plasma [insulin], increased peripheral glucose uptake, enhanced skeletal muscle carbohydrate oxidation, which positively affect muscle function (Lee-Young *et al.*, 2006). However, the glucose-induced increase in plasma [insulin] likely simultaneously also stimulated the skeletal muscle NKA, increased the K^+ -uptake by muscle, thereby affecting K^+ homeostasis, which also affects muscle function (Alvestrand *et al.*, 1984; Chibalin *et al.*, 2001). This was evident in Study 1 with a lower venous plasma [K^+] during exercise and recovery following glucose ingestion. This may be a result of insulin-induced phosphorylation of the NKA α subunits (Feraille *et al.*, 1999; Chibalin *et al.*, 2001) which has been demonstrated to increase [3H]ouabain-sensitive $^{86}Rb^+$ uptake in cultured human skeletal muscle cells (Al-Khalili *et al.*, 2004).

Several studies have previously suggested that insulin also induces translocation of NKA isoforms from an intracellular location to the plasma membrane. Immunofluorescence results from Study 3 showed that the α_2 and β_1 isoforms were more highly expressed in the plasma membrane than in the intracellular region. Several studies report that NKA α_2 is the primary NKA α isoform involved in translocation following activation by insulin (Brodsky, 1990; Aledo & Hundal, 1995; Al-Khalili *et al.*, 2003b). One study examining translocation in rat skeletal muscle demonstrated that insulin had no effect on NKA α_1 or β_2 , and that the main insulin-responsive enzyme was an $\alpha_2:\beta_1$ dimer (Hundal *et al.*, 1992). There is evidence providing support for insulin-

induced translocation (Omatsu-Kanbe & Kitasato, 1990; Lavoie *et al.*, 1996; Al-Khalili *et al.*, 2003b) and against (McKenna *et al.*, 2003), but the mechanisms responsible for this are still being examined, with phosphorylation of the α subunits suggested to be involved (Chibalin *et al.*, 2001; Al-Khalili *et al.*, 2003a). With advancements in techniques allowing separate analysis of different cellular compartments and growing supportive research, translocation appears a likely process, most probably from the caveolae to the plasma membrane, but more investigation is required to determine the exact mechanisms involved in the process.

6.1.3 Exercise, supplementation and NKA protein abundance

The effects of acute exercise with prior glucose, or NaHCO₃ versus placebo on skeletal muscle NKA isoform protein abundance were examined with a high intensity intermittent cycling protocol in Study 1, and the repeated sprint exercise protocol in Study 2. Neither type of acute exercise induced changes in abundance of any of the NKA α_{1-3} isoforms. This supports previous research using continuous exercise models that found no change in NKA isoform protein abundance following acute high intensity exercise (Juel *et al.*, 2000a; Murphy *et al.*, 2004). An interesting finding in Study 1 in the CON trial was an increase in NKA β_3 abundance, but this finding was not detected for the CHO trial, nor was it repeated in the placebo trial in Study 2. This discrepancy between trials may be due to the different exercise protocols used. Whilst both trials involved high intensity exercise (130% VO_{2peak} vs. all-out effort), the total exercise duration for Study 1 was more than three times that of Study 2, potentially providing a greater stimulus to initiate NKA protein synthesis. However, the protocols used in both trials were still of a very short duration, being approximately 3.25 min for Study 1, and 60 sec for Study 2.

An increase in NKA β_1 was found for the PRE-NaHCO₃ trial, but this was a treatment main effect, thus combining the pre- and post-exercise biopsies, and with no pre-ingestion biopsy, it is not possible to determine the timing of the protein increase. These differing results suggest that the combination of acute high intensity exercise with prior glucose or NaHCO₃ supplementation may increase the NKA upregulation sometimes seen following acute exercise.

In Study 2, chronic NaHCO₃ supplementation taken during 4 wks of RSE training, compared to the RSE training in the absence of NaHCO₃, decreased β_1 and increased β_3 protein abundance, but had no effect on the NKA α_{1-3} or β_2 isoforms in vastus lateralis muscle. The lack of increased NKA α_{1-3} protein abundance following 4 wks RSE training in both conditions was surprising, and might simply be due to the RSE training protocol utilised having insufficient training volume to stimulate increased NKA isoform protein synthesis. However, the decrease in β_1 and also tendency for lower NKA β_2 isoform abundance following RSE training with NaHCO₃ may also in part be related to the previously reported K⁺-lowering effects of NaHCO₃ supplementation (Sostaric *et al.*, 2006). Animal studies have demonstrated reductions in skeletal muscle β_1 and β_2 protein abundance following chronic K⁺ deprivation (Thompson & McDonough, 1996). It is thus possible that chronic NaHCO₃ ingestion with training may result in a similar response, but the reduction in plasma [K⁺] is likely much greater with chronic K⁺ deprivation compared to NaHCO₃ supplementation. However, plasma [K⁺] was not monitored during the training phase, therefore it is not possible to conclude on this postulated mechanism. Furthermore, training can also result in a lowering of the resting plasma [K⁺] albeit by only a small amount (McKenna *et al.*, 1997; Nielsen *et al.*, 2004a). This possible effect should be investigated further with chronic NaHCO₃ supplementation during a training protocol previously demonstrated to

increase NKA protein abundance, and with the added inclusion of plasma $[K^+]$ monitoring periodically throughout the training program, in conjunction with measures of skeletal muscle NKA protein abundance.

6.1.4 Cellular localisation

This final study examined the cellular localisation of the six NKA isoforms expressed in human skeletal muscle, $\alpha_1 - \alpha_3$ and $\beta_1 - \beta_3$, by quantitatively analysing and comparing fluorescence from the plasma membrane and intracellular regions, which encompassed the t-tubules, sarcoplasm and cytoskeleton, as well as fluorescence between type I and type II fibres. Both the NKA α_2 and β_1 isoforms were expressed with greater density in the plasma membrane, regardless of fibre type (Table 6.1). Previous immunofluorescence research has been of a qualitative nature on rat skeletal muscle (Williams *et al.*, 2001; Zhang *et al.*, 2006), so the relative distribution between regions cannot be accurately compared between studies. Analysis of NKA isoform expression in fibre types revealed NKA α_1 and α_3 were expressed with greater density in type II and type I fibres, respectively (Tables 6.1 - 6.2). This has possible functional relevance for NKA activity levels, with NKA α_3 having a lower affinity for $[Na^+]_i$ compared to α_1 and α_2 (Munzer *et al.*, 1994) and potentially resulting in a lower NKA activity in type I fibres.

Table 6.1 Summary of immunofluorescence localisation in human vastus lateralis muscle results from Study 3.

NKA isoform	Location	Fibre type difference
α_1	PM \approx IC	I < II
α_2	PM 2x > IC	I \approx II
α_3	PM \approx IC	I 2x > II
β_1	PM 47% > IC	I \approx II
β_2	PM 44% > IC	I \approx II
β_3	PM \approx IC	NM

PM plasma membrane; IC intracellular; NM not measured.

The fibre type specific expression of the NKA α_1 and α_3 also has important implications for studies investigating changes in NKA isoforms following exercise interventions. Most human muscle analyses are performed on biopsies obtained from the vastus lateralis muscle, which is of a mixed fibre type (Staron *et al.*, 2000). If adaptations occur in specific fibre types specific to the exercise mode utilised, then results from mixed whole homogenates may not provide an accurate representation of changes in different fibre types. This could contribute to the lack of change seen in protein abundance in both Study 1 and Study 2. As both of these utilised high intensity exercise, suggesting NKA changes would most likely be seen in type II fibres, which constitute approximately only half of the fibres present in the vastus lateralis. Analysis of dissected human vastus lateralis muscle segments demonstrated that following acute high intensity exercise, phosphorylation of FXVD1 (PLM) was increased only in type II fibres and unchanged in type I fibres (Thomassen *et al.*, 2013). If the protein analysis involved had examined type I and type II fibres separately, it would likely have been more sensitive to detect any changes that occurred.

Table 6.2 Summary of NKA immunofluorescence density in human vastus lateralis muscle results from Study 3.

NKA isoform	PM Density (a.u.)	
	MHC I	MHC II
α_1	7.2	9.0
α_2	7.9	7.5
α_3	9.2	3.9
β_1	14.4	13.9
β_2	4.6	4.3
β_3	NM	NM

a.u. arbitrary units; NM not measured.

All three α isoforms, as well as the β_1 isoform demonstrated strong intracellular fluorescence, which appeared likely to be localisation of the isoforms within the t-tubular system. T-tubular localisation of the NKA is consistent with previous studies on NKA α_2 in developing mouse skeletal muscle (Cougnon *et al.*, 2002) and immunofluorescence labelling of NKA α_1 and α_2 in rat EDL (Williams *et al.*, 2001). It has been previously shown that during strenuous exercise the plasma $[K^+]$ in venous blood draining contracting muscle can double from resting values (Sjøgaard *et al.*, 1985; Bangsbo *et al.*, 1996) and reach even higher values in the muscle interstitium (Nordsborg *et al.*, 2003). Electrical stimulation of surface fibres of the EDL of rats showed that $[K^+]$ in the innermost t-tubules, estimated via modelling, reached approximately 13 mmol.l^{-1} when stimulated at 30 Hz (Fraser *et al.*, 2011). Therefore, the change in K^+ homeostasis in the t-tubules may be particularly pronounced following activation, and K^+ released in to the t-tubule can likely only be rapidly removed by reuptake mediated by transport proteins located within the t-tubule membrane (Kristensen & Juel, 2010). This suggests that the localisation of NKA α_1 and α_2 within the t-tubules is functionally very important.

6.2 Conclusions

The major conclusions from this thesis are:

Study 1

1. An acute oral glucose load elevated arterial plasma [insulin], decreased arterial and venous plasma $[K^+]$ and also increased the plasma $[K^+]_{a-v \text{ diff}}$ across the relatively inactive forearm musculature.
2. Acute high-intensity intermittent exercise did not change skeletal muscle NKA α_{1-3} , β_1 or β_2 isoform protein abundance.
3. Acute high-intensity intermittent exercise increased the skeletal muscle NKA β_3 isoform protein abundance.

Study 2

4. Acute RSE exercise did not change the skeletal muscle NKA α_{1-3} or β_{1-3} isoform protein abundance.
5. Four weeks of RSE training with chronic NaHCO_3 supplementation did not change the skeletal muscle NKA α_{1-3} , β_2 or β_3 isoform protein abundances, but decreased the NKA β_1 protein abundance.

Study 3

Immunofluorescence analysis of localisation in human vastus lateralis muscle showed that:

6. NKA α_1 is expressed with a 24% greater density in type II fibres, while NKA α_3 is expressed with a 90% greater density in type I fibres.
7. NKA α_2 and β_1 isoforms were expressed with greater density in the plasma membrane than in the intracellular region which encompassed the t-tubules, sarcoplasm and cytoskeleton, but with a strong t-tubular localisation suggested by DHPR localisation analysis.

8. NKA β_2 co-localised with the cell nuclei.
9. NKA β_3 demonstrated a possible co-localisation with vascular tissue.

6.3 Recommendations for future studies

Several recommendations for future directions of research follow on from this thesis. As Study 3 demonstrated fibre type specific expression of NKA α_1 and α_3 isoforms, it is recommended that future analyses of mixed fibre type muscle, such as the vastus lateralis muscle, include analysis techniques which enable the NKA protein expression to be analysed and compared between the different fibre types.

The technique of quantifying NKA localisation using immunofluorescence could be used to also examine the fibre type distribution and cellular localisation in human skeletal muscle of other transport proteins such as the Na^+/H^+ exchanger, the $\text{Na}^+, \text{K}^+, \text{Cl}^-$ co-transporter, and the MCT family of lactate transporters. This technique should also be further investigated to determine if it is suitable for investigation of translocation and movement of proteins between different cellular locations; however the use of higher magnification or confocal imaging may be needed to assist in the identification of other intracellular locations or “pools” of transport proteins.

The inclusion of immunofluorescence localisation analysis of skeletal muscle following glucose ingestion and insulin infusion could be utilised to investigate insulin-induced translocation of NKA isoforms from intracellular locations to the plasma membrane. The investigation of varying concentrations of insulin infusion and the addition of measures of blood flow would allow for quantification of muscle K^+ uptake alongside any changes in NKA protein abundance or location.

The suggested adverse effects of chronic NaHCO_3 supplementation during exercise training on NKA isoforms is also an area for further investigation. By utilising a

training protocol that has been reliably demonstrated to increase NKA protein abundance, the effects of chronic NaHCO_3 supplementation could be further investigated. This would also require the addition of regular monitoring of plasma $[\text{K}^+]$ during the training phase to monitor for NaHCO_3 -induced hypokalaemia. The inclusion of immunofluorescence localisation analysis and confocal scanning could also be used to investigate possible exercise-induced translocation of the NKA isoforms.

It has also been recently identified that mutations of the NKA α_3 isoform are associated with some neurological disorders, most notably rapid-onset dystonia parkinsonism and alternating hemiplegia of childhood (Heinzen *et al.*, 2014). Therefore it is suggested that the localisation and expression of the NKA α_3 isoform in skeletal muscle be examined in populations expressing this mutation and compared to normal populations. By including an exercise intervention, a comparison between the clinical population and healthy controls could also be done to examine for any impairments in K^+ regulation during exercise in people with NKA α_3 mutations. Investigations should include, but not be limited to comparisons of fibre type specific NKA isoform expression, [^3H]ouabain binding and NKA activity. Consideration should also be given to the mechanisms involved in NKA regulation in skeletal muscle, such as the aforementioned phosphorylation of the α subunits. This will help improve the understanding of the role the NKA plays in skeletal muscle function within both healthy and clinical populations.

REFERENCES

- Al-Khalili L, Kotova O, Tsuchida H, Ehren I, Feraille E, Krook A & Chibalin AV. (2004). ERK1/2 mediates insulin stimulation of Na⁺,K⁺-ATPase by phosphorylation of the alpha-subunit in human skeletal muscle cells. *Journal of Biological Chemistry* **279**, 25211-25218.
- Al-Khalili L, Krook A & Chibalin AV. (2003a). Phosphorylation of the Na⁺,K⁺-ATPase in skeletal muscle: potential mechanism for changes in pump cell-surface abundance and activity. *Ann N Y Acad Sci* **986**, 449-452.
- Al-Khalili L, Yu M & Chibalin AV. (2003b). Na⁺,K⁺-ATPase trafficking in skeletal muscle: insulin stimulates translocation of both alpha 1- and alpha 2-subunit isoforms. *FEBS Lett* **536**, 198-202.
- Aledo JC & Hundal HS. (1995). Sedimentation and immunological analyses of GLUT4 and alpha 2-Na,K-ATPase subunit-containing vesicles from rat skeletal muscle: evidence for segregation. *FEBS Lett* **376**, 211-215.
- Alvestrand A, Wahren J, Smith D & DeFronzo RA. (1984). Insulin-mediated potassium uptake is normal in uremic and healthy subjects. *American Journal of Physiology* **246**, E174-180.
- Andres R, Baltzan MA, Cader G & Zierler KL. (1962). Effect of insulin on carbohydrate metabolism and on potassium in the forearm of man. *Journal of Clinical Investigation* **41**, 108-115.
- Aughey RJ, Gore CJ, Hahn AG, Garnham AP, Clark SA, Petersen AC, Roberts AD & McKenna MJ. (2005). Chronic intermittent hypoxia and incremental cycling exercise independently depress muscle in vitro maximal Na⁺-K⁺-ATPase activity in well-trained athletes. *Journal of applied physiology* **98**, 186-192.
- Aughey RJ, Murphy KT, Clark SA, Garnham AP, Snow RJ, Cameron-Smith D, Hawley JA & McKenna MJ. (2007). Muscle Na⁺-K⁺-ATPase activity and isoform adaptations to intense interval exercise and training in well-trained athletes. *Journal of applied physiology* **103**, 39-47.
- Azuma KK, Hensley CB, Putnam DS & McDonough AA. (1991). Hypokalemia decreases Na⁺-K⁺-ATPase alpha 2- but not alpha 1-isoform abundance in heart, muscle, and brain. *American Journal Physiology* **260**, C958-964.
- Balog EM & Fitts RH. (1996). Effects of fatiguing stimulation on intracellular Na⁺ and K⁺ in frog skeletal muscle. *Journal of applied physiology* **81**, 679-685.
- Balog EM, Thompson LV & Fitts RH. (1994). Role of sarcolemma action potentials and excitability in muscle fatigue. *Journal of applied physiology* **76**, 2157-2162.
- Bangsbo J, Gunnarsson TP, Wendell J, Nybo L & Thomassen M. (2009). Reduced volume and increased training intensity elevate muscle Na⁺-K⁺ pump alpha2-

- subunit expression as well as short- and long-term work capacity in humans. *Journal of applied physiology* **107**, 1771-1780.
- Bangsbo J, Madsen K, Kiens B & Richter EA. (1996). Effect of muscle acidity on muscle metabolism and fatigue during intense exercise in man. *Journal of physiology* **495 (Pt 2)**, 587-596.
- Batterham AM & Hopkins WG. (2006). Making meaningful inferences about magnitudes. *Int J Sports Physiol Perform* **1**, 50-57.
- Beggah AT, Jaunin P & Geering K. (1997). Role of glycosylation and disulfide bond formation in the beta subunit in the folding and functional expression of Na,K-ATPase. *Journal of Biological Chemistry* **272**, 10318-10326.
- Berry RG, Despa S, Fuller W, Bers DM & Shattock MJ. (2007). Differential distribution and regulation of mouse cardiac Na⁺/K⁺-ATPase alpha₁ and alpha₂ subunits in T-tubule and surface sarcolemmal membranes. *Cardiovascular Research* **73**, 92-100.
- Bevegard BS & Shepherd JT. (1966). Reaction in man of resistance and capacity vessels in forearm and hand to leg exercise. *Journal of applied physiology* **21**, 123-132.
- Bishop D, Edge J, Davis C & Goodman C. (2004). Induced metabolic alkalosis affects muscle metabolism and repeated-sprint ability. *Med Sci Sports Exerc* **36**, 807-813.
- Blanco G & Mercer RW. (1998). Isozymes of the Na-K-ATPase: heterogeneity in structure, diversity in function. *American Journal Physiology* **275**, F633-650.
- Boenisch T, ed. (2001). *Handbook of immunochemical staining methods*. DAKO Corporation, Carpinteria, CA, USA.
- Bolte S & Cordelieres FP. (2006). A guided tour into subcellular colocalization analysis in light microscopy. *J Microsc* **224**, 213-232.
- Bossuyt J, Despa S, Han F, Hou Z, Robia SL, Lingrel JB & Bers DM. (2009). Isoform specificity of the Na/K-ATPase association and regulation by phospholemman. *Journal of biological chemistry* **284**, 26749-26757.
- Boucllin R, Charbonneau E & Renaud JM. (1995). Na⁺ and K⁺ effect on contractility of frog sartorius muscle: implication for the mechanism of fatigue. *American Journal Physiology* **268**, C1528-1536.
- Broch-Lips M, Overgaard K, Praetorius HA & Nielsen OB. (2007). Effects of extracellular HCO₃ on fatigue, pH_i, and K⁺ efflux in rat skeletal muscles. *Journal of applied physiology* **103**, 494-503.
- Brodsky JL. (1990). Insulin activation of brain Na⁺-K⁺-ATPase is mediated by alpha 2-form of enzyme. *American Journal Physiology* **258**, C812-817.

- Cairns SP, Buller SJ, Loiselle DS & Renaud JM. (2003). Changes of action potentials and force at lowered $[Na^+]_o$ in mouse skeletal muscle: implications for fatigue. *American Journal Physiology: Cell Physiology* **285**, C1131-1141.
- Cairns SP, Hing WA, Slack JR, Mills RG & Loiselle DS. (1997). Different effects of raised $[K^+]_o$ on membrane potential and contraction in mouse fast- and slow-twitch muscle. *American Journal Physiology* **273**, C598-611.
- Cairns SP & Lindinger MI. (2008). Do multiple ionic interactions contribute to skeletal muscle fatigue? *Journal of Physiology* **586**, 4039-4054.
- Cairns SP, Ruzhynsky V & Renaud JM. (2004). Protective role of extracellular chloride in fatigue of isolated mammalian skeletal muscle. *American Journal Physiology: Cell Physiology* **287**, C762-770.
- Carranza ML, Rousselot M, Chibalin AV, Bertorello AM, Favre H & Feraille E. (1998). Protein kinase A induces recruitment of active Na^+,K^+ -ATPase units to the plasma membrane of rat proximal convoluted tubule cells. *Journal of Physiology* **511** (Pt 1), 235-243.
- Chibalin AV, Kovalenko MV, Ryder JW, Feraille E, Wallberg-Henriksson H & Zierath JR. (2001). Insulin- and glucose-induced phosphorylation of the Na^+,K^+ -adenosine triphosphatase alpha-subunits in rat skeletal muscle. *Endocrinology* **142**, 3474-3482.
- Chow DC & Forte JG. (1995). Functional significance of the beta-subunit for heterodimeric P-type ATPases. *Journal of Experimental Biology* **198**, 1-17.
- Clausen T. (1986). Regulation of active Na^+-K^+ transport in skeletal muscle. *Physiological Reviews* **66**, 542-580.
- Clausen T. (1996). The Na^+, K^+ pump in skeletal muscle: quantification, regulation and functional significance. *Acta physiologica Scandinavica* **156**, 227-235.
- Clausen T. (2003). Na^+-K^+ pump regulation and skeletal muscle contractility. *Physiological Reviews* **83**, 1269-1324.
- Clausen T. (2008). Role of Na^+,K^+ -pumps and transmembrane Na^+,K^+ -distribution in muscle function. The FEPS lecture - Bratislava 2007. *Acta Physiologica* **192**, 339-349.
- Clausen T. (2010). Hormonal and pharmacological modification of plasma potassium homeostasis. *Fundamental and clinical pharmacology* **24**, 595-605.
- Clausen T. (2013). Quantification of Na^+,K^+ pumps and their transport rate in skeletal muscle: functional significance. *Journal of general physiology* **142**, 327-345.

- Clausen T, Andersen SL & Flatman JA. (1993). Na⁺-K⁺ pump stimulation elicits recovery of contractility in K⁺-paralysed rat muscle. *Journal of Physiology* **472**, 521-536.
- Clausen T & Kohn PG. (1977). The effect of insulin on the transport of sodium and potassium in rat soleus muscle. *Journal of Physiology* **265**, 19-42.
- Colognato H & Yurchenco PD. (2000). Form and function: the laminin family of heterotrimers. *Developmental Dynamics* **218**, 213-234.
- Cougnon MH, Moseley AE, Radzyukevich TL, Lingrel JB & Heiny JA. (2002). Na,K-ATPase alpha- and beta-isoform expression in developing skeletal muscles: alpha2 correlates with t-tubule formation. *Pflugers Archives* **445**, 123-131.
- Coyle EF, Coggan AR, Hemmert MK & Ivy JL. (1986). Muscle glycogen utilization during prolonged strenuous exercise when fed carbohydrate. *Journal of applied physiology* **61**, 165-172.
- Coyle EF, Hagberg JM, Hurley BF, Martin WH, Ehsani AA & Holloszy JO. (1983). Carbohydrate feeding during prolonged strenuous exercise can delay fatigue. *Journal of applied physiology* **55**, 230-235.
- Cunningham JN, Jr., Carter NW, Rector FC, Jr. & Seldin DW. (1971). Resting transmembrane potential difference of skeletal muscle in normal subjects and severely ill patients. *Journal of clinical investigation* **50**, 49-59.
- de Paoli FV, Overgaard K, Pedersen TH & Nielsen OB. (2007). Additive protective effects of the addition of lactic acid and adrenaline on excitability and force in isolated rat skeletal muscle depressed by elevated extracellular K⁺. *Journal of Physiology* **581**, 829-839.
- DeFronzo RA. (1988). Obesity is associated with impaired insulin-mediated potassium uptake. *Metabolism* **37**, 105-108.
- DeFronzo RA, Felig P, Ferrannini E & Wahren J. (1980). Effect of graded doses of insulin on splanchnic and peripheral potassium metabolism in man. *American Journal Physiology* **238**, E421-427.
- Di Biase V & Franzini-Armstrong C. (2005). Evolution of skeletal type e-c coupling: a novel means of controlling calcium delivery. *Journal of Cell Biology* **171**, 695-704.
- Dombrowski L, Roy D, Marcotte B & Marette A. (1996). A new procedure for the isolation of plasma membranes, T tubules, and internal membranes from skeletal muscle. *American Journal Physiology* **270**, E667-676.
- Dorup I & Clausen T. (1995). Insulin-like growth factor I stimulates active Na⁺-K⁺ transport in rat soleus muscle. *American Journal Physiology* **268**, E849-857.

- Dufer M, Haspel D, Krippeit-Drews P, Aguilar-Bryan L, Bryan J & Drews G. (2009). Activation of the Na⁺/K⁺-ATPase by insulin and glucose as a putative negative feedback mechanism in pancreatic beta-cells. *Pflugers Archives* **457**, 1351-1360.
- Dutka TL & Lamb GD. (2007). Na⁺-K⁺ pumps in the transverse tubular system of skeletal muscle fibers preferentially use ATP from glycolysis. *American Journal Physiology: Cell Physiology* **293**, C967-977.
- Dutka TL, Murphy RM, Stephenson DG & Lamb GD. (2008). Chloride conductance in the transverse tubular system of rat skeletal muscle fibres: importance in excitation-contraction coupling and fatigue. *Journal of Physiology* **586**, 875-887.
- Erlj D & Grinstein S. (1976). The number of sodium ion pumping sites in skeletal muscle and its modification by insulin. *Journal of Physiology* **259**, 13-31.
- Everts ME & Clausen T. (1992). Activation of the Na-K pump by intracellular Na in rat slow- and fast-twitch muscle. *Acta physiologica Scandinavica* **145**, 353-362.
- Everts ME & Clausen T. (1994). Excitation-induced activation of the Na⁺-K⁺ pump in rat skeletal muscle. *American Journal Physiology* **266**, C925-934.
- Evertsen F, Medbo JJ, Jebens E & Nicolaysen K. (1997). Hard training for 5 mo increases Na⁺-K⁺ pump concentration in skeletal muscle of cross-country skiers. *American Journal of Physiology* **272**, R1417-1424.
- Ewart HS & Klip A. (1995). Hormonal regulation of the Na⁺-K⁺-ATPase: mechanisms underlying rapid and sustained changes in pump activity. *American Journal Physiology* **269**, C295-311.
- Fambrough DM & Bayne EK. (1983). Multiple forms of Na⁺,K⁺-ATPase in the chicken. Selective detection of the major nerve, skeletal muscle, and kidney form by a monoclonal antibody. *Journal of biological chemistry* **258**, 3926-3935.
- Feraille E, Carranza ML, Gonin S, Beguin P, Pedemonte C, Rousselot M, Caverzasio J, Geering K, Martin PY & Favre H. (1999). Insulin-induced stimulation of Na⁺,K⁺-ATPase activity in kidney proximal tubule cells depends on phosphorylation of the alpha-subunit at Tyr-10. *Mol Biol Cell* **10**, 2847-2859.
- Feraille E, Rousselot M, Rajerison R & Favre H. (1995). Effect of insulin on Na⁺,K⁺-ATPase in rat collecting duct. *Journal of Physiology* **488 (Pt 1)**, 171-180.
- Ferrannini E, Taddei S, Santoro D, Natali A, Boni C, Del Chiaro D & Buzzigoli G. (1988). Independent stimulation of glucose metabolism and Na⁺-K⁺ exchange by insulin in the human forearm. *American Journal Physiology* **255**, E953-958.
- Fitts RH. (1994). Cellular mechanisms of muscle fatigue. *Physiological Reviews* **74**, 49-94.
- Fitts RH. (2008). The cross-bridge cycle and skeletal muscle fatigue. *Journal of applied physiology* **104**, 551-558.

- Fitts RH & Balog EM. (1996). Effect of intracellular and extracellular ion changes on E-C coupling and skeletal muscle fatigue. *Acta physiologica Scandinavica* **156**, 169-181.
- Fowles JR, Green HJ & Ouyang J. (2004). Na⁺-K⁺-ATPase in rat skeletal muscle: content, isoform, and activity characteristics. *Journal of applied physiology* **96**, 316-326.
- Fowles JR, Green HJ, Tupling R, O'Brien S & Roy BD. (2002). Human neuromuscular fatigue is associated with altered Na⁺-K⁺-ATPase activity following isometric exercise. *Journal of applied physiology* **92**, 1585-1593.
- Fraser JA, Huang CL & Pedersen TH. (2011). Relationships between resting conductances, excitability, and t-system ionic homeostasis in skeletal muscle. *Journal of general physiology* **138**, 95-116.
- Fraser SF, Li JL, Carey MF, Wang XN, Sangkabuttra T, Sostaric S, Selig SE, Kjeldsen K & McKenna MJ. (2002). Fatigue depresses maximal in vitro skeletal muscle Na⁺-K⁺-ATPase activity in untrained and trained individuals. *Journal of applied physiology* **93**, 1650-1659.
- Fraser SF & McKenna MJ. (1998). Measurement of Na⁺, K⁺-ATPase activity in human skeletal muscle. *Anal Biochem* **258**, 63-67.
- Fugmann A, Lind L, Andersson PE, Millgard J, Hanni A, Berne C & Lithell H. (1998). The effect of euglucaemic hyperinsulinaemia on forearm blood flow and glucose uptake in the human forearm. *Acta Diabetologica* **35**, 203-206.
- Fuller W, Eaton P, Bell JR & Shattock MJ. (2004). Ischemia-induced phosphorylation of phospholemman directly activates rat cardiac Na/K-ATPase. *FASEB journal* **18**, 197-199.
- Gaitanos GC, Nevill ME, Brooks S & Williams C. (1991). Repeated bouts of sprint running after induced alkalosis. *J Sports Sci* **9**, 355-370.
- Gavryck WA, Moore RD & Thompson RC. (1975). Effect of insulin upon membrane-bound Na⁺,K⁺-ATPase extracted from frog skeletal muscle. *Journal of Physiology* **252**, 43-58.
- Geering K. (2001). The functional role of beta subunits in oligomeric P-type ATPases. *Journal of Bioenergetics and Biomembranes* **33**, 425-438.
- Geering K. (2006). FXYD proteins: new regulators of Na-K-ATPase. *American Journal of Physiology: Renal Physiology* **290**, F241-250.
- Geering K, Beguin P, Garty H, Karlsh S, Fuzesi M, Horisberger JD & Crambert G. (2003). FXYD proteins: new tissue- and isoform-specific regulators of Na,K-ATPase. *Ann N Y Acad Sci* **986**, 388-394.

- Golovina VA, Song H, James PF, Lingrel JB & Blaustein MP. (2003). Na⁺ pump alpha 2-subunit expression modulates Ca²⁺ signaling. *American Journal Physiology: Cell Physiology* **284**, C475-486.
- Green HJ. (1997). Mechanisms of muscle fatigue in intense exercise. *J Sports Sci* **15**, 247-256.
- Green HJ, Barr DJ, Fowles JR, Sandiford SD & Ouyang J. (2004). Malleability of human skeletal muscle Na⁺-K⁺-ATPase pump with short-term training. *Journal of applied physiology* **97**, 143-148.
- Green HJ, Chin ER, Ball-Burnett M & Ranney D. (1993). Increases in human skeletal muscle Na⁺-K⁺-ATPase concentration with short-term training. *American Journal Physiology* **264**, C1538-1541.
- Green HJ, Duhamel TA, Foley KP, Ouyang J, Smith IC & Stewart RD. (2007a). Glucose supplements increase human muscle in vitro Na⁺-K⁺-ATPase activity during prolonged exercise. *American Journal of Physiology: Regulatory, Integrative and Comparative Physiology* **293**, R354-362.
- Green HJ, Duhamel TA, Holloway GP, Moule JW, Ouyang J, Ranney D & Tupling AR. (2007b). Muscle Na⁺-K⁺-ATPase response during 16 h of heavy intermittent cycle exercise. *American Journal of Physiology: Endocrinology and Metabolism* **293**, E523-530.
- Grounds MD, Sorokin L & White J. (2005). Strength at the extracellular matrix-muscle interface. *Scandinavian Journal of Medicine and Science in Sports* **15**, 381-391.
- Hansen O & Clausen T. (1988). Quantitative determination of Na⁺-K⁺-ATPase and other sarcolemmal components in muscle cells. *American Journal Physiology* **254**, C1-7.
- Hansen PS, Clarke RJ, Buhagiar KA, Hamilton E, Garcia A, White C & Rasmussen HH. (2007). Alloxan-induced diabetes reduces sarcolemmal Na⁺-K⁺ pump function in rabbit ventricular myocytes. *American Journal Physiology: Cell Physiology* **292**, C1070-1077.
- Harmer AR, McKenna MJ, Sutton JR, Snow RJ, Ruell PA, Booth J, Thompson MW, Mackay NA, Stathis CG, Crameri RM, Carey MF & Eager DM. (2000). Skeletal muscle metabolic and ionic adaptations during intense exercise following sprint training in humans. *Journal of applied physiology* **89**, 1793-1803.
- Harrison MH. (1985). Effects on thermal stress and exercise on blood volume in humans. *Physiological Reviews* **65**, 149-209.
- Hawke TJ & Garry DJ. (2001). Myogenic satellite cells: physiology to molecular biology. *Journal of applied physiology* **91**, 534-551.
- He S, Shelly DA, Moseley AE, James PF, James JH, Paul RJ & Lingrel JB. (2001). The alpha₁- and alpha₂-isoforms of Na-K-ATPase play different roles in skeletal

- muscle contractility. *American Journal of Physiology: Regulatory, Integrative and Comparative Physiology* **281**, R917-925.
- Heinzen EL, Arzimanoglou A, Brashear A, Clapcote SJ, Gurrieri F, Goldstein DB, Johannesson SH, Mikati MA, Neville B, Nicole S, Ozelius LJ, Poulsen H, Schyns T, Sweadner KJ, van den Maagdenberg A & Vilsen B. (2014). Distinct neurological disorders with ATP1A3 mutations. *Lancet Neurol* **13**, 503-514.
- Hodgkin AL & Huxley AF. (1952). Propagation of electrical signals along giant nerve fibers. *Proceedings of the Royal Society of London Series B, Containing papers of a Biological character* **140**, 177-183.
- Hopkins WG. (2006). Spreadsheets for analysis of controlled trials with adjustment for a predictor. *Sportscience* **10**, 46-50.
- Hsu YM & Guidotti G. (1991). Effects of hypokalemia on the properties and expression of the Na⁺,K⁺-ATPase of rat skeletal muscle. *Journal of Biological Chemistry* **266**, 427-433.
- Hu YK & Kaplan JH. (2000). Site-directed chemical labeling of extracellular loops in a membrane protein. The topology of the Na,K-ATPase alpha-subunit. *Journal of Biological Chemistry* **275**, 19185-19191.
- Hundal HS, Marette A, Mitumoto Y, Ramlal T, Blostein R & Klip A. (1992). Insulin induces translocation of the alpha 2 and beta 1 subunits of the Na⁺/K⁺-ATPase from intracellular compartments to the plasma membrane in mammalian skeletal muscle. *Journal of Biological Chemistry* **267**, 5040-5043.
- Hundal HS, Marette A, Ramlal T, Liu Z & Klip A. (1993). Expression of beta subunit isoforms of the Na⁺,K⁺-ATPase is muscle type-specific. *FEBS Lett* **328**, 253-258.
- Hundal HS, Maxwell DL, Ahmed A, Darakhshan F, Mitumoto Y & Klip A. (1994). Subcellular distribution and immunocytochemical localization of Na,K-ATPase subunit isoforms in human skeletal muscle. *Molecular Membrane Biology* **11**, 255-262.
- Iaia FM, Thomassen M, Kolding H, Gunnarsson T, Wendell J, Rostgaard T, Nordsborg N, Krstrup P, Nybo L, Hellsten Y & Bangsbo J. (2008). Reduced volume but increased training intensity elevates muscle Na⁺-K⁺ pump α 1-subunit and NHE1 expression as well as short-term work capacity in humans. *American Journal of Physiology: Regulatory, Integrative and Comparative Physiology* **294**, R966-974.
- Jaimovich E, Donoso P, Liberona JL & Hidalgo C. (1986). Ion pathways in transverse tubules. Quantification of receptors in membranes isolated from frog and rabbit skeletal muscle. *Biochimica et Biophysica Acta* **855**, 89-98.
- James JH, Fang CH, Schrantz SJ, Hasselgren PO, Paul RJ & Fischer JE. (1996). Linkage of aerobic glycolysis to sodium-potassium transport in rat skeletal

- muscle. Implications for increased muscle lactate production in sepsis. *Journal of Clinical Investigation* **98**, 2388-2397.
- Jewell EA & Lingrel JB. (1991). Comparison of the substrate dependence properties of the rat Na,K-ATPase alpha 1, alpha 2, and alpha 3 isoforms expressed in HeLa cells. *Journal of Biological Chemistry* **266**, 16925-16930.
- Juel C. (1988). Muscle action potential propagation velocity changes during activity. *Muscle and nerve* **11**, 714-719.
- Juel C. (2009). Na⁺-K⁺-ATPase in rat skeletal muscle: muscle fiber-specific differences in exercise-induced changes in ion affinity and maximal activity. *American Journal of Physiology: Regulatory, Integrative and Comparative Physiology* **296**, R125-132.
- Juel C, Grunnet L, Holse M, Kenworthy S, Sommer V & Wulff T. (2001). Reversibility of exercise-induced translocation of Na⁺-K⁺ pump subunits to the plasma membrane in rat skeletal muscle. *Pflugers Archives* **443**, 212-217.
- Juel C, Klarskov C, Nielsen JJ, Krstrup P, Mohr M & Bangsbo J. (2004). Effect of high-intensity intermittent training on lactate and H⁺ release from human skeletal muscle. *American Journal of Physiology: Endocrinology and Metabolism* **286**, E245-251.
- Juel C, Nielsen JJ & Bangsbo J. (2000a). Exercise-induced translocation of Na⁺-K⁺ pump subunits to the plasma membrane in human skeletal muscle. *American Journal of Physiology: Regulatory, Integrative and Comparative Physiology* **278**, R1107-1110.
- Juel C, Nordsborg NB & Bangsbo J. (2013). Exercise-induced increase in maximal in vitro Na-K-ATPase activity in human skeletal muscle. *American Journal of Physiology: Regulatory, Integrative and Comparative Physiology* **304**, R1161-1165.
- Juel C, Pilegaard H, Nielsen JJ & Bangsbo J. (2000b). Interstitial K⁺ in human skeletal muscle during and after dynamic graded exercise determined by microdialysis. *American Journal of Physiology: Regulatory, Integrative and Comparative Physiology* **278**, R400-406.
- Kaplan JH. (2002). Biochemistry of Na,K-ATPase. *Annual Review of Biochemistry* **71**, 511-535.
- Karelis AD, Peronnet F & Gardiner PF. (2002). Glucose infusion attenuates muscle fatigue in rat plantaris muscle during prolonged indirect stimulation in situ. *Experimental Physiology* **87**, 585-592.
- Karelis AD, Peronnet F & Gardiner PF. (2003). Insulin does not mediate the attenuation of fatigue associated with glucose infusion in rat plantaris muscle. *Journal of applied physiology* **95**, 330-335.

- Kowalchuk JM, Heigenhauser GJ, Lindinger MI, Obminski G, Sutton JR & Jones NL. (1988a). Role of lungs and inactive muscle in acid-base control after maximal exercise. *Journal of applied physiology* **65**, 2090-2096.
- Kowalchuk JM, Heigenhauser GJ, Lindinger MI, Sutton JR & Jones NL. (1988b). Factors influencing hydrogen ion concentration in muscle after intense exercise. *Journal of applied physiology* **65**, 2080-2089.
- Kristensen M, Albertsen J, Rentsch M & Juel C. (2005). Lactate and force production in skeletal muscle. *The Journal of physiology* **562**, 521-526.
- Kristensen M & Juel C. (2010). Potassium-transporting proteins in skeletal muscle: cellular location and fibre-type differences. *Acta Physiologica* **198**, 105-123.
- Kristensen M, Rasmussen MK & Juel C. (2008). Na⁺-K⁺ pump location and translocation during muscle contraction in rat skeletal muscle. *Pflugers Archives* **456**, 979-989.
- Lansbery KL, Burcea LC, Mendenhall ML & Mercer RW. (2006). Cytoplasmic targeting signals mediate delivery of phospholemman to the plasma membrane. *American Journal Physiology: Cell Physiology* **290**, C1275-1286.
- Lau YH, Caswell AH, Garcia M & Letellier L. (1979). Ouabain binding and coupled sodium, potassium, and chloride transport in isolated transverse tubules of skeletal muscle. *Journal of general physiology* **74**, 335-349.
- Lavoie L, Levenson R, Martin-Vasallo P & Klip A. (1997). The molar ratios of alpha and beta subunits of the Na⁺-K⁺-ATPase differ in distinct subcellular membranes from rat skeletal muscle. *Biochemistry* **36**, 7726-7732.
- Lavoie L, Roy D, Ramlal T, Dombrowski L, Martin-Vasallo P, Marette A, Carpentier JL & Klip A. (1996). Insulin-induced translocation of Na⁺-K⁺-ATPase subunits to the plasma membrane is muscle fiber type specific. *American Journal Physiology* **270**, C1421-1429.
- Lee-Young RS, Palmer MJ, Linden KC, LePlastrier K, Canny BJ, Hargreaves M, Wadley GD, Kemp BE & McConell GK. (2006). Carbohydrate ingestion does not alter skeletal muscle AMPK signaling during exercise in humans. *American Journal of Physiology: Endocrinology and Metabolism* **291**, E566-573.
- Liang M, Tian J, Liu L, Pierre S, Liu J, Shapiro J & Xie ZJ. (2007). Identification of a pool of non-pumping Na/K-ATPase. *Journal of Biological Chemistry* **282**, 10585-10593.
- Lindinger MI, Franklin TW, Lands LC, Pedersen PK, Welsh DG & Heigenhauser GJ. (2000). NaHCO₃ and KHCO₃ ingestion rapidly increases renal electrolyte excretion in humans. *Journal of applied physiology* **88**, 540-550.
- Lindinger MI & Heigenhauser GJ. (1988). Ion fluxes during tetanic stimulation in isolated perfused rat hindlimb. *American Journal of Physiology* **254**, R117-126.

- Lindinger MI, Heigenhauser GJ, McKelvie RS & Jones NL. (1990a). Role of nonworking muscle on blood metabolites and ions with intense intermittent exercise. *American Journal of Physiology* **258**, R1486-1494.
- Lindinger MI, Heigenhauser GJ, McKelvie RS & Jones NL. (1992). Blood ion regulation during repeated maximal exercise and recovery in humans. *American Journal Physiology* **262**, R126-136.
- Lindinger MI, Heigenhauser GJ & Spriet LL. (1990b). Effects of alkalosis on muscle ions at rest and with intense exercise. *Can J Physiol Pharmacol* **68**, 820-829.
- Lindinger MI, Leung M, Trajcevski KE & Hawke TJ. (2011). Volume regulation in mammalian skeletal muscle: the role of sodium-potassium-chloride cotransporters during exposure to hypertonic solutions. *Journal of physiology* **589**, 2887-2899.
- Lindinger MI & Sjøgaard G. (1991). Potassium regulation during exercise and recovery. *Sports Medicine* **11**, 382-401.
- Lindinger MI, Spriet LL, Hultman E, Putman T, McKelvie RS, Lands LC, Jones NL & Heigenhauser GJ. (1994). Plasma volume and ion regulation during exercise after low- and high-carbohydrate diets. *American Journal of Physiology* **266**, R1896-1906.
- Liu JX, Eriksson PO, Thornell LE & Pedrosa-Domellof F. (2002). Myosin heavy chain composition of muscle spindles in human biceps brachii. *Journal of Histochemistry and Cytochemistry* **50**, 171-183.
- Liu L & Askari A. (2006). Beta-subunit of cardiac Na⁺-K⁺-ATPase dictates the concentration of the functional enzyme in caveolae. *American Journal Physiology: Cell Physiology* **291**, C569-578.
- Lundvall J, Mellander S, Westling H & White T. (1972). Fluid transfer between blood and tissues during exercise. *Acta physiologica Scandinavica* **85**, 258-269.
- Magyar JP, Bartsch U, Wang ZQ, Howells N, Aguzzi A, Wagner EF & Schachner M. (1994). Degeneration of neural cells in the central nervous system of mice deficient in the gene for the adhesion molecule on Glia, the beta 2 subunit of murine Na,K-ATPase. *Journal of cell biology* **127**, 835-845.
- Marette A, Krischer J, Lavoie L, Ackerley C, Carpentier JL & Klip A. (1993). Insulin increases the Na⁺-K⁺-ATPase alpha 2-subunit in the surface of rat skeletal muscle: morphological evidence. *American Journal Physiology* **265**, C1716-1722.
- Mauro A & Adams WR. (1961). The structure of the sarcolemma of the frog skeletal muscle fiber. *Journal of Biophysical and Biochemical Cytology* **10(4)Suppl**, 177-185.

- McConnell G, Fabris S, Proietto J & Hargreaves M. (1994). Effect of carbohydrate ingestion on glucose kinetics during exercise. *Journal of applied physiology* **77**, 1537-1541.
- McDonough AA, Zhang Y, Shin V & Frank JS. (1996). Subcellular distribution of sodium pump isoform subunits in mammalian cardiac myocytes. *American Journal Physiology* **270**, C1221-1227.
- McKenna MJ, Gissel H & Clausen T. (2003). Effects of electrical stimulation and insulin on Na⁺-K⁺-ATPase [³H]ouabain binding in rat skeletal muscle. *Journal of Physiology* **547**, 567-580.
- McKenna MJ, Heigenhauser GJ, McKelvie RS, MacDougall JD & Jones NL. (1997). Sprint training enhances ionic regulation during intense exercise in men. *Journal of Physiology* **501 (Pt 3)**, 687-702.
- McKenna MJ, Perry BD, Serpiello FR, Caldow MK, Levinger P, Cameron-Smith D & Levinger I. (2012). Unchanged [³H]ouabain binding site content but reduced Na⁺-K⁺ pump alpha2-protein abundance in skeletal muscle in older adults. *Journal of applied physiology* **113**, 1505-1511.
- McKenna MJ, Schmidt TA, Hargreaves M, Cameron L, Skinner SL & Kjeldsen K. (1993). Sprint training increases human skeletal muscle Na⁺-K⁺-ATPase concentration and improves K⁺ regulation. *Journal of applied physiology* **75**, 173-180.
- McNaughton L, Backx K, Palmer G & Strange N. (1999). Effects of chronic bicarbonate ingestion on the performance of high-intensity work. *Eur J Appl Physiol Occup Physiol* **80**, 333-336.
- McNaughton LR. (1992). Bicarbonate ingestion: effects of dosage on 60 s cycle ergometry. *J Sports Sci* **10**, 415-423.
- Medved I, Brown MJ, Bjorksten AR, Leppik JA, Sostaric S & McKenna MJ. (2003). N-acetylcysteine infusion alters blood redox status but not time to fatigue during intense exercise in humans. *Journal of applied physiology* **94**, 1572-1582.
- Mercer RW, Biemesderfer D, Bliss DP, Jr., Collins JH & Forbush B, 3rd. (1993). Molecular cloning and immunological characterization of the gamma polypeptide, a small protein associated with the Na,K-ATPase. *Journal of Cell Biology* **121**, 579-586.
- Mohr M, Nordsborg N, Nielsen JJ, Pedersen LD, Fischer C, Krstrup P & Bangsbo J. (2004). Potassium kinetics in human muscle interstitium during repeated intense exercise in relation to fatigue. *Pflugers Archives* **448**, 452-456.
- Moore RD. (1973). Effect of insulin upon the sodium pump in frog skeletal muscle. *Journal of Physiology* **232**, 23-45.

- Morth JP, Pedersen BP, Toustrup-Jensen MS, Sorensen TL, Petersen J, Andersen JP, Vilsen B & Nissen P. (2007). Crystal structure of the sodium-potassium pump. *Nature* **450**, 1043-1049.
- Mueller SM, Gehrig SM, Frese S, Wagner CA, Boutellier U & Toigo M. (2013). Multiday acute sodium bicarbonate intake improves endurance capacity and reduces acidosis in men. *J Int Soc Sports Nutr* **10**, 16.
- Munzer JS, Daly SE, Jewell-Motz EA, Lingrel JB & Blostein R. (1994). Tissue- and isoform-specific kinetic behavior of the Na,K-ATPase. *Journal of Biological Chemistry* **269**, 16668-16676.
- Murphy KT, Aughey RJ, Petersen AC, Clark SA, Goodman C, Hawley JA, Cameron-Smith D, Snow RJ & McKenna MJ. (2007). Effects of endurance training status and sex differences on Na⁺,K⁺-pump mRNA expression, content and maximal activity in human skeletal muscle. *Acta Physiologica* **189**, 259-269.
- Murphy KT, Petersen AC, Goodman C, Gong X, Leppik JA, Garnham AP, Cameron-Smith D, Snow RJ & McKenna MJ. (2006). Prolonged submaximal exercise induces isoform-specific Na⁺-K⁺-ATPase mRNA and protein responses in human skeletal muscle. *Am J Physiol Regul Integr Comp Physiol* **290**, R414-424.
- Murphy KT, Snow RJ, Petersen AC, Murphy RM, Mollica J, Lee JS, Garnham AP, Aughey RJ, Leppik JA, Medved I, Cameron-Smith D & McKenna MJ. (2004). Intense exercise up-regulates Na⁺,K⁺-ATPase isoform mRNA, but not protein expression in human skeletal muscle. *Journal of Physiology* **556**, 507-519.
- Murphy RM & Lamb GD. (2013). Important considerations for protein analyses using antibody based techniques: down-sizing Western blotting up-sizes outcomes. *Journal of physiology* **591**, 5823-5831.
- Murphy RM, Mollica JP & Lamb GD. (2009). Plasma membrane removal in rat skeletal muscle fibers reveals caveolin-3 hot-spots at the necks of transverse tubules. *Exp Cell Res* **315**, 1015-1028.
- Muto S, Sebata K, Watanabe H, Shoji F, Yamamoto Y, Ohashi M, Yamada T, Matsumoto H, Mukouyama T, Yonekura T, Namiki S & Kusano E. (2005). Effect of oral glucose administration on serum potassium concentration in hemodialysis patients. *American Journal of Kidney Disease* **46**, 697-705.
- Natali A, Quinones Galvan A, Santoro D, Pecori N, Taddei S, Salvetti A & Ferrannini E. (1993). Relationship between insulin release, antinatriuresis and hypokalaemia after glucose ingestion in normal and hypertensive man. *Clinical Science* **85**, 327-335.
- Nelson CR & Fitts RH. (2014). Effects of low cell pH and elevated inorganic phosphate on the pCa-force relationship in single muscle fibers at near-physiological temperatures. *American Journal of Physiology: Cell Physiology* **306**, C670-678.

- Nielsen JJ, Mohr M, Klarskov C, Kristensen M, Krstrup P, Juel C & Bangsbo J. (2004a). Effects of high-intensity intermittent training on potassium kinetics and performance in human skeletal muscle. *J Physiol* **554**, 857-870.
- Nielsen OB, de Paoli F & Overgaard K. (2001). Protective effects of lactic acid on force production in rat skeletal muscle. *Journal of Physiology* **536**, 161-166.
- Nielsen OB & de Paoli FV. (2007). Regulation of Na⁺-K⁺ homeostasis and excitability in contracting muscles: implications for fatigue. *Applied Physiology, Nutrition and Metabolism* **32**, 974-984.
- Nielsen OB & Harrison AP. (1998). The regulation of the Na⁺,K⁺ pump in contracting skeletal muscle. *Acta physiologica Scandinavica* **162**, 191-200.
- Nielsen OB, Ortenblad N, Lamb GD & Stephenson DG. (2004b). Excitability of the T-tubular system in rat skeletal muscle: roles of K⁺ and Na⁺ gradients and Na⁺-K⁺ pump activity. *Journal of physiology* **557**, 133-146.
- Nordsborg N, Mohr M, Pedersen LD, Nielsen JJ, Langberg H & Bangsbo J. (2003). Muscle interstitial potassium kinetics during intense exhaustive exercise: effect of previous arm exercise. *American Journal of Physiology: Regulatory, Integrative and Comparative Physiology* **285**, R143-148.
- Nordsborg N, Ovesen J, Thomassen M, Zangenberg M, Jons C, Iaia FM, Nielsen JJ & Bangsbo J. (2008). Effect of dexamethasone on skeletal muscle Na⁺,K⁺ pump subunit specific expression and K⁺ homeostasis during exercise in humans. *Journal of physiology* **586**, 1447-1459.
- Nordsborg N, Thomassen M, Lundby C, Pilegaard H & Bangsbo J. (2005). Contraction-induced increases in Na⁺-K⁺-ATPase mRNA levels in human skeletal muscle are not amplified by activation of additional muscle mass. *American Journal of Physiology: Regulatory, Integrative and Comparative Physiology* **289**, R84-91.
- Norgaard A, Kjeldsen K & Clausen T. (1984). A method for the determination of the total number of ³H-ouabain binding sites in biopsies of human skeletal muscle. *Scandinavian Journal of Clinical and Laboratory Investigation* **44**, 509-518.
- Novel-Chate V, Rey V, Chioloro R, Schneiter P, Leverve X, Jequier E & Tappy L. (2001). Role of Na⁺-K⁺-ATPase in insulin-induced lactate release by skeletal muscle. *American Journal of Physiology: Endocrinology and Metabolism* **280**, E296-300.
- Okamoto K, Wang W, Rounds J, Chambers EA & Jacobs DO. (2001). ATP from glycolysis is required for normal sodium homeostasis in resting fast-twitch rodent skeletal muscle. *American Journal of Physiology: Endocrinology and Metabolism* **281**, E479-488.

- Omatsu-Kanbe M & Kitasato H. (1990). Insulin stimulates the translocation of Na⁺/K⁺-dependent ATPase molecules from intracellular stores to the plasma membrane in frog skeletal muscle. *Biochemical Journal* **272**, 727-733.
- Overgaard K, Lindstrom T, Ingemann-Hansen T & Clausen T. (2002). Membrane leakage and increased content of Na⁺-K⁺ pumps and Ca²⁺ in human muscle after a 100-km run. *Journal of applied physiology* **92**, 1891-1898.
- Overgaard K, Nielsen OB & Clausen T. (1997). Effects of reduced electrochemical Na⁺ gradient on contractility in skeletal muscle: role of the Na⁺-K⁺ pump. *Pflugers Archives* **434**, 457-465.
- Overgaard K, Nielsen OB, Flatman JA & Clausen T. (1999). Relations between excitability and contractility in rat soleus muscle: role of the Na⁺-K⁺ pump and Na⁺/K⁺ gradients. *Journal of Physiology* **518 (Pt 1)**, 215-225.
- Peachey LD & Eisenberg BR. (1978). Helicoids in the T system and striations of frog skeletal muscle fibers seen by high voltage electron microscopy. *Biophys J* **22**, 145-154.
- Pedersen TH, de Paoli F & Nielsen OB. (2005). Increased excitability of acidified skeletal muscle: role of chloride conductance. *J Gen Physiol* **125**, 237-246.
- Pedersen TH, Nielsen OB, Lamb GD & Stephenson DG. (2004). Intracellular acidosis enhances the excitability of working muscle. *Science* **305**, 1144-1147.
- Petersen AC, Murphy KT, Snow RJ, Leppik JA, Aughey RJ, Garnham AP, Cameron-Smith D & McKenna MJ. (2005). Depressed Na⁺-K⁺-ATPase activity in skeletal muscle at fatigue is correlated with increased Na⁺-K⁺-ATPase mRNA expression following intense exercise. *American Journal of Physiology: Regulatory, Integrative and Comparative Physiology* **289**, R266-274.
- Pette D & Staron RS. (2000). Myosin isoforms, muscle fiber types, and transitions. *Microscopy Research and Technique* **50**, 500-509.
- Poortmans JR, Delescaille-Vanden Bossche J & Leclercq R. (1978). Lactate uptake by inactive forearm during progressive leg exercise. *J Appl Physiol Respir Environ Exerc Physiol* **45**, 835-839.
- Presti CF, Jones LR & Lindemann JP. (1985a). Isoproterenol-induced phosphorylation of a 15-kilodalton sarcolemmal protein in intact myocardium. *Journal of biological chemistry* **260**, 3860-3867.
- Presti CF, Scott BT & Jones LR. (1985b). Identification of an endogenous protein kinase C activity and its intrinsic 15-kilodalton substrate in purified canine cardiac sarcolemmal vesicles. *Journal of biological chemistry* **260**, 13879-13889.

- Radzyukevich TL, Lingrel JB & Heiny JA. (2009). The cardiac glycoside binding site on the Na,K-ATPase α_2 isoform plays a role in the dynamic regulation of active transport in skeletal muscle. *Proc Natl Acad Sci U S A* **106**, 2565-2570.
- Radzyukevich TL, Neumann JC, Rindler TN, Oshiro N, Goldhamer DJ, Lingrel JB & Heiny JA. (2013). Tissue-specific role of the Na,K-ATPase α_2 isozyme in skeletal muscle. *Journal of biological chemistry* **288**, 1226-1237.
- Ramlal T, Ewart HS, Somwar R, Deems RO, Valentin MA, Young DA & Klip A. (1996). Muscle subcellular localization and recruitment by insulin of glucose transporters and $\text{Na}^+\text{-K}^+\text{-ATPase}$ subunits in transgenic mice overexpressing the GLUT4 glucose transporter. *Diabetes* **45**, 1516-1523.
- Rasmussen MK, Kristensen M & Juel C. (2008). Exercise-induced regulation of phospholemman (FXD1) in rat skeletal muscle: implications for $\text{Na}^+\text{/K}^+\text{-ATPase}$ activity. *Acta Physiologica*.
- Raymer GH, Marsh GD, Kowalchuk JM & Thompson RT. (2004). Metabolic effects of induced alkalosis during progressive forearm exercise to fatigue. *Journal of applied physiology* **96**, 2050-2056.
- Renaud KJ, Inman EM & Fambrough DM. (1991). Cytoplasmic and transmembrane domain deletions of Na,K-ATPase beta-subunit. Effects on subunit assembly and intracellular transport. *Journal of Biological Chemistry* **266**, 20491-20497.
- Resh MD, Nemenoff RA & Guidotti G. (1980). Insulin stimulation of ($\text{Na}^+\text{,K}^+\text{)-adenosine triphosphatase-dependent } ^{86}\text{Rb}^+$ uptake in rat adipocytes. *Journal of Biological Chemistry* **255**, 10938-10945.
- Rosic NK, Standaert ML & Pollet RJ. (1985). The mechanism of insulin stimulation of $\text{Na}^+\text{,K}^+\text{-ATPase}$ transport activity in muscle. *Journal of Biological Chemistry* **260**, 6206-6212.
- Rudnick J, Puttmann B, Tesch PA, Alkner B, Schoser BG, Salanova M, Kirsch K, Gunga HC, Schiffl G, Luck G & Blottner D. (2004). Differential expression of nitric oxide synthases NOS₁₋₃ in human skeletal muscle following exercise countermeasure during 12 weeks of bed rest. *FASEB journal* **18**, 1228-1230.
- Sargeant RJ, Liu Z & Klip A. (1995). Action of insulin on $\text{Na}^+\text{-K}^+\text{-ATPase}$ and the $\text{Na}^+\text{-K}^+\text{-2Cl}^-$ cotransporter in 3T3-L1 adipocytes. *American Journal Physiology* **269**, C217-225.
- Schmidt TA, Hasselbalch S, Farrell PA, Vestergaard H & Kjeldsen K. (1994). Human and rodent muscle $\text{Na}^+\text{-K}^+\text{-ATPase}$ in diabetes related to insulin, starvation, and training. *Journal of applied physiology* **76**, 2140-2146.
- Segall L, Daly SE & Blostein R. (2001). Mechanistic basis for kinetic differences between the rat α_1 , α_2 , and α_3 isoforms of the Na,K-ATPase. *Journal of Biological Chemistry* **276**, 31535-31541.

- Sejersted OM & Sjøgaard G. (2000). Dynamics and consequences of potassium shifts in skeletal muscle and heart during exercise. *Physiological Reviews* **80**, 1411-1481.
- Serpiello FR, McKenna MJ, Stepto NK, Bishop DJ & Aughey RJ. (2011). Performance and physiological responses to repeated-sprint exercise: a novel multiple-set approach. *Eur J Appl Physiol* **111**, 669-678.
- Shelly DA, He S, Moseley A, Weber C, Stegemeyer M, Lynch RM, Lingrel J & Paul RJ. (2004). Na⁺ pump alpha 2-isoform specifically couples to contractility in vascular smooth muscle: evidence from gene-targeted neonatal mice. *American Journal Physiology: Cell Physiology* **286**, C813-820.
- Silverman BZ, Fuller W, Eaton P, Deng J, Moorman JR, Cheung JY, James AF & Shattock MJ. (2005). Serine 68 phosphorylation of phospholemman: acute isoform-specific activation of cardiac Na/K ATPase. *Cardiovascular Research* **65**, 93-103.
- Sjøgaard G. (1983). Electrolytes in slow and fast muscle fibers of humans at rest and with dynamic exercise. *American Journal Physiology* **245**, R25-31.
- Sjøgaard G, Adams RP & Saltin B. (1985). Water and ion shifts in skeletal muscle of humans with intense dynamic knee extension. *American Journal Physiology* **248**, R190-196.
- Skou JC. (1998). Nobel Lecture. The identification of the sodium pump. *Bioscience Reports* **18**, 155-169.
- Sostaric SM, Skinner SL, Brown MJ, Sangkabutra T, Medved I, Medley T, Selig SE, Fairweather I, Rutar D & McKenna MJ. (2006). Alkalosis increases muscle K⁺ release, but lowers plasma [K⁺] and delays fatigue during dynamic forearm exercise. *Journal of Physiology* **570**, 185-205.
- Spriet LL, Lindinger MI, McKelvie RS, Heigenhauser GJ & Jones NL. (1989). Muscle glycogenolysis and H⁺ concentration during maximal intermittent cycling. *Journal of applied physiology* **66**, 8-13.
- Stainsby WN, Brechue WF & O'Drobinak DM. (1991). Regulation of muscle lactate production. *Med Sci Sports Exerc* **23**, 907-911.
- Staron RS, Hagerman FC, Hikida RS, Murray TF, Hostler DP, Crill MT, Ragg KE & Toma K. (2000). Fiber type composition of the vastus lateralis muscle of young men and women. *journal of histochemistry and cytochemistry* **48**, 623-629.
- Stephens TJ, McKenna MJ, Canny BJ, Snow RJ & McConell GK. (2002). Effect of sodium bicarbonate on muscle metabolism during intense endurance cycling. *Med Sci Sports Exerc* **34**, 614-621.
- Stephenson DG, Lamb GD & Stephenson GM. (1998). Events of the excitation-contraction-relaxation (E-C-R) cycle in fast- and slow-twitch mammalian

- muscle fibres relevant to muscle fatigue. *Acta physiologica Scandinavica* **162**, 229-245.
- Summa V, Camargo SM, Bauch C, Zecevic M & Verrey F. (2004). Isoform specificity of human Na⁺, K⁺-ATPase localization and aldosterone regulation in mouse kidney cells. *Journal of Physiology* **555**, 355-364.
- Sweadner KJ. (1989). Isozymes of the Na⁺/K⁺-ATPase. *Biochimica et Biophysica Acta* **988**, 185-220.
- Sweeney G, Niu W, Canfield VA, Levenson R & Klip A. (2001). Insulin increases plasma membrane content and reduces phosphorylation of Na⁺-K⁺ pump alpha₁-subunit in HEK-293 cells. *American Journal Physiology: Cell Physiology* **281**, C1797-1803.
- Swift F, Tovsrud N, Sjaastad I, Sejersted OM, Niggli E & Egger M. (2010). Functional coupling of alpha₂-isoform Na⁺/K⁺-ATPase and Ca²⁺ extrusion through the Na⁺/Ca²⁺-exchanger in cardiomyocytes. *Cell Calcium* **48**, 54-60.
- Tanaka H, Shimizu S, Ohmori F, Muraoka Y, Kumagai M, Yoshizawa M & Kagaya A. (2006). Increases in blood flow and shear stress to nonworking limbs during incremental exercise. *Med Sci Sports Exerc* **38**, 81-85.
- Therien AG & Blostein R. (2000). Mechanisms of sodium pump regulation. *American Journal Physiology: Cell Physiology* **279**, C541-566.
- Thomassen M, Christensen PM, Gunnarsson TP, Nybo L & Bangsbo J. (2010). Effect of 2 weeks intensified training and inactivity on muscle Na⁺/K⁺ pump expression, phospholemman (FXYP1) phosphorylation and performance in soccer players. *Journal of applied physiology* **108**, 898-905.
- Thomassen M, Murphy RM & Bangsbo J. (2013). Fibre type-specific change in FXYP1 phosphorylation during acute intense exercise in humans. *Journal of physiology* **591**, 1523-1533.
- Thompson CB & McDonough AA. (1996). Skeletal muscle Na,K-ATPase alpha and beta subunit protein levels respond to hypokalemic challenge with isoform and muscle type specificity. *Journal of Biological Chemistry* **271**, 32653-32658.
- Trenerry MK, Carey KA, Ward AC & Cameron-Smith D. (2007). STAT3 signaling is activated in human skeletal muscle following acute resistance exercise. *Journal of applied physiology* **102**, 1483-1489.
- Tsakiridis T, Wong PP, Liu Z, Rodgers CD, Vranic M & Klip A. (1996). Exercise increases the plasma membrane content of the Na⁺-K⁺ pump and its mRNA in rat skeletal muscles. *Journal of applied physiology* **80**, 699-705.
- Vagin O, Tokhtaeva E & Sachs G. (2006). The role of the beta1 subunit of the Na,K-ATPase and its glycosylation in cell-cell adhesion. *Journal of Biological Chemistry* **281**, 39573-39587.

- Varley MC. (2013). Acceleration and fatigue in soccer. In *College of Exercise and Sport Science*. Victoria University, Melbourne, Australia.
- Venosa RA & Horowicz P. (1981). Density and apparent location of the sodium pump in frog sartorius muscle. *Journal of membrane biology* **59**, 225-232.
- Vollestad NK & Sejersted OM. (1988). Biochemical correlates of fatigue. A brief review. *Eur J Appl Physiol Occup Physiol* **57**, 336-347.
- Wahren J, Felig P, Ahlborg G & Jorfeldt L. (1971). Glucose metabolism during leg exercise in man. *Journal of clinical investigation* **50**, 2715-2725.
- Weil E, Sasson S & Gutman Y. (1991). Mechanism of insulin-induced activation of Na⁺-K⁺-ATPase in isolated rat soleus muscle. *American Journal Physiology* **261**, C224-230.
- Welinder C & Ekblad L. (2011). Coomassie staining as loading control in Western blot analysis. *J Proteome Res* **10**, 1416-1419.
- Williams MW, Resneck WG, Kaysser T, Ursitti JA, Birkenmeier CS, Barker JE & Bloch RJ. (2001). Na,K-ATPase in skeletal muscle: two populations of beta-spectrin control localization in the sarcolemma but not partitioning between the sarcolemma and the transverse tubules. *J Cell Sci* **114**, 751-762.
- Wyckelsma VL. (2014). Na⁺,K⁺-ATPase in single skeletal muscle fibres and the effects of ageing, training and inactivity. In *College of Sport and Exercise Science*. Victoria University, Melbourne, Australia.
- Xie Z & Askari A. (2002). Na⁺/K⁺-ATPase as a signal transducer. *European Journal of Biochemistry* **269**, 2434-2439.
- Yki-Jarvinen H, Young AA, Lamkin C & Foley JE. (1987). Kinetics of glucose disposal in whole body and across the forearm in man. *Journal of Clinical Investigation* **79**, 1713-1719.
- Yuan X, Luo S, Lin Z & Wu Y. (2006). Cyclic stretch translocates the alpha₂-subunit of the Na pump to plasma membrane in skeletal muscle cells in vitro. *Biochemical and Biophysical Research Communications* **348**, 750-757.
- Zhang L, Morris KJ & Ng YC. (2006). Fiber type-specific immunostaining of the Na⁺,K⁺-ATPase subunit isoforms in skeletal muscle: age-associated differential changes. *Biochimica et Biophysica Acta* **1762**, 783-793.
- Zierler KL & Rabinowitz D. (1964). Effect of Very Small Concentrations of Insulin on Forearm Metabolism. Persistence of Its Action on Potassium and Free Fatty Acids without Its Effect on Glucose. *Journal of Clinical Investigation* **43**, 950-962.

Appendix 1. Participant information, consent form, and risk factor questionnaires

A1.1 Study 1 Information for Participants

INFORMATION FOR PARTICIPANTS INVOLVED IN RESEARCH

TITLE OF PROJECT:

Glucose ingestion, insulin, potassium homeostasis and exercise performance.

INVESTIGATORS:

Professor Michael McKenna

Ms Collene Steward

AIMS OF THE STUDY

The major aim of this project is to investigate the effects of a standard glucose load on insulin and potassium regulation in blood and muscle during rest and exercise in healthy young participants.

While insulin is important in regulating blood glucose, it is also important in regulating potassium. The ingestion of glucose causes an increase in plasma insulin concentration, which is sufficient to produce a lowering of the potassium concentration in the blood. This action occurs as a result of insulin acutely increasing the activity of an enzyme located in muscle. This enzyme is vital in preserving muscle potassium levels and the capacity for repeated contractions. We are therefore investigating the effects of insulin on potassium regulation and muscular performance in healthy individuals. This study will improve fundamental knowledge about insulin effects on muscle potassium regulation, exercise performance and muscle function in healthy individuals.

PARTICIPANT INVOLVEMENT AND OVERVIEW OF TESTING

You will be requested to attend the Exercise Physiology Laboratory at Victoria University, Footscray Park Campus (Room L305, building L) on six separate occasions for exercise testing trials, over approximately 9 weeks. Whilst each test is tiring, you will recover very quickly. Please refrain from eating overnight before visits 5 and 6.

Visit 1. Involves attending the Laboratory for initial screening purposes to ensure that only healthy individuals can enter the study.

Visit 2. This session will involve familiarisation with the high-intensity cycle ergometer exercise test, to be used in the final two experimental trials. All familiarisation trials will simulate the exact protocols of the experiments in the following weeks. No invasive procedures are undertaken during the familiarisation trials.

Visit 3 and 4. During the *third and fourth visit*, you will undergo *variability testing* of the high-intensity cycle exercise test. These tests will be repeated, separated by 5-7 days, to document the variability of each participant during the muscle performance tests. No invasive procedures are undertaken during these variability trials.

Visits 5 and 6. Visits 5 and 6 will require approximately 3 hours each and will involve (i) a single glucose load (Oral Glucose Tolerance Test) or placebo, (ii) a 1 hour rest with

periodic blood sampling, (iii) followed by the high-intensity cycling exercise test with blood and muscle sampling. In the 24 hours prior to each visit, you will be asked to avoid any intense exercise and substances such as caffeine, alcohol, or other drugs and to record all exercise, fluid and food intake. These visits will be conducted one month apart.

EXERCISE TESTING PROCEDURES

Safety Procedures

Each exercise test is completed when you become too tired to continue (wish to stop), or unless we stop the test due to you having an abnormal response to exercise, such as unusual heart rhythm, inappropriate heart rate or sweating responses, chest pain or severe shortness of breath. We will closely monitor you and your heart electrical activity (ECG) during exercise to ensure your safety. The most common event associated with maximal exercise testing is fainting. This will be prevented using our standard laboratory procedures. In the unlikely event of emergency situations, a medical practitioner will be in attendance, two members of the research team have current CPR (cardio pulmonary resuscitation) qualifications and the Western Hospital is minutes away by ambulance.

Cycling Exercise Tests Procedures

You will be asked to undertake cycling exercise tests over several laboratory visits. On Visit 1 you will be asked to perform an incremental cycling test, in which the workrate is progressively increased until your muscles fatigue. This test is used to determine your aerobic fitness, by measurement of the peak oxygen consumption ($\dot{V}O_{2peak}$). Visit 2 will be a familiarisation session using the high-intensity cycling exercise protocol which involves cycling at 70 revolutions per minute for three 45 second bouts at 130% of the peak incremental workrate attained during visit 1 (i.e. 130% of the workrate corresponding to $\dot{V}O_{2peak}$), with each bout separated by 135 seconds, followed by a fourth bout at 130% of the workrate corresponding to $\dot{V}O_{2peak}$ continued until fatigue, defined as an inability to maintain pedal cadence above 60 revolutions per minute. Visits 3 and 4 will be variability trials of the high-intensity cycling exercise. On Visits 5 and 6 you will be asked to perform the high-intensity cycling, and these 2 visits will include blood sampling and muscle biopsies.

ORAL GLUCOSE TOLERANCE TEST

The Oral Glucose Tolerance Test (OGTT) involves participants ingesting 300 ml of fluid with 75 g of glucose to stimulate insulin secretion, with blood samples to monitor the changes in glucose prior to performing exercise to fatigue. This will be performed to determine the effects of lowering potassium on exercise performance.

MUSCLE BIOPSIES

On Visits 5 and 6, two muscle biopsies will be taken from the thigh muscle of participants, at rest, and following the cycling test. Thus three biopsies will be taken on each visit, giving an overall total of six biopsies. Muscle biopsies are routinely carried out in our laboratory, with no serious adverse effects.

The muscle biopsy procedure is used to obtain small samples of your muscle tissue for analysis of enzymes and energy sources. An injection of a local anaesthetic is made in the skin overlying the muscle in your thigh, and then a small incision (approx. 0.6 cm long) is made in the skin. The biopsy needle is then inserted into your muscle and a small piece of tissue removed from the muscle. During this part of the procedure you

will feel pressure and this will be quite uncomfortable and you may also experience some pain, but will last for only about 1-2 seconds. When the small piece of muscle is removed you may also experience a mild muscle cramp, but this only persists for a few seconds. The size of muscle removed by the biopsy needle is similar to a grain of rice. This poses no long-term effects for your muscle and will not be noticeable to others apart from a small scar on the skin for a few months. Following the biopsy the incision will be closed using a steri-strip and covered by a transparent waterproof dressing. Then a pressure bandage will be applied which should be maintained for 24-48 hours. Steri-strip closure should be maintained for a few days. You should not exercise for 24 hours after biopsies and you should avoid heavy knocks. It is common for participants to experience some mild soreness in the muscle over the next 2-3 days, however this passes and does not restrict movement. The soreness is due to slight bleeding within the muscle and is best treated by “ice, compression and elevation”. An ice pack will be applied over the biopsy site after the biopsy procedure to minimise any bleeding and therefore soreness. In some rare cases mild haematomas have been reported, but these symptoms disappear within a week. A medical practitioner will perform the whole procedure under sterile conditions. On very rare occasions, some people have reported altered sensation (numbness or tingling) in the skin near the site of the biopsy. This is due to a very small nerve being cut, but this sensation disappears over a period of a few weeks-to-months. Although the possibility of infection, significant bruising and altered sensation is quite small, if by chance it does eventuate, please inform us immediately and we will immediately consult the doctor who performed the biopsy to review the reported problems and recommend appropriate action.

VENOUS CATHETERISATION

Blood samples will be taken during rest, exercise and recovery via a catheter placed in the arm. The catheter consists of a needle and teflon tubing. The tubing is fed over the top of the needle on entering the vein. The needle is then withdrawn, leaving only the teflon tubing in your vein for the remainder of the experiment. A tap (stopcock) is placed into the tubing so the flow of blood along the tubing can be altered at will. This procedure allows the taking of multiple blood samples without the need for multiple venepuncture (puncturing of the vein). Each time a blood sample is taken, a small volume of fluid will be injected to keep the catheter from clotting. Catheterisation is slightly uncomfortable, with minimal possibility of bruising and infection. The use of sterile, disposable catheters, syringes, single dose vials and aseptic techniques will markedly reduce the possibility of infection. Only staff qualified and experienced in venepuncture will be used in order to prevent complications. Although the possibility of infection, bleeding, local blood clots, local swelling and redness, and bruising are remote, should any one of these conditions eventuate, please inform us immediately and then consult your doctor.

ARTERIAL CATHETERISATION

A similar catheter will be used as above, but will be inserted into the radial artery (wrist) of the other arm after the hand has been pre-warmed by holding the hand in warm water or under a warm-air hand dryer for approximately 5 minutes. Arterial puncture and catheterisation is more difficult and may involve more discomfort and bruising formation than with venous punctures. Pain is minimised by use of a local anaesthetic in the skin and near the artery, whilst bleeding and bruising are minimised through use of appropriate pressure techniques for an adequate amount of time after arterial puncture or removal of the catheter. Infection is unlikely as only sterile, unused

disposable instruments; single dose vials and aseptic techniques will be used. An experienced medical practitioner, who will remain throughout the entire testing and recovery procedures, will perform all arterial catheterisations.

CONTACT NUMBERS

Professor Michael McKenna (w) 9919 4499

michael.mckenna@vu.edu.au

Ms Collene Steward (w)99194207

collene.steward@research.vu.edu.au

Any queries about your participation in this project may be directed to the researcher Professor Michael McKenna, 9919 4499. If you have any queries or complaints about the way you have been treated, you may contact the Secretary, Victoria University Human Research Ethics Committee, Victoria University, PO Box 14428, Melbourne, VIC, 8001 phone (03) 9919 4710

A1.2 Study 1 Consent Form

CONSENT FORM FOR PARTICIPANTS INVOLVED IN RESEARCH

INFORMATION TO PARTICIPANTS:

We would like to invite you to be a part of a study investigating the effects of glucose on skeletal muscle fatigue.

INVESTIGATORS:

Professor Michael McKenna

Ms Collene Steward

AIMS OF THE STUDY

The major aim of this project is to investigate the effects of glucose on insulin and potassium regulation in blood and muscle during rest and exercise in healthy young participants.

PARTICIPANT INVOLVEMENT AND OVERVIEW OF TESTING

Participants will be requested to attend the Exercise Physiology Laboratory at Victoria University, Footscray Park Campus (Room L305, building L) on six separate occasions for exercise testing trials, over approximately 9 weeks. Whilst each test is tiring, you will recover very quickly. Please refrain from eating overnight before visits 5 and 6.

EXERCISE TESTING PROCEDURES

Participants will be asked to undertake high-intensity cycling exercise tests over several visits.

ORAL GLUCOSE TOLERANCE TEST

The Oral Glucose Tolerance Test (OGTT) involves participants ingesting 300 ml of fluid with 75 g of glucose to stimulate insulin secretion prior to performing exercise to fatigue with blood samples taken to monitor changes in glucose.

MUSCLE BIOPSIES

The muscle biopsy procedure is used to obtain small samples of your muscle tissue for analysis of enzymes and energy sources. On Visits 5 and 6, muscle biopsies will be taken from the thigh muscle of participants, at rest, and following the cycling test. Three biopsies will be taken on each visit, giving an overall total of six biopsies. During the procedure you will feel pressure and this will be quite uncomfortable and you may also experience some pain, but this will last for only about 1-2 seconds. Muscle biopsies are routinely carried out in our laboratory, with no serious adverse effects.

VENOUS CATHETERISATION

Blood samples will be taken during rest, exercise and recovery via a catheter placed in the arm. This procedure allows the taking of multiple blood samples without the need for multiple venepuncture (puncturing of the vein). Catheterisation is slightly uncomfortable, with minimal possibility of bruising and infection.

ARTERIAL CATHETERISATION

After pre-warming the hand, a similar catheter will be used as above, but will be inserted into the radial artery (wrist) of the other arm. Arterial puncture and catheterisation is more difficult and may involve more discomfort and bruising formation than with venous punctures. An experienced medical practitioner, who will remain throughout the entire testing and recovery procedures, will perform all arterial catheterisations.

CERTIFICATION BY SUBJECT

I, (participant name)
of (suburb)

certify that I am at least 18* years old and that I am voluntarily giving my consent to participate in the study: *Glucose ingestion, insulin, potassium homeostasis and exercise performance*, being conducted at Victoria University by: Professor Michael McKenna.

I certify that the objectives of the study, together with any risks and safeguards associated with the procedures listed hereunder to be carried out in the research, have been fully explained to me by:

Ms Collene Steward

and that I freely consent to participation involving the use on me of these procedures:

- Preliminary pre-participation screening
- Maximal incremental cycling test
- High-intensity exercise on cycle ergometer
- Glucose and placebo administration under experimental conditions
- Arterial catheterisation and blood sampling during rest, exercise and recovery
- Antecubital venous catheterisation and blood sampling during rest, exercise and recovery
- Muscle biopsies at rest and during exercise

I certify that I have had the opportunity to have any questions answered and that I understand that I can withdraw from this study at any time and that this withdrawal will not jeopardise me in any way.

I have been informed that the information I provide will be kept confidential.

Signed:

Witness other than the researcher:

Date:

Any queries about your participation in this project may be directed to the researcher Professor Michael McKenna, 9919 4499. If you have any queries or complaints about the way you have been treated, you may contact the Secretary, Victoria University Human Research Ethics Committee, Victoria University, PO Box 14428, Melbourne, VIC, 8001 phone (03) 9919 4710

[*please note: Where the participant/s are aged under 18, separate parental consent is required; where the participant/s are unable to answer for themselves due to mental illness or disability, parental or guardian consent may be required.]

A1.3 Risk Factor Questionnaires

MUSCLE BIOPSY, ARTERIAL & VENOUS CATHETERISATION QUESTIONNAIRE

Glucose ingestion, insulin, potassium homeostasis and exercise performance.

NAME: _____

ADDRESS: _____

DATE: _____

AGE: _____ years

1. Have you or your family suffered from any tendency to bleed excessively? (eg. Haemophilia) or bruise very easily? Yes No Don't Know

If yes, please elaborate _____

2. Are you allergic to local anaesthetic? Yes No Don't Know

If yes, please elaborate _____

3. Do you have any skin allergies? Yes No Don't Know

If yes, please elaborate _____

4. Have you any other allergies? Yes No Don't Know

If yes, please elaborate _____

5. Are you currently on any medication? Yes No

If yes, what is the medication? _____

6. Do you have any other medical problems? Yes No

If yes, please elaborate _____

7. Have you ever fainted when you had an injection or blood sample taken?

Yes No Don't know

If yes, please elaborate _____

8. Have you previously had heparin infused or injected?

Yes No Don't know

If yes, please elaborate _____

9. Do you or other members of your family have Raynauds disease, or suffer from very poor circulation in the fingers, leading to painful fingers that turn white/blue?

Yes No Don't know

If yes, please elaborate _____

To the best of my knowledge, the above questionnaire has been completely accurately and truthfully.

Signature: _____ Date: _____

Appendix 2. Individual data from Study 1 (Chapter 3)

A2.1 Participant Characteristics.

	Age (yrs)	Height (cms)	Weight (kg)	$\dot{V}O_{2peak}$ (l.min ⁻¹)	$\dot{V}O_{2peak}$ (ml.kg ⁻¹ .min ⁻¹)	Peak Power (watts)	130% Power (watts)
1	23	165	73	3.17	43.4	275	341
2	24	177	84	3.75	44.7	325	400
3	33	173	79	3.16	40.0	275	346
4	25	189	80	3.13	39.1	300	387
5	22	185	90	4.09	45.5	325	414
6	21	180	59	3.89	65.9	375	474
7	31	160	65	2.59	39.8	225	246
8	19	171	63	2.87	45.5	250	272
n	8	8	8	8	8	8	8
Mean	24.8	175.0	74.1	3.33	45.5	294	360
SD	4.9	9.8	11.0	0.52	8.6	48	75

A2.2 CON Arterial plasma insulin concentration (pmol.l⁻¹)

	Rest	R+20	R+40	R+60	Fatigue
1	46.4	62.9	44.2	39.2	54.6
2	1.4	84.2	64.9	54.3	125.7
3	109.3	58.6	46.6	41.6	54.1
4	91.5	26.9	163.8	105.0	117.6
5	83.6		21.2	25.8	39.1
6	26.4	56.8	25.9	28.0	52.8
7	74.6	102.9	119.7	53.8	54.4
8		132.7	73.9	106.3	230.1
n	7	7	8	8	8
Mean	61.9	75.0	70.0	56.7	91.0
SD	38.6	34.8	49.1	31.9	64.9

A2.3 CHO Arterial plasma insulin concentration (pmol.l⁻¹)

	Rest	R+20	R+40	R+60	Fatigue
1	50.9	321.2	223.3	148.2	98.6
2		109.4	357.3	357.3	188.5
3	64.5	282.8	435.2	384.3	154.9
4	54.3	626.3	613.3	437.4	191.9
5	83.6	386.2	342.5	322.3	229.4
6	38.9	165.2	283.3	208.4	144.5
7	46.9	102.6	251.1	197.0	123.7
8	74.5	664.6	872.1	460.2	346.6
n	7	8	8	8	8
Mean	59.1	332.3	422.3	314.4	184.8
SD	15.9	218.0	219.7	117.0	77.4

A2.4 CON arterial [K⁺]

	Rest	R+10	R+20	R+40	R+60	Post EB 1	Pre EB 2	Post EB 2	Pre EB 3	Post EB 3	Pre EB 4	F	F+1	F+2	F+5	F+10	F+20	F+30
1	3.68	3.54	3.41	3.47	3.57	3.99	3.49	4.03	3.48	4.03	3.60	6.17	4.53	3.59	3.28	3.47	3.49	3.69
2	3.90	3.97	3.93	4.02	4.03	5.54	4.17	5.47	4.03	5.19	4.06	6.56	5.22	3.93	3.82	3.95	4.08	3.99
3	3.73	3.65	3.61	3.59	3.61	4.54	3.68	4.32	3.58	3.70	3.83	5.21	4.73	3.74	3.26	3.28	3.63	3.38
4	3.66	3.70	3.76	3.60	3.69	4.82	3.95	4.72	3.83	4.78	3.80	6.25	4.72	3.70	3.51	3.60	3.76	3.76
5	4.15	4.08	4.09	4.19	4.26	4.25	5.13	4.81	4.14	4.78	4.03	6.57	5.11	3.97	3.44	4.01	4.13	4.16
6	3.91	3.81	3.85	3.83	3.77	4.97	4.73	4.67	3.71				4.67	3.26	3.31	3.55	3.83	3.74
7	3.88	3.76	3.71	4.07	4.09	5.26	3.84	5.23	3.91	5.33	3.95	5.42	4.42	3.96	3.43	3.69	3.60	3.75
8	3.86	3.81	3.52	3.66	3.73	5.19	3.87	4.69	3.62	4.80	3.47	4.92	3.97	3.42	3.49	3.49	3.62	3.55
n	8	8	8	8	8	8	8	8	8	7	7	7	8	8	8	8	8	8
Mean	3.84	3.79	3.73	3.80	3.84	4.82	4.11	4.74	3.79	4.66	3.82	5.87	4.67	3.70	3.44	3.63	3.77	3.75
SD	0.16	0.17	0.22	0.26	0.25	0.53	0.55	0.46	0.23	0.59	0.22	0.68	0.39	0.26	0.18	0.25	0.23	0.24

A2.5 CHO arterial [K⁺]

	Rest	R+10	R+20	R+40	R+60	Post EB 1	Pre EB 2	Post EB 2	Pre EB 3	Post EB 3	Pre EB 4	F	F+1	F+2	F+5	F+10	F+20	F+30
1	3.60	3.59	3.55	3.57	3.61	4.76	3.65	4.77	3.61	4.43	3.69	5.7	5.07	3.84	3.28	3.41	3.68	3.68
2	3.94	3.99	3.88	3.91	3.87	5.64	4.03	5.12	3.88	5.19	4.00	6.3	4.26	3.73	3.75	3.85	3.96	3.97
3	3.91	3.86	3.85	3.65	3.76	4.73	3.41	4.21	3.49	4.12	3.53	5.15	4.55	3.39	3.1	3.32	3.48	3.52
4	3.87	3.79	3.63	3.79	3.69	5.36	4.03	5	3.67	5.02	3.69	6.26	4.34	3.72	3.32	3.65	3.78	3.74
5	3.74	3.56	3.69	3.66	3.66	4.3	3.79	4.06	3.72	4.13	3.53	5.71	4.46	3.56	3.42	3.48	3.78	3.79
6	3.74	3.52	3.59	3.51	3.49	5.39	3.48	5.98	3.41	5.23	3.21	4.69	3.4	3.11	3.06	3.18	3.44	3.7
7	3.80	3.66	3.72	3.93	3.81	5.47	3.72	5.01	3.6	4.55	3.61	6.1	3.9	3.53	3.13	3.46	3.53	3.67
8	3.71	3.38	3.3	3.54	3.98	5.28	3.47	4.53	3.63	5.51	3.63	4.77	4.03	3.55	3.4	3.42	3.9	3.54
n	8	8	8	8	8	8	8	8	8	8	8	8	8	8	8	8	8	8
Mean	3.79	3.67	3.65	3.70	3.73	5.12	3.70	4.84	3.63	4.77	3.61	5.59	4.25	3.55	3.31	3.47	3.69	3.70
SD	0.11	0.20	0.18	0.16	0.15	0.46	0.24	0.60	0.14	0.53	0.22	0.65	0.49	0.23	0.22	0.20	0.19	0.14

A2.6 CON venous [K⁺]

	Rest	R+10	R+20	R+40	R+60	Post EB 1	Pre EB 2	Post EB 2	Pre EB 3	Post EB 3	Pre EB 4	F	F+1	F+2	F+5	F+10	F+20	F+30
1	3.70	3.72	3.7	3.58	3.59	3.62	3.66	3.73	3.68	3.73	3.72	3.77	4.21	3.85	3.36	3.51	3.85	3.78
2	3.91	3.78	3.86	3.93	3.99	4.11	4.11	4.29	4.09	4.01	4.21	4.55	4.48	4.2	3.94	3.98	4.13	4.04
3	3.92	3.91	3.92	3.77	3.71	3.96	3.67	3.64	3.71	3.63	3.66	5.35	4.25	3.56	3.35	3.13	3.49	3.45
4	3.74	3.88	3.95	4.02	3.67	3.48	3.465	3.67	3.535	3.725	3.465	3.855	4.075	3.66	3.405	3.375	3.46	3.455
5	4.30	4.19	4.24	4.15	4.42	4.85	4.44	4.8	4.37	4.53	4.44	4.81	4.72			4.09	4.11	4.17
6	3.90	3.86	3.87	3.87	3.82	3.93	4.14	4.04										
7	4.05	3.92	3.72	4	4.09	4.23	4.02	4.56	3.97	4.36	4.09	4.89	4.8	4.11	3.6	3.77	3.8	3.72
8	3.80	3.8	3.71	3.4	3.71	3.96	3.9	4.12	3.64	4.37	3.54	4.34	3.72	3.63	3.25	3.58	3.74	3.61
n	8	8	8	8	8	8	8	8	7	7	7	7	7	6	6	7	7	7
Mean	3.91	3.88	3.87	3.84	3.88	4.02	3.93	4.11	3.86	4.05	3.88	4.51	4.32	3.84	3.48	3.63	3.80	3.75
SD	0.19	0.14	0.18	0.25	0.28	0.42	0.32	0.43	0.30	0.37	0.37	0.57	0.38	0.27	0.25	0.34	0.27	0.28

A2.7 CHO venous [K⁺]

	Rest	R+10	R+20	R+40	R+60	Post EB 1	Pre EB 2	Post EB 2	Pre EB 3	Post EB 3	Pre EB 4	F	F+1	F+2	F+5	F+10	F+20	F+30
1	3.78	4.01	3.93	3.9	3.82											3.49	3.68	3.7
2	3.97	3.76	3.99	3.94	3.88	4.18											4.05	
3	4.16	4.21	4.22	4	3.79	3.54	3.59	3.66	3.4	3.49	3.55	3.57	4.01	3.5	3.35	3.28	3.78	3.66
4	3.58	3.88	3.73	3.82	3.64						4				3.5	3.65	3.78	3.73
5	3.69	3.77	3.58	3.59	3.58		3.77		3.71									
6	3.75	3.84	3.73	3.59	3.52	3.6	3.68	3.42	3.55	3.94	3.36	3.54	3.51	3.3	3.2	3.2	3.37	3.49
7	3.96	4.02	3.98	3.82	3.7	3.47	3.28	4	3.14	3.86	3.36	3.5	3.74	3.55	3.07	3.44	3.54	3.89
8	3.78	3.58	3.18	3.66	3.33	3.39	3.13	3.34	3.26	3.48	3.18	3.4	3.74	3.37	3.37	3.24	3.46	3.5
n	8	8	8	8	8	5	5	4	5	4	5	4	4	4	5	6	7	6
Mean	3.83	3.88	3.79	3.79	3.66	3.64	3.49	3.61	3.41	3.69	3.49	3.50	3.75	3.43	3.30	3.38	3.67	3.66
SD	0.18	0.19	0.32	0.16	0.18	0.31	0.27	0.30	0.23	0.24	0.31	0.07	0.20	0.12	0.17	0.17	0.23	0.15

A2.8 CON [K⁺]_{a-v} diff

	Rest	R+10	R+20	R+40	R+60	Post EB 1	Pre EB 2	Post EB 2	Pre EB 3	Post EB 3	Pre EB 4	F	F+1	F+2	F+5	F+10	F+20	F+30
1	-0.02	-0.18	-0.29	-0.11	-0.02	0.37	-0.17	0.30	-0.20	0.30	-0.12	2.40	0.32	-0.26	-0.08	-0.04	-0.36	-0.09
2	-0.01	0.19	0.07	0.09	0.04	1.43	0.06	1.18	-0.06	1.18	-0.15	2.01	0.74	-0.27	-0.12	-0.03	-0.05	-0.05
3	-0.19	-0.26	-0.31	-0.18	-0.10	0.58	0.01	0.68	-0.13	0.07	0.17	-0.14	0.48	0.18	-0.09	0.15	0.14	-0.07
4	-0.08	-0.19	-0.20	-0.42	0.02	1.34	0.48	1.05	0.30	1.05	0.33	2.39	0.65	0.03	0.11	0.22	0.30	0.30
5	-0.15	-0.11	-0.15	0.04	-0.16	-0.60	0.69	0.01	-0.23	0.25	-0.41	1.76	0.39			-0.08	0.02	-0.01
6	0.01	-0.05	-0.02	-0.04	-0.05	1.04	0.59	0.63										
7	-0.17	-0.16	-0.01	0.07	0.00	1.03	-0.18	0.67	-0.06	0.97	-0.14	0.53	-0.38	-0.15	-0.17	-0.08	-0.20	0.03
8	0.06	0.01	-0.19	0.26	0.02	1.23	-0.03	0.57	-0.02	0.43	-0.07	0.58	0.25	-0.21	0.24	-0.09	-0.12	-0.06
n	8	8	8	8	8	8	8	8	7	7	7	7	7	6	6	7	7	7
Mean	-0.07	-0.09	-0.14	-0.04	-0.03	0.80	0.18	0.64	-0.06	0.61	-0.06	1.36	0.35	-0.11	-0.02	0.01	-0.04	0.01
SD	0.09	0.14	0.14	0.21	0.07	0.67	0.35	0.37	0.17	0.45	0.24	1.02	0.37	0.18	0.16	0.13	0.22	0.14

A2.9 CHO [K⁺]_{a-v} diff

	Rest	R+10	R+20	R+40	R+60	Post EB 1	Pre EB 2	Post EB 2	Pre EB 3	Post EB 3	Pre EB 4	F	F+1	F+2	F+5	F+10	F+20	F+30
1	-0.18	-0.20	-0.19	-0.19	-0.19											-0.08	0.00	-0.02
2	-0.03	-0.01	-0.02	-0.02	-0.02	1.46											-0.09	
3	-0.25	-0.26	-0.25	-0.25	-0.25	1.19	-0.18	0.55	0.09	0.63	-0.02	1.58	0.54	-0.11	-0.25	0.04	-0.30	-0.14
4	0.29	0.28	0.29	0.28	0.28						-0.31				-0.18	0.00	0.00	0.01
5	0.05	0.06	0.06	0.06	0.06		0.02		0.01									
6	-0.01	-0.04	-0.03	-0.03	-0.03	1.79	-0.20	2.56	-0.14	1.29	-0.15	1.15	-0.11	-0.19	-0.14	-0.02	0.07	0.21
7	-0.16	-0.13	-0.14	-0.13	-0.14	2.00	0.44	1.01	0.46	0.69	0.25	2.60	0.16	-0.02	0.06	0.02	-0.01	-0.22
8	-0.08	0.02	-0.03	-0.01	-0.02	1.89	0.34	1.19	0.37	2.03	0.45	1.37	0.29	0.18	0.03	0.18	0.44	0.04
n	8	8	8	8	8	5	5	4	5	4	5	4	4	4	5	6	7	6
Mean	-0.05	-0.03	-0.04	-0.04	-0.04	1.67	0.08	1.33	0.16	1.16	0.04	1.68	0.22	-0.04	-0.10	0.02	0.02	-0.02
SD	0.17	0.17	0.17	0.17	0.17	0.33	0.29	0.86	0.25	0.65	0.31	0.64	0.27	0.16	0.14	0.09	0.22	0.15

A2.10 CON arterial $\Delta[K^+]$

	Rest	R+10	R+20	R+40	R+60	Post EB 1	Pre EB 2	Post EB 2	Pre EB 3	Post EB 3	Pre EB 4	F	F+1	F+2	F+5	F+10	F+20	F+30
1	0.00	-0.14	-0.27	-0.21	-0.11	0.32	-0.19	0.36	-0.20	0.36	-0.07	2.50	0.86	-0.09	-0.40	-0.21	-0.19	0.02
2	0.00	0.07	0.03	0.12	0.13	1.64	0.27	1.57	0.13	1.29	0.16	2.66	1.32	0.03	-0.08	0.05	0.18	0.09
3	0.00	-0.08	-0.12	-0.14	-0.12	0.81	-0.05	0.59	-0.15	-0.03	0.10	1.48	1.00	0.01	-0.47	-0.45	-0.10	-0.35
4	0.00	0.03	0.09	-0.06	0.02	1.16	0.28	1.06	0.17	1.11	0.13	2.58	1.06	0.03	-0.15	-0.07	0.10	0.09
5	0.00	-0.07	-0.06	0.04	0.11	0.10	0.98	0.66	-0.01	0.63	-0.12	2.42	0.96	-0.18	-0.71	-0.14	-0.02	0.01
6	0.00	-0.10	-0.06	-0.08	-0.14	1.06	0.82	0.76	-0.20				0.76	-0.65	-0.60	-0.36	-0.08	-0.17
7	0.00	-0.12	-0.17	0.20	0.22	1.39	-0.04	1.36	0.04	1.46	0.08	1.55	0.55	0.09	-0.45	-0.19	-0.28	-0.13
8	0.00	-0.04	-0.34	-0.20	-0.13	1.34	0.02	0.84	-0.24	0.95	-0.39	1.07	0.12	-0.44	-0.37	-0.37	-0.24	-0.31
n	8	8	8	8	8	8	8	8	8	7	7	7	8	8	8	8	8	8
Mean	0.00	-0.06	-0.11	-0.04	0.00	0.98	0.26	0.90	-0.06	0.82	-0.02	2.04	0.83	-0.15	-0.40	-0.22	-0.08	-0.09
SD	0.00	0.07	0.14	0.15	0.14	0.54	0.43	0.41	0.16	0.53	0.19	0.65	0.37	0.26	0.21	0.17	0.16	0.17

A2.11 CHO arterial $[\Delta K^+]$

	Rest	R+10	R+20	R+40	R+60	Post EB 1	Pre EB 2	Post EB 2	Pre EB 3	Post EB 3	Pre EB 4	F	F+1	F+2	F+5	F+10	F+20	F+30
1	0.00	0.00	-0.04	-0.02	0.02	1.17	0.06	1.18	0.02	0.84	0.10	2.11	1.48	0.25	-0.32	-0.19	0.09	0.09
2	0.00	0.06	-0.06	-0.02	-0.06	1.71	0.10	1.19	-0.06	1.26	0.06	2.37	0.33	-0.21	-0.19	-0.09	0.02	0.04
3	0.00	-0.05	-0.06	-0.26	-0.15	0.82	-0.50	0.30	-0.42	0.21	-0.38	1.24	0.64	-0.52	-0.81	-0.59	-0.43	-0.39
4	0.00	-0.08	-0.24	-0.08	-0.18	1.50	0.17	1.14	-0.20	1.16	-0.18	2.40	0.48	-0.15	-0.55	-0.22	-0.09	-0.13
5	0.00	-0.18	-0.05	-0.08	-0.08	0.56	0.05	0.32	-0.02	0.39	-0.21	1.97	0.72	-0.18	-0.32	-0.26	0.04	0.05
6	0.00	-0.22	-0.15	-0.23	-0.25	1.66	-0.26	2.25	-0.33	1.50	-0.53	0.96	-0.34	-0.63	-0.68	-0.56	-0.30	-0.04
7	0.00	-0.14	-0.08	0.13	0.01	1.67	-0.08	1.21	-0.20	0.75	-0.19	2.30	0.10	-0.27	-0.67	-0.34	-0.27	-0.13
8	0.00	-0.33	-0.41	-0.17	0.28	1.58	-0.24	0.83	-0.08	1.81	-0.08	1.07	0.33	-0.16	-0.31	-0.29	0.20	-0.17
n	8	8	8	8	8	8	8	8	8	8	8	8	8	8	8	8	8	8
Mean	0.00	-0.12	-0.13	-0.09	-0.05	1.33	-0.09	1.05	-0.16	0.99	-0.17	1.80	0.47	-0.23	-0.48	-0.31	-0.09	-0.08
SD	0.00	0.12	0.13	0.13	0.16	0.44	0.23	0.61	0.15	0.54	0.21	0.61	0.52	0.26	0.23	0.18	0.22	0.15

A2.12 CON venous $\Delta[K^+]$

	Rest	R+10	R+20	R+40	R+60	Post EB 1	Pre EB 2	Post EB 2	Pre EB 3	Post EB 3	Pre EB 4	F	F+1	F+2	F+5	F+10	F+20	F+30
1	0.00	0.02	0.00	-0.12	-0.11	-0.08	-0.04	0.03	-0.02	0.03	0.02	0.07	0.51	0.15	-0.34	-0.19	0.15	0.08
2	0.00	-0.13	-0.05	0.02	0.08	0.20	0.20	0.38	0.18	0.10	0.30	0.64	0.57	0.29	0.03	0.07	0.22	0.13
3	0.00	-0.01	0.00	-0.15	-0.21	0.04	-0.25	-0.28	-0.21	-0.29	-0.26	1.43	0.33	-0.36	-0.57	-0.79	-0.43	-0.47
4	0.00	0.14	0.21	0.28	-0.07	-0.26	-0.28	-0.07	-0.21	-0.02	-0.28	0.12	0.34	-0.08	-0.34	-0.37	-0.28	-0.29
5	0.00	-0.11	-0.05	-0.15	0.13	0.56	0.15	0.51	0.08	0.24	0.15	0.52	0.43			-0.21	-0.19	-0.13
6	0.00	-0.04	-0.03	-0.03	-0.08	0.03	0.24	0.14										
7	0.00	-0.13	-0.33	-0.04	0.04	0.19	-0.03	0.52	-0.07	0.32	0.04	0.85	0.76	0.07	-0.45	-0.28	-0.25	-0.33
8	0.00	0.00	-0.09	-0.40	-0.09	0.17	0.11	0.33	-0.16	0.58	-0.26	0.55	-0.07	-0.17	-0.55	-0.22	-0.05	-0.19
n	8	8	8	8	8	8	8	8	7	7	7	7	7	6	6	7	7	7
Mean	0.00	-0.03	-0.04	-0.07	-0.04	0.10	0.01	0.19	-0.06	0.14	-0.04	0.59	0.41	-0.02	-0.37	-0.28	-0.12	-0.17
SD	0.00	0.09	0.15	0.19	0.11	0.24	0.20	0.29	0.15	0.27	0.23	0.46	0.26	0.23	0.22	0.26	0.24	0.22

A2.13 CHO venous $\Delta[K^+]$

	Rest	R+10	R+20	R+40	R+60	Post EB 1	Pre EB 2	Post EB 2	Pre EB 3	Post EB 3	Pre EB 4	F	F+1	F+2	F+5	F+10	F+20	F+30
1	0.00	0.24	0.16	0.13	0.04											-0.29	-0.09	-0.07
2	0.00	-0.21	0.02	-0.03	-0.09	0.21											0.08	
3	0.00	0.05	0.06	-0.16	-0.37	-0.62	-0.57	-0.50	-0.76	-0.67	-0.61	-0.59	-0.15	-0.66	-0.81	-0.88	-0.38	-0.50
4	0.00	0.31	0.16	0.25	0.06						0.43				-0.08	0.07	0.21	0.16
5	0.00	0.08	-0.11	-0.10	-0.11		0.08		0.02									
6	0.00	0.09	-0.02	-0.16	-0.23	-0.15	-0.07	-0.33	-0.20	0.19	-0.39	-0.21	-0.24	-0.45	-0.55	-0.55	-0.38	-0.26
7	0.00	0.06	0.02	-0.14	-0.26	-0.49	-0.68	0.04	-0.82	-0.10	-0.60	-0.46	-0.22	-0.41	-0.89	-0.52	-0.42	-0.06
8	0.00	-0.20	-0.60	-0.12	-0.45	-0.39	-0.65	-0.44	-0.52	-0.30	-0.60	-0.38	-0.04	-0.41	-0.41	-0.54	-0.32	-0.28
n	8	8	8	8	8	5	5	4	5	4	5	4	4	4	5	6	7	6
Mean	0.00	0.05	-0.04	-0.04	-0.17	-0.29	-0.38	-0.31	-0.45	-0.22	-0.35	-0.41	-0.16	-0.48	-0.55	-0.45	-0.19	-0.17
SD	0.00	0.18	0.24	0.15	0.18	0.33	0.35	0.24	0.36	0.36	0.44	0.16	0.09	0.12	0.32	0.32	0.25	0.22

A2.14 CON $\Delta[K^+]_{a-v}$ diff

	Rest	R+10	R+20	R+40	R+60	Post EB 1	Pre EB 2	Post EB 2	Pre EB 3	Post EB 3	Pre EB 4	F	F+1	F+2	F+5	F+10	F+20	F+30
1	0.00	-0.16	-0.27	-0.09	0.00	0.40	-0.15	0.33	-0.18	0.33	-0.10	2.43	0.35	-0.24	-0.06	-0.01	-0.34	-0.06
2	0.00	0.20	0.08	0.10	0.05	1.44	0.07	1.19	-0.05	1.19	-0.14	2.02	0.75	-0.26	-0.11	-0.02	-0.04	-0.04
3	0.00	-0.07	-0.12	0.01	0.09	0.77	0.20	0.87	0.06	0.26	0.36	0.05	0.67	0.37	0.10	0.34	0.33	0.12
4	0.00	-0.11	-0.12	-0.34	0.09	1.42	0.56	1.13	0.37	1.13	0.41	2.47	0.72	0.11	0.18	0.30	0.38	0.38
5	0.00	0.03	-0.01	0.19	-0.02	-0.46	0.83	0.15	-0.09	0.40	-0.27	1.91	0.54			0.06	0.16	0.14
6	0.00	-0.06	-0.03	-0.05	-0.06	1.03	0.58	0.62										
7	0.00	0.01	0.16	0.24	0.17	1.20	-0.01	0.84	0.11	1.14	0.03	0.70	-0.21	0.02	0.00	0.09	-0.03	0.20
8	0.00	-0.05	-0.25	0.20	-0.04	1.17	-0.09	0.51	-0.08	0.37	-0.13	0.52	0.19	-0.27	0.18	-0.15	-0.18	-0.12
n	8	8	8	8	8	8	8	8	7	7	7	7	7	6	6	7	7	7
Mean	0.00	-0.02	-0.07	0.03	0.04	0.87	0.25	0.70	0.02	0.69	0.02	1.44	0.43	-0.04	0.05	0.09	0.04	0.09
SD	0.00	0.11	0.15	0.19	0.08	0.64	0.36	0.37	0.18	0.44	0.26	0.99	0.35	0.26	0.12	0.18	0.26	0.17

A2.15 CHO $\Delta[K^+]_{a-v}$ diff

	Rest	R+10	R+20	R+40	R+60	Post EB 1	Pre EB 2	Post EB 2	Pre EB 3	Post EB 3	Pre EB 4	F	F+1	F+2	F+5	F+10	F+20	F+30
1	0.00	-0.02	-0.01	-0.01	-0.01											0.10	0.18	0.16
2	0.00	0.02	0.01	0.02	0.01	1.50											-0.05	
3	0.00	-0.01	-0.01	-0.01	-0.01	1.44	0.07	0.80	0.34	0.88	0.23	1.83	0.79	0.14	0.00	0.29	-0.05	0.11
4	0.00	-0.01	-0.01	-0.01	-0.01						-0.60				-0.47	-0.29	-0.29	-0.28
5	0.00	0.01	0.00	0.01	0.01		-0.03		-0.04									
6	0.00	-0.02	-0.01	-0.02	-0.01	1.81	-0.19	2.58	-0.13	1.31	-0.14	1.17	-0.10	-0.18	-0.13	-0.01	0.08	0.23
7	0.00	0.03	0.01	0.02	0.02	2.16	0.60	1.17	0.62	0.85	0.41	2.76	0.32	0.14	0.22	0.18	0.15	-0.07
8	0.00	0.09	0.05	0.07	0.06	1.97	0.42	1.27	0.45	2.11	0.53	1.45	0.37	0.26	0.11	0.26	0.52	0.12
n	8	8	8	8	8	5	5	4	5	4	5	4	4	4	5	6	7	6
Mean	0.00	0.01	0.01	0.01	0.01	1.77	0.17	1.45	0.25	1.28	0.08	1.80	0.34	0.09	-0.06	0.09	0.08	0.04
SD	0.00	0.04	0.02	0.03	0.02	0.31	0.32	0.78	0.32	0.59	0.46	0.69	0.36	0.18	0.26	0.21	0.25	0.19

A2.16 CON arterial [Na⁺]

	Rest	R+10	R+20	R+40	R+60	Post EB 1	Pre EB 2	Post EB 2	Pre EB 3	Post EB 3	Pre EB 4	F	F+1	F+2	F+5	F+10	F+20	F+30
1	131.5	132.8	126.4	130.7	135.8	133.9	131.6	130.0	136.8	135.8	137.7	143.2	136.1	140.6	138.5	136.0	118.2	127.8
2	138.0	136.3	136.3	137.1	138.1	142.1	139.9	144.6	140.4	145.4	139.8	146.0	144.5	142.3	139.4	137.8	135.7	137.4
3	133.8	132.1	132.7	134.2	134.2	135.9	139.7	141.2	142.8	139.1	138.7	143.9	143.8	141.3	138.3	135.6	136.6	137.2
4	138.6	138.7	138.7	138.3	140.5	142.7	141.2	143.3	142.0	143.9	142.8	150.7	146.4	144.4	143.4	140.5	139.8	139.2
5	135.9	136.0	134.9	135.2	135.5	137.7	137.9	138.0	139.3	139.1	138.5	145.3	142.5	141.6	139.1	137.0	136.0	135.5
6	134.2	133.6	133.4	132.5	132.2	135.8	143.7	143.0	142.8			139.3	136.5	136.3	135.3	135.6		
7	132.0	130.3	126.6	133.0	131.0	140.7	132.6	137.2	136.6	141.1	137.3	140.1	141.4	137.7	135.1	134.2	134.0	136.0
8	137.7	135.5	125.8	134.8	138.0	144.6	144.9	147.3	145.1	149.4	147.0	148.8	148.4	144.2	142.7	139.2	138.6	139.1
n	8	8	8	8	8	8	8	8	8	7	7	8	8	8	8	8	7	7
Mean	135.2	134.4	131.9	134.5	135.7	139.2	138.9	140.6	140.7	142.0	140.3	144.7	142.4	141.1	139.0	137.0	134.1	136.0
SD	2.7	2.7	5.0	2.5	3.2	3.9	4.8	5.4	3.0	4.6	3.5	3.9	4.4	2.9	3.0	2.1	7.3	3.9

A2.17 CHO arterial [Na⁺]

	Rest	R+10	R+20	R+40	R+60	Post EB 1	Pre EB 2	Post EB 2	Pre EB 3	Post EB 3	Pre EB 4	F	F+1	F+2	F+5	F+10	F+20	F+30
1	135.2	133.2	133.1	135.6	137.4	139.4	141.9	144.4	142.3	143.6	144.2	148.0	149.8	144.2	145.5	140.1	138.3	138.2
2	137.5	137.3	136.5	136.1	137.1	142.4	139.0	142.2	140.7	144.6	140.5	149.7	141.3	141.2	141.3	138.7	140.7	139.8
3	132.6	136.5	136.0	133.6	135.3	137.8	138.6	141.8	141.4	142.6	142.2	148.9	147.2	141.3	141.7	137.1	132.7	136.3
4	137.8	136.9	137.0	137.4	139.0	140.6	140.1	143.3	141.7	145.2	142.9	146.9	146.1	144.3	141.7	139.9	138.8	138.3
5	134.2	136.3	136.6	136.1	134.3	136.0	138.7	138.0	139.9	140.9	137.2	147.3	144.6	142.3	144.6	138.6	138.2	138.1
6	138.5	135.3	139.0	137.0	139.8	143.5	146.4	152.1	149.1	153.2	150.7	153.6	145.7	147.1	145.7	143.3	139.7	137.5
7	136.5	136.3	134.7	134.4	135.0	140.7	134.9	138.7	135.1	138.4	134.6	144.2	139.1	138.8	135.1	134.0	133.5	134.1
8	136.1	138.0	137.0	136.1	135.7	143.2	139.9	142.8	146.8	148.2	146.4	147.4	147.1	142.9	142.6	140.3	143.3	137.6
n	8	8	8	8	8	8	8	8	8	8	8	8	8	8	8	8	8	8
Mean	136.0	136.2	136.2	135.8	136.7	140.5	139.9	142.9	142.1	144.6	142.3	148.3	145.1	142.8	142.3	139.0	138.2	137.5
SD	2.0	1.5	1.7	1.3	2.0	2.6	3.3	4.3	4.3	4.5	5.1	2.7	3.4	2.5	3.4	2.7	3.5	1.7

A2.18 CON venous [Na⁺]

	Rest	R+10	R+20	R+40	R+60	Post EB 1	Pre EB 2	Post EB 2	Pre EB 3	Post EB 3	Pre EB 4	F	F+1	F+2	F+5	F+10	F+20	F+30
1	137.6	138.2	135.6	136.9	138.0	136.8	138.2	138.8	140.1	139.9	140.0	141.4	144.2	147.4	145.8	142.5	140.1	139.5
2	137.2	134.1	137.6	137.4	137.4	139.0	137.4	138.9	137.7	138.6	140.1	141.0	139.1	142.4	141.4	139.6	138.8	136.7
3	138.0	134.8	136.3	137.1	137.8	135.6	134.7	129.1	139.7	140.7	138.1	136.9	146.4	140.4	141.8	139.6	135.9	136.7
4	139.6	140.9	140.5	140.2	140.9	140.7	140.4	140.3	141.8	143.2	142.4	143.8	145.0	144.3	144.2	142.3	141.5	141.5
5	137.8	136.4	135.8	135.2	135.9	137.4	136.8	136.1	136.8	137.0	136.9	137.6	140.2			137.4	136.0	135.9
6	136.7	136.4	136.1	135.8	135.6	137.8	137.8	135.4										
7	134.3	134.4	126.3	133.4	134.0	132.9	134.6	138.7	130.2	135.5	134.6	137.8	130.6	136.9	136.6	134.3	134.6	134.8
8	133.4	136.5	136.0	123.6	137.1	136.9	139.9	140.0	135.4	141.6	140.6	146.0	141.7	142.0	131.4	140.8	136.4	135.2
n	8	8	8	8	8	8	8	8	7	7	7	7	7	6	6	7	7	7
Mean	136.8	136.5	135.5	134.9	137.1	137.1	137.5	137.2	137.4	139.5	139.0	140.6	141.0	142.2	140.2	139.5	137.6	137.2
SD	2.0	2.2	4.1	5.0	2.0	2.3	2.1	3.7	3.8	2.7	2.6	3.4	5.3	3.5	5.3	2.9	2.5	2.4

A2.19 CHO venous [Na⁺]

	Rest	R+10	R+20	R+40	R+60	Post EB 1	Pre EB 2	Post EB 2	Pre EB 3	Post EB 3	Pre EB 4	F	F+1	F+2	F+5	F+10	F+20	F+30
1	134.4	136.2	135.7	135.6	134.9	133.0	133.8	138.7		133.6			140.4	140.9	142.7	137.0	138.4	139.4
2	138.6	127.4	140.5	135.5	138.5	138.3											142.5	
3	134.3	135.1	132.5	135.8	133.3	133.5	140.1	141.3	139.9	139.4	140.7	141.7	141.5	136.6	140.1	132.5	137.2	137.1
4	138.2	138.7	138.1	137.0	136.9						142.8				142.7	139.9	137.9	139.4
5	137.4	138.5	132.5	138.1	137.7		139.1	138.2	139.7						142.4		138.4	
6	139.5	137.9	135.4	135.5	135.4	135.7	137.0	138.0	137.9	141.7	142.6	141.0	141.7	142.3	143.1	141.0	139.8	138.3
7	132.6	129.4	130.5	129.1	128.5	131.8	129.9	133.0	133.2	134.0	131.3	134.5	135.5	136.6	136.1	133.4	134.0	133.0
8	139.3	139.1	125.4	137.5	138.8	139.6	139.8	137.6	140.8	140.9	141.4	142.1	142.8	143.7	141.3	140.0	139.6	138.5
n	8	8	8	8	8	6	6	6	5	5	5	4	5	5	7	6	8	6
Mean	136.8	135.3	133.8	135.5	135.5	135.3	136.6	137.8	138.3	137.9	139.8	139.8	140.4	140.0	141.2	137.3	138.5	137.6
SD	2.6	4.5	4.7	2.8	3.4	3.1	4.0	2.7	3.0	3.9	4.8	3.6	2.9	3.3	2.5	3.6	2.4	2.4

A2.20 CON [Na⁺]_{a-v} diff

	Rest	R+10	R+20	R+40	R+60	Post EB 1	Pre EB 2	Post EB 2	Pre EB 3	Post EB 3	Pre EB 4	F	F+1	F+2	F+5	F+10	F+20	F+30
1	-6.1	-5.4	-9.2	-6.2	-2.2	-2.9	-6.6	-8.8	-3.3	-4.1	-2.3	1.8	-8.1	-6.8	-7.3	-6.5	-21.9	-11.7
2	0.8	2.2	-1.3	-0.3	0.7	3.1	2.5	5.7	2.7	6.8	-0.3	5.0	5.4	-0.1	-2.0	-1.8	-3.1	0.7
3	-4.2	-2.7	-3.6	-2.9	-3.7	0.3	5.0	12.1	3.1	-1.6	0.6	7.0	-2.6	0.9	-3.5	-4.0	0.7	0.5
4	-1.0	-2.2	-1.8	-1.8	-0.5	2.0	0.8	3.0	0.2	0.7	0.4	6.9	1.3	0.1	-0.8	-1.8	-1.8	-2.3
5	-1.9	-0.4	-0.9	0.0	-0.4	0.3	1.1	1.9	2.5	2.1	1.6	7.7	2.3			-0.4	0.0	-0.4
6	-2.5	-2.8	-2.7	-3.3	-3.4	-2.0	5.9	7.6										
7	-2.3	-4.1	0.3	-0.4	-3.0	7.8	-2.0	-1.5	6.4	5.6	2.7	2.3	10.8	0.8	-1.5	-0.1	-0.6	-1.6
8	4.3	-1.0	-10.2	11.2	0.9	7.7	5.0	7.3	9.7	7.8	6.4	2.8	6.7	2.2	11.3	-1.6	2.2	3.9
n	8	8	8	8	8	8	8	8	7	7	7	7	7	6	6	7	7	7
Mean	-1.6	-2.1	-3.7	-0.5	-1.4	2.0	1.5	3.4	3.0	2.5	1.3	4.8	2.3	-0.5	-0.6	-2.3	-3.5	-1.6
SD	3.1	2.3	3.9	5.1	1.8	4.0	4.2	6.4	4.2	4.5	2.7	2.5	6.2	3.2	6.3	2.2	8.3	4.9

A2.21 CHO [Na⁺]_{a-v} diff

	Rest	R+10	R+20	R+40	R+60	Post EB 1	Pre EB 2	Post EB 2	Pre EB 3	Post EB 3	Pre EB 4	F	F+1	F+2	F+5	F+10	F+20	F+30
1	0.8	-3.0	-2.6	0.0	2.5	6.4	8.1	5.7		10.0			4.4	3.3	2.8	3.1	-0.1	-1.2
2	-1.1	9.9	-4.0	0.6	-1.4	4.1												-1.8
3	-1.7	1.4	3.5	-2.2	2.0	4.3	-1.5	0.5	1.5	3.2	1.5	7.2	5.7	4.7	1.6	4.6	-4.5	-0.8
4	-0.3	-1.8	-1.1	0.4	2.1						0.1				-1.0	0.0	0.9	-1.1
5	-3.2	-2.2	4.1	-2.0	-3.4		-0.4	-0.2	0.2						2.2		-0.2	
6	-1.0	-2.6	3.6	1.5	4.4	7.8	9.4	14.1	11.2	11.5	8.1	12.6	4.0	4.8	2.6	2.3	-0.1	-0.6
7	4.0	6.9	4.2	5.3	6.5	8.9	5.0	5.7	1.9	4.4	3.3	9.7	3.6	2.2	-1.0	0.6	-0.5	1.1
8	-3.2	-1.1	11.6	-1.4	-3.1	3.6	0.1	5.2	6.0	7.3	5.0	5.3	4.3	-0.8	1.3	0.3	3.7	-0.9
n	8	8	8	8	8	6	6	6	5	5	5	4	5	5	7	6	8	6
Mean	-0.7	0.9	2.4	0.3	1.2	5.9	3.5	5.2	4.2	7.3	3.6	8.7	4.4	2.8	1.2	1.8	-0.3	-0.6
SD	2.3	4.9	5.0	2.4	3.5	2.2	4.7	5.1	4.5	3.5	3.1	3.2	0.8	2.3	1.6	1.8	2.3	0.9

A2.22 CON arterial [glucose]

	Rest	R+10	R+20	R+40	R+60	Post EB 1	Pre EB 2	Post EB 2	Pre EB 3	Post EB 3	Pre EB 4	F	F+1	F+2	F+5	F+10	F+20	F+30
1	4.91	4.99	5.36	5.34	4.88	5.02	5.19	5.21	5.36	5.32	5.42	5.53	5.68	5.82	6.46	6.22	6.11	6.04
2	5.39	5.51	5.54	5.32	5.29	4.70	5.49	5.72	5.82	5.81	6.00	6.36	6.34	6.99	6.79	6.71	6.19	6.22
3	4.80	4.56	5.73	5.14	4.77	5.43	5.56	5.67	6.28	5.69	6.64	6.90	7.27	8.11	8.33	7.80	6.53	5.80
4	4.65	4.71	4.73	6.78	5.83	5.59	5.51	5.51	5.40	5.35	5.45	5.53	5.64	5.73	5.79	5.54	4.83	4.28
5	5.17	5.30	5.46	5.11	5.04	5.44	5.33	5.38	5.55	5.52	5.63	5.93	6.14	6.38	6.54	6.06	5.80	5.66
6	4.65	5.09	5.28	4.73	4.48	4.83	5.54	6.13	7.20			7.21	6.82	6.64	6.47	5.85		
7	5.04	5.37	5.52	5.07	5.00	5.33	5.15	5.54	5.67	5.87	6.08	6.35	6.95	7.27	7.35	7.38	7.22	
8	5.15	5.35	5.50	5.11	5.39	5.25	5.43	5.58	5.78	5.92	6.27	6.56	6.40	6.68	6.54	6.41	6.28	5.86
n	8	8	8	8	8	8	8	8	8	7	7	8	8	8	8	8	7	6
Mean	4.97	5.11	5.39	5.32	5.08	5.20	5.40	5.59	5.88	5.64	5.93	6.30	6.40	6.70	6.78	6.50	6.14	5.64
SD	0.26	0.34	0.30	0.62	0.42	0.32	0.16	0.27	0.60	0.25	0.45	0.61	0.58	0.77	0.76	0.77	0.73	0.70

A2.23 CHO arterial [glucose]

	Rest	R+10	R+20	R+40	R+60	Post EB 1	Pre EB 2	Post EB 2	Pre EB 3	Post EB 3	Pre EB 4	F	F+1	F+2	F+5	F+10	F+20	F+30
1	5.36	8.14	10.80	9.51	7.74	5.84	5.58	5.42	5.27	5.25	5.14	5.13	5.06	5.18	4.86	4.59	4.20	4.11
2	5.45	5.83	7.72	10.90	10.40	9.06	8.08	7.74	7.05	6.85	5.40	6.08	5.81	5.70	5.76	5.13	4.51	4.51
3	5.11	6.58	7.67	9.43	9.07	6.80	6.90	6.64	7.02	7.16	7.28	7.48	7.68	8.06	8.29	7.82	6.54	5.67
4	4.69	6.92	8.46	9.47	8.47	7.62	6.69	6.70	6.70	6.42	6.31	6.38	5.85	5.95	5.57	5.25	4.23	3.53
5	5.09	7.12	8.79	10.10	9.52	8.40	8.50	8.23	8.01	7.58	7.22	6.96	6.94	6.80	6.42	5.52	4.56	3.91
6	4.57	6.19	7.18	10.40	10.06	8.77	8.86	8.50	8.73	8.81	8.81	8.52	8.23	8.11	7.74	7.23	6.01	
7	5.13	6.66	6.84	9.29	8.78	7.76	7.49	7.50	7.49	7.60	7.48	7.73	7.54	7.70	7.73	7.48	7.25	6.89
8	4.46	7.42	8.76	9.80	7.67	7.60	7.53	7.58		7.41	7.42	7.47	7.52	7.66	7.38	7.15	6.21	5.48
n	8	8	8	8	8	8	8	8	7	8	8	8	8	8	8	8	8	7
Mean	4.98	6.86	8.28	9.86	8.96	7.73	7.45	7.29	7.18	7.13	6.88	6.97	6.83	6.89	6.72	6.27	5.44	4.87
SD	0.37	0.72	1.25	0.56	1.00	1.06	1.06	1.00	1.09	1.03	1.21	1.07	1.12	1.15	1.24	1.27	1.20	1.19

A2.24 CON venous [glucose]

	Rest	R+10	R+20	R+40	R+60	Post EB 1	Pre EB 2	Post EB 2	Pre EB 3	Post EB 3	Pre EB 4	F	F+1	F+2	F+5	F+10	F+20	F+30
1	4.81	4.96	5.07	5.16	4.84	4.66	4.84	4.59		4.65				5.07	6.22	5.97	5.94	6.04
2	4.91	4.98	5.32	5.19	5.25	5.18	5.25	5.30	5.33	5.28	5.50	5.61	5.53	6.01	6.48	6.38	6.09	5.45
3	4.64	4.68	4.98	4.65	4.64	4.48	4.35	4.55	5.32	4.84	5.19	5.29	5.58	5.74	7.21	7.16	6.67	6.35
4	4.73	4.71	4.57	6.10	5.39	4.83	4.68	4.84	4.66	4.80	4.70	4.96	5.11	5.33	5.57	5.28	4.84	4.37
5	4.95	5.01	5.21	5.08	4.85	5.06	4.76	5.04	4.70	5.00	4.99	5.24	5.35	6.05		5.91	5.89	5.67
6	4.49	4.65	4.92	4.72	4.48	4.49	4.55	4.43										
7	5.30	5.26	5.57	5.34	5.21	5.20	5.25	5.49	5.33	5.51	5.67	6.05	5.95	6.53	7.45	7.07	7.14	7.06
8	5.20	5.24	5.37	4.82	4.97	5.07	4.97	5.00	5.11	5.31	5.38	5.82	5.69	5.59	5.93	6.29	6.13	5.71
n	8	8	8	8	8	8	8	8	6	7	6	6	6	7	6	7	7	7
Mean	4.88	4.94	5.13	5.13	4.95	4.87	4.83	4.90	5.07	5.06	5.24	5.49	5.54	5.76	6.48	6.29	6.10	5.81
SD	0.27	0.24	0.31	0.46	0.32	0.30	0.32	0.38	0.32	0.32	0.35	0.40	0.29	0.49	0.73	0.66	0.71	0.83

A2.25 CHO venous [glucose]

	Rest	R+10	R+20	R+40	R+60	Post EB 1	Pre EB 2	Post EB 2	Pre EB 3	Post EB 3	Pre EB 4	F	F+1	F+2	F+5	F+10	F+20	F+30
1	4.82	5.28	7.44	8.17	5.80	4.99	3.83	4.23	3.67	4.15	3.61	4.21	3.92	4.40	4.72	4.20	4.18	3.93
2	5.06	4.79	6.40	9.39	9.15	8.56									5.23	5.22	4.90	4.50
3	5.08	5.71	6.42	7.64	7.68	5.35	4.80	5.04	4.42	4.76	4.80		5.51	5.55	7.94	7.07	6.43	5.46
4	4.38	4.79	6.03	7.46	7.43						5.76				5.53	5.24	4.25	3.67
5	4.42	4.84	6.20	6.70	5.91		6.42	6.00	4.88		6.78					5.52	4.46	
6	4.57	5.15	6.27	8.92	7.83	7.47	6.54	6.36	5.67	6.99	6.60	6.60	6.62	6.27	7.27	6.64	5.91	4.92
7	5.12	5.67	6.36	7.92	8.40	7.05	6.92	7.26	7.05	7.15	6.91	7.21	6.98	7.20	7.41	7.33	7.11	6.71
8	4.40	5.73	7.08	8.11	7.45	6.87	6.26	6.57	6.34	6.76	6.93	6.82	6.85	6.89	7.50	7.17	6.45	5.60
n	8	8	8	8	8	6	6	6	6	5	7	4	5	5	7	8	8	7
Mean	4.73	5.24	6.52	8.04	7.45	6.71	5.79	5.91	5.34	5.96	5.91	6.21	5.98	6.06	6.51	6.05	5.46	4.97
SD	0.33	0.42	0.48	0.84	1.14	1.34	1.21	1.10	1.25	1.40	1.28	1.36	1.29	1.12	1.30	1.16	1.15	1.05

A2.26 CON [glucose]_{a-v diff}

	Rest	R+10	R+20	R+40	R+60	Post EB 1	Pre EB 2	Post EB 2	Pre EB 3	Post EB 3	Pre EB 4	F	F+1	F+2	F+5	F+10	F+20	F+30
1	0.10	0.03	0.29	0.18	0.04	0.36	0.35	0.63		0.67				0.75	0.25	0.26	0.18	0.00
2	0.48	0.53	0.22	0.13	0.04	-0.48	0.24	0.42	0.49	0.53	0.50	0.75	0.81	0.98	0.31	0.33	0.10	0.77
3	0.17	-0.13	0.74	0.50	0.13	0.96	1.22	1.12	0.97	0.85	1.45	1.62	1.69	2.37	1.12	0.65	-0.14	-0.55
4	-0.08	0.00	0.16	0.68	0.44	0.76	0.83	0.67	0.74	0.55	0.75	0.57	0.53	0.40	0.22	0.26	-0.01	-0.09
5	0.22	0.29	0.25	0.03	0.19	0.38	0.57	0.34	0.85	0.52	0.64	0.69	0.79	0.33		0.15	-0.09	-0.01
6	0.16	0.44	0.36	0.00	0.00	0.34	0.99	1.71										
7	-0.26	0.11	-0.06	-0.28	-0.21	0.14	-0.10	0.04	0.34	0.36	0.41	0.30	1.00	0.74	-0.10	0.32	0.07	
8	-0.05	0.11	0.13	0.29	0.42	0.18	0.46	0.58	0.67	0.61	0.89	0.74	0.71	1.09	0.61	0.12	0.15	0.15
n	8	8	8	8	8	8	8	8	6	7	6	6	6	7	6	7	7	6
Mean	0.09	0.17	0.26	0.19	0.13	0.33	0.57	0.69	0.68	0.58	0.77	0.78	0.92	0.95	0.40	0.30	0.04	0.04
SD	0.22	0.23	0.23	0.30	0.22	0.43	0.43	0.51	0.23	0.15	0.37	0.44	0.40	0.68	0.42	0.17	0.12	0.43

A2.27 CHO [glucose]_{a-v diff}

	Rest	R+10	R+20	R+40	R+60	Post EB 1	Pre EB 2	Post EB 2	Pre EB 3	Post EB 3	Pre EB 4	F	F+1	F+2	F+5	F+10	F+20	F+30
1	0.55	2.86	3.37	1.34	1.95	0.85	1.75	1.19	1.60	1.10	1.53	0.92	1.14	0.78	0.14	0.40	0.02	0.18
2	0.40	1.04	1.32	1.51	1.25	0.50									0.53	-0.09	-0.39	0.01
3	0.03	0.87	1.26	1.79	1.39	1.45	2.10	1.60	2.60	2.40	2.48		2.17	2.51	0.35	0.74	0.12	0.22
4	0.31	2.13	2.43	2.01	1.04						0.55				0.04	0.01	-0.02	-0.14
5	0.67	2.28	2.59	3.40	3.61		2.08	2.23	3.13		0.44					0.00	0.10	
6	0.00	1.05	0.91	1.48	2.23	1.31	2.32	2.15	3.06	1.82	2.21	1.93	1.61	1.84	0.47	0.58	0.09	
7	0.01	1.00	0.48	1.38	0.38	0.71	0.57	0.25	0.45	0.45	0.57	0.53	0.56	0.50	0.32	0.15	0.14	0.18
8	0.06	1.69	1.68	1.69	0.22	0.73	1.27	1.01		0.65	0.49	0.65	0.67	0.77	-0.12	-0.02	-0.24	-0.12
n	8	8	8	8	8	6	6	6	5	5	7	4	5	5	7	8	8	6
Mean	0.25	1.61	1.75	1.82	1.51	0.92	1.68	1.40	2.17	1.28	1.18	1.01	1.23	1.28	0.25	0.22	-0.02	0.05
SD	0.27	0.74	0.97	0.68	1.09	0.37	0.65	0.75	1.14	0.81	0.88	0.64	0.67	0.86	0.24	0.31	0.19	0.16

A2.28 CON arterial [lactate]

	Rest	R+10	R+20	R+40	R+60	Post EB 1	Pre EB 2	Post EB 2	Pre EB 3	Post EB 3	Pre EB 4	F	F+1	F+2	F+5	F+10	F+20	F+30
1	0.94	0.94	0.94	1.29	1.39	1.47	10.40	10.15	14.05	13.75	16.70	18.40	20.60	20.70	21.40	20.50	16.95	12.75
2	0.62	0.60	0.58	0.60	0.62	2.52	10.80	10.70	14.30	13.20	16.40	17.60	18.70	18.30	16.80	14.70	9.27	7.14
3	0.40	0.64	0.75	0.88	0.75	1.82	12.70	12.45	17.70	15.20	19.95	20.40	23.95	23.50	20.45	18.80	11.80	7.60
4	0.64	0.63	0.62	0.95	0.93	2.31	10.65	9.45	14.25	12.80	17.00	18.40	19.95	20.70	19.20	17.95	11.65	7.41
5	0.92	0.91	0.87	0.84	0.88	8.30	1.49	7.65	11.90	10.50	13.80	15.70	19.20	19.10	19.20	18.00	14.00	10.60
6	0.64	0.61	0.58	0.64	0.59	1.86	19.80	20.90	24.25			22.70	20.45	16.60	11.95	8.18		
7	0.73	0.70	0.63	0.65	0.65	8.72	8.93	10.50	12.55	13.05	15.85	19.15	18.85	18.40	16.55	15.05	9.14	
8	1.84	1.74	1.58	1.71	1.91	3.83	13.40	12.70	17.30	16.80	19.10	20.00	19.80	19.90	18.00	17.30	13.90	10.20
n	8	8	8	8	8	8	8	8	8	7	7	8	8	8	8	8	7	6
Mean	0.84	0.85	0.82	0.94	0.97	3.85	11.02	11.81	15.79	13.61	16.97	19.04	20.19	19.65	17.94	16.31	12.39	9.28
SD	0.44	0.39	0.34	0.38	0.46	2.96	5.09	4.01	3.98	1.98	2.05	2.08	1.67	2.07	2.94	3.79	2.79	2.26

A2.29 CHO arterial [lactate]

	Rest	R+10	R+20	R+40	R+60	Post EB 1	Pre EB 2	Post EB 2	Pre EB 3	Post EB 3	Pre EB 4	F	F+1	F+2	F+5	F+10	F+20	F+30
1	0.56	0.61	0.57	0.60	0.62	1.47	10.40	10.15	14.05	13.75	16.70	18.40	20.90	20.15	21.30	20.75	17.80	13.60
2	0.68	0.78	0.71	0.94	1.19	2.52	10.80	10.70	14.30	13.20	16.40	17.60	17.90	17.00	17.40	12.60	7.53	5.10
3	1.25	1.26	1.22	1.39	1.43	1.82	12.70	12.45	17.70	15.20	19.95	20.40	23.05	21.65	20.25	17.85	11.20	7.11
4	0.57	0.60	0.61	0.94	1.14	2.31	10.65	9.45	14.25	12.80	17.00	18.40	20.90	21.20	20.60	19.00	13.20	8.91
5	0.55	0.55	0.63	0.94	1.19	8.30	1.49	7.65	11.90	10.50	13.80	15.70	18.50	18.10	18.70	17.00	13.00	9.52
6	0.60	0.66	0.58	0.73	0.88	1.86	19.80	20.90	24.25			22.70	25.00	24.25	23.20	21.90	17.00	
7	0.66	0.70	0.71	1.07	1.60	8.72	8.93	10.50	12.55	13.05	15.85	19.15	17.60	17.55	17.10	15.25	10.75	7.56
8	0.76	1.08	1.53	2.73	2.51	3.83	13.40	12.70	17.30	16.80	19.10	20.00	20.50	20.30	17.70	16.80	12.10	8.93
n	8	8	8	8	8	8	8	8	8	7	7	8	8	8	8	8	8	7
Mean	0.70	0.78	0.82	1.16	1.32	3.85	11.02	11.81	15.79	13.61	16.97	19.04	20.54	20.03	19.53	17.64	12.82	8.67
SD	0.23	0.25	0.36	0.67	0.57	2.96	5.09	4.01	3.98	1.98	2.05	2.08	2.57	2.42	2.16	2.97	3.34	2.63

A2.30 CON venous [lactate]

	Rest	R+10	R+20	R+40	R+60	Post EB 1	Pre EB 2	Post EB 2	Pre EB 3	Post EB 3	Pre EB 4	F	F+1	F+2	F+5	F+10	F+20	F+30
1	0.99	1.02	0.96	1.37	1.40	1.53	2.64	3.18	5.15	5.63	6.65	6.53	9.71	14.50	20.05	18.40	16.95	11.75
2	0.60	0.91	0.87	0.86	0.63	0.87	2.96	4.16	5.01	5.38	6.84	8.59	8.35	10.60	14.60	12.60	8.93	6.58
3	0.77	0.76	0.79	1.25	0.77	0.93	2.00	3.13	6.03	5.99	5.91	7.50	8.22	8.97	13.55	14.55	11.85	8.32
4	0.72	0.78	0.73	0.87	0.84	1.03	1.85	2.53	3.53	4.86	4.96	8.21	12.70	13.90	16.95	15.15	10.40	6.59
5	0.96	1.04	0.94	1.05	0.82	1.20	1.98	2.63	3.22	4.07	4.80	6.16	10.40	14.70		14.20	13.70	10.60
6	0.88	0.83	0.82	0.78	0.67	0.90	2.04	3.38										
7	0.92	1.04	0.95	0.86	0.82	1.27	2.95	4.96	4.90	5.74	7.30	10.00	9.48	11.00	15.75	12.70	9.25	7.24
8	1.92	1.63	1.53	1.65	1.78	1.89	3.31	3.91	6.46	8.84	8.68	10.90	9.22	9.58	13.20	14.80	12.00	9.07
n	8	8	8	8	8	8	8	8	7	7	7	7	7	7	6	7	7	7
Mean	0.97	1.00	0.95	1.08	0.97	1.20	2.46	3.48	4.90	5.79	6.45	8.27	9.72	11.89	15.68	14.63	11.87	8.59
SD	0.40	0.28	0.25	0.31	0.41	0.36	0.56	0.82	1.19	1.49	1.36	1.74	1.52	2.42	2.55	1.94	2.79	2.01

A2.31 CHO venous [lactate]

	Rest	R+10	R+20	R+40	R+60	Post EB 1	Pre EB 2	Post EB 2	Pre EB 3	Post EB 3	Pre EB 4	F	F+1	F+2	F+5	F+10	F+20	F+30
1	0.87	0.93	0.94	0.91	0.84	1.75	2.34	3.53		4.63				12.85	19.05	18.25	12.60	11.05
2	0.99	1.02	1.03	1.15	1.34	1.53									9.97	10.50	7.83	5.82
3	1.05	1.14	1.14	1.17	1.27	1.65	2.34	2.95	3.53	4.25	5.03		8.64	7.91	13.45	12.40	9.16	6.48
4	1.03	1.27	1.17	1.30	1.41						12.00				20.20	17.90	13.00	9.35
5	0.83	0.96	0.85	1.04	1.10		1.82	2.35	3.79		10.50					16.40	12.30	
6	0.79	0.78	0.80	0.82	1.08	1.18	3.10	5.41	6.85	11.95	11.60	12.65	13.20	12.35	18.65	17.05	13.25	11.15
7	1.05	1.11	0.98	1.12	1.52	2.83	3.25	4.56	4.70	5.60	5.84	8.09	8.27	12.70	14.80	14.30	10.10	6.94
8	0.93	1.20	1.34	2.23	2.29	2.38	3.96	5.51	6.25	8.51	10.30	10.50	12.70	12.70	16.00	14.10	11.90	8.75
n	8	8	8	8	8	6	6	6	5	5	6	3	4	5	7	8	8	7
Mean	0.94	1.05	1.03	1.22	1.36	1.88	2.80	4.05	5.02	6.99	9.21	10.41	10.70	11.70	16.02	15.11	11.27	8.51
SD	0.10	0.16	0.18	0.44	0.44	0.61	0.78	1.31	1.47	3.24	3.01	2.28	2.61	2.13	3.61	2.76	1.99	2.16

A2.32 CON [lactate]_{a-v} diff

	Rest	R+10	R+20	R+40	R+60	Post EB 1	Pre EB 2	Post EB 2	Pre EB 3	Post EB 3	Pre EB 4	F	F+1	F+2	F+5	F+10	F+20	F+30
1	-0.05	-0.08	-0.03	-0.09	-0.01	-0.05	7.77	6.97	8.90	8.13	10.05	11.87	10.90	6.20	1.35	2.10	0.00	1.00
2	0.02	-0.31	-0.30	-0.25	-0.01	1.65	7.84	6.54	9.29	7.82	9.56	9.01	10.35	7.70	2.20	2.10	0.34	0.56
3	-0.37	-0.12	-0.04	-0.37	-0.02	0.89	10.70	9.33	11.67	9.21	14.04	12.90	15.73	14.54	6.90	4.25	-0.05	-0.72
4	-0.08	-0.15	-0.11	0.08	0.09	1.28	8.80	6.92	10.73	7.94	12.05	10.19	7.25	6.80	2.25	2.80	1.25	0.82
5	-0.04	-0.13	-0.07	-0.21	0.06	7.10	-0.49	5.02	8.68	6.43	9.00	9.54	8.80	4.40		3.80	0.30	0.00
6	-0.23	-0.22	-0.24	-0.14	-0.08	0.95	17.77	17.53										
7	-0.19	-0.34	-0.32	-0.21	-0.17	7.45	5.98	5.55	7.66	7.31	8.56	9.16	9.38	7.40	0.80	2.35	-0.10	
8	-0.07	0.11	0.05	0.06	0.13	1.94	10.09	8.79	10.84	7.96	10.42	9.10	10.58	10.32	4.80	2.50	1.90	1.13
n	8	8	8	8	8	8	8	8	7	7	7	7	7	7	6	7	7	6
Mean	-0.13	-0.16	-0.13	-0.14	0.00	2.65	8.56	8.33	9.68	7.83	10.52	10.25	10.43	8.19	3.05	2.84	0.52	0.46
SD	0.13	0.14	0.14	0.15	0.10	2.91	5.09	3.99	1.43	0.84	1.92	1.54	2.65	3.31	2.33	0.85	0.76	0.70

A2.33 CHO [lactate]_{a-v} diff

	Rest	R+10	R+20	R+40	R+60	Post EB 1	Pre EB 2	Post EB 2	Pre EB 3	Post EB 3	Pre EB 4	F	F+1	F+2	F+5	F+10	F+20	F+30
1	-0.31	-0.32	-0.37	-0.31	-0.21	-0.28	8.07	6.62		9.12				7.30	2.25	2.50	5.20	2.55
2	-0.31	-0.25	-0.32	-0.21	-0.15	0.99									7.43	2.10	-0.30	-0.72
3	0.20	0.12	0.08	0.22	0.16	0.18	10.36	9.50	14.18	10.95	14.93		14.41	13.74	6.80	5.45	2.05	0.63
4	-0.46	-0.67	-0.56	-0.36	-0.27						5.00				0.40	1.10	0.20	-0.44
5	-0.29	-0.41	-0.22	-0.11	0.09		-0.33	5.30	8.11		3.30					0.60	0.70	
6	-0.19	-0.12	-0.22	-0.09	-0.20	0.68	16.70	15.50	17.41			10.05	11.80	11.90	4.55	4.85	3.75	
7	-0.38	-0.41	-0.28	-0.05	0.08	5.89	5.68	5.95	7.86	7.46	10.02	11.07	9.34	4.85	2.30	0.95	0.66	0.62
8	-0.17	-0.12	0.19	0.50	0.22	1.45	9.44	7.19	11.05	8.29	8.80	9.50	7.80	7.60	1.70	2.70	0.20	0.18
n	8	8	8	8	8	6	6	6	5	4	5	3	4	5	7	8	8	6
Mean	-0.24	-0.27	-0.21	-0.05	-0.04	1.48	8.32	8.34	11.72	8.95	8.41	10.21	10.84	9.08	3.63	2.53	1.56	0.47
SD	0.20	0.24	0.24	0.29	0.19	2.24	5.61	3.79	4.09	1.49	4.55	0.79	2.90	3.64	2.68	1.79	1.96	1.16

A2.34 CON arterial [H⁺]

	Rest	R+10	R+20	R+40	R+60	Post EB 1	Pre EB 2	Post EB 2	Pre EB 3	Post EB 3	Pre EB 4	F	F+1	F+2	F+5	F+10	F+20	F+30
1	38.2	39.3	38.6	39.4	38.6	36.7	50.2	44.5	53.3	48.8	56.6	59.7	67.9	67.5	68.7	69.3	59.2	50.1
2	37.1	36.3	37.0	36.2	34.4	38.6	45.0	40.6	47.9	44.8	52.6	52.1	59.3	54.3	57.4	51.2	43.9	42.0
3	38.9	38.5	38.1	40.9	35.6	35.5	45.6	43.9	56.1	50.4	56.4	54.8	65.6	65.9	71.4	71.3	55.3	47.0
4	38.3	39.4	39.4	41.4	40.9	33.0	46.6	40.2	53.2	45.1	56.6	50.4	58.3	60.0	64.1	66.4	53.7	42.6
5	37.7	38.1	37.2	38.7	37.3	34.8	41.6	42.1	47.1	45.3	50.6	44.8	58.1	61.9	65.0	65.2	56.6	48.1
6	40.8	40.2	38.1	40.7	40.6	38.4	62.1	60.8	75.5					82.0	78.0	67.8	51.3	44.0
7	32.3	37.1	37.4	35.6	35.2	39.5	41.1	43.6	47.5	49.0	50.2	57.1	63.0	57.9	61.5	58.5	43.9	41.0
8	38.4	39.0	38.4	38.8	37.8	36.1	48.6	44.9	58.6	50.8	60.7	59.7	65.5	63.2	68.5	67.8	58.6	50.1
n	8	8	8	8	8	8	8	8	8	7	7	7	7	8	8	8	8	8
Mean	37.7	38.5	38.0	39.0	37.6	36.6	47.6	45.0	54.9	47.7	54.8	54.1	62.5	64.1	66.8	64.7	52.8	45.6
SD	2.5	1.3	0.8	2.1	2.4	2.2	6.6	6.6	9.3	2.6	3.8	5.4	4.0	8.4	6.3	6.6	6.1	3.7

A2.35 CHO arterial [H⁺]

	Rest	R+10	R+20	R+40	R+60	Post EB 1	Pre EB 2	Post EB 2	Pre EB 3	Post EB 3	Pre EB 4	F	F+1	F+2	F+5	F+10	F+20	F+30
1	39.2	39.8	39.1	38.2	38.2	37.4	50.9	45.1	55.8	51.1	60.4	57.5	70.5	69.0	73.6	74.6	62.7	51.8
2	36.4	36.3	36.0	36.4	38.5	38.4	44.5	40.3	47.6	44.3	51.4	50.6	56.9	57.0	54.3	49.7	42.0	39.6
3	39.4	39.3	39.4	40.5	37.8	37.7	47.5	44.4	56.9	52.2	59.2	64.0	67.8	66.5	74.3	67.1	53.2	45.2
4	34.8	35.8	34.8	37.6	39.6	29.2	47.3	39.1	52.5	43.4	54.3	49.3	55.7	63.2	62.1	63.1	52.2	
5	37.9	41.7	38.5	40.2	37.5	36.2	44.2	41.5	48.9	44.6	48.9	52.4	58.1	56.8	63.5	61.7	50.5	44.4
6	39.6	39.3	41.1	39.6	38.5	43.1	57.1	54.8	74.8	76.0	86.5	88.1	90.4	90.2	93.5	86.7	66.7	
7	36.4	36.9	35.6	36.6	37.7	35.2	43.3	45.0	44.3	48.1	49.5	59.0	66.1	61.2	64.4	58.1	48.2	41.1
8	37.2	37.8	36.6	37.1	35.6	44.6	43.5	46.8		55.8	56.9	60.5	65.5	62.2	66.1	63.4	49.0	48.0
n	8	8	8	8	8	8	8	8	7	8	8	8	8	8	8	8	8	6
Mean	37.6	38.3	37.6	38.3	37.9	37.7	47.3	44.6	54.4	51.9	58.4	60.2	66.4	65.8	69.0	65.5	53.1	45.0
SD	1.7	2.0	2.2	1.6	1.1	4.7	4.8	4.9	10.1	10.7	12.1	12.4	11.1	10.7	11.8	11.1	8.0	4.4

A2.36 CON venous [H⁺]

	Rest	R+10	R+20	R+40	R+60	Post EB 1	Pre EB 2	Post EB 2	Pre EB 3	Post EB 3	Pre EB 4	F	F+1	F+2	F+5	F+10	F+20	F+30
1	42.0	44.1	43.6	44.0	45.3	45.9	49.4	49.8	52.8	53.7	55.3	56.1	61.4	65.8	69.3	68.9	59.8	53.5
2	36.8	38.9	41.2	39.9	39.1	38.5	39.3	43.2	43.4	46.3	48.3	49.0	49.9	53.5	57.7	53.6	44.8	38.7
3	41.4	42.8	43.1	43.9	41.4	37.3	41.5	44.9	51.2	51.1	52.0	55.6	58.2	62.5	69.2	69.0	57.0	49.0
4	41.9	42.6	44.7	44.3	43.9	45.2	44.3	47.9	49.3	50.5	51.8	55.6	57.3	55.3	64.0	64.3	52.5	48.1
5	40.3	40.6	40.7	39.8	41.6	40.7	41.7	42.7	44.7	47.5	46.6	48.6	54.5	59.8		63.7	57.3	49.8
6	40.7	42.2	41.6	40.4	41.7	41.8	44.5	48.8										
7	35.6	37.9	38.7	38.1	38.5	34.0	38.9	41.8	44.1	45.7	48.6	52.2	56.9	56.6	62.4	57.8	48.9	44.8
8	40.7	43.4	42.1	40.7	40.9	41.3	44.5	47.5	53.0	55.2	58.1	60.1	59.4	60.7	66.7	66.5	59.8	54.8
n	8	8	8	8	8	8	8	8	7	7	7	7	7	7	6	7	7	7
Mean	39.9	41.5	42.0	41.4	41.5	40.6	43.0	45.8	48.3	50.0	51.5	53.9	56.8	59.2	64.9	63.4	54.3	48.4
SD	2.4	2.2	1.8	2.3	2.2	4.0	3.4	3.1	4.2	3.7	4.1	4.2	3.7	4.3	4.5	5.8	5.8	5.4

A2.37 CHO venous [H⁺]

	Rest	R+10	R+20	R+40	R+60	Post EB 1	Pre EB 2	Post EB 2	Pre EB 3	Post EB 3	Pre EB 4	F	F+1	F+2	F+5	F+10	F+20	F+30
1	43.0	44.3	44.9	44.6	43.9	43.1	45.3	47.1		49.2		52.0		70.5	71.6	72.9	66.2	56.6
2	39.0	39.4	38.7	39.6	40.6	39.7									55.7	50.2	44.0	43.7
3	40.8	42.1	42.0	43.7	42.9	46.9	47.8	48.4	50.5	52.1	52.8		66.7	61.9	67.3	64.3	54.1	48.1
4	38.6	39.9	40.4	42.4	41.0	42.7			49.8	52.1	52.1	53.1	56.6	59.7	63.2	64.3		
5	42.6	42.9	41.9	43.2	43.2		44.3	44.8	49.4		49.7				60.5	58.7	50.7	
6	40.6	41.5	41.0	41.6	43.1	41.6	48.9	51.5	57.9	66.5	67.8	72.4	75.7	73.6	89.1	81.5	64.9	55.6
7	37.8	39.6	39.4	39.8	37.7	42.3	43.8	47.4	46.8	47.1	50.0	54.5	60.3	63.7	63.5	59.8	51.1	46.2
8	37.3	39.7	38.6	42.3	41.9	41.9	45.2	46.3	48.0	51.5	57.8	58.2	64.6	64.7	66.1	62.8	57.1	50.5
n	8	8	8	8	8	7	6	6	6	6	6	5	5	6	8	8	7	6
Mean	40.0	41.2	40.9	42.1	41.8	42.6	45.9	47.6	50.4	53.1	55.0	58.0	64.8	65.7	67.1	64.3	55.4	50.1
SD	2.1	1.8	2.1	1.7	2.0	2.2	2.0	2.3	3.9	6.9	6.9	8.4	7.2	5.3	10.0	9.4	8.0	5.2

A2.38 CON [H⁺]_{a-v} diff

	Rest	R+10	R+20	R+40	R+60	Post EB 1	Pre EB 2	Post EB 2	Pre EB 3	Post EB 3	Pre EB 4	F	F+1	F+2	F+5	F+10	F+20	F+30
1	-1.1	-0.5	-0.4	1.2	0.4	-0.7	-0.7	-0.6	-2.5	-2.3	-3.8	2.2	-2.5	-1.6	-4.9	-5.3	-3.5	-1.6
2	0.6	0.0	1.0	-0.2	-4.0	0.3	0.5	0.3	0.2	0.5	1.2	1.5	2.4	-2.7	3.1	1.5	1.9	2.3
3	-0.5	-0.7	-1.2	0.5	-2.2	-2.2	-1.9	-0.5	-0.8	-1.9	-2.8	-9.1	-2.1	-0.6	-2.9	4.1	2.1	1.8
4	3.5	3.6	4.6	3.8	1.3	3.8	-0.8	1.1	0.7	1.7	2.3	1.0	2.6	-3.3	2.0	3.3	1.5	
5	-0.3	-3.6	-1.3	-1.5	-0.2	-1.4	-2.6	0.6	-1.8	0.7	1.7	-7.6	0.0	5.2	1.5	3.5	6.2	3.7
6	1.3	0.9	-3.0	1.1	2.0	-4.7	4.9	6.0	0.7					-8.1	-15.6	-18.9	-15.4	
7	-4.1	0.2	1.8	-1.0	-2.5	4.4	-2.1	-1.4	3.3	0.9	0.7	-1.9	-3.1	-3.3	-2.9	0.4	-4.3	-0.1
8	1.2	1.2	1.8	1.7	2.1	-8.4	5.2	-1.9		-5.0	3.8	-0.8	0.0	1.0	2.5	4.4	9.6	2.1
n	8	8	8	8	8	8	8	8	7	7	7	7	7	8	8	8	8	6
Mean	0.1	0.1	0.4	0.7	-0.4	-1.1	0.3	0.4	0.0	-0.8	0.4	-2.1	-0.4	-1.7	-2.1	-0.9	-0.2	1.4
SD	2.2	2.0	2.4	1.7	2.3	4.2	3.1	2.5	1.9	2.4	2.7	4.5	2.3	3.8	6.2	7.9	7.6	1.9

A2.39 CON [H⁺]_{a-v} diff

	Rest	R+10	R+20	R+40	R+60	Post EB 1	Pre EB 2	Post EB 2	Pre EB 3	Post EB 3	Pre EB 4	F	F+1	F+2	F+5	F+10	F+20	F+30
1	-3.7	-4.4	-5.8	-6.4	-5.7	-5.6	5.6	-2.0		1.8		5.5		-1.4	2.0	1.7	-3.6	-4.9
2	-2.6	-3.0	-2.8	-3.2	-2.2	-1.3									-1.4	-0.6	-2.0	-4.0
3	-1.5	-2.8	-2.6	-3.2	-5.0	-9.2	-0.2	-4.1	6.4	0.1	6.3		1.1	4.6	7.0	2.9	-0.9	-2.9
4	-3.8	-4.1	-5.6	-4.8	-1.4	-13.4			2.7	-8.8	2.2	-3.8	-0.9	3.5	-1.2	-1.2		
5	-4.7	-1.2	-3.4	-3.0	-5.7		-0.1	-3.3	-0.6		-0.8				3.0	2.9	-0.2	
6	-1.0	-2.2	0.1	-2.0	-4.5	1.5	8.3	3.3	16.9	9.5	18.7	15.7	14.7	16.5	4.4	5.2	1.8	
7	-1.4	-2.7	-3.8	-3.2	0.0	-7.1	-0.5	-2.4	-2.5	1.0	-0.5	4.6	5.8	-2.4	0.9	-1.8	-2.9	-5.1
8	-0.1	-2.0	-2.1	-5.2	-6.2	2.7	-1.7	0.4		4.3	-0.9	2.3	0.9	-2.5	0.0	0.6	-8.2	-2.5
n	8	8	8	8	8	7	6	6	5	6	6	5	5	6	8	8	7	5
Mean	-2.4	-2.8	-3.2	-3.9	-3.8	-4.7	1.9	-1.3	4.6	1.3	4.2	4.9	4.3	3.0	1.8	1.2	-2.3	-3.9
SD	1.6	1.1	1.9	1.4	2.3	5.9	4.1	2.7	7.7	6.0	7.6	7.0	6.3	7.3	2.9	2.4	3.2	1.2

A2.40 CON arterial [Hb]

	Rest	R+10	R+20	R+40	R+60	Post EB 1	Pre EB 2	Post EB 2	Pre EB 3	Post EB 3	Pre EB 4	F	F+1	F+2	F+5	F+10	F+20	F+30
1	14.9	15.1	15.0	14.6	14.7	15.4	15.9	16.1	16.1	16.3	16.5	16.9	16.9	16.9	16.8	16.4	15.9	15.7
2	14.0	13.9	13.8	13.9	14.2	14.9	15.1	15.4	15.3	15.8	15.5	16.0	15.7	15.4	15.3	14.9	14.2	13.9
3	13.8	13.5	13.5	13.9	13.7	14.3	14.7	15.0	14.9	13.9	15.0	15.7	15.3	15.2	15.0	14.8	14.2	13.6
4	14.8	14.8	14.7	14.5	14.8	15.6	15.6	16.1	16.0	16.3	16.3	16.9	16.5	16.5	16.6	16.0	15.4	15.3
5	15.9	15.9	15.7	15.6	16.3	16.6	16.8	17.0	17.2	17.2	17.4	18.0	17.8	17.8	17.4	17.1	16.5	16.1
6	14.1	14.2	13.6	13.9	14.0	14.6	15.4	15.6	15.4					15.2	14.9	14.5	14.3	14.0
7	13.7	13.3	13.3	13.4	14.0	14.7	14.6	14.9	14.7	15.1	15.1	15.1	14.8	15.0	14.8	14.2	13.3	
8	13.7	13.8	13.7	13.8	14.1	15.0	15.5	15.6	15.9	16.0	16.0	16.2	16.0	15.5	15.6	15.4	14.7	14.4
n	8	8	8	8	8	8	8	8	8	7	7	7	7	8	8	8	8	7
Mean	14.3	14.3	14.2	14.2	14.5	15.1	15.4	15.7	15.7	15.8	16.0	16.4	16.1	15.9	15.8	15.4	14.8	14.7
SD	0.8	0.9	0.9	0.7	0.8	0.7	0.7	0.7	0.8	1.0	0.8	0.9	1.0	1.0	1.0	1.0	1.0	1.0

A2.41 CHO arterial [Hb]

	Rest	R+10	R+20	R+40	R+60	Post EB 1	Pre EB 2	Post EB 2	Pre EB 3	Post EB 3	Pre EB 4	F	F+1	F+2	F+5	F+10	F+20	F+30
1	14.6	14.7	14.3	14.4	14.7	15.5	15.5	16.0	16.0	16.2	16.4	16.8	16.6	16.5	16.3	15.9	15.4	15.1
2	14.2	14.3	14.3	14.0	14.0	14.7	15.1	15.3	14.3	15.7	15.6	15.8	15.6	15.7	15.5	15.0	14.6	14.7
3	13.8	13.5	13.6	13.4	13.8	14.6	14.8	14.9	14.8	15.5	14.9	15.0	15.0	14.8	14.6	14.0	13.7	13.7
4	15.4	15.6	15.3	15.4	15.3	16.1	16.3	16.8	16.5	16.9	16.9	17.4	17.2	17.0	16.5	16.4	16.1	15.8
5	15.2	15.2	15.0	15.1	15.0	15.4	15.8	15.9	16.3	16.3	16.4	17.0	16.9	16.9	16.5	16.0	15.8	15.5
6				14.2	14.4	15.2	15.7	16.0	16.0	16.2	16.1	16.2	16.1	16.0	15.7	15.6	15.1	
7	13.7	14.1	13.9	14.0	14.1	14.8	14.6	15.0	15.2	15.2	15.1	15.8	15.4	15.2	15.2	14.5	14.2	13.9
8	14.2	14.0	13.8	13.8	14.3	15.1	15.0	15.5		15.7		15.5	15.9	15.7	15.4	15.1	14.3	14.1
n	7	7	7	8	8	8	8	8	7	8	7	8	8	8	8	8	8	7
Mean	14.4	14.5	14.3	14.3	14.4	15.2	15.3	15.7	15.6	16.0	15.9	16.2	16.1	16.0	15.7	15.3	14.9	14.7
SD	0.7	0.7	0.6	0.7	0.5	0.5	0.6	0.6	0.8	0.5	0.7	0.8	0.8	0.8	0.7	0.8	0.8	0.8

A2.42 CON venous [Hb]

	Rest	R+10	R+20	R+40	R+60	Post EB 1	Pre EB 2	Post EB 2	Pre EB 3	Post EB 3	Pre EB 4	F	F+1	F+2	F+5	F+10	F+20	F+30
1	15.0	14.8	14.7	14.7	14.8	14.5	15.2	15.2	15.8	15.8	15.9	15.7	16.7	16.6	16.7	16.3	16.0	15.7
2	14.3	14.1	14.0	14.0	14.2	14.4	14.6	14.9	15.0	14.9	15.3	15.2	15.2	15.2	15.3	14.7	14.3	14.0
3	13.4	13.4	13.4	13.6	13.7	13.9	13.9	14.0	14.4	12.9	14.5	13.6	13.5	13.8	14.9	14.2	14.1	13.7
4	14.6	14.7	14.8	14.6	14.8	14.9	16.1	15.4	15.9	16.1	16.0	16.2	16.5	16.5	16.5	16.1	15.4	15.3
5	15.9	16.0	15.8	15.6	16.1	16.2	16.2	16.5	16.6	16.6	16.8	17.0	17.4	17.6		16.7	16.5	16.2
6	14.1	13.9	13.8	13.9	14.0	14.5	14.6	14.8	14.2									
7	13.5	13.7	13.4	13.2	13.3	13.6	13.9	14.6	14.1	14.4	14.8	14.8	14.9	14.6	14.6	14.5	13.6	13.1
8	13.8	14.0		13.8	14.1	14.7	14.8	15.3	15.2	15.7	15.6	15.7	15.8	15.6	15.5	15.4	14.7	14.4
n	8	8	7	8	8	8	8	8	8	7	7	7	7	7	6	7	7	7
Mean	14.3	14.3	14.3	14.2	14.4	14.6	14.9	15.1	15.1	15.2	15.6	15.5	15.7	15.7	15.6	15.4	14.9	14.6
SD	0.8	0.8	0.9	0.7	0.8	0.8	0.9	0.7	0.9	1.2	0.8	1.1	1.3	1.3	0.9	1.0	1.1	1.1

A2.43 CHO venous [Hb]

	Rest	R+10	R+20	R+40	R+60	Post EB 1	Pre EB 2	Post EB 2	Pre EB 3	Post EB 3	Pre EB 4	F	F+1	F+2	F+5	F+10	F+20	F+30
1	14.5	14.8	14.5	14.6	14.9	15.0	15.2	15.3		15.6				16.8	16.3	15.9	15.3	15.1
2	14.3	14.2	14.1	14.0	13.9	14.5					15.4				14.8	14.8	14.6	14.1
3	13.6	13.4	13.4	13.4	13.5	14.3	14.5	14.6	14.6	14.9	14.8		14.8	14.4	14.6	13.9	13.8	13.3
4	15.3	15.4	15.3	15.3	15.2	15.9					16.6	17.0			16.8	16.5	16.1	15.8
5	15.2	15.1	15.1	14.5	15.1		15.3	15.4	15.8		16.4				16.7	16.2	15.7	
6	14.5	14.3	14.4	14.0	14.5	14.5	14.7	14.0	15.5	15.1	15.8	15.3	15.6	15.9	15.8	15.5	15.2	14.8
7	13.7	13.7	13.8	14.0	14.1		14.0	14.9	14.2	14.7	14.9	15.2	14.9	15.4	14.9	14.8	14.1	13.9
8	13.6	13.8	13.6	13.7	13.9	14.4	14.3	14.8	14.7	14.9	15.1	15.2	15.6	15.4	15.3	14.9	14.5	14.0
n	8	8	8	8	8	6	6	6	5	5	7	4	4	5	8	8	8	7
Mean	14.3	14.3	14.3	14.2	14.4	14.8	14.7	14.8	15.0	15.0	15.6	15.7	15.2	15.6	15.6	15.3	14.9	14.4
SD	0.7	0.7	0.7	0.6	0.6	0.6	0.5	0.5	0.7	0.3	0.7	0.9	0.4	0.9	0.9	0.9	0.8	0.8

A2.44 CON arterial [Hct]

	Rest	R+10	R+20	R+40	R+60	Post EB 1	Pre EB 2	Post EB 2	Pre EB 3	Post EB 3	Pre EB 4	F	F+1	F+2	F+5	F+10	F+20	F+30
1	42.5	42.0	42.7	42.6	43.2	43.7	46.5	45.7	46.6	47.9	47.7	51.0	51.5	50.5	50.2	48.4	47.8	45.5
2	37.8	38.6	37.5	38.3	39.0	41.7	41.8	42.6	42.0	43.8	42.5	44.3	43.2	41.6	42.9	40.7	39.3	38.4
3	39.0	37.2	37.4	38.6	37.8	39.8	41.4	41.4	39.7	38.6	42.0	43.0	44.2	42.3	41.5	40.9	40.5	37.3
4	41.7	41.8	41.3	41.1	42.0	44.4	44.8	43.7	43.1	44.0	44.0	45.9	46.4	44.8	45.9	44.3	41.8	41.1
5	42.3	42.8	41.1	41.3	43.4	42.9	44.9	45.3	46.4	46.9	46.4	47.2	49.0	48.4	48.4	45.9	44.8	42.7
6	38.3	38.6	37.2	38.0	38.5	38.4	44.6	43.2	43.1					42.4	41.8	41.2	39.2	39.2
7	36.8	36.6	36.6	35.8	37.1	39.7	39.0	41.0	40.1	41.2	40.8	42.1	39.9	41.6	40.8	39.0	36.7	
8	38.3	38.4	38.3	38.5	39.6	41.2	44.0	42.6	44.5	45.6	45.8	45.0	46.5	43.8	43.9	43.2	41.2	41.0
n	8	8	8	8	8	8	8	8	8	7	7	7	7	8	8	8	8	7
Mean	39.6	39.5	39.0	39.3	40.1	41.5	43.4	43.2	43.2	44.0	44.2	45.5	45.8	44.4	44.4	42.9	41.4	40.7
SD	2.2	2.4	2.3	2.2	2.5	2.1	2.4	1.7	2.6	3.2	2.5	3.0	3.8	3.3	3.4	3.1	3.5	2.8

A2.45 CHO arterial [Hct]

	Rest	R+10	R+20	R+40	R+60	Post EB 1	Pre EB 2	Post EB 2	Pre EB 3	Post EB 3	Pre EB 4	F	F+1	F+2	F+5	F+10	F+20	F+30
1	40.9	41.0	40.9	41.4	41.1	44.3	44.9	45.6	45.0	44.6	46.2	48.1	48.2	46.6	46.1	46.1	43.5	43.0
2	39.1	38.6	37.9	38.1	38.5	41.2	41.5	41.8	42.0	43.6	42.7	42.4	43.4	43.8	42.7	42.1	40.7	39.6
3	37.8	38.6	38.0	37.3	37.9	40.6	41.3	41.9	41.8	42.8	42.4	41.9	42.8	41.6	41.0	40.4	38.7	37.9
4	42.5	41.8	40.4	40.8	40.3	42.2	44.1	45.6	44.7	45.9	45.8	46.6	46.7	46.5	45.7	45.4	43.2	42.8
5	40.8	40.6	39.8	40.7	40.7	41.2	42.1	43.6	45.1	45.2	45.1	46.4	45.4	45.7	46.0	44.4	43.7	42.3
6				37.7	38.6	39.7	42.8	43.9	42.6	42.7	44.6	44.8	45.0	43.7	44.4	42.8	40.5	
7	38.0	37.5	37.0	37.9	38.7	40.8	39.7	41.4	41.8	40.9	42.7	43.5	41.5	42.4	42.8	40.2	38.8	38.1
8	39.5	39.2	37.6	38.4	39.5	42.1	42.1	44.2		44.0		43.9	45.1	43.2	43.2	43.3	40.7	40.2
n	7	7	7	8	8	8	8	8	7	8	7	8	8	8	8	8	8	7
Mean	39.8	39.6	38.8	39.0	39.4	41.5	42.3	43.5	43.3	43.7	44.2	44.7	44.8	44.2	44.0	43.1	41.2	40.5
SD	1.7	1.5	1.5	1.6	1.2	1.4	1.6	1.7	1.6	1.6	1.6	2.2	2.2	1.9	1.8	2.1	2.0	2.2

A2.46 CON venous [Hct]

	Rest	R+10	R+20	R+40	R+60	Post EB 1	Pre EB 2	Post EB 2	Pre EB 3	Post EB 3	Pre EB 4	F	F+1	F+2	F+5	F+10	F+20	F+30
1	43.0	42.1	42.0	41.4	40.8	41.4	43.8	42.7	45.6	44.8	45.4	46.0	47.8	47.4	48.0	47.3	45.1	44.3
2	39.3	38.8	38.2	38.0	38.6	40.0	39.9	41.4	42.1	41.4	42.6	42.0	42.3	42.3	42.4	41.7	38.2	38.5
3	37.0	37.5	38.3	37.4	38.0	38.2	37.8	35.8	41.3	36.9	40.2	38.6	38.6	39.8	42.4	39.2	39.1	37.1
4	41.3	41.0	41.4	40.9	41.5	43.0	42.7	42.0	43.4	43.2	44.0	44.3	45.5	45.4	44.9	44.3	42.0	41.9
5	42.2	42.0	42.3	41.6	43.0	43.5	44.4	44.7	44.6	44.3	44.9	46.7	47.0	47.9		45.7	44.7	43.1
6	37.2	39.3	37.3	38.8	37.4	39.8	39.9	41.2	38.3									
7	35.7	36.9	35.9	36.6	36.1	36.5	38.0	40.8	38.4	39.7	39.3	40.8	41.2	41.5	39.6	40.4	38.0	36.2
8	38.0	38.5	38.6	38.9	38.7	40.4	41.5	42.3	43.3	43.5	44.3	44.0	44.9	43.8	43.8	43.6	42.1	41.1
n	8	8	8	8	8	8	8	8	8	7	7	7	7	7	6	7	7	7
Mean	39.2	39.5	39.2	39.2	39.2	40.3	41.0	41.4	42.1	42.0	42.9	43.2	43.9	44.0	43.5	43.2	41.3	40.3
SD	2.7	2.0	2.4	1.9	2.3	2.3	2.5	2.5	2.7	2.8	2.4	2.9	3.3	3.0	2.8	2.9	3.0	3.1

A2.47 CHO venous [Hct]

	Rest	R+10	R+20	R+40	R+60	Post EB 1	Pre EB 2	Post EB 2	Pre EB 3	Post EB 3	Pre EB 4	F	F+1	F+2	F+5	F+10	F+20	F+30
1	39.3	40.5	40.2	40.4	42.0	43.2	44.3	43.7		45.9				49.2	47.8	46.2	43.5	42.4
2	39.3	39.8	38.4	38.4	37.4	40.0					42.7				41.3	41.1	40.5	39.5
3	38.8	38.6	38.1	38.0	38.8	40.3	39.7	40.2	40.5	41.8	41.4		41.7	41.3	41.3	38.0	38.3	38.1
4	40.8	41.8	41.4	41.5	40.6	43.9					44.6	45.8			45.6	44.6	42.6	42.8
5	41.3	40.8	40.6	40.4	40.5		41.1	41.2	42.8		44.4				46.2	44.7	42.9	
6	38.8	38.6	38.7	37.5	38.6	39.7	39.0	38.3	42.3	40.8	42.1	41.3	42.4	44.3	43.9	42.5	40.1	39.7
7	38.3	36.9	37.4	36.5	36.1		38.2	39.7		40.0	39.4	42.2	40.3	40.3	41.2	40.6	38.2	38.1
8	37.7	39.3	39.0	37.9	38.1	40.8	39.6	40.9	41.5	41.8	40.8	42.7	44.3	43.0	42.5	43.2	40.8	39.7
n	8	8	8	8	8	6	6	6	4	5	7	4	4	5	8	8	8	7
Mean	39.3	39.5	39.2	38.8	39.0	41.3	40.3	40.7	41.8	42.1	42.2	43.0	42.2	43.6	43.7	42.6	40.9	40.0
SD	1.2	1.5	1.4	1.7	1.9	1.8	2.2	1.8	1.0	2.3	1.9	1.9	1.7	3.5	2.6	2.6	2.0	1.9

A2.48 CON arterial Δ PV

	Rest	R+10	R+20	R+40	R+60	Post EB 1	Pre EB 2	Post EB 2	Pre EB 3	Post EB 3	Pre EB 4	F	F+1	F+2	F+5	F+10	F+20	F+30
1	0	0.0	-0.5	2.4	0.6	-4.8	-12.4	-12.2	-13.6	-16.8	-17.5	-24.5	-25.3	-23.7	-22.8	-18.1	-14.5	-9.6
2	0	-0.1	2.1	0.0	-2.9	-11.5	-13.1	-16.0	-14.3	-19.9	-16.1	-21.3	-18.3	-14.3	-15.7	-10.1	-3.7	0.1
3	0	2.9	2.5	-2.3	0.4	-6.9	-11.8	-13.6	-10.5	-2.3	-14.5	-19.7	-19.3	-16.0	-13.8	-11.7	-7.3	2.0
4	0	0.0	1.6	3.0	-0.3	-9.6	-10.0	-11.0	-9.9	-12.6	-12.7	-18.9	-17.7	-15.2	-17.4	-11.8	-4.2	-2.4
5	0	-1.0	3.2	3.9	-4.4	-5.1	-9.7	-11.4	-14.2	-15.0	-14.9	-19.0	-21.1	-20.2	-18.4	-12.9	-7.6	-1.8
6	0	-2.1	4.5	1.0	-0.6	-4.5	-18.6	-17.6	-16.4					-14.2	-11.6	-8.2	-3.7	-1.7
7	0	2.7	2.7	3.3	-3.2	-11.6	-9.9	-14.7	-12.2	-16.1	-15.5	-17.4	-12.5	-16.1	-13.8	-7.4	2.6	
8	0	-2.4	-1.4	-2.5	-5.9	-13.9	-20.9	-19.5	-23.4	-25.6	-25.9	-25.4	-26.9	-20.6	-21.3	-19.0	-12.2	-10.1
n	8	8	8	8	8	8	8	8	8	7	7	7	7	8	8	8	8	7
Mean	0	0.0	1.8	1.1	-2.0	-8.5	-13.3	-14.5	-14.3	-15.5	-16.7	-20.9	-20.1	-17.5	-16.8	-12.4	-6.3	-3.4
SD	0	2.0	2.0	2.5	2.4	3.7	4.2	3.0	4.2	7.1	4.3	3.0	4.9	3.5	3.9	4.2	5.4	4.7

A2.49 CHO arterial Δ PV

	Rest	R+10	R+20	R+40	R+60	Post EB 1	Pre EB 2	Post EB 2	Pre EB 3	Post EB 3	Pre EB 4	F	F+1	F+2	F+5	F+10	F+20	F+30
1	0	-2.5	0.5	-0.7	-2.3	-12.4	-13.7	-17.1	-16.3	-16.9	-20.1	-24.9	-24.2	-21.3	-19.7	-17.6	-10.8	-8.0
2	0	-0.1	1.3	3.0	2.4	-7.3	-9.6	-11.6	-5.8	-16.4	-14.3	-15.4	-15.4	-16.5	-13.8	-10.4	-5.6	-4.2
3	0	-0.9	-0.6	2.0	-1.9	-11.3	-13.6	-15.0	-14.3	-19.6	-15.7	-15.6	-16.9	-14.0	-11.9	-7.2	-2.5	-1.2
4	0	4.2	8.9	7.3	8.6	0.0	-4.5	-9.6	-6.5	-11.1	-10.5	-14.3	-13.5	-12.4	-8.3	-7.3	-1.7	0.8
5	0	0.3	2.7	0.5	1.3	-2.3	-6.1	-9.2	-13.5	-13.7	-14.3	-19.0	-17.3	-17.5	-16.2	-11.1	-8.4	-4.6
6																		
7	0	-3.9	-1.8	-3.9	-5.8	-13.3	-10.5	-15.3	-17.0	-15.7	-17.8	-22.5	-17.7	-17.9	-18.5	-10.6	-6.6	-3.5
8	0	0.8	5.0	3.6	-1.8	-11.0	-10.4	-16.4		-17.2		-16.0	-19.8	-16.0	-14.4	-12.8	-3.7	-1.5
n	7	7	7	7	7	7	7	7	6	7	6	7	7	7	7	7	7	7
Mean	0	-0.3	2.3	1.7	0.1	-8.2	-9.8	-13.5	-12.2	-15.8	-15.5	-18.2	-17.8	-16.5	-14.7	-11.0	-5.6	-3.2
SD	0	2.6	3.7	3.6	4.6	5.2	3.5	3.3	4.9	2.7	3.3	4.1	3.4	2.9	3.9	3.6	3.3	2.9

A2.50 CON venous ΔPV

	Rest	R+10	R+20	R+40	R+60	Post EB 1	Pre EB 2	Post EB 2	Pre EB 3	Post EB 3	Pre EB 4	F	F+1	F+2	F+5	F+10	F+20	F+30
1	0	2.6	3.5	4.5	4.9	6.0	-3.0	-1.1	-9.7	-8.4	-9.9	-9.8	-18.0	-16.9	-18.3	-15.2	-10.0	-7.0
2	0	7.2	9.4	9.9	6.9	3.0	2.0	-2.8	-4.6	-2.8	-7.0	-5.6	-5.8	-6.1	-6.6	-1.9	7.2	9.0
3	0	-6.7	-7.9	-7.9	-9.5	-11.1	-10.5	-8.3	-18.5	-2.2	-17.5	-9.7	-9.0	-12.8	-22.7	-14.4	-13.6	-8.2
4	0	1.1	-0.7	2.0	-0.4	-3.6	-10.4	-5.2	-10.4	-11.1	-12.2	-13.7	-17.1	-17.0	-16.2	-13.2	-5.5	-4.7
5	0	-0.9	-0.1	2.7	-2.9	-4.6	-6.0	-8.3	-8.6	-8.2	-10.2	-14.2	-16.4	-19.0		-11.1	-8.3	-3.6
6	0	-2.0	1.9	-1.2	0.3	-6.9	-7.6	-10.9	-2.5									
7	0	-3.0	0.7	1.2	1.2	-1.7	-6.1	-14.6	-8.0	-11.8	-13.6	-15.8	-16.9	-15.6	-12.9	-13.4	-4.0	2.6
8	0	-4.0		-3.2	-5.0	-11.7	-13.9	-17.6	-18.7	-21.4	-22.2	-22.1	-23.9	-21.3	-20.8	-20.0	-14.3	-10.6
n	8	8	7	8	8	8	8	8	8	7	7	7	7	7	6	7	7	7
Mean	0	-0.7	1.0	1.0	-0.6	-3.8	-6.9	-8.6	-10.1	-9.4	-13.2	-13.0	-15.3	-15.5	-16.3	-12.7	-6.9	-3.2
SD	0	4.3	5.2	5.3	5.3	6.2	4.9	5.6	5.8	6.5	5.1	5.3	6.0	4.9	5.9	5.5	7.3	6.8

A2.51 CHO venous ΔPV

	Rest	R+10	R+20	R+40	R+60	Post EB 1	Pre EB 2	Post EB 2	Pre EB 3	Post EB 3	Pre EB 4	F	F+1	F+2	F+5	F+10	F+20	F+30
1	0	-3.1	-1.1	-2.0	-6.3	-8.9	-11.7	-11.4		-16.5				-27.2	-23.2	-18.8	-11.4	-8.1
2	0	0.4	3.5	4.7	6.7	-2.0					-11.9				-6.1	-5.7	-3.1	1.6
3	0	-1.0	-0.2	0.0	-2.0	-9.8	-10.1	-11.5	-11.9	-15.6	-14.4		-14.9	-11.9	-13.1	-3.6	-3.4	0.6
4	0	-1.4	-0.2	0.0	2.3	-8.0					-13.1	-16.6			-15.4	-12.4	-6.7	-5.3
5	0	0.3	0.6	5.2	0.8		-1.3	-2.4	-7.1		-13.3				-17.5	-12.6	-6.7	
6	0	4.8	3.9	9.0	3.4	1.5	1.3	8.1	-9.1	-4.3	-10.5	-6.3	-9.9	-14.5	-13.3	-9.4	-3.8	-0.5
7	0	2.3	0.7	0.7	0.6		-2.0	-10.1		-9.4	-9.7	-15.6	-11.0	-13.9	-12.4	-10.9	-2.7	-1.1
8	0	-2.6	-0.7	0.4	-1.4	-9.0	-6.5	-11.6	-11.9	-13.5	-13.2	-16.5	-20.9	-18.0	-16.8	-15.6	-9.6	-4.6
n	8	8	8	8	8	6	6	6	4	5	7	4	4	5	8	8	8	7
Mean	0	0.0	0.8	2.2	0.5	-6.0	-5.0	-6.5	-10.0	-11.8	-12.3	-13.8	-14.2	-17.1	-14.7	-11.1	-5.9	-2.5
SD	0	2.6	1.9	3.7	3.9	4.6	5.2	8.0	2.3	5.0	1.7	5.0	5.0	6.1	4.9	4.9	3.3	3.6

A2.52 CON arterial Δ BV

	Rest	R+10	R+20	R+40	R+60	Post EB 1	Pre EB 2	Post EB 2	Pre EB 3	Post EB 3	Pre EB 4	F	F+1	F+2	F+5	F+10	F+20	F+30
1	0	-0.7	0.0	2.7	2.0	-2.6	-5.7	-6.8	-6.8	-8.0	-9.1	-11.2	-11.2	-11.2	-10.7	-8.5	-5.7	-4.5
2	0	1.4	1.8	1.1	-0.7	-5.4	-7.0	-8.8	-7.9	-11.1	-9.1	-11.9	-10.2	-8.5	-7.9	-5.4	-1.1	1.4
3	0	0.7	0.7	-2.2	-0.7	-4.9	-7.5	-9.3	-8.7	-2.2	-9.3	-13.4	-11.1	-10.5	-9.3	-8.1	-4.2	0.0
4	0	0.3	1.0	2.1	0.3	-5.1	-4.8	-7.8	-7.5	-8.9	-8.9	-12.4	-10.3	-10.3	-10.8	-7.5	-3.9	-3.3
5	0	-0.4	0.8	1.8	-2.9	-4.3	-5.8	-6.9	-7.9	-7.9	-8.7	-11.8	-11.0	-11.0	-9.0	-7.4	-3.7	-1.3
6	0	-2.1	2.2	0.0	-0.7	-4.8	-9.7	-10.9	-9.7					-8.6	-6.7	-4.1	-2.8	-0.7
7	0	2.3	2.3	1.5	-2.9	-7.5	-6.8	-8.7	-7.5	-9.9	-9.9	-9.9	-8.1	-9.3	-8.1	-4.2	2.3	
8	0	-1.8	-1.1	-1.8	-3.6	-9.4	-12.6	-13.1	-14.5	-15.3	-15.3	-16.1	-15.3	-12.6	-13.1	-11.7	-7.5	-5.6
n	8	8	8	8	8	8	8	8	8	7	7	7	7	8	8	8	8	7
Mean	0	0.0	1.0	0.7	-1.1	-5.5	-7.5	-9.0	-8.8	-9.0	-10.1	-12.4	-11.0	-10.3	-9.5	-7.1	-3.3	-2.0
SD	0	1.5	1.1	1.8	1.9	2.1	2.5	2.1	2.5	4.0	2.3	1.9	2.2	1.4	2.0	2.5	2.9	2.5

A2.53 CHO arterial Δ BV

	Rest	R+10	R+20	R+40	R+60	Post EB 1	Pre EB 2	Post EB 2	Pre EB 3	Post EB 3	Pre EB 4	F	F+1	F+2	F+5	F+10	F+20	F+30
1	0	-1.7	1.0	0.7	-1.4	-6.5	-6.8	-9.4	-9.4	-10.8	-11.6	-14.0	-13.0	-12.4	-11.3	-9.1	-6.2	-4.0
2	0	-1.2	-1.1	1.0	1.1	-4.3	-6.3	-7.8	-1.4	-10.0	-9.3	-10.8	-9.3	-9.9	-8.7	-6.0	-3.4	-3.8
3	0	0.7	0.0	1.5	-1.4	-6.8	-8.1	-8.7	-8.1	-12.3	-8.7	-9.3	-9.3	-8.1	-6.8	-2.9	-0.7	-0.7
4	0	0.3	2.3	1.6	2.0	-3.1	-4.3	-6.9	-5.3	-7.9	-7.4	-10.1	-9.0	-8.2	-5.5	-4.9	-2.9	-1.3
5	0	-0.3	0.7	0.0	0.7	-1.9	-4.4	-5.0	-7.1	-7.1	-7.9	-10.9	-10.7	-10.4	-8.5	-5.6	-4.1	-2.6
6	0																	
7	0	-4.3	-2.9	-3.6	-4.3	-8.8	-7.5	-10.0	-11.2	-11.2	-10.6	-14.6	-12.3	-11.2	-11.2	-6.9	-4.9	-2.9
8	0	0.0	1.4	1.4	-2.1	-7.3	-6.7	-9.7		-10.8		-9.7	-11.9	-10.8	-9.1	-7.3	-2.1	-0.7
n	8	7	7	7	7	7	7	7	6	7	6	7	7	7	7	7	7	7
Mean	0	-0.9	0.2	0.4	-0.8	-5.5	-6.3	-8.2	-7.1	-10.0	-9.3	-11.3	-10.8	-10.2	-8.7	-6.1	-3.5	-2.3
SD	0	1.7	1.7	1.8	2.1	2.5	1.5	1.8	3.4	1.9	1.6	2.1	1.6	1.6	2.1	2.0	1.8	1.4

A2.54 CON venous Δ BV

	Rest	R+10	R+20	R+40	R+60	Post EB 1	Pre EB 2	Post EB 2	Pre EB 3	Post EB 3	Pre EB 4	F	F+1	F+2	F+5	F+10	F+20	F+30
1	0	1.4	2.0	2.0	1.4	3.4	-1.3	-1.3	-5.1	-5.1	-5.7	-4.5	-10.2	-9.6	-10.2	-8.0	-6.3	-4.5
2	0	4.3	5.4	5.4	3.5	2.1	1.0	-1.3	-2.0	-1.3	-3.6	-3.3	-3.0	-3.3	-3.6	0.0	3.2	5.4
3	0	-3.0	-3.0	-4.4	-5.1	-6.5	-6.5	-7.1	-9.7	0.8	-10.3	-4.4	-3.7	-5.8	-12.8	-8.5	-7.8	-5.1
4	0	0.0	-1.0	0.7	-0.7	-1.3	-8.7	-4.6	-7.6	-8.7	-8.4	-9.6	-11.2	-11.2	-11.2	-9.0	-4.9	-4.2
5	0	-0.9	0.3	1.9	-1.2	-2.2	-2.2	-3.9	-4.5	-4.5	-5.7	-6.8	-8.6	-9.9		-5.1	-3.9	-1.9
6	0	0.7	1.4	0.7	0.0	-3.4	-4.1	-5.4	-1.4									
7	0	-1.5	0.7	2.3	1.5	-0.7	-2.9	-7.5	-4.3	-6.3	-8.8	-8.8	-9.4	-7.5	-7.5	-6.9	-0.7	3.1
8	0	-2.7		-1.3	-3.4	-7.7	-8.3	-11.0	-10.7	-13.3	-13.0	-13.3	-13.9	-12.8	-12.2	-11.6	-7.7	-5.5
n	8	8	7	8	8	8	8	8	8	7	7	7	7	7	6	7	7	7
Mean	0	-0.2	0.8	0.9	-0.5	-2.0	-4.1	-5.3	-5.7	-5.5	-7.9	-7.2	-8.6	-8.6	-9.6	-7.0	-4.0	-1.8
SD	0	2.4	2.6	2.9	2.8	3.8	3.5	3.3	3.4	4.7	3.2	3.6	3.9	3.3	3.5	3.7	4.0	4.3

A2.55 CHO venous Δ BV

	Rest	R+10	R+20	R+40	R+60	Post EB 1	Pre EB 2	Post EB 2	Pre EB 3	Post EB 3	Pre EB 4	F	F+1	F+2	F+5	F+10	F+20	F+30
1	0	-1.4	0.3	-0.3	-2.0	-2.7	-4.0	-4.6		-6.4				-13.1	-10.7	-8.5	-4.9	-3.3
2	0	1.4	2.1	3.2	3.6	-0.7					-6.5				-2.7	-2.7	-1.0	2.1
3	0	0.0	0.0	0.0	-0.7	-6.3	-7.6	-8.2	-8.2	-10.1	-9.5		-9.5	-6.9	-8.2	-3.6	-2.9	0.8
4	0	-0.6	0.0	0.3	1.0	-3.8					-8.0	-9.7			-8.7	-7.3	-4.7	-2.9
5	0	0.0	0.0	4.1	0.0		-1.1	-1.9	-4.1		-7.9				-9.6	-6.8	-3.5	
6	0	1.4	0.7	3.6	0.0	0.0	-1.4	3.9	-6.5	-4.0	-8.2	-5.2	-7.1	-8.8	-8.2	-6.5	-4.6	-2.0
7	0	0.0	-0.7	-2.1	-2.8		-2.1	-8.1	-3.5	-6.8	-8.1	-9.9	-8.1	-11.0	-8.1	-7.4	-2.8	-1.4
8	0	-1.1	0.4	-0.4	-1.8	-5.2	-4.5	-7.8	-7.1	-8.4	-9.6	-10.2	-12.5	-11.4	-10.8	-8.4	-5.9	-2.5
n	8	8	8	8	8	6	6	6	5	5	7	4	4	5	8	8	8	7
Mean	0	0.0	0.4	1.1	-0.4	-3.1	-3.4	-4.4	-5.9	-7.1	-8.3	-8.8	-9.3	-10.3	-8.4	-6.4	-3.8	-1.3
SD	0	1.0	0.8	2.3	2.0	2.5	2.5	4.8	2.0	2.3	1.0	2.4	2.4	2.4	2.5	2.1	1.5	2.0

A2.56 CON $\Delta PV_{a-v \text{ diff}}$

	Rest	R+10	R+20	R+40	R+60	Post EB 1	Pre EB 2	Post EB 2	Pre EB 3	Post EB 3	Pre EB 4	F	F+1	F+2	F+5	F+10	F+20	F+30
1	-1.4	1.9	3.3	1.4	3.5	10.5	9.9	11.8	3.8	9.3	8.3	18.6	8.9	8.2	5.0	2.8	4.5	2.2
2	-4.7	-2.2	-2.3	0.1	0.4	6.1	7.1	5.5	1.4	10.6	1.0	9.3	5.0	-0.2	1.0	-0.6	1.5	-0.8
3	6.1	0.3	-0.7	4.2	-0.3	5.6	12.3	17.4	0.7	10.7	6.7	24.4	24.7	14.8	-0.9	7.2	3.1	-0.4
4	1.7	2.2	-1.3	0.0	0.9	7.7	0.5	7.6	0.4	2.7	1.6	7.4	1.7	-1.1	2.5	-0.6	-0.3	-1.4
5	0.1	0.8	-2.6	-0.5	2.3	1.1	4.6	4.1	7.1	8.6	6.2	6.7	6.6	2.2		2.8	-0.2	-1.3
6	1.9	1.0	-1.6	-1.3	1.8	-1.6	14.4	9.1	17.6									
7	3.3	-3.4	0.3	0.3	6.9	13.8	6.8	2.4	7.2	7.5	4.6	4.3	-2.8	2.9	3.4	-4.3	-4.2	
8	-0.1	-1.2		-0.2	1.5	3.1	9.4	2.9	6.6	6.1	5.5	5.1	4.6	-0.4	1.2	-0.7	-1.9	-0.1
n	8	8	7	8	8	8	8	8	8	7	7	7	7	7	6	7	7	6
Mean	0.8	-0.1	-0.7	0.5	2.1	5.8	8.1	7.6	5.6	7.9	4.8	10.8	7.0	3.8	2.0	0.9	0.3	-0.3
SD	3.2	2.0	2.0	1.7	2.3	5.0	4.4	5.1	5.6	2.8	2.7	7.6	8.7	5.8	2.1	3.7	3.0	1.3

A2.57 CHO $\Delta PV_{a-v \text{ diff}}$

	Rest	R+10	R+20	R+40	R+60	Post EB 1	Pre EB 2	Post EB 2	Pre EB 3	Post EB 3	Pre EB 4	F	F+1	F+2	F+5	F+10	F+20	F+30
1	3.0	0.6	-0.3	0.0	-2.9	5.4	3.5	8.2		1.7				-6.4	-3.2	-0.2	0.6	1.1
2	-1.2	-1.4	0.2	-0.3	2.2	3.7					0.9				6.9	3.2	0.6	4.0
3	-0.5	0.7	1.3	-1.1	0.7	2.6	4.9	5.0	3.7	5.8	2.4		3.3	3.3	-0.5	4.8	-0.1	2.7
4	4.0	1.1	-2.1	-0.5	0.6	-1.7					3.6	4.0			-1.4	0.8	1.3	0.2
5	-1.1	0.1	-2.0	4.7	-0.4		5.2	7.6	7.5		1.3				-1.6	-1.7	2.0	
6				1.8	-0.7	4.8	13.9	26.2	3.8	10.8	6.5	12.6	8.1	-0.4	0.3	1.2	0.0	
7	-0.5	3.9	0.1	2.3	4.2		6.9	3.6		5.0	7.2	6.3	5.5	2.3	4.9	-2.7	1.7	0.0
8	7.3	1.3	-0.8	1.5	5.3	7.2	9.4	10.9		9.5		4.2	3.4	2.3	1.9	1.5	-1.5	1.6
n	7	7	7	8	8	6	6	6	3	5	6	4	4	5	8	8	8	6
Mean	1.6	0.9	-0.5	1.0	1.1	3.7	7.3	10.3	5.0	6.6	3.6	6.8	5.1	0.2	0.9	0.9	0.6	1.6
SD	3.3	1.6	1.2	1.9	2.7	3.1	3.8	8.2	2.2	3.7	2.7	4.0	2.2	3.9	3.5	2.4	1.1	1.5

NKA protein results from western blotting

A2.58 NKA alpha 1

	CON			CHO		
	rest	60min	fat	rest	60min	fat
1	1.00	1.01	1.62	2.24	1.31	1.02
2	1.00	1.23	2.06	1.30	1.71	1.44
3	1.00	1.13	0.74	0.78	0.22	0.74
4	1.00	0.72	0.55	0.39	0.78	0.79
5	1.00	1.09	0.48	0.67	0.83	0.70
6	1.00	1.27	0.76	0.87	0.91	1.22
7	1.00	1.63	2.10	1.07	1.84	1.34
8	1.00	1.49	2.29	1.03	1.74	0.87
n	8.00	8.00	8.00	8.00	8.00	8.00
Mean	1.00	1.20	1.33	1.04	1.17	1.01
SD	0.00	0.28	0.77	0.55	0.58	0.29

A2.59 NKA alpha 2

	CON			CHO		
	rest	60min	fat	rest	60min	fat
1	1.00	0.84	0.92	1.16	0.99	1.33
2	1.00	1.16	1.88	0.96	1.28	1.02
3	1.00	0.89	0.82	0.60	0.45	0.41
4	1.00	1.11	1.25	0.91	1.26	0.82
5	1.00	0.73	1.03	1.13	1.21	0.74
6	1.00	0.97	0.59	1.20	1.42	1.12
7	1.00	0.96	1.22	0.14	0.45	0.88
8	1.00	1.09	1.20	1.10	1.87	1.17
n	8.00	8.00	8.00	8.00	8.00	8.00
Mean	1.00	0.97	1.11	0.90	1.11	0.94
SD	0.00	0.15	0.38	0.36	0.48	0.29

A2.60 NKA alpha 3

	CON			CHO		
	rest	60min	fat	rest	60min	fat
1	1.00	0.69	0.54	1.97	0.53	0.62
2	1.00	1.35	1.33	0.94	1.55	0.52
3	1.00	4.59	2.75	3.13	1.46	2.09
4	1.00	0.45	0.38	0.35	0.73	0.76
5	1.00	0.49	0.28	0.60	0.64	0.59
6	1.00	0.94	0.32	1.41	0.50	0.72
7	1.00	1.46	0.91	1.46	0.92	0.80
8	1.00	1.32	0.85	1.54	1.59	0.38
n	8.00	8.00	8.00	8.00	8.00	8.00
Mean	1.00	1.41	0.92	1.43	0.99	0.81
SD	0.00	1.34	0.82	0.87	0.47	0.54

A2.61 NKA beta 1

	CON			CHO		
	rest	60min	fat	rest	60min	fat
1	1.00	1.16	0.61	1.50	1.74	2.32
2	1.00	1.41	1.35	0.83	1.01	0.75
3	1.00	0.95	0.46	0.46	0.18	0.19
4	1.00	1.59	1.43	1.29	1.63	1.87
5	1.00	1.00	0.66	0.59	0.91	0.58
6	1.00	1.03	0.36	0.98	1.11	1.56
7	1.00	1.01	1.13	0.65	0.70	0.89
8	1.00	2.48	2.21	2.63	4.75	2.24
n	8.00	8.00	8.00	8.00	8.00	8.00
Mean	1.00	1.33	1.03	1.12	1.50	1.30
SD	0.00	0.52	0.63	0.71	1.40	0.80

A2.62 NKA beta 2

	CON			CHO		
	rest	60min	fat	rest	60min	fat
1	1.00	0.88	1.20	1.05	1.17	1.10
2	1.00	0.93	1.20	1.21	1.06	0.79
3	1.00	1.21	0.85	1.57	1.31	3.32
4	1.00	0.83	0.59	0.30	0.47	0.68
5	1.00	1.18	0.76	0.85	0.91	0.96
6	1.00	2.70		0.79	0.54	1.06
7	1.00	0.77	0.39	1.00	1.14	1.23
8	1.00	2.20	1.59	2.70	4.85	1.70
n	8.00	8.00	7.00	8.00	8.00	8.00
Mean	1.00	1.34	0.94	1.19	1.43	1.36
SD	0.00	0.72	0.41	0.71	1.41	0.85

A2.63 NKA beta 3

	CON			CHO		
	rest	60min	fat	rest	60min	fat
1	1.00	1.11	2.04	0.57	1.60	1.46
2	1.00	0.48	1.25	0.44	0.65	1.00
3	1.00	1.18	2.90	1.72	1.60	1.19
4	1.00	0.66	0.83	0.36	0.57	0.45
5	1.00	0.74	1.83	1.72	2.49	1.56
6	1.00	0.62	0.75	3.21	2.84	1.77
7	1.00	0.69	1.40	0.50	0.51	0.50
8	1.00	0.95	1.54	1.75	1.58	2.04
n	8.00	8.00	8.00	8.00	8.00	8.00
Mean	1.00	0.80	1.57	1.28	1.48	1.25
SD	0.00	0.25	0.70	1.00	0.88	0.57

Appendix 3. Individual data from Study 2 (Chapter 4)

A3.1 Participant Characteristics

	Age (yrs)	Height (cms)	Weight (kg)	$\dot{V}O_{2peak}$ (ml.kg ⁻¹ .min ⁻¹)
1	23	156	62.8	45.3
2	24	180	62	60
3	19	183	75.9	53.47
4	21	182	81.5	52.48
5	21	168	61	46.4
6	21	174	71.5	49.17
7	24	178	75	54.7
n	7	7	7	7
Mean	21.9	174.4	70.0	51.6
SD	1.9	9.6	8.1	5.1

NKA protein results from western blotting

A3.2 NKA alpha 1

	PRE-CaCO ₂		PRE-NaHCO ₃		POST-CaCO ₂	
	Pre-ex	Post-ex	Pre-ex	Post-ex	Pre-ex	Post-ex
1	1.00	2.9	1.4	0.9	1.0	1.0
2	1.00	1.6	1.9	2.6	2.7	1.3
3	1.00	1.2	0.9	0.8	0.9	1.4
4	1.00	1.1	1.7	1.0	0.8	0.7
5	1.00	0.9	1.2	1.7	1.6	1.9
6	1.00	1.3	1.0	0.7	1.0	1.0
7	1.00	0.7	0.6	0.8	0.9	0.6
n	7	7	7	7	7	7
Mean	1.00	1.37	1.25	1.23	1.29	1.13
SD	0.00	0.72	0.45	0.70	0.66	0.44

A3.3 NKA alpha 2

	PRE-CaCO ₂		PRE-NaHCO ₃		POST-CaCO ₂	
	Pre-ex	Post-ex	Pre-ex	Post-ex	Pre-ex	Post-ex
1	1.00	1.1	1.2	0.8	1.0	1.2
2	1.00	1.3	0.8	1.5	1.1	0.7
3	1.00	1.6	1.2	1.5	1.1	1.2
4	1.00	1.2	2.1	1.6	1.1	1.0
5	1.00	0.8	1.1	0.9	0.9	0.8
6	1.00	1.6	1.2	1.3	1.7	1.5
7	1.00	0.9	1.1	0.9	1.4	0.8
n	7	7	7	7	7	7
Mean	1.00	1.21	1.25	1.21	1.20	1.05
SD	0.00	0.31	0.39	0.34	0.28	0.28

A3.4 NKA alpha 3

	PRE-CaCO ₂		PRE-NaHCO ₃		POST-CaCO ₂	
	Pre-ex	Post-ex	Pre-ex	Post-ex	Pre-ex	Post-ex
1	1.0	35.5	28.6	40.5	1.9	5.8
2	1.0	1.0	1.0	29.8	2.5	2.7
3	1.0	0.9	2.0	2.6	1.1	0.6
4	1.0	3.1	0.5	2.5	1.8	20.0
5	1.0	16.6	19.9	1.8	8.9	3.7
6	1.0	1.3	1.0	0.9	1.3	1.1
7	1.0	1.2	1.2	1.2	1.7	0.7
n	7	7	7	7	7	7
Mean	1.0	8.5	7.7	11.3	2.7	4.9
SD	0.0	13.2	11.6	16.6	2.7	6.9

A3.5 NKA beta 1

	PRE-CaCO ₂		PRE-NaHCO ₃		POST-CaCO ₂	
	Pre-ex	Post-ex	Pre-ex	Post-ex	Pre-ex	Post-ex
1	1.00	1.3	1.7	1.7	1.0	0.8
2	1.00	1.1	1.2	1.5	0.8	0.6
3	1.00	1.1	1.3	1.5	0.9	0.7
4	1.00	1.0	1.4	0.7	0.9	0.8
5	1.00	0.6	1.3	0.6	0.7	0.6
6	1.00	1.0	1.4	0.7	0.8	0.7
7	1.00	1.1	1.4	0.7	0.7	0.6
n	7	7	7	7	7	7
Mean	1.00	1.04	1.40	1.05	0.81	0.68
SD	0.00	0.23	0.18	0.49	0.10	0.08

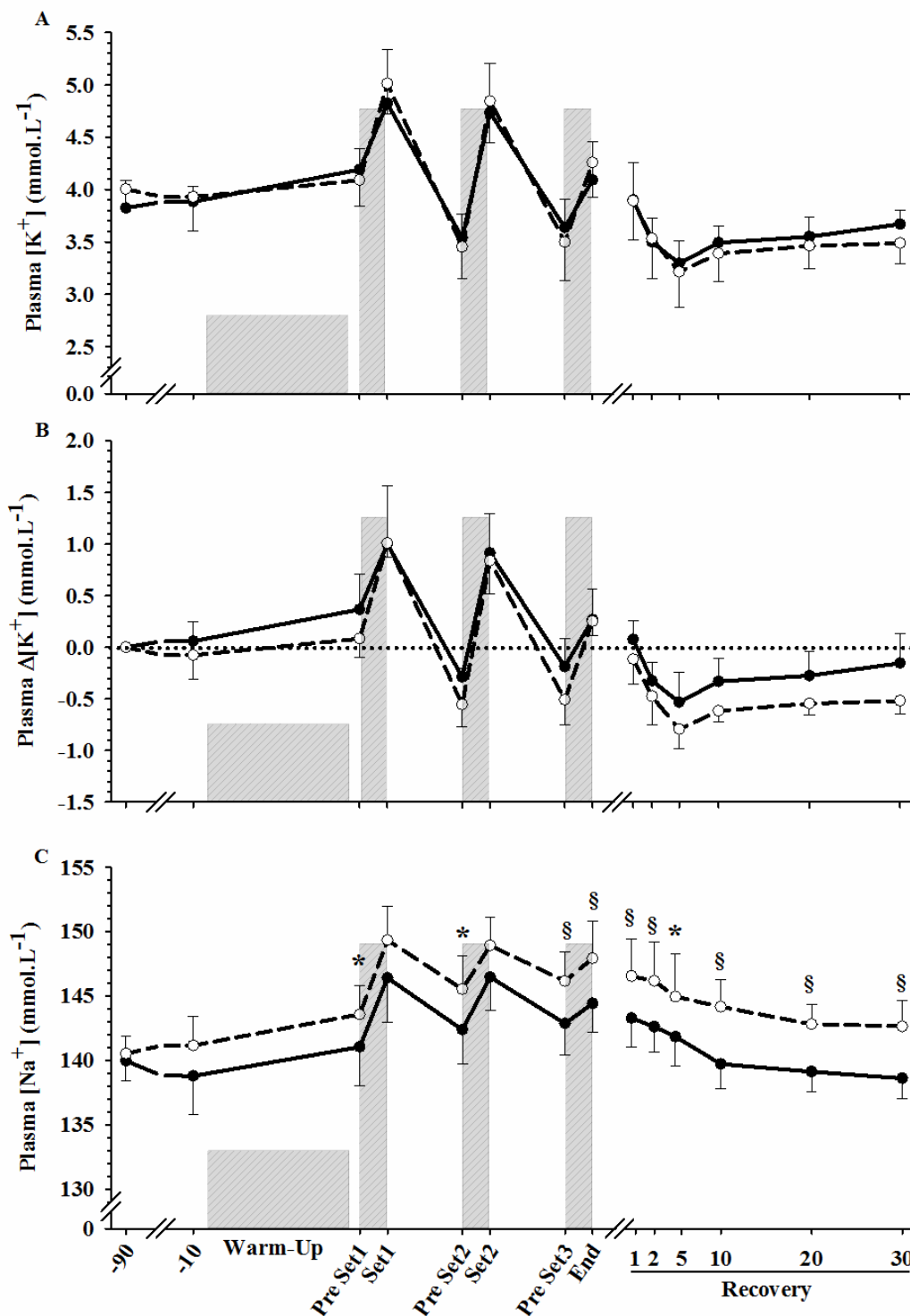
A3.6 NKA beta 2

	PRE-CaCO ₂		PRE-NaHCO ₃		POST-CaCO ₂	
	Pre-ex	Post-ex	Pre-ex	Post-ex	Pre-ex	Post-ex
1	1.0	1.2	1.1	1.1	1.3	1.0
2	1.0	0.8	0.7	0.6	0.7	0.7
3	1.0	0.6	0.8	0.8	0.7	0.5
4	1.0	1.1	1.0	1.8	1.4	1.0
5	1.0	1.9	1.5	1.9	2.1	1.8
6	1.0	2.4	2.1	1.7	3.2	1.8
7	1.0	0.6	0.9	0.7	0.9	0.3
n	7	7	7	7	7	7
Mean	1.00	1.23	1.16	1.24	1.47	1.01
SD	0.0	0.7	0.5	0.6	0.9	0.6

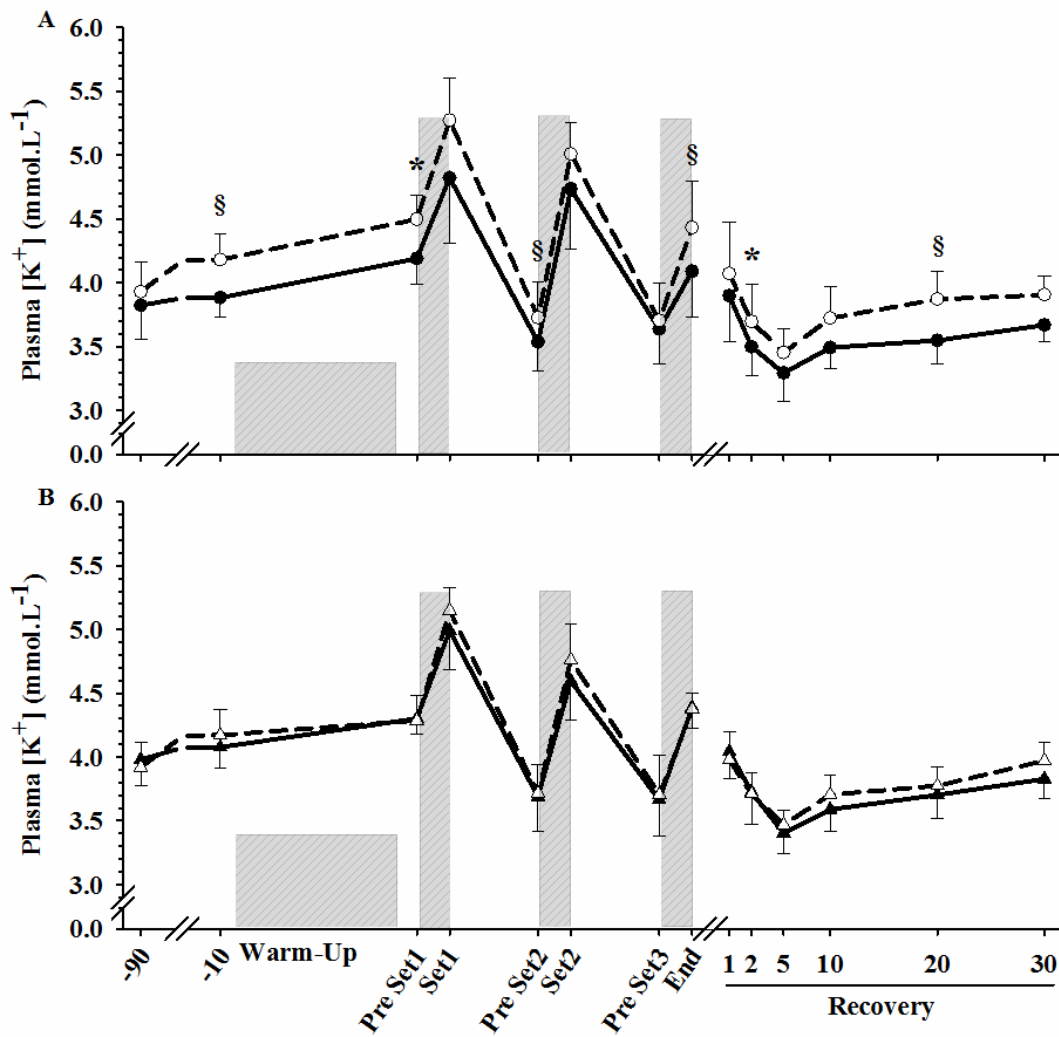
A3.7 NKA beta 3

	PRE-CaCO ₂		PRE-NaHCO ₃		POST-CaCO ₂	
	Pre-ex	Post-ex	Pre-ex	Post-ex	Pre-ex	Post-ex
1	1.00	4.3	2.2	0.6	1.4	3.4
2	1.00	15.1	2.9	13.3	10.7	7.7
3	1.00	9.2	2.2	4.8	4.1	6.5
4						
5	1.00	0.4	0.4	0.9	0.8	0.7
6	1.00	1.4	1.5	0.6	0.8	2.1
7	1.00	1.4	0.4	0.5	2.1	0.5
n	6	6	6	6	6	6
Mean	1.00	5.31	1.60	3.44	3.33	3.47
SD	0.00	5.77	1.04	5.10	3.84	3.03

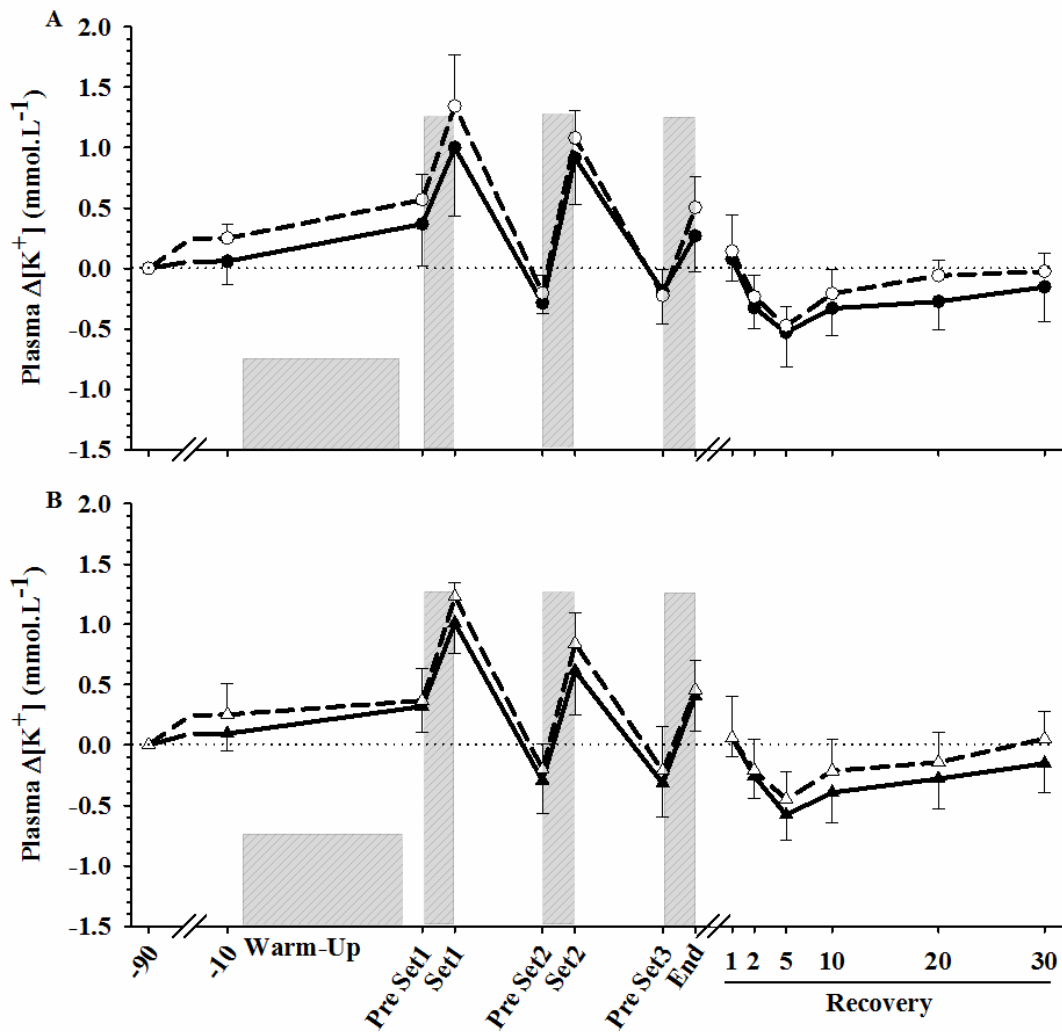
Appendix 4. Plasma K⁺ data from Study 2 (Chapter 4)



A4.1 Pre-training venous plasma [K⁺] (A), plasma Δ[K⁺] (B) and plasma [Na⁺] (C) during RSE and recovery for EXP group (n=7) during PRE-EXP (placebo ingestion, closed circles) and ACUTE-EXP (NaHCO₃ ingestion, open circles). Data are mean ± SD. * = greater than PRE-EXP (P<0.05), § = greater than PRE-EXP (P<0.01). Shaded area indicates exercise.



A4.2 Venous plasma [K⁺] during RSE and recovery during PRE (closed symbols) and POST (open symbols) testing for EXP (circles), (A) and CON (triangles), n=7 (B) groups. Data are mean ± SD. * = greater than pre-training (P<0.05), § = greater than pre-training (P<0.01). Both groups ingested CaCO₃ prior to exercise during PRE and POST testing. Shaded area indicates exercise.

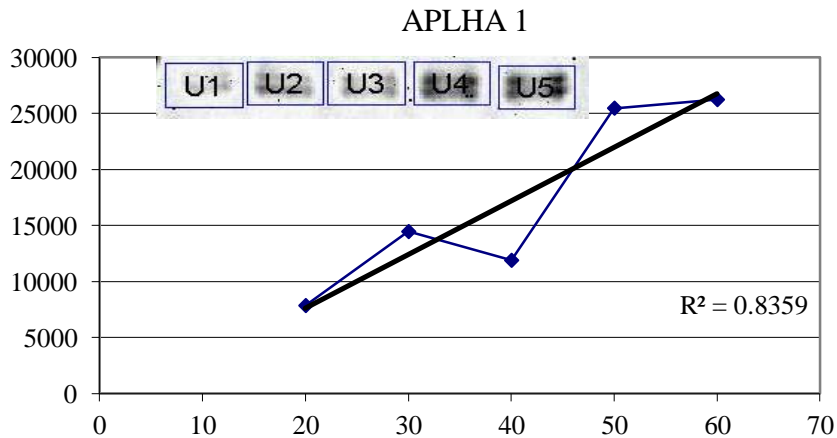


A4.3 Venous plasma $\Delta[K^+]$ during RSE and recovery during PRE (closed symbols) and POST (open symbols) testing for EXP (circles), (A) and CON (triangles), $n=7$ (B) groups. Data are mean \pm SD. Both groups ingested $CaCO_3$ prior to exercise during PRE and POST testing. Shaded area indicates exercise

Appendix 5. Western blot protein linearity

A5.1a Protein loading volume (μg) and density for NKA α_1

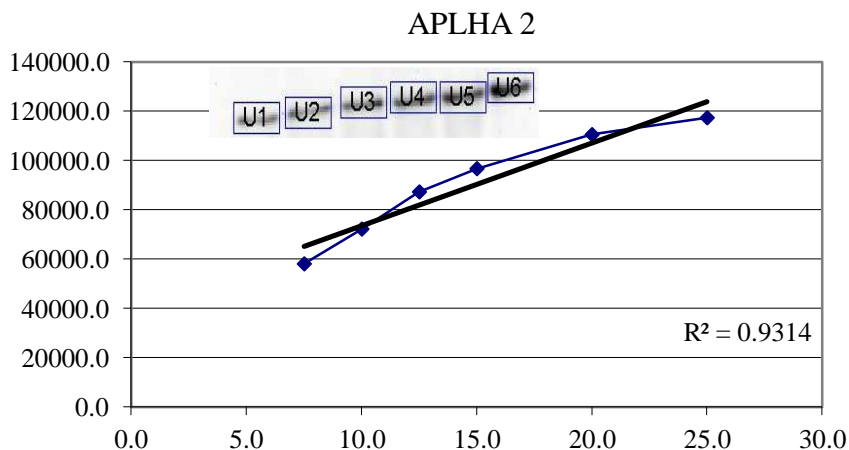
Lane	Protein Loaded (μg)	Density
1	20.0	7844.17
2	30.0	14449.08
3	40.0	11884.46
4	50.0	25468.8
5	60.0	26234.86



A5.1b Protein loading volume (μg) and density for NKA α_1

A5.2a Protein loading volume (μg) and density for NKA α_2

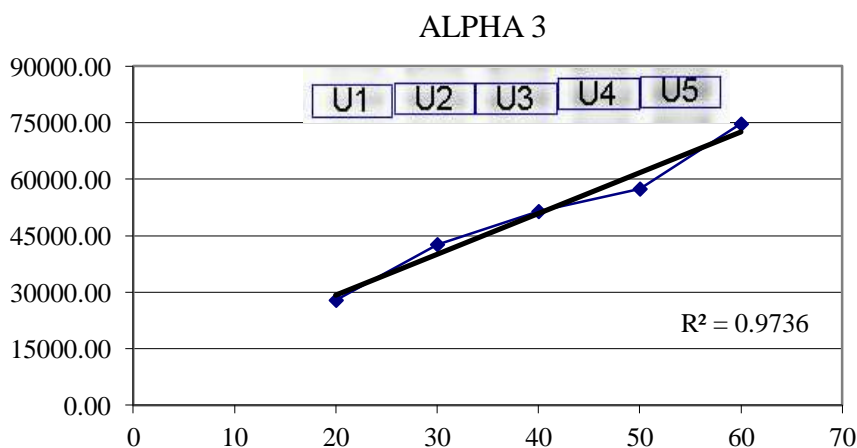
Lane	Protein Loaded (μg)	Density
1	7.5	57994.1
2	10.0	72105.0
3	12.5	87179.0
4	15.0	96610.8
5	20.0	110422.9
6	25.0	117253.0



A5.2b Protein loading volume (μg) and density for NKA α_2

A5.3a Protein loading volume (μg) and density for NKA α_3

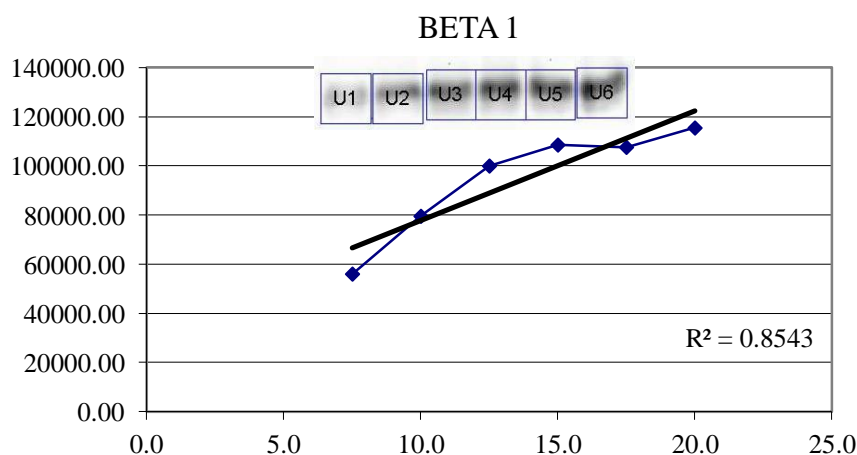
Lane	Protein Loaded (μg)	Density
1	20.0	27888.89
2	30.0	42675.10
3	40.0	51461.26
4	50.0	57436.31
5	60.0	74697.44



A5.3b Protein loading volume (μg) and density for NKA α_3

A5.4a Protein loading volume (μg) and density for NKA β_1

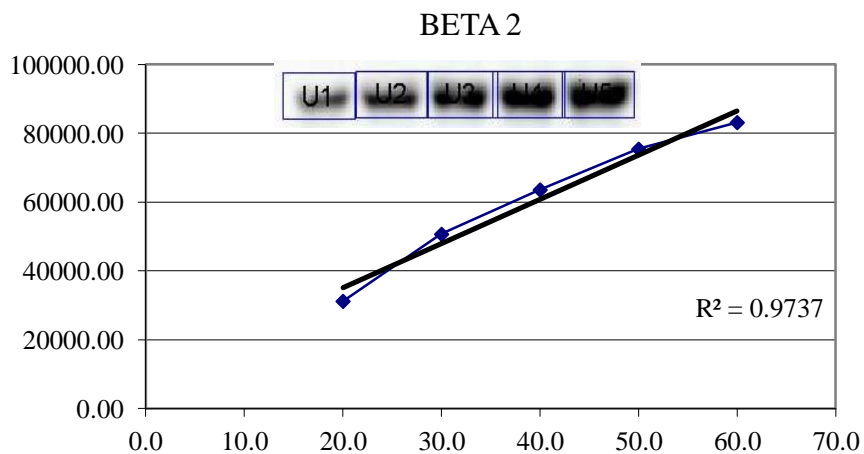
Lane	Protein Loaded (μg)	Density
1	7.5	56032.56
2	10.0	79557.83
3	12.5	100003.43
4	15.0	108557.06
5	17.5	107611.25
6	20.0	115483.86



A5.4b Protein loading volume (μg) and density for NKA β_1

A5.5a Protein loading volume (μg) and density for NKA β_2

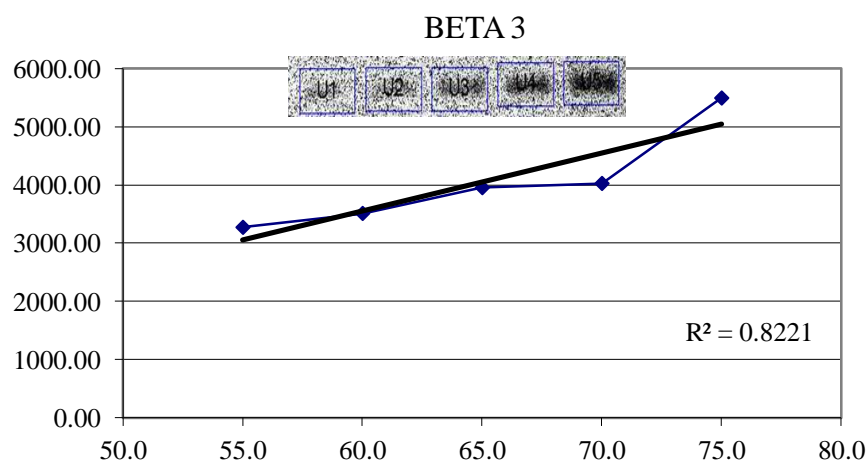
Lane	Protein Loaded (μg)	Density
1	20.0	31205.64
2	30.0	50691.45
3	40.0	63582.40
4	50.0	75429.05
5	60.0	83162.38



A5.5b Protein loading volume (μg) and density for NKA β_2

A5.6a Protein loading volume (μg) and density for NKA β_3

Lane	Protein Loaded (μg)	Density
1	55.0	3271.67
2	60.0	3510.34
3	65.0	3952.94
4	70.0	4025.21
5	75.0	5493.21



A5.6b Protein loading volume (μg) and density for NKA β_3

Appendix 6. Individual data from Study 3 (Chapter 5)

A6.1 alpha 1 Intracellular

	MHC I			MHC II		
	n	mean	St dev	n	mean	St dev
1	19	7.03	0.98	44	7.78	0.81
2	37	6.60	0.43	29	7.30	0.50
3	30	5.15	1.09	55	7.82	2.90
4	88	9.96	1.48	46	11.59	1.30
5	72	5.65	1.04	35	8.78	1.52
6	61	6.08	1.04	47	8.99	1.53
n	6	6	6	6	6	6
Mean	51.17	6.75	1.01	42.67	8.71	1.43
SD	26.72	1.71	0.34	9.27	1.55	0.83

A6.2 alpha 1 Plasma Membrane

	MHC I		MHC II	
	mean	St dev	mean	St dev
1	6.68	0.80	8.23	0.60
2	7.11	0.54	8.00	1.02
3	4.48	0.40	7.47	3.23
4	12.87	1.90	13.87	2.33
5	4.93	0.84	6.02	1.14
6	6.82	1.33	10.67	4.09
n	6	6	6	6
Mean	7.15	0.97	9.04	2.07
SD	3.01	0.56	2.80	1.39

A6.3 alpha 2 Intracellular

	MHC I			MHC II		
	n	mean	St dev	n	mean	St dev
1	8	3.44	1.08	21	3.08	0.30
2	102	3.24	0.30	44	3.49	0.44
3	38	3.24	0.70	59	3.55	0.91
4	64	5.06	0.69	33	5.16	0.79
5	72	5.65	1.04	39	3.32	0.54
6	57	4.19	0.56	34	3.99	0.57
n	6	6	6	6	6	6
Mean	56.83	4.14	0.73	38.33	3.77	0.59
SD	31.81	1.03	0.29	12.71	0.75	0.23

A6.4 alpha 2 Plasma Membrane

	MHC I		MHC II	
	mean	St dev	mean	St dev
1	4.94	1.47	6.90	3.35
2	6.65	1.95	6.22	1.75
3	8.09	2.42	8.43	2.49
4	13.12	3.23	9.75	3.88
5	5.91	1.70	4.65	0.77
6	8.87	2.06	9.27	1.87
n	6	6	6	6
Mean	7.93	2.14	7.54	2.35
SD	2.91	0.62	1.96	1.14

A6.5 alpha 3 Intracellular

	MHC I			MHC II		
	n	mean	St dev	n	mean	St dev
1	17	4.20	0.84	44	2.10	0.32
2	115	5.20	0.87	61	2.94	0.38
3	34	19.71	3.22	63	4.37	0.93
4	78	8.63	1.36	36	6.76	1.11
5	74	16.35	3.2	39	2.92	0.53
6	30	9.02	2.11	25	2.31	0.35
n	6	6	6	6	6	6
Mean	58.00	10.52	1.94	44.67	3.57	0.60
SD	37.27	6.20	1.09	14.81	1.76	0.33

A6.6 alpha 3 Plasma Membrane

	MHC I		MHC II	
	mean	St dev	mean	St dev
1	3.60	0.64	2.22	0.18
2	4.94	0.58	3.14	0.44
3	15.46	2.46	5.07	0.81
4	8.08	1.16	6.71	0.93
5	13.75	3.94	2.84	0.52
6	9.68	2.54	3.48	0.90
n	6	6	6	6
Mean	9.25	1.89	3.91	0.63
SD	4.71	1.32	1.67	0.30

A6.7 beta 1 Intracellular

	MHC I			MHC II		
	n	mean	St dev	n	mean	St dev
1	16	5.35	0.84	41	5.88	0.75
2	101	6.83	0.88	53	7.05	0.71
3	51	12.77	1.73	71	14.18	2.12
4	71	3.83	0.34	36	4.15	0.45
5	78	13.38	3.36	39	12.74	2.22
6	70	9.22	1.35	46	9.98	1.16
n	6	6	6	6	6	6
Mean	64.50	8.56	1.42	47.67	9.00	1.24
SD	28.71	3.93	1.06	12.89	3.97	0.76

A6.8 beta 1 Plasma Membrane

	MHC I		MHC II	
	mean	St dev	mean	St dev
1	7.48	1.11	7.67	1.29
2	8.71	1.21	8.42	0.85
3	21.40	2.89	20.59	3.42
4	6.40	1.23	6.64	1.55
5	22.80	5.56	19.25	3.72
6	19.60	3.83	20.90	5.12
n	6	6	6	6
Mean	14.40	2.64	13.91	2.66
SD	7.63	1.81	6.99	1.68

A6.9 beta 2 Intracellular

	MHC I			MHC II		
	n	mean	St dev	n	mean	St dev
1	7	3.33	0.25	16	3.12	0.26
2	104	1.91	0.13	49	1.91	0.20
3						
4	23	3.29	0.28	8	3.45	0.16
5						
6						
n	3	3	3	3	3	3
Mean	44.67	2.84	0.22	24.33	2.83	0.20
SD	52.00	0.81	0.08	21.73	0.81	0.05

A6.10 beta 2 Plasma Membrane

	MHC I		MHC II	
	mean	St dev	mean	St dev
1	5.89	2.00	4.88	0.87
2	3.27	0.86	3.13	0.88
3				
4	4.66	0.68	4.88	0.78
5				
6				
n	3	3	3	3
Mean	4.61	1.18	4.30	0.85
SD	1.31	0.71	1.01	0.06

A6.11 beta 3 Intracellular

	n	mean	St dev
1	37	1.81	0.12
2	184	1.77	0.28
3	146	1.63	0.37
4	181	1.69	0.31
5	43	1.63	0.28
6	219	1.65	0.32
n	6	6	6
Mean	135.00	1.70	0.28
SD	77.15	0.08	0.09

A6.12 beta 3 Plasma Membrane

	mean	St dev
1	2.15	1.10
2	1.91	1.09
3	2.06	1.17
4	1.90	0.51
5	2.08	1.19
6	1.77	0.47
n	6	6
Mean	1.98	0.92
SD	0.14	0.34